Outer Boundary Conditions in Numerical Relativity

Deadman, E

2009

MIMS EPrint: **2010.92**

Manchester Institute for Mathematical Sciences
School of Mathematics

The University of Manchester

Reports available from: http://eprints.maths.manchester.ac.uk/
And by contacting: The MIMS Secretary
School of Mathematics
The University of Manchester
Manchester, M13 9PL, UK

ISSN 1749-9097

Outer Boundary Conditions in Numerical Relativity

Edvin Deadman
St Catharine's College, Cambridge

November 4, 2009

A dissertation submitted to the
University of Cambridge
for the degree of
Doctor of Philosophy

Declaration

This thesis is based on work carried out under the supervision of Dr John M Stewart at the Department of Applied Mathematics and Theoretical Physics, University of Cambridge, from October 2006. Chapter 3 is based on work done in collaboration with my supervisor and published in a joint paper [40]. The remaining chapters are all my own work. No part of this thesis has been submitted towards any other qualification.

Acknowledgements

I would like to express my thanks to my supervisor, Dr John Stewart. His advice, encouragement and constant flow of ideas throughout this research project have been invaluable to me.

Financial support from the Engineering and Physical Sciences Research Council is gratefully acknowledged.

I would also like to thank my office mates James Fergusson and Jorge Santos for their friendship and advice, and Dr Oliver Rinne for many useful discussions.

Abstract

This thesis is concerned with outer boundary conditions in numerical relativity. In numerical simulations, the spatially infinite universe is typically modelled using a finite spatial domain, on the edge of which boundary conditions are imposed. These boundary conditions should mirror the unbounded physical domain as closely as possible. They should be transparent to outgoing gravitational radiation and should not introduce spurious incoming radiation via reflections of outgoing radiation off the boundary.

The concepts of incoming and outgoing gravitational radiation are only well understood in certain specific charts and tetrads. The first half of this thesis investigates the relationship between these charts and tetrads and those used in numerical relativity.

We begin by studying a previous calculation [134], in which quantities such as the Bondi mass and the news function were expressed in terms of the Newman-Penrose scalars in an axisymmetric spacetime. The calculation is generalized to spacetimes with no symmetries.

The results above still require a specific choice of tetrad. By supposing that the region of spacetime far from an isolated gravitating source is in some sense Minkowskian, we demonstrate how to transform between the charts and tetrads used in theoretical studies of gravitational radiation and the charts and tetrads used in numerical relativity. This enables us to provide "numerical relativity recipes" in which the Weyl scalars, the Bondi mass and news function are expressed in terms of the metric variables in a numerical chart.

The second half of this thesis addresses the problem of absorbing boundary conditions in numerical relativity. Using Hertz potentials, the far-field region of a spacetime can be expressed as a linear perturbation about Minkowski, Schwarzschild or Kerr backgrounds. The resulting field equations enable us to investigate the propagation of linearized gravitational radiation. On a Minkowski background, incoming and outgoing waves propagate independently. The presence of a curved background creates a "gravitational tail" whose behaviour near future null infinity we are able to estimate. This enables us to formulate absorbing boundary conditions for numerical relativity.

Finally, we link the two threads mentioned above. The boundary conditions are expressed in terms of the metric variables in a numerical relativity chart.

Contents

Chapter 1

Introduction

Albert Einstein's theory of general relativity [42, 43] changed the way we view space and time. In previous physical theories, fields evolved on a fixed spacetime geometry. In general relativity, the geometry itself forms part of the field equations and evolves dynamically. The geometry of the spacetime is related to the presence of matter by a set of field equations. The curvature of the spacetime in turn determines the motion of matter. Newton's notion of a gravitational force then becomes an essentially geometric concept.

In general relativity, the spacetime is described by a four dimensional pseudo-Riemannian manifold $\mathcal{M}$ admitting a Lorentzian metric g_{ik}. The Einstein field equations are

$$R_{ik} - \frac{1}{2} R g_{ik} = \kappa T_{ik}, \tag{1.1}$$

where R_{ik} is the Ricci curvature tensor, R is the Ricci scalar, κ is a constant and T_{ik} is the stress-energy tensor of any matter or energy present. In a vacuum, the field equations reduce to

$$R_{ik} = 0. \tag{1.2}$$

In the tensor notation used above, the field equations appear deceptively simple. In fact they form a complicated set of ten coupled, nonlinear, second-order partial differential equations for the ten independent metric variables. This makes them exceedingly difficult to solve in all but the simplest of scenarios. Hence, in the century since its discovery by Einstein, general relativity remains at the forefront of research in theoretical physics.

Obtaining analytical closed-form solutions to the field equations coupled

to matter (1.1) is particularly difficult, and even in a vacuum the problem is non-trivial. Simplifications must be made by, for example, considering spacetimes with symmetries, or by perturbing the spacetime about a known background solution. Many such solutions are known (see e.g. [132]), but each one corresponds to a particular special case of the field equations. The field equations corresponding to more general dynamical situations, spacetimes with no symmetries, or exotic types of energy-momentum tensor remain analytically intractable. However, the advent of computers and the rapid increase in computing power and memory in the past few decades mean that it is now possible to try to solve the field equations numerically. This field is known as numerical relativity.

1.1 An Overview of Results Obtained in Numerical Relativity

Only very modest computing power was available in the 1960s. Early simulations in the nascent field of numerical relativity focused on either spherically symmetric or axisymmetric spacetimes. The symmetries significantly reduced the computational cost of the simulations since "dimensional reduction" could be used to reduce the number of field equations to be solved. The first documented numerical study in relativity appears to be that of Hahn & Lindquist [69], followed several years later by Eppley [44]. The first realistic numerical study of gravitational collapse was performed in 1985 [131], using axisymmetry.

Axisymmetric evolutions are particularly interesting because they reduce the computational effort required, whilst still permitting the study of gravitational radiation (Birkhoff's theorem [15] implies that spherically symmetric spacetimes do not contain gravitational waves). However, if standard cylindrical polar coordinates are used, then a coordinate singularity is present on the axis. This problem has only recently been solved [118]. This has led to improved simulations of axisymmetric gravitational waves (Brill waves) [115].

The speed and memory of computers today is such that many simulations are now carried out in spacetimes with no symmetries at all. For example, in [2], highly nonlinear gravitational radiation was modelled in three spatial

dimensions. Waves were found that were strong enough to undergo gravitational collapse and form black holes due to their own self-gravity.

The importance of numerical relativity became apparent in the 1990s with the discovery of critical phenomena in gravitational collapse [28]. Numerical relativity had uncovered behaviour that had never before been seen in analytical studies of general relativity. The central ideas of critical collapse are as follows. Consider a one parameter family of asymptotically flat, smooth initial data. Let p^* be the critical value of the parameter p separating solutions whose fields disperse from solutions which form black holes. For slightly supercritical data, the mass M of the resulting black hole obeys the relation

$$M \propto (p - p^*)^\gamma, \tag{1.3}$$

where γ is independent of the family of initial data chosen. In addition, the critical solution itself is independent of the initial data and exhibits self-similar behaviour. The study of critical phenomena has since developed into a thriving field of research in its own right. We refer the reader to the recent review article by Gundlach & Martin-Garcia [63] for more information.

Current research in numerical relativity can be divided into two main areas. The astrophysical community focuses on modelling the Einstein field equations coupled to various types of matter. By seeking realistic equations of state for the matter, the general relativistic behaviour of celestial bodies can be investigated. For example, in relativistic hydrodynamics and magnetohydrodynamics accurate models of self-gravitating fluids are studied [46]. This has increased our understanding of the interiors of stars and neutron stars, and the behaviour of accretion discs.

This thesis, however, is concerned primarily with the second branch of numerical relativity; the study of the geometry of spacetime. Solutions to the field equations are investigated in the absence of matter, typically by considering vacuum black hole spacetimes. Many numerical relativity groups are now focusing on evolving binary systems of black holes, white dwarves and neutron stars and obtaining the resulting gravitational wave signatures.

The evolution of a binary black hole system can be divided into three phases. Initially the black holes orbit each other, the distance between them

decreasing. This is known as "inspiral". The second phase is known as the "merger". The two black holes coalesce into a single highly-deformed black hole. The "no hair" theorem [70,119,120] states that a black hole is completely characterized by only three externally observable parameters: mass, charge and angular momentum. Therefore, the new black hole will now rid itself of its deformity by emitting gravitational radiation characteristic of the mass and angular momentum of the final state of the black hole. This process is known as "ringdown".

The study of binary black hole systems was pioneered by Smarr [130], who studied the head-on collision of two black holes in axisymmetry. The full three-dimensional problem has proved considerably more difficult to solve. The first long term, stable evolution of a binary black hole system in three spatial dimensions was achieved by Pretorius [108]. The collision of two non-rotating, equal-mass black holes was simulated through inspiral, merger and ringdown. Recent investigations have extended these results [24, 72, 127]. Numerical relativity groups around the world are performing increasingly accurate simulations, and there is now a wealth of literature on the subject. For a very recent summary we direct the reader to the study of Scheel et al. [126].

The numerical study of binary black holes is of interest to experimental physicists as well as theorists. The first generation of gravitational wave detectors has been gathering data for several years now. These detectors (such as LIGO, VIRGO and TAMA 300) usually use "laser interferometry" and each detector is designed to detect a different range of frequencies of radiation. The resolution of these instruments is not currently high enough to detect gravitational radiation with any degree of certainty. However, as the second generation of gravitational wave detectors begins to take over (for example Enhanced LIGO and LISA), gravitational wave observations are expected in the coming years. Sathyaprakash & Schutz [125] have written a recent review article summarising this area of research.

The most likely source of measurable gravitational radiation is from large-scale astrophysical events such as binary black hole merger or the collision of neutron stars (other sources of radiation are too weak to be detected on Earth). There is therefore a strong demand for waveform templates from these events, to enable gravitational wave detectors to correctly interpret their data. Hence, as well as investigating the evolution of binary systems of massive objects, nu-

merical relativists are also attempting to calculate the resulting gravitational waveforms which propagate into the far-field region. The detection of gravitational waves from the coalescence of two black holes would provide one of the best experimental verifications to date of the strong-field predictions of general relativity.

1.2 Techniques used in Numerical Relativity

Numerical relativity calculations are typically based on either the Cauchy problem or the characteristic initial value problem.

In the Cauchy problem the spacetime is foliated with spacelike hypersurfaces. Initial data are specified on one such hypersurface (see e.g. [35]) and the system is evolved from one hypersurface to the next. The evolution is performed by decomposing the Einstein field equations into spatial and temporal parts. This results in a set of "constraint equations" which are imposed on each spacelike hypersurface, and a set of "evolution equations" governing the evolution of the system between hypersurfaces. The first such decomposition was the Arnowitt-Deser-Misner $3 + 1$ formulation (see for example [5, 148]) in which the ten field equations were separated into six constraint equations and four evolution equations. In reality this particular decomposition is rarely used in numerical relativity due to stability issues, but many other formalisms are available. For a general summary of the Cauchy problem in general relativity we refer the reader to Rendall's review article [112]. Aspects of the Cauchy problem pertinent to numerical relativity were studied in more detail by Stewart [136]. This will be discussed in more detail shortly.

In a Lorentzian manifold, there is typically no preferred Cauchy foliation. The alternative to the Cauchy problem is the characteristic initial value problem, which is more suited to the study of gravitational radiation. Data are specified on two characteristic (null) hypersurfaces and the spacetime is foliated accordingly. The characteristic initial value problem was used to carry out the first stable numerical simulations of black holes moving in three dimensions [58]. One of the drawbacks of this technique is the tendency for caustics to develop and the subsequent loss of stability in the evolution. Winicour [147] has written an up-to-date review on the use of the characteristic initial value problem in numerical relativity.

The characteristic initial value problem will be used later in this thesis in order to study gravitational waves, but for the remainder of this chapter we focus on the Cauchy problem, which is more commonly used in numerical relativity. Before a particular formulation of the Cauchy problem can be used numerically, the problems of "well-posedness" and "constraint violations" must be addressed. These are discussed below.

If an analytical solution to the Cauchy problem is not known then one must ask if the problem is "well-posed". Does a solution even exist? If so, is it stable under small perturbations of the initial data? Once well-posedness has been established one must be able to ascertain that the simulation gives an acceptably small numerical error. These rather imprecise conditions were dealt with more rigorously by Stewart [136] who showed that they are satisfied if the system of equations can be shown to have a strongly hyperbolic principal part. Thus many studies have been devoted to developing strongly hyperbolic formulations of the Cauchy problem. One such formulation is the Z4 formulation [16] in which a covariant term is added to the Einstein equations such that the resulting 3+1 decomposition is strongly hyperbolic. This was applied in axisymmetry by Rinne & Stewart [113,118]. An alternative approach is the first order formulation of Alvi [3] which is symmetrizable hyperbolic.

Recent attempts to find strongly hyperbolic formulations of the Cauchy problem have focused on "generalized harmonic coordinates". These are coordinates which, when regarded as scalars, satisfy the wave equation, $\Box x^a = 0$. They enable terms in the Ricci tensor to be simplified so that symmetric hyperbolic decompositions of the Einstein field equations (1.1) can be obtained [90]. Unfortunately, many of the gauge choices which are useful in numerical relativity do not preserve the hyperbolicity of generalized harmonic representations of the Einstein equations. The technique has recently been extended by Lindblom et al. [89] to circumvent this problem.

As described earlier in this section, in the Cauchy problem, the Einstein field equations are decomposed into constraint equations and evolution equations. Constraint equations are defined on each spacelike hypersurface. If the constraint equations are satisfied on one such hypersurface and the evolution equations are satisfied, then analytically the constraint equations will be satisfied on all the hypersurfaces in the foliation. A numerical relativist can make use of this fact by imposing the constraint equations on the initial data only.

This is known as a "free" or "unconstrained evolution". However, numerical errors within the computational domain and the choice of boundary conditions imposed on the edge of the computational domain can both cause constraint violations to arise (see, for example, [74] for further details on the problem of constraint violations). The alternative to an unconstrained evolution is to impose the constraint equations on each hypersurface; a "constrained evolution". This is more accurate but computationally expensive. Attention has therefore turned to obtaining strongly hyperbolic formulations of the field equations with "constraint-damping" behaviour, so that any constraint violations decay as the evolution progresses. For example, the Z4 formulation was extended by Gundlach et al. [62], in which additional terms were added which dampen any constraint violations. The evolution system of Lindblom et al. [90] also has built in constraint-damping behaviour.

Once a suitable formulation of the Einstein field equations has been obtained, the equations must be discretized in order to be programmed into a computer. The most common method is the "finite difference technique" [64]. Here the spatial domain is covered by a discrete grid and differential operators are translated into finite differences using Taylor expansions. The majority of numerical relativity simulations use the finite difference method (for example, some recent simulations of black holes [4] and Brill waves [113] have successfully implemented the technique).

An alternative discretization method is to expand the numerical solution in terms of a given set of basis functions, typically using a fast Fourier transform. These techniques are known as "spectral methods". They have excellent stability and error properties, but compared to the finite difference method they do not cope well with shocks and non-smooth data. For an up-to-date and comprehensive review of spectral methods in numerical relativity, we refer the reader to the article by Grandclément et al. [60].

In order to increase numerical accuracy with a minimal increase in computational cost, many numerical relativity groups now use "adaptive mesh refinement" (AMR) algorithms. The resolution of the computational grid is altered dynamically as the evolution progresses. A finer grid is used in areas where the solution is highly oscillatory in nature or contains interesting features, and a coarser grid is used when the solution has fewer such features. Adaptive

mesh refinement was originally devised by the computational physics community [11–13]. It was first implemented in numerical relativity by Choptuik [28].

Finally in this section, we discuss singularities and horizons in numerical relativity. Most black hole simulations are only concerned with the region of spacetime outside the event horizon. Since the interior of the horizon is not causally connected to the exterior, it is possible in principle to remove this region from any numerical simulation without affecting the resulting solution. This process is known as "excision", and requires the event horizon to be accurately tracked during the evolution. Various methods have been devised to locate event and apparent horizons numerically [144].

The excision process is not applicable to spacetimes containing naked singularities or to simulations of the interior of an event horizon. In these cases the singularities must be dealt with explicitly [10].

1.3 Outer Boundary Conditions in Numerical Relativity

The Cauchy problem is defined on a spatially unbounded domain. This poses a severe problem for numerical relativists, since computers do not have the luxury of an unbounded domain. The standard approach is to truncate the spacetime $\mathcal{M}$ by considering the Cauchy problem on a "computational domain" $\Omega \in \mathcal{M}$, with an artificial boundary $\partial\Omega$. There are however some alternative approaches, which we briefly review below.

Rather than truncating the spatial domain, it is possible to compactify spatial infinity, so that the entire domain is mapped into a finite region [51]. The resulting Cauchy problem can then be solved numerically. Recent numerical studies [29, 108] have successfully implemented this technique. However, the disadvantage of this approach is the loss of resolution in the far-field region.

Alternatively, if hyperboloidal slices are used to foliate the spacetime (this is known as the hyperboloidal initial value problem), then null infinity can be compactified instead [48]. The theoretical study of Moncrief & Rinne [94] suggests that this may be a fruitful area of research, circumventing the bound-

ary condition problem. For a more detailed review of the Penrose conformal approach and its applications in numerical relativity see [47].

Another alternative to truncating the spatial domain is "Cauchy-characteristic matching". The need for an artificial boundary is eliminated by "matching" the Cauchy evolution to a characteristic evolution, in which the radiated waveform can be calculated at null infinity [147]. The technique combines the best features of characteristic and Cauchy evolutions. To date, however, stability issues have prevented this technique from being implemented in fully nonlinear three-dimensional numerical relativity simulations.

This thesis is concerned with the standard technique in which an artificial boundary $\partial\Omega$ is introduced. In order for the Cauchy evolution to be well defined, *outer boundary conditions* must be imposed on $\partial\Omega$. Obtaining appropriate boundary conditions is one of the outstanding problems in numerical relativity.

Outer boundary conditions must have the following properties.

(i) The resulting initial boundary value problem should be well-posed (see §1.2).

(ii) They should be constraint-preserving — constraint violations must not be introduced on the boundary.

(iii) They should be *absorbing*. The boundary conditions should mirror as closely as possible the physical problem on the spatially unbounded domain.

The goal of this thesis is to address the third item above.

The concept of absorbing boundary conditions is best understood by considering gravitational radiation. An astrophysical event such as the coalescence of two black holes will produce gravitational radiation that will propagate outwards towards $\partial\Omega$. The outer boundary conditions should allow all such radiation to pass through the boundary without introducing any spurious incoming radiation into Ω by reflection of the outgoing radiation off $\partial\Omega$. Spurious incoming radiation would significantly alter any gravitational waveform templates produced by the numerical evolution.

In the far-field region, it is reasonable to suppose that gravitational radiation is weak and that the spacetime geometry can accurately be described by

a linear perturbation about a known background. Typically then, a solution in the far field will consist of

(i) outgoing linearized gravitational waves originating from the source in the near-field region,
(ii) the effect on these waves of the background Weyl curvature (this effect will be made precise later),
(iii) incoming linearized gravitational waves caused by the reflection of outgoing waves off $\partial\Omega$.

On a Minkowski background there is no Weyl curvature. Absorbing boundary conditions should therefore remove all reflected, incoming radiation whilst remaining transparent to outgoing radiation. However, on a curved background the notions of "incoming" and "outgoing" radiation are less clear. The effect of the Weyl curvature on the propagation of gravitational waves must be taken into consideration when formulating boundary conditions.

The boundary condition problem can then be divided into two parts. The first is the study of gravitational radiation. What is meant by "incoming" and "outgoing" radiation? How can we use these definitions to formulate absorbing boundary conditions? Secondly there is the problem of "wave extraction". How do we obtain the radiative parts of the solution from a numerically calculated metric, so that the boundary conditions can actually be implemented? To motivate our approach to these problems we will first review some of the techniques currently in use by numerical relativity groups worldwide.

In the full nonlinear theory of general relativity, much is known about gravitational radiation. Bondi and his co-workers [18] considered asymptotic expansions of the vacuum field equations in the far-field region and were able to demonstrate that gravitational waves carry energy. They quantified this phenomenon by introducing the "news function" and the "Bondi mass" (see chapters 2 and 3). Newman & Unti [100] adopted a different approach. They used asymptotic expansions in the Newman-Penrose formalism of vacuum relativity [97, 98] to describe gravitational radiation in terms of the Weyl scalars.

Gravitational radiation has also been investigated using linear perturbations about fixed background spacetimes. For example Regge & Wheeler [111] and Zerilli [149] considered perturbations on a Schwarzschild background. This

work was later expressed in a gauge invariant form by Moncrief [93]. Nagar & Rezzolla [95] have produced a recent review of these results. One of the restrictions of linearized theory is that in general it is not known *a priori* which fixed background metric to choose. Nevertheless, the simplifications afforded by a perturbative approach prove to be very fruitful when formulating absorbing boundary conditions.

The investigations mentioned above all made use of very specific choices of coordinate chart and tetrad, cleverly constructed to enable theoretical results to be obtained. Similarly, the formulation of theoretically absorbing boundary conditions will require a careful choice of chart and tetrad. However, the charts and tetrads used in numerical relativity are chosen for completely different reasons (see e.g. [17]). How do we relate theoretical results in one chart to numerical results in another chart?

One approach is to seek gauge-invariant quantities which can be evaluated in any coordinate chart. In [9], for example, a scalar curvature invariant is found which vanishes in regions of spacetime which are free of gravitational radiation. This idea has since been implemented numerically [25]. Although they are chart-independent, such quantities are often tetrad-dependent. For instance, the scalar invariant above uses a *Kinnersley frame* [79]. By constructing a so called *quasi*-Kinnersley frame which approximates the background Kinnersley frame when the spacetime is modelled as a perturbation about a Kerr geometry, Nerozzi et al. [8, 96] have demonstrated how to construct such scalar invariants numerically.

Although there has been some success using quasi-Kinnersley frames, the technique has some drawbacks. A perturbative approach only enables weak field calculations to be performed. Furthermore a Kinnersley frame is not the most natural frame in which to study gravitational radiation. These limitations are found in many other studies of wave extraction methods in numerical relativity (see, for example, [121] in which recent results on wave extraction techniques were collated, all of which are only valid perturbatively and require the numerical relativist to make an appropriate choice of tetrad). A more desirable approach would be to describe gravitational radiation in terms of gauge-invariant quantities in a Bondi-type frame, and to find a way of expressing such quantities in terms of the metric variables in a typical numerical chart.

Our approach to wave extraction (chapters 2 and 3) is motivated by the desire to evaluate useful gauge-invariant quantities (such as the Bondi mass or the Weyl scalars) in the full nonlinear theory of relativity, in a numerical chart. The investigations of Bondi et al. [18] and Newman & Unti [100] suggest that a method based on asymptotic expansions in an asymptotically flat spacetime may be successful. This approach will enable us to relate a chart and tetrad that might be used in numerical relativity to the Bondi chart and tetrad in which gravitational radiation is best understood. The Weyl scalars in a Bondi frame can then be expressed purely in terms of the metric variables in the numerical chart. The use of asymptotic expansions will allow us to remain in the full nonlinear theory of relativity and will highlight the limitations of working in linearized theory.

Absorbing boundary conditions were first investigated by the computational physics community. In 1980 Bayliss & Turkel [7] constructed a sequence of absorbing boundary conditions for wave-like equations, with each boundary condition in the hierarchy accurate to higher order than the previous one. More recently, stable numerical implementations of these boundary conditions have been obtained [66,67]. Higdon [73] adopted a different approach, in which discrete boundary conditions for the finite difference approximation to the wave equation were found. Sequences of Bayliss & Turkel-type boundary conditions typically involve high radial derivatives, which are difficult to estimate numerically. By defining a sequence of *auxiliary variables* on $\partial\Omega$ and expressing the boundary conditions in terms of these variables, the radial derivatives can be removed [54, 55, 68].

The construction of absorbing boundary conditions in numerical relativity is particularly difficult because the geometrical structure of the spacetime varies dynamically during the evolution. The standard way of dealing with this problem is to treat the spacetime near $\partial\Omega$ as a linear perturbation about a known background. In the far-field region, this is a valid approximation but, as we will see in chapter 3, it is nevertheless important to understand the limitations of the perturbative approach.

As a first approximation when constructing absorbing boundary conditions, one can "freeze" the value of the Weyl scalar Ψ_0 (which, in linearized theory, is dominated by incoming radiation, as illustrated in chapter 5) on $\partial\Omega$ to its ini-

tial value [78,90,114,124]. The resulting boundary conditions, are not perfectly absorbing; they are known as "radiation-controlling" boundary conditions.

The first use of absorbing boundary conditions in numerical relativity appears to be by Novak & Bonazzola [101], who considered the scalar wave equation on a flat background. They obtained boundary conditions which are perfectly absorbing for quadrupole radiation on a Minkowski background. More recently, Buchman & Sarbach [22, 23] applied this idea to gravitational multipole radiation on a Schwarzschild background. They were able to incorporate the first order contribution from the mass parameter M into their boundary conditions. They analysed the initial boundary value problem for Einstein's field equations, treating the region near $\partial\Omega$ first as a perturbation about flat space and then as a perturbation about a Schwarzschild spacetime. By expanding the linearized Weyl tensor in terms of spherical tensor harmonics, a wave equation was obtained which admits sensible definitions of in- and out-going gravitational radiation. This enabled a hierarchy of boundary conditions $\mathcal{B}_L$ to be defined. The $\mathcal{B}_L$ are perfectly absorbing for gravitational modes with angular momentum number $l \leq L$, when applied to Ψ_0. The boundary condition $\mathcal{B}_1$ corresponds to the freezing Ψ_0 condition mentioned above.

As mentioned previously, due to the strict gauge choices that must be made in theoretical studies of gravitational radiation, boundary conditions are typically non-trivial to implement numerically. Ruiz et al. [122] showed that the boundary conditions of Buchman & Sarbach form a well-posed initial value problem. Recently, Rinne et al. [116] have taken this work further. The boundary conditions of Buchman & Sarbach were reformulated in terms of Regge-Wheeler-Zerilli scalars and imposed on the Einstein equations in harmonic gauge. To leading order on a Minkowski background, the boundary condition $\mathcal{B}_L$ was shown to be perfectly absorbing.

On a Schwarzschild background, the boundary conditions of Buchman & Sarbach are accurate to first order in M/R, where R is the radial coordinate. In principle, their calculation could be extended to second order. However, if the background spacetime is rotating (a Kerr background), then at second order, the angular momentum of the background will also contribute. At present their method cannot be applied to perturbations about a Kerr background.

Since it is dominated by incoming radiation near future null infinity, Ψ_0 would appear to be the natural gauge-invariant quantity on which to base

absorbing boundary conditions. However, in chapter 3 we will argue that Ψ_0 cannot be estimated accurately using linearized theory, since nonlinear effects arise in the leading order terms. Of the Weyl scalars, Ψ_4 can most accurately be obtained. However, we will show in chapter 5 that we would need to evaluate Ψ_4 to fifth order in order to use it in an absorbing boundary condition, since incoming radiation is not present in the lower order terms. This is unlikely to be possible numerically. Therefore a compromise is required. This can be achieved by formulating boundary conditions in terms of Ψ_2, in which incoming and outgoing radiation are on an equal footing. In chapter 3 we will show that the leading order term in Ψ_2 can be estimated using linearized theory.

The ultimate goal of this thesis is to obtain absorbing boundary conditions for Ψ_2, which take into account the mass and angular momentum of the background spacetime. Our approach is slightly different from that of Buchman & Sarbach. Whereas they started from the initial boundary value problem on a compact domain Ω, we will consider the propagation of linearized gravitational radiation near future null infinity. In [116], the Regge-Wheeler-Zerilli formalism was used to construct absorbing boundary conditions on a Minkowski background. It can also be used to construct boundary conditions on a Schwarzschild background [23]. However it cannot be used to describe perturbations on a Kerr background. Instead of the Regge-Wheeler-Zerilli formalism, the use of Hertz potentials will enable us to describe perturbations about Minkowski, Schwarzschild and Kerr backgrounds in a unified manner and obtain boundary conditions for gravitational radiation linearized about each of these backgrounds.

1.4 Outline of this Thesis

The aim of this thesis is to obtain absorbing boundary conditions for numerical relativity. Since these boundary conditions will be imposed in the far-field region, away from any gravitational sources, we begin with an investigation into the asymptotic behaviour of gravitational fields near future null infinity. This enables us to establish a link between the charts and tetrads used in the theoretical study of general relativity and those used in numerical relativity. Next we use Hertz potentials to describe linearized gravitational perturbations about known spacetime backgrounds. This enables us to obtain theoretically absorbing boundary conditions in a specific choice of chart and tetrad. Using the machinery developed earlier we are then able to express these boundary conditions in terms of the metric variables in a numerical chart.

In chapter 2 we use a Bondi-type coordinate system, with a careful choice of tetrad, to investigate the asymptotic behaviour of a gravitational field in the far-field region of an asymptotically flat spacetime. This enables us to obtain coordinate independent definitions of the Bondi mass and the news function. In chapter 3, we generalize these results by considering the asymptotic expansion of a chart and tetrad that might be used by a numerical relativist. The Weyl scalars, the Bondi mass and the news function can be expressed in terms of the metric variables in this chart and we are able to demonstrate how to transform from the theoretical chart into the numerical one. By working in the full nonlinear theory of relativity we are also able to investigate the limitations of linearized theory. We find that the leading order terms in Ψ_4, Ψ_3 and Ψ_2 can be evaluated in linearized theory but the leading order terms in Ψ_1 and Ψ_0 cannot. This suggests that absorbing boundary conditions derived within linearized theory should not be formulated in terms of Ψ_0 or Ψ_1.

Chapter 4 contains an introduction to Hertz potentials, which can be used to describe linearized gravitational perturbations about background spacetimes of Petrov type D. On a Minkowski background (chapter 5) the resulting field equations can be solved exactly. The solutions consist of "incoming" and "outgoing" radiative parts. We use these solutions to formulate absorbing boundary conditions for linearized gravitational fields on a flat background. We formulate a hierarchy of absorbing boundary conditions $\hat{O}_L$ for Ψ_2, which are very similar in form to the boundary conditions obtained by Bayliss &

Turkel [7], and are perfectly absorbing for gravitational waves with angular momentum number $l \leq L$.

In chapters 6 and 7, we generalize these results by considering linearized gravitational radiation on Schwarzschild and Kerr backgrounds respectively. Now, the non-vanishing Weyl curvature alters the propagation of the radiation. The field equations can no longer be solved explicitly, but the leading order behaviour in the region near future null infinity can be determined, and boundary conditions can be obtained. In the Schwarzschild case, our choice of coordinate chart results in logarithmic terms in the solution to the field equation. The resulting boundary conditions are rather cumbersome and unlikely to be useful for numerical relativity. A careful choice of coordinates in chapter 7 circumvents this problem and we obtain a sequence of absorbing boundary conditions for gravitational waves on a Kerr background, similar to the boundary conditions of Bayliss & Turkel. These boundary conditions are considerably simpler in form than those of chapter 6. Boundary conditions on a Schwarzschild background can therefore be obtained by taking the limit $a \to 0$, where a is the angular momentum parameter of the Kerr background.

In chapter 8 we express these boundary conditions in a chart that might be used by a numerical relativist. This is done in two stages. Firstly, we use the machinery of chapter 3 to evaluate Ψ_2 in terms of the metric variables in the numerical chart. Secondly, coordinate transformations are applied to the boundary conditions themselves to express them in the numerical chart.

1.5 Notation and Conventions

The Einstein summation convention is used for tensor indices, spinor indices and tetrad indices.

In general, a quantity with lower case indices is a tensor, e.g. R_{abcd}. These indices run over $0, 1, 2, 3$ unless otherwise stated. A quantity with upper case indices is a spinor, e.g. Ψ_{ABCD} (the use of spinors is confined to chapter 4). In addition, a dash ($'$) on the index and a bar (-) across the spinor denote its complex conjugate. Thus $\bar{o}^{A'}$ is the complex conjugate of o^A. Greek letters are used to denote tetrad indices. For example $e_\alpha{}^a$ is the a^{th} component of the tetrad vector e_α, and $R_{\alpha\beta} = R_{ab} e_\alpha{}^a e_\beta{}^b$ (the use of tetrad indices is confined to chapter 3 and appendix A.2).

Round brackets on the indices denote symmetrization and square brackets denote anti-symmetrization:

$$\begin{aligned} T_{(ab)} &= \frac{1}{2}(T_{ab} + T_{ba}), \\ T_{[ab]} &= \frac{1}{2}(T_{ab} - T_{ba}). \end{aligned} \tag{1.4}$$

Throughout this thesis we use a Lorentzian metric with signature $(+---)$. A comma (,) denotes partial differentiation, e.g. $f_{a,b}$. A semicolon (;) denotes covariant differentiation, e.g. $f_{a;b}$.

We use geometric units in which Newton's constant G and the speed of light c are both equal to 1 so that in Einstein's equations (1.1) we have $\kappa = 8\pi$.

Chapter 2

The Bondi Mass and the Outgoing Radiation Condition

In the latter part of this thesis, the propagation, in the far-field region, of gravitational waves linearized about various background spacetimes will be investigated, in order to obtain absorbing boundary conditions. However, general relativity is an intrinsically nonlinear theory. It is therefore important to understand the restrictions of linearized theory before using it. Hence we begin by investigating gravitational radiation in the full nonlinear theory of general relativity. In the far-field region, this is made possible by expanding the metric variables in powers of a dimensionless parameter $\epsilon = r_0/r$, where r is a suitable radial coordinate and r_0 is a suitable scale length. In the literature it is customary to set $r_0 = 1$.

The idea of making $1/r$ expansions in the asymptotic limit of spacetimes proves to be a particularly fruitful one. In chapter 3 it will be used to investigate the link between the specific charts chosen to simplify theoretical calculations and the charts and tetrads used in numerical relativity. The ability to move between theoretical and numerical charts and tetrads will enable us to obtain general formulae for quantities such as the Bondi mass and the news function in numerical relativity. Furthermore, it will allow us to formulate the boundary conditions derived in chapters 5, 6 and 7 in a numerical chart.

We start by reviewing the theoretical approach to gravitational radiation. It is widely believed that the region of spacetime far from an isolated gravitating body is, in some sense, asymptotically Minkowskian. Already in 1962

Bondi and his co-workers [18, 123] developed asymptotic expansions for the solution of the full nonlinear vacuum field equations, leading to a rigorous concept of gravitational radiation in the far-field. Soon afterwards Newman and Unti [100] produced an alternative version using the NP null tetrad formalism [97, 98]. A key ingredient in this and later work was the careful choice of a suitable coordinate chart involving a "retarded time" coordinate u. Both groups introduced a (u, r, θ, ϕ) chart, where θ and ϕ were spherical polar coordinates. They both developed asymptotic expansions as $r \to \infty$, holding the other coordinates fixed. Subsequent work by Penrose [103] showed that by a process of "conformal compactification", infinity could be adjoined to the spacetime manifold and then treated by standard methods. Most modern theoretical treatments use the Penrose conformal approach, and the "old-fashioned" chart-based approach has fallen out of fashion. However it is closer to what most numerical relativists are calculating, and for this reason we shall use it here.

The two groups used different u and r coordinates and different dependent variables. Bondi [18] chose a (u, r, θ, ϕ) chart where r was an area coordinate and θ and ϕ were standard spherical polar coordinates (see below). Their primary dependent variables were the metric components. Newman & Unti [100] produced an alternative version using a null "retarded time" coordinate u. Then the null vector $l^a = g^{ab}u_{,b}$ is geodesic and their coordinate r was chosen to be an affine parameter for the integral curves of l^a, along which the other three coordinates were fixed. Their primary dependent variables were the tetrad connection components and the tetrad components of the Weyl curvature tensor. The ten independent Weyl tensor components are usually described by five complex scalar functions Ψ_n where $n = 0, 1, \ldots, 4$. (For a covariant physical interpretation of the Weyl tensor see e.g. [140].)

Both groups were considering the limit $r \to \infty$ with the other coordinates fixed. In the Penrose geometrical picture [103] this region is called *future null infinity*. Of course both groups could have considered an "advanced time" coordinate v, where the corresponding limit is *past null infinity*. The Ψ_n in that case have similar properties and interpretations to Ψ_{4-n} near future null infinity.

If one wants to consider an isolated system with no extrinsic incoming radiation, then the natural place to impose this is past null infinity. However,

both groups looked for a condition to be imposed near future null infinity. Bondi [18] introduced an "outgoing radiation condition" which required the vanishing of certain terms in the asymptotic expansion of two of the metric components. This condition is stated more precisely below, and in §3.2. Newman & Unti [100] made a "peeling assumption": near future null infinity $\Psi_0 = O(r^{-5})$, and with this assumption they were able to demonstrate a so-called "peeling theorem": $\Psi_n = O(r^{n-5})$. Then $\Psi_4 = O(r^{-1})$ is interpreted as the leading term in the outgoing radiation. In the picture of Bondi et al. [18], the equivalent role is taken by the "Bondi news function" built from first derivatives of metric components. For a comparison of the conditions in the two schemes, showing that the outgoing radiation condition implies the peeling assumption see e.g. Valiente Kroon [81] and §3.4.

By reversing the direction of time, swapping advanced time for retarded time, one could carry out an almost identical study near past null infinity. There, assuming the analogous peeling condition, $\Psi_0 = O(r^{-1})$ is to be interpreted as the leading term in the extrinsic incoming radiation, and a natural "incoming radiation condition" near past null infinity would be $\Psi_4 = O(r^{-5})$.

Both the "outgoing radiation condition" and the "peeling assumption" do not actually preclude the presence of incoming radiation near future null infinity. Even within linearized theory the "peeling theorem" allows modest amounts of incoming radiation (see §5.3.3). Note that the outgoing radiation condition is in fact also a consistency condition on the type of asymptotic expansion that is used to describe the spacetime (see for example [30] and §3.5.1). Without it, logarithmic terms arise in the asymptotic expansions and so the $1/r$ expansion is no longer valid.

Bondi et al. [18] originally studied only axisymmetric spacetimes. These results were then generalized to non-axisymmetric spacetimes by Sachs [123]. Sachs wrote the metric in the form

$$\begin{aligned} ds^2 = &\left(\frac{V\mathrm{e}^{2\beta}}{r} + r^2 h_{AB}U^A U^B\right)\mathrm{d}u^2 - 2\mathrm{e}^{2\beta}\mathrm{d}u\mathrm{d}r \\ &- 2r^2 h_{AB}U^B \mathrm{d}x^A \mathrm{d}u + r^2 h_{AB}\mathrm{d}x^A \mathrm{d}x^B, \end{aligned} \tag{2.1}$$

where V, β, δ and γ are suitable functions of u, θ and ϕ, and

$$h_{AB} = \begin{pmatrix} \frac{1}{2}\left(\mathrm{e}^{2\gamma} + \mathrm{e}^{2\delta}\right) & \sin\theta \sinh(\gamma - \delta) \\ \sin\theta \sinh(\gamma - \delta) & \frac{1}{2}\sin^2\theta \left(\mathrm{e}^{-2\gamma} + \mathrm{e}^{-2\delta}\right) \end{pmatrix}. \tag{2.2}$$

The indices above run over θ and ϕ, so that $(x^\theta, x^\phi) = (\theta, \phi)$. The coordinate chart (u, r, θ, ϕ) will be defined more precisely later. The restriction to axisymmetry is obtained by removing the $\phi-$dependence from the metric variables and setting $\gamma = \delta$. Sachs found that the news function was now a complex valued scalar function of the coordinates.

The outgoing radiation condition can now be stated more precisely. It requires the vanishing of the $O(r^{-2})$ terms in the asymptotic expansions of γ and δ.

The Newman-Penrose formalism, used by Newman & Unti [100], casts the vacuum Einstein field equations into a manifestly chart-independent (but tetrad-dependent) form. Hence, a sensible first step, when working with gravitational radiation in numerical relativity, would be to express the results of Bondi et al. [18] in Newman-Penrose language. This was first done by Stewart [134], who expressed the Bondi mass and the news function in terms of the Newman-Penrose scalars and the Weyl scalars. However, the analogous calculation based on Sachs' approach (i.e. without axisymmetry) has never been performed. The aim of this chapter is to perform this calculation.

Stewart [134] started from the axisymmetric metric used by Bondi et al. [18], and chose a suitable Newman-Penrose (NP) tetrad. The leading order terms in Ψ_4, Ψ_3 and Ψ_2 were obtained, and the peeling property of the Weyl scalars was shown to hold. Furthermore the leading order terms of various NP scalars were calculated and formulae for the Bondi mass and the news function in terms of the Weyl scalars and the NP scalars were then obtained. A conformal transformation was made to show that these formulae were in agreement with the *Bondi-Sachs 4-momentum* defined at null infinity [105].

In §2.1 we apply Stewart's approach to a spacetime which is not necessarily axisymmetric, taking Sachs' form of the metric (2.1) as our starting point. It is found that, when the assumption of axisymmetry is relaxed, we are unable to estimate the leading order term in Ψ_2 without using higher order terms in the asymptotic expansions of the metric variables. In §2.2 these higher

order terms are introduced. This enables us to express the Bondi mass in terms of the NP scalars, confirming that the formulae obtained by Stewart [134] apply in non-axisymmetric spacetimes. We are also able to calculate the asymptotic behaviour of the Weyl scalars and explicitly demonstrate the relationship between the outgoing radiation condition and the Newman-Unti constraint $\Psi_0 = O(r^{-5})$. Imposing the Einstein field equations (i.e. demanding that the Ricci curvature vanishes) provides us with a set of constraints for the asymptotic expansions of the metric variables. Using these constraints, we are able to show that the outgoing radiation condition is in fact a necessary condition to avoid coordinate singularities at $\theta = 0$ or $\theta = \pi$ in our particular choice of chart.

The definitions of the Bondi mass and the news function derived in §2.2 are still only valid in the tetrad introduced in §2.1. Therefore, in §2.3 we investigate the effect of Lorentz transformations of the tetrad on these quantities. We find that under spins, boosts or null rotations about l, the formulae remain valid.

2.1 The Leading Order Calculation

We begin by introducing the framework used by Sachs [123]. Consider a space-time foliated by null hypersurfaces, labelled by $u = \text{const.}$, where u is a null coordinate. The null geodesic generators of these hypersurfaces are labelled by spherical polar coordinates (θ, ϕ). The coordinate r is a parameter along these geodesics, and is chosen so that the area element of the surface $u = \text{const.}$, $r = \text{const.}$ is $r^2 \mathrm{d}S$, where $\mathrm{d}S = \sin\theta \mathrm{d}\theta \mathrm{d}\phi$ is the area element of the unit sphere. In this section, capital Latin indices range over the θ and ϕ coordinates. The metric will be taken to be

$$\begin{aligned} \mathrm{d}s^2 = &\left(V\mathrm{e}^{2b} - r^2 h_{AB} U^A U^B\right) \mathrm{d}u^2 + 2\mathrm{e}^{2b} \mathrm{d}u\mathrm{d}r \\ &+ 2r^2 h_{AB} U^B \mathrm{d}x^A \mathrm{d}u - r^2 h_{AB} \mathrm{d}x^A \mathrm{d}x^B, \end{aligned} \tag{2.3}$$

where

$$h_{AB} = \begin{pmatrix} \frac{1}{2}\left(\mathrm{e}^{2g} + \mathrm{e}^{2d}\right) & \sin\theta \sinh(g-d) \\ \sin\theta \sinh(g-d) & \frac{1}{2}\sin^2\theta \left(\mathrm{e}^{-2g} + \mathrm{e}^{-2d}\right) \end{pmatrix},$$

and V, U^A, g, b and d are functions of the coordinates. Note that we have adopted a different signature from Sachs [123]. Furthermore, to avoid confusion when calculating the NP scalars, the β, γ and δ found in (2.1) have been replaced by b, g and d respectively, and V there has been replaced with rV here.

Sachs argued that the following conditions are sufficient for asymptotic flatness:

(i) the limit along a null geodesic generator (in our case $r \to \infty$ whilst u, θ and ϕ are held constant) exists (this is called future null infinity),
(ii) under such a limiting process $V \to 1$ and $rU^A, b, g, d \to 0$,
(iii) V, U^A, g, b and d can be expanded in powers of r^{-1}.

This motivates the following asymptotic expansions:

$$\begin{aligned} V &= 1 - 2Mr^{-1} + O(r^{-2}), & b &= b_2 r^{-2} + O(r^{-3}), \\ g &= g_1 r^{-1} + O(r^{-2}), & d &= d_1 r^{-1} + O(r^{-2}), \\ U^\theta &= U_2^\theta r^{-2} + O(r^{-3}), & U^\phi &= U_2^\phi r^{-2} + O(r^{-3}), \end{aligned} \tag{2.4}$$

where M, g_1, d_1, b_2, U_2^θ and U_2^ϕ are functions of u, θ and ϕ only. Note that one might expect b to contain a $O(r^{-1})$ term but this can be removed by a suitable coordinate transformation (as was done in [18]).

In the axisymmetric version of this calculation [134], $g = d$. Furthermore, the freedom in the origin of r was used to remove the $O(r^{-2})$ term in g. This idea will be revisited later. Here we use the freedom in the origin of r to eliminate the $O(r^{-2})$ term in $g + d$.

Using the asymptotic expansions listed above, and the Newman-Penrose tetrad

$$\begin{aligned} l^a &= \mathrm{e}^{-2b}\frac{\partial}{\partial r}, \\ n^a &= \frac{\partial}{\partial u} - \frac{1}{2}V\frac{\partial}{\partial r} + U^\theta\frac{\partial}{\partial \theta} + U^\phi\frac{\partial}{\partial \phi}, \\ m^a &= 2^{-1/2}r^{-1}h_{\theta\theta}^{-1/2}\left[(1 + ih_{\theta\phi}\csc\theta)\frac{\partial}{\partial \theta} - ih_{\theta\theta}\csc\theta\frac{\partial}{\partial \phi}\right], \end{aligned} \tag{2.5}$$

the NP scalars are found to be

$$\begin{aligned} \alpha &= -2^{-3/2}r^{-1}\cot\theta + O(r^{-2}), \\ \beta &= 2^{-3/2}r^{-1}\cot\theta + O(r^{-2}), \\ \gamma &= \frac{1}{4}i\partial_u(g_1 - d_1)r^{-1} + O(r^{-2}), \\ \epsilon &= -\frac{1}{4}i\partial_u(g_1 - d_1)r^{-2} + O(r^{-3}), \\ \lambda &= \frac{1}{2}\partial_u(g_1 + d_1)r^{-1} + \frac{1}{2}i\partial_u(g_1 - d_1)r^{-1} + O(r^{-2}), \\ \mu &= -\frac{1}{2}r^{-1} + \left(M + \frac{1}{2}\partial_\theta U_2^\theta + \frac{1}{2}\partial_\phi U_2^\phi + \frac{1}{2}U_2^\theta\cot\theta\right)r^{-2} + O(r^{-3}), \\ \pi &= -2^{-1/2}(U_2^\theta + iU_2^\phi\sin\theta)r^{-2} + O(r^{-3}), \\ \nu &= -2^{-1/2}(\partial_\theta M + i\partial_\phi M)r^{-2} + O(r^{-3}), \\ \rho &= -r^{-1} + 2b_2r^{-3} + O(r^{-4}), \\ \tau &= -2^{-1/2}(U_2^\theta - iU_2^\phi\sin\theta)r^{-2} + O(r^{-3}), \\ \kappa &= 0, \\ \sigma &= \frac{1}{2}(g_1 + d_1)r^{-2} - \frac{1}{2}i(g_1 - d_1)r^{-2} + O(r^{-3}). \end{aligned} \tag{2.6}$$

Since we are performing the calculation in the far-field region we will as-

sume that for large r we have a vacuum spacetime. We can therefore obtain constraints on the metric variables by demanding that the Ricci tensor vanishes (1.2). In the Newman-Penrose formalism this equates to demanding that the quantities Φ_{ij} (for $i,j = 0,1,2$) and Λ all vanish. We impose $\Phi_{ij} = 0$ and $\Lambda = 0$ at $O(r^{-1})$ and $O(r^{-2})$. This results in the following four independent constraint equations:

$$b_2 = -\frac{1}{8}(g_1^2 + d_1^2), \tag{2.7}$$

$$U_2^\theta = -(g_1 + d_1)\cot\theta - \frac{1}{2}\partial_\theta(g_1 + d_1) - \frac{1}{2}\partial_\phi(g_1 - d_1)\csc\theta, \tag{2.8}$$

$$\begin{aligned} U_2^\phi = &-(g_1 - d_1)\cot\theta\csc\theta \\ &-\frac{1}{2}\partial_\theta(g_1 - d_1)\csc\theta + \frac{1}{2}\partial_\phi(g_1 + d_1)\csc^2\theta, \end{aligned} \tag{2.9}$$

$$0 = \partial_u\left(2M + U_2^\theta\cot\theta + \partial_\theta U_2^\theta + \partial_\phi U_2^\phi\right) + (\partial_u g_1)^2 + (\partial_u d_1)^2. \tag{2.10}$$

As expected, all the metric variables are determined by the two functions g_1 and d_1. Thus we define the *Bondi news function*

$$\mathcal{N} = \frac{1}{2}\partial_u(g_1 + d_1) + \frac{1}{2}i\partial_u(g_1 - d_1), \tag{2.11}$$

which determines the leading order behaviour of the gravitational field as we approach future null infinity. The news function can be expressed in terms of an NP scalar:

$$\mathcal{N} = \lim_{r\to\infty} r\lambda. \tag{2.12}$$

Furthermore, on each hypersurface $u = \text{const.}$, we define the *Bondi mass* $M_B(u)$ by integrating over the sphere $r = \text{const.}$

$$4\pi M_B(u) = \lim_{r\to\infty}\int\int M(u,\theta,\phi)\mathrm{d}S. \tag{2.13}$$

Integrating the constraint (2.10) over the sphere (noting that several terms vanish upon integration) results in the standard mass loss formula

$$\begin{aligned} 4\pi\partial_u M_B(u) &= -\int\int |\mathcal{N}|^2\mathrm{d}S \\ &= -\lim_{r\to\infty}\int\int r^2|\lambda|^2\mathrm{d}S. \end{aligned} \tag{2.14}$$

This was first obtained for axisymmetric spacetimes by Bondi et al. [18] and subsequently by Sachs [123] for more general spacetimes. Here we have expressed the rate of mass loss in terms of NP scalars rather than the metric variables.

Following Stewart's calculation [134], we will attempt to express the Bondi mass in terms of a combination of the NP scalars and the Weyl scalar Ψ_2. However, the lack of axisymmetry causes problems. Because we have only used the leading order terms in the asymptotic expansions of the metric variables (2.4), the only information we can obtain about the Weyl scalars is

$$\begin{aligned}
\Psi_4 &= -\frac{1}{2}\left\{\partial_u^2(g_1+d_1)+\mathrm{i}\partial_u^2(g_1-d_1)\right\}r^{-1}+O(r^{-2}) \\
&= -\partial_u\mathcal{N}r^{-1}+O(r^{-2}), \\
\Psi_3 &= 2^{-1/2}\partial_u\left\{-\frac{1}{2}(g_1-d_1)+\frac{1}{2}\partial_\phi(g_1+d_1)\csc\theta\right. \\
&\quad -(g_1-d_1)\cot\theta+\frac{1}{2}U_2^\theta \\
&\quad +i\left[-\frac{1}{2}(g_1+d_1)-\frac{1}{2}\partial_\phi(g_1-d_1)\csc\theta\right. \\
&\quad \left.\left.-(g_1+d_1)\cot\theta+\frac{1}{2}U_2^\phi\sin\theta\right]\right\}r^{-2}+O(r^{-3}), \\
\Psi_2 &= O(r^{-3}), \\
\Psi_1 &= O(r^{-4}), \\
\Psi_0 &= O(r^{-4}).
\end{aligned} \tag{2.15}$$

We are unable to evaluate the leading order terms in Ψ_2, Ψ_1 or Ψ_0. This means that we are not able to find a definition for the Bondi mass in terms of Ψ_2, and we cannot investigate under what conditions the peeling property of the curvature might hold. In order to make further progress we must look at higher order terms in the expansions of the metric variables.

2.2 The Second Order Calculation

In order to investigate the asymptotic behaviour of the Weyl scalars we refine the $1/r$ expansions of the metric variables

$$\begin{aligned} V &= 1 - 2Mr^{-1} + M_2 r^{-2} + O(r^{-3}), & g &= g_1 r^{-1} + g_2 r^{-2} + g_3 r^{-3} + O(r^{-4}), \\ d &= d_1 r^{-1} - g_2 r^{-2} + d_3 r^{-3} + O(r^{-3}), & b &= b_2 r^{-2} + b_3 r^{-3} + O(r^{-4}), \\ U^\theta &= U_2^\theta r^{-2} + U_3^\theta r^{-3} + O(r^{-4}), & U^\phi &= U_2^\phi r^{-2} + U_3^\phi r^{-3} + O(r^{-4}). \end{aligned} \tag{2.16}$$

Recall that we have already chosen the origin of r such that the $O(r^{-2})$ term in $g + d$ vanishes, hence the presence of $-g_2 r^{-2}$ in the asymptotic expansion of d.

Calculating the Weyl scalars to second order is most easily done using a computer algebra package (the author used a *Reduce 3.8* script). Algorithms are available to facilitate such a process [26]. The asymptotic expansion of Ψ_2 is found to be

$$\Psi_2 = \Psi_2^{(3)} r^{-3} + O(r^{-4}), \tag{2.17}$$

where

$$\begin{aligned} \Psi_2^{(3)} = &- M + \frac{1}{6}(g_1 + d_1) - \frac{1}{3}(g_1 \partial_u g_1 + d_1 \partial_u d_1) - \frac{1}{4}\cot\theta\, \partial_\theta (g_1 + d_1) \\ &- \frac{1}{6}\partial_\phi (g_1 - d_1)\cot\theta \csc\theta - \frac{1}{12}\partial_\theta^2 (g_1 + d_1) - \frac{1}{6}\csc\theta\, \partial_{\theta\phi}^2 (g_1 - d_1) \\ &+ \frac{1}{12}\partial_\phi^2 (g_1 + d_1)\csc^2\theta - \frac{1}{6}(\partial_\theta U_2^\theta + \partial_\phi U_2^\phi + U_2^\theta \cot\theta) + \frac{2}{3}\partial_u b_2 \\ &+ \frac{1}{2} i \left[g_1 \partial_u d_1 - d_1 \partial_u g_1 + U_2^\phi \cos\theta + \sin\theta\, \partial_\theta U_2^\phi - \partial_\phi U_2^\theta \csc\theta \right]. \end{aligned} \tag{2.18}$$

Note that a very useful cancellation has occurred among the second order terms so that $\Psi_2^{(3)}$ only depends on the leading order terms in the expansions of the metric variables (2.16).

Stewart's definition of the Bondi mass in axisymmetry [134] involved the combination $\Psi_2 + \sigma\lambda$. Motivated by this, we calculate the $O(r^{-3})$ term in $\Psi_2 + \sigma\lambda$. Applying the constraints (2.7)-(2.9), integrating over the sphere (noting that the imaginary part of the integrand vanishes upon integration),

and using the definition of the Bondi mass (2.13), we obtain

$$4\pi M_B(u) = -\lim_{r\to\infty} \int\int r^3 \left(\Psi_2 + \sigma\lambda\right) \, \mathrm{d}S \tag{2.19}$$

$$= -\lim_{r\to\infty} \int\int \left(r^3\Psi_2 + r^2\sigma\mathcal{N}\right) \, \mathrm{d}S. \tag{2.20}$$

Therefore the formula for the Bondi mass in terms of NP and Weyl scalars, previously obtained for axisymmetric spacetimes, is also valid if the assumption of axisymmetry is relaxed. A conformal transformation (as was carried out in [134]) would show that these results are consistent with the Bondi-Sachs 4-momentum [105].

We now investigate the peeling property of the curvature. The Weyl scalar Ψ_0 is found to be

$$\Psi_0 = 2ig_2 r^{-4} + O(r^{-5}). \tag{2.21}$$

In order to obtain the standard peeling result, $\Psi_i = O(r^{i-5})$, we must therefore set $g_2 = 0$. This is precisely the same as imposing the outgoing radiation condition. Valiente Kroon [81] showed that in general the outgoing radiation condition implies that $\Psi_i = O(r^{i-5})$ but the converse is not necessarily true. However, for this particular choice of coordinate chart and tetrad, the outgoing radiation condition and the condition $\Psi_0 = O(r^{-5})$ are equivalent to each other and are necessary and sufficient for the peeling property of the Weyl curvature to hold.

At first glance, the results of the previous paragraph would seem to contradict Stewart's calculation [134], in which the peeling property of the curvature was obtained without imposing either of the two conditions mentioned above. However, the choice of r which removed the $O(r^{-2})$ terms in his g meant that the outgoing radiation was automatically satisfied, so there is no contradiction. Thus in the axisymmetric case, the outgoing radiation condition can be satisfied by a careful gauge choice. Any logarithmic terms that one might expect to arise in the asymptotic expansion are also removed by this choice of gauge. This is not true in the more general case considered in this chapter. Here it appears that the outgoing radiation condition (and therefore the removal of logarithmic terms in the asymptotic expansion) cannot automatically be satisfied by a choice of gauge.

By demanding that the Ricci curvature vanishes (so that the quantities Φ_{ij} and Λ vanish) and looking at higher order terms in $1/r$, we obtain further constraints on the additional variables defined in (2.16). Specifically, by demanding $\Phi_{20} \pm \Phi_{02} = 0$ and $\Phi_{10} = 0$ and using (2.7)-(2.9) to simplify the results, we obtain

$$\partial_u g_2 = 0, \tag{2.22}$$

$$\partial_\phi g_2 = 0, \tag{2.23}$$

$$\partial_\theta g_2 = -2 g_2 \cot\theta, \tag{2.24}$$

and we deduce

$$g_2 \propto \csc^2\theta. \tag{2.25}$$

Unless we impose the outgoing radiation condition $g_2 = 0$, the covariant form of the metric will contain coordinate singularities at $\theta = 0, \pi$. In our particular choice of chart, the outgoing radiation condition can therefore be interpreted as the condition that the covariant form of the metric on the unit $2-$sphere $r = \text{const.}$ $u = \text{const.}$ is well-behaved at $\theta = 0$ and $\theta = \pi$. Note, however, that the coordinate singularities at $\theta = 0$ and $\theta = \pi$ can easily be removed by a coordinate transformation.

2.3 Transformations of the Tetrad

The arguments presented in §2.2 are valid only in the tetrad (2.5). What happens to the formulae (2.12), (2.14) and (2.19) if we perform a change of tetrad (a Lorentz transformation) into a more general frame?

The most important characteristics of the tetrad (2.5) are that l^a is geodesic ($\kappa = 0$) and asymptotically affinely parameterized ($\epsilon + \bar{\epsilon} = O(r^{-3})$). We will consider only tetrad changes that preserve these properties. The behaviour of the NP scalars under spins, boosts and null rotations about l and n can be read off from appendix B of [135]. The following transformations preserve $\kappa = 0$ and $\epsilon + \bar{\epsilon} = 0$:

(i) a null rotation about l, by a complex parameter c

$$l \to l, \quad n \to n + cm + \bar{c}\bar{m} + c\bar{c}l, \quad m \to m + \bar{c}l, \tag{2.26}$$

(ii) a spin through an angle ψ

$$l \to l, \quad n \to n, \quad m \to e^{2i\psi}m, \tag{2.27}$$

(iii) a boost by the real parameter a, where $\partial_r a = 0$

$$l \to a^2 l, \quad n \to a^{-2}n, \quad m \to m. \tag{2.28}$$

Under a null rotation c about l, the scalars Ψ_2, λ and σ transform in the following way:

$$\begin{aligned} \Psi_2 &\to \Psi_2 + 2c\Psi_1 + c^2\Psi_0, \\ \lambda &\to \lambda + c\pi + 2c\alpha + c^2(\rho + 2\epsilon) + c^3\kappa + cl^a c_{;a} + \bar{m}^a c_{;a}, \\ \sigma &\to \sigma + \bar{c}\kappa. \end{aligned} \tag{2.29}$$

Under a spin ψ and a boost a

$$\begin{aligned} \Psi_2 &\to \Psi_2, \\ \lambda &\to a^{-2}e^{-4i\psi}\lambda, \\ \sigma &\to a^2 e^{4i\psi}\sigma. \end{aligned} \tag{2.30}$$

Consider first the Bondi mass (2.19). Under spins and boosts, the integrand in (2.19) is unchanged. We expect that $c = O(r^{-1})$ as $r \to \infty$. Then we find that under a null rotation about l, the leading order term in $\Psi_2 + \sigma\lambda$ is invariant and hence the right hand side of (2.19) is unchanged.

Consider now the news function, defined by (2.12). Under a null rotation about l, with $c = O(r^{-1})$ as $r \to \infty$, the leading order term in λ will be unchanged and so $\mathcal{N}$ will be invariant. Under a spin through an angle ψ, the news will undergo a phase shift of $e^{-4i\psi}$. Under a boost a, the news will be scaled by a factor of a^{-2}. This is not unexpected, since l is also scaled, $l \to a^2 l$.

Finally we discuss the mass loss formula (2.14). Under a null rotation about l, if we once again demand that $c = O(r^{-1})$ as $r \to \infty$, then the leading order term in λ is unchanged and so the integrand in (2.14) is invariant. Under a spin through an angle ψ, there is the phase shift $\lambda \to e^{-4i\psi}\lambda$. Again, the integrand in (2.14) is unchanged. Finally under a boost, $\lambda \to a^{-2}\lambda$, the integrand will scale by a factor of a^{-4}. This is expected, since $l_a = (\mathrm{d}u)_a$ and so the left-hand side of (2.14) undergoes a similar transformation. We conclude that the mass loss formula (2.14) remains valid under the spins, boosts and null rotations of the tetrad that were considered above.

In summary, the Bondi mass, the news function and the rate of mass loss are quantities which can be defined in terms of the Newman-Penrose scalars and the Weyl scalars by (2.19), (2.12) and (2.14) respectively. The Newman-Penrose scalars are evaluated in a very specific *Bondi tetrad*. If we perform a Lorentz transformation of the tetrad which preserves the direction of l, then the formulae (2.12), (2.14) and (2.19) will still apply when evaluated using the NP scalars in the "new" frame, although the news function may undergo a phase shift. In §3.4 we will extend this discussion to consider null rotations about n.

2.4 Some Preliminary Conclusions

The main results of this chapter are as follows.

(i) The expressions for the news function and the Bondi mass in terms of the Weyl scalars and the Newman-Penrose scalars in an axisymmetric spacetime [134] can be generalized to a non-axisymmetric spacetime, but extra terms in the asymptotic expansions of the metric variables are required in order to perform the calculation. The expressions for the Bondi mass (2.19), the rate of mass loss (2.14) and the news function (2.12) remain valid under spins, boosts and null rotations about l (although the news function will undergo a phase shift associated with the spin).

(ii) The Bondi mass, the news function and the Weyl scalars Ψ_4, Ψ_3, Ψ_2 only depend on the leading order terms in the $1/r$ expansions of the metric variables. This lends credence to the idea that a numerical relativist might be able to accurately calculate these quantities.

(iii) We have a clear illustration of Valiente Kroon's result [81] on the relationship between the outgoing radiation condition and the condition $\Psi_0 = O(r^{-5})$. In the chart and tetrad used in this chapter, the conditions are equivalent to each other and are necessary and sufficient for peeling to occur.

(iv) In our particular choice of coordinate chart, the outgoing radiation condition is a necessary condition to avoid coordinate singularities in the covariant form of the metric at $\theta = 0$ and $\theta = \pi$ (although these singularities can be removed by a coordinate transformation).

The results of this chapter are still of limited use in numerical relativity. We have taken a first step in linking theoretical studies of gravitational radiation with numerical studies, by obtaining definitions of the Bondi mass and the news function in terms of the Newman-Penrose and Weyl scalars. However these definitions still require a careful choice of tetrad, and it is still not obvious how to evaluate such quantities in numerical relativity. Furthermore, the limitations of linearized theory remain unclear. Chapter 3 examines these problems in more detail.

Chapter 3

Numerical Relativity and Asymptotic Flatness

In this chapter [40], we investigate the link between theoretical studies of gravitational radiation (such as the study in chapter §2) and numerical relativity.

In recent years, researchers have expended considerable effort on the numerical evolution of asymptotically flat spacetimes. A minority of researchers have adopted the Penrose conformal approach, but most have chosen to evolve the spacetime as far out (both in space and time) as is feasible, truncating the spatial domain with an artificial boundary $\partial\Omega$ (see §1.3). Then some matching process is required to interpret their numerical data in the Bondi or Newman-Unti pictures in which gravitational radiation is best understood. This, the goal of this chapter, turns out to be far from trivial. The choice of a coordinate chart is an intrinsic part of the numerical evolution and the final data are available only in this chosen chart. Each numerical relativity group has its own favoured chart or charts and they usually bear little resemblance to the Bondi or Newman-Unti ones. Furthermore the numerical data do not contain complete information because the inevitable occurrence of numerical errors will corrupt the values of higher derivatives—from it one can construct reliably only a few leading terms in the asymptotic expansions[1].

[1]Consider an asymptotic expansion, as $r \to \infty$,

$$f(r) = f_0 + f_1 r^{-1} + f_2 r^{-2} + \dots .$$

We interpret this as the Taylor series for $f(q)$ about $q = 0$, where $q = r^{-1}$. Then the f_n are, up to numerical factors, the n^{th}-derivatives of f with respect to q, evaluated at $q = 0$.

The usual approach adopted by numerical relativists is to argue that, far from the isolated source, the gravitational field is weak, and so linearized theory can be used to match the numerical and the Bondi or Newman-Unti pictures. Bondi argued strongly against such an approximation, pointing out the fundamental nonlinearity of general relativity. Even if plausible arguments in its favour could be found, linearization carries its own difficulties. The first is that, in a non-compactified spacetime, the matching process is a global one. Furthermore, given a spacetime, the choice of a simpler second spacetime of which the first can be considered a linearized perturbation, is not unambiguous. Even if such a choice could be justified, the transformation between the charts in the two spacetimes would not, in general, be smooth.

As a concrete example illustrating these points, consider the well-known Schwarzschild metric in the standard (t, r, θ, ϕ) chart

$$g^S_{ab} = \mathrm{diag}(F, -F^{-1}, -r^2, -r^2 \sin^2\theta), \tag{3.1}$$

where $F = 1 - 2M/r$. In the region where $r \gg 2M$ this might appear to be a small perturbation of Minkowski spacetime with metric

$$g^M_{ab} = \mathrm{diag}(1, -1, -r^2, -r^2 \sin^2\theta), \tag{3.2}$$

but this is deceptive. Consider the scalar wave equation $g^{ab}\Psi_{;ab} = 0$ on the two spacetimes. We would measure outgoing radiation at *future null infinity* by taking the limit $r \to \infty$ holding u constant, where u is a retarded time coordinate. Two standard choices for u are

$$u^M = t - r, \qquad u^S = t - r^*, \tag{3.3}$$

where

$$r^* = \int F^{-1}\,\mathrm{d}r = r + 2M \log\left|\frac{r}{2M} - 1\right| + \text{const.} \tag{3.4}$$

Thus

$$u^M = u^S + 2M \log\left|\frac{r}{2M} - 1\right| + \text{const.} \tag{3.5}$$

The Schwarzschild null infinity is given by $r \to \infty$ holding u^S constant, which implies $u^M \to \infty$. This is known as *future timelike infinity* for the Minkowski spacetime. Equivalently the Minkowski null infinity involves taking the limit

$r \to \infty$ with u^M constant, which corresponds to $r \to \infty$, with $u^S \to -\infty$. This is known as *spacelike infinity* for the Schwarzschild spacetime. Thus the limits in the two charts are different. This happens because of the global nature of the limiting process.

In order to achieve comparable limiting processes we need to redefine the two charts. Here, both spacetimes are static and so it is simplest to retain the t-coordinate. Suppose we invert (for $r > 2M$) the relation (3.4), $r^* = r^*(r)$ giving $r = r(r^*)$ and introduce a new chart (t, r^*, θ, ϕ). Then the Schwarzschild line element (3.1) becomes

$$g^S_{ab} = \mathrm{diag}(F, -F, -r^2, -r^2 \sin^2\theta). \tag{3.6}$$

Using the same chart the Minkowski line element is

$$g^M_{ab} = \mathrm{diag}(1, -1, -r^2, -r^2 \sin^2\theta). \tag{3.7}$$

Now the two metrics (3.6) and (3.7) are not only small perturbations of each other (for large r^*), but they share the same causal structure, $u = t - r^*$ in both cases. (There are of course many other ways of doing this, e.g. retain the r's and change the t's, which is the approach to be adopted in this chapter.) Note also the appearance of logarithms, which means that the transformations are not smooth.

The purpose of this chapter is to examine in more detail these issues from the point of view of the numerical relativist. In §3.1 we state what information we believe is available in a typical numerical evolution, and we assume that this information is expressed in terms of a given chart $X^a = (T, R, \Theta, \Phi)$ which is asymptotically Minkowskian. Section 3.2 addresses the construction of an approximate Bondi-like chart $x^a = (u, r, \theta, \phi)$ using this information. This circumvents the problem referred to above. We write down here the explicit form of the Bondi et al. outgoing radiation condition. We introduce a Newman-Penrose (NP) tetrad [97] adapted to the problem by Newman & Unti [100] in §3.3. At leading order this is the usual NP tetrad for Minkowski spacetime. At each order, r^{-1}, r^{-2}, ..., there are 16 real coefficients describing the tetrad. However from §3.2 we know that only 10 coefficients are needed to describe the metric. There are six coefficients which describe an infinitesimal Lorentz transformation at each order, and, for the moment, we do not make a particular

choice for them.

In §3.4 we obtain the asymptotic solution of the full nonlinear vacuum Einstein equations. The vanishing of the Ricci curvature provides us with constraints on the metric variables in a similar manner to §2.1 and §2.2. As we obtain the asymptotic solution of the field equations, we fine-tune our chart and NP tetrad to make them closer to those of Bondi et al. and Newman-Unti. Once we have set the Ricci curvature, to the best of our abilities, to zero, we turn to the Weyl curvature described by the Weyl scalars Ψ_n referred to earlier. We find that $\Psi_n = O(r^{n-5})$ for $n = 4, 3, 2, 1$, but $\Psi_0 = O(r^{-4})$, which would appear to violate the Newman-Unti peeling assumption. However using the information gleaned from solving the vacuum field equations and the fine-tuning of the chart and tetrad, we can show that the Bondi outgoing radiation condition implies the Newman-Unti peeling condition so that the peeling theorem then holds. These results are consistent with those of the previous chapter.

The bad news is that the leading order terms in the Weyl scalars $\Psi_0 = O(r^{-5})$ and $\Psi_1 = O(r^{-4})$ cannot be estimated using the information we judge to be available from the numerical data in §3.1. Although these scalars can be computed in linearized theory, the results would appear to be inconsistent with the full nonlinear theory of relativity near future null infinity.

The good news is that we can compute the leading terms in $\Psi_4 = O(r^{-1})$, equivalent to the "Bondi news function" (and we can compute this scalar accurately within linearized theory). The same holds for $\Psi_3 = O(r^2)$, which involves nonlinear terms, but these can be removed by the fine-tuning process. We can also compute $\Psi_2 = O(r^{-3})$ which involves nonlinear terms in an essential way. This means that we can offer reliable estimates of the "Bondi mass" $M_B(u)$ of the isolated system[2], and its rate of decrease $\mathrm{d}M_B/\mathrm{d}u \leq 0$, presumably due to the radiation of energy, both manifestly inaccessible to linearized theory.

The final section §3.5 translates these results back into the X^a chart of §3.1 used by a typical numerical relativist. From her/his standpoint there is no need to go through the elaborate construction of a theoretical chart and NP

[2]The "Bondi mass" is of course the timelike component of a 4-vector and so frame dependent. But a numerical relativity evolution singles out a well-defined frame, and that is the one in which the mass is computed.

tetrad carried out in the intermediate sections. Instead, we offer "numerical relativity recipes" so that they can compute the key quantities referred to in the previous paragraph in their own preferred chart.

The key ideas in this chapter are at least forty years old, and one might ask why were these results not given before? The nonlinear calculations of [18], [123] and [100] were made possible by careful, clever, a priori choices of chart and tetrad. In this chapter, we have to start from more or less arbitrary choices and so the resulting expressions are horrendously complicated. In order to handle them accurately we have utilized a computer algebra system. We used *Reduce 3.8*. This choice reflected experience and knowledge of one particular computer algebra system, but used no features not available in some other systems.

3.1 The Numerical Data

Many numerical relativists might choose a quasi-spherical polar chart $X^a = (T, R, \Theta, \Phi)$ for the numerical evolution of the spacetime surrounding an isolated gravitational source. We could also define an associated quasi-Cartesian chart $Y^a = (T, X, Y, Z)$ where

$$X = R\sin\Theta\cos\Phi, \quad Y = R\sin\Theta\sin\Phi, \quad Z = R\cos\Theta.$$

We shall be interested in the limit $R \to \infty$. As stated this limit is meaningless unless we specify the behaviour of the other three coordinates under the limiting process, and we shall rectify this omission shortly. It proves very convenient to introduce the notation

$$O_n = O(R^{-n}) \text{ as } R \to \infty. \tag{3.8}$$

Our fundamental assumption is that the spacetime outside an isolated source is asymptotically Minkowskian, expressed by the idea that, as seen in the Y^a chart,

$$g_{ab} = \eta_{ab} + g^{(1)}_{ab}R^{-1} + g^{(2)}_{ab}R^{-2} + O_3, \tag{3.9}$$

where $\eta_{ab} = \text{diag}(1, -1, -1, -1)$ and the $g^{(n)}_{ab}$ are supposed to remain constant during the limiting process. Transforming from the Minkowskian chart to the spherical polar one we find that the metric components in the X^a chart look like

$$\begin{aligned}
g_{00} &= 1 + h_{00}R^{-1} + k_{00}R^{-2} + O_3,\\
g_{01} &= h_{01}R^{-1} + k_{01}R^{-2} + O_3,\\
g_{02} &= h_{02} + k_{02}R^{-1} + O_2,\\
g_{03} &= h_{03} + k_{03}R^{-1} + O_2,\\
g_{11} &= -1 + h_{11}R^{-1} + k_{11}R^{-2} + O_3,\\
g_{12} &= h_{12} + k_{12}R^{-1} + O_2,\\
g_{13} &= h_{13} + k_{13}R^{-1} + O_2,\\
g_{22} &= -R^2 + h_{22}R + k_{22} + O_1,\\
g_{23} &= h_{23}R + k_{23} + O_1,\\
g_{33} &= -R^2\sin^2\Theta + h_{33}R + k_{33} + O_1.
\end{aligned} \tag{3.10}$$

Here the functions $\{h_{ab}\}$ and $\{k_{ab}\}$ are required to remain constant during the limiting process.

We will also need the asymptotic form of the inverse metric g^{ab} which is readily obtained from the relation $g^{ac}g_{cb} = \delta^a{}_b$. We find

$$\begin{aligned}
g^{00} &= 1 + h^{00}R^{-1} + k^{00}R^{-2} + O_3, \\
g^{01} &= h^{01}R^{-1} + k^{01}R^{-2} + O_3, \\
g^{02} &= h^{02}R^{-2} + k^{02}R^{-3} + O_4, \\
g^{03} &= h^{03}R^{-2} + k^{03}R^{-3} + O_4, \\
g^{11} &= -1 + h^{11}R^{-1} + k^{11}R^{-2} + O_3, \\
g^{12} &= h^{12}R^{-2} + k^{12}R^{-3} + O_4, \\
g^{13} &= h^{13}R^{-2} + k^{13}R^{-3} + O_4, \\
g^{22} &= -R^{-2} + h^{22}R^{-3} + k^{22}R^{-4} + O_5, \\
g^{23} &= h^{23}R^{-3} + k^{23}R^{-4} + O_5, \\
g^{33} &= -R^{-2}\csc^2\Theta + h^{33}R^{-3} + k^{33}R^{-4} + O_5.
\end{aligned} \tag{3.11}$$

Explicit formulae for the h^{ab} and the k^{ab} are given by equations (A.1) and (A.2) in appendix A.1. At this level of approximation

$$g^{ac}g_{cb} = \delta^a{}_b + O_3.$$

A numerical evolution in which the dependent variables include both g_{ab} and $g_{ab,c}$ (usually called a "first order formulation") should produce accurate values for h_{ab} and its first derivatives, and for k_{ab}. Otherwise we assume that these variables are available for discrete ranges of T, Θ and Φ so that the corresponding derivatives can be estimated.

3.2 The Bondi Chart

Most of the theoretical work which has been done on outgoing gravitational radiation involves a "Bondi chart" (u, r, θ, ϕ) in which u is a retarded time coordinate (see e.g. [18], [97], [100] and chapter 2).

Here we take the viewpoint that the $X^a = (T, R, \Theta, \Phi)$ chart introduced in §3.1 is the fundamental one in which, ultimately, all numerical calculations will be performed. Starting from this chart we need to construct an $x^a = (u, r, \theta, \phi)$ one which has all the essential features of a Bondi chart. We start by studying the function $u(T, R, \Theta, \Phi)$.

Because u is a null coordinate it has to satisfy the *relativistic eikonal equation*

$$g^{ab}u_{,a}u_{,b} = 0. \tag{3.12}$$

This is a well-known nonlinear equation with four independent variables which is exceedingly difficult to solve with any generality. (Even the restriction of (3.12) to Minkowski spacetime leads to the surprisingly rich structure of light ray caustics, see e.g. [135].) Note that there is a "gauge freedom"—if u is a solution then so is $U(u)$ for any differentiable function U.

The standard procedure is to specify u on a spacelike hypersurface in spacetime, and then existence and local uniqueness of u is guaranteed by standard theorems. However, the standard procedure is of little utility in this context, for no obvious choice of data suggests itself, and so we adopt a different approach.

Consider first the special case of a Minkowski spacetime, where (3.12) can be rewritten as

$$(u_{,T})^2 - (u_{,R})^2 = R^{-2}\left[(u_{,\Theta})^2 + \csc^2\Theta(u_{,\Phi})^2\right] = O_2. \tag{3.13}$$

Suppose we look for spherically symmetric solutions $u = u(T, R)$. Setting $\omega = u_{,R}/u_{,T}$ in (3.13) we find $\omega^2 = 1$. Using the gauge freedom mentioned earlier we may impose $u_{,T} = 1$ to find

$$\mathrm{d}u = \mathrm{d}T \pm \mathrm{d}R,$$

which implies

$$u = T \pm R + \text{const.}$$

$T - R$ is called *retarded time* and $T + R$ is called *advanced time*.

Although the special case appears trivial it is the key to the general one. Within this paragraph only let the indices i, j range over $0, 1$ and let the indices I, J range over $2, 3$. Perusal of the display (3.11) shows that g^{ij} is O_0 while both g^{iJ} and g^{IJ} are O_2. Thus the eikonal equation takes the form

$$g^{ij} u_{,i} u_{,j} = O_2, \tag{3.14}$$

which should be compared with (3.13) above. As boundary conditions (as $R \to \infty$) we impose

$$u_{,T} = 1 + O_1, \qquad u_{,I} = O_1. \tag{3.15}$$

This means that the eikonal equation takes the form

$$g^{ij} u_{,i} u_{,j} = O_3, \tag{3.16}$$

which we can write as a quadratic equation for $\omega = u_{,R}/u_{,T}$. Choosing the sign appropriate for a retarded time coordinate, we find the solution

$$u_{,R} = -\left(1 + \frac{2m_1}{R} + \frac{2m_2}{R^2}\right) u_{,T} + O_3, \tag{3.17}$$

where

$$m_1 = -\frac{1}{4}(h_{00} + 2h_{01} + h_{11}), \tag{3.18}$$

and

$$\begin{aligned} m_2 = -\frac{1}{16}\big[&4k_{00} + 8k_{01} + 4k_{11} + (h_{00} - h_{11})^2 \\ &- 4(h_{00} + h_{01})^2 + 4(h_{02} + h_{12})^2 + 4(h_{03} + h_{13})^2 \csc^2\theta\big]. \end{aligned} \tag{3.19}$$

Thus

$$\mathrm{d}u = u_{,T}\,\mathrm{d}T - u_{,T}\left(1 + \frac{2m_1}{R} + \frac{2m_2}{R^2}\right)\mathrm{d}R + O_3. \tag{3.20}$$

We leave some freedom in u by setting

$$u_{,T} = 1 + \frac{q_1}{R} + \frac{q_2}{R^2} + O_3, \tag{3.21}$$

where q_1 and q_2 are R-independent functions. At the moment they are arbitrary. The requirement that the vacuum Einstein equations hold then determines inter alia q_1, see §3.4. In our calculation, q_2 is not used directly.

We need next to specify a radial coordinate $r = r(T, R, \Theta, \Phi)$. The simplest choice is $r = R$. This has the great practical advantage that $O_n = O(R^{-n}) = O(r^{-n})$. It could be argued that our choice of r is neither the Bondi area coordinate nor an affine parameter along the outgoing null rays as favoured by [100]. However, since both of those approaches are known to be essentially equivalent (see chapter 2), it would seem that the discussion is not sensitive to the precise choice of r.

Then (3.20) implies

$$\mathrm{d}T = \left(1 - \frac{q_1}{r} - \frac{q_2 - {q_1}^2}{r^2}\right) \mathrm{d}u + \left(1 + \frac{2m_1}{r} + \frac{2m_2}{r^2}\right) \mathrm{d}r + O_3, \tag{3.22}$$

and so

$$\left(\frac{\partial T}{\partial u}\right)_r = 1 - \frac{q_1}{r} - \frac{q_2 - {q_1}^2}{r^2} + O_3, \quad \left(\frac{\partial R}{\partial u}\right)_r = 0, \tag{3.23}$$

$$\left(\frac{\partial T}{\partial r}\right)_u = 1 + \frac{2m_1}{r} + \frac{2m_2}{r^2} + O_3, \quad \left(\frac{\partial R}{\partial r}\right)_u = 1. \tag{3.24}$$

Finally we consider the choice of angular coordinates $\theta = \theta(T, R, \Theta, \Phi)$ and $\phi = \phi(T, R, \Theta, \Phi)$. We shall require $\theta = \Theta + O_1$ and $\phi = \Phi + O_1$, and so the relations, being close to the identity, are invertible. It is more convenient to posit

$$\Theta = \theta + \frac{y_2}{r} + \frac{z_2}{r^2} + O_3, \qquad \Phi = \phi + \frac{y_3}{r} + \frac{z_3}{r^2} + O_3, \tag{3.25}$$

where the functions y_J and z_J do not depend on r but are otherwise arbitrary. Equations (3.25) are certainly consistent with the boundary conditions (3.15).

We can now specify the limiting process as $r \to \infty$ holding u, θ and ϕ constant. Thus we are regarding m_n, q_n, y_J, z_J, $\{h_{ab}\}$ and $\{k_{ab}\}$ as functions of u, θ and ϕ.

Because we know the Jacobian $(\partial X^a/\partial x^b)$ we can write down the metric components in the $x^a = (u, r, \theta, \phi)$ chart

$$\begin{aligned}
g_{00} &= 1 + a_{00}r^{-1} + b_{00}r^{-2} + O_3, \\
g_{01} &= 1 + a_{01}r^{-1} + b_{01}r^{-2} + O_3, \\
g_{02} &= -ry_{2,u} + a_{02} + b_{02}r^{-1} + O_2, \\
g_{03} &= -rz_{2,u}\sin^2\theta + a_{03} + b_{03}r^{-1} + O_2, \\
g_{11} &= a_{11}r^{-1} + b_{11}r^{-2} + O_3, \\
g_{12} &= a_{12} + b_{12}r^{-1} + O_2, \\
g_{13} &= a_{13} + b_{13}r^{-1} + O_2, \\
g_{22} &= -r^2 + a_{22}r + b_{22} + O_1, \\
g_{23} &= a_{23}r + b_{23} + O_1, \\
g_{33} &= -r^2\sin^2\theta + a_{33}r + b_{33} + O_1.
\end{aligned} \tag{3.26}$$

Two points should be noted here. Firstly the leading terms in g_{02} and g_{03}, if non-zero, would violate our notion of an asymptotically Minkowskian space-time, for they are not present in the standard Minkowski line element. Thus we need to impose the conditions or "constraints"

$$y_{2,u} = z_{2,u} = 0. \tag{3.27}$$

Explicit formulae for the a_{mn} in terms of the h_{mn}, q_1, m_1, y_2 and z_2 (after imposing (3.27)) are given as (A.3) in appendix A.1. We could also give explicit formulae for the b_{mn} in terms of $\{h_{mn}\}$, $\{k_{mn}\}$, q_n, m_n, y_n and z_n but they are rather lengthy, and are most easily generated using a computer algebra package.

Next recall that the u-coordinate was constructed as a solution of the eikonal equation (3.16). Thus, as seen in the (u, r, θ, ϕ) chart, $g^{00} = O_3$. This implies $g_{11} = O_2$ and so $a_{11} = 0$. One may verify this directly by comparing the explicit expression for a_{11} given in (A.3) with (3.18). We will show later that by making a suitable choice for y_2 and y_3, we can achieve $b_{11} = 0$ so that $g_{11} = O_3$ as expected.

We now have sufficient notation available to write down the "outgoing

radiation condition" of [18] as

$$a_{33} = -a_{22}\sin^2\theta, \qquad b_{33} = b_{22}\sin^2\theta, \qquad b_{23} = 0, \tag{3.28}$$

which we shall invoke later. The outgoing radiation condition is deduced by inspecting the real and imaginary parts of the O_4 term in Ψ_0 (3.55) and requiring that they vanish so that the peeling property holds.

3.3 The Newman-Penrose Tetrad

Since most recent studies of gravitational radiation use a Newman-Penrose null tetrad [97], we need to introduce one. The basics of tetrad formalisms are due to Schouten [129]. Many textbooks contain more readable, but often succinct accounts, and [27] chapter 1, section 7, is a good pedagogic compromise. With small, but necessary, changes in notation this is summarised in appendix A.2. The specialisation of this approach to the original NP formalism is given in [26]. It turns out that the calculations that we need to perform become surprisingly intricate, and so are most conveniently handled using a computer algebra system.

We use a tetrad of vectors ${e_\alpha}^a$ and the dual tetrad of covectors ${e^\alpha}_a$. (The tetrad indices are Greek characters and always occur first.) Tetrad indices are lowered and raised using $\epsilon_{\alpha\beta}$ and $\epsilon^{\alpha\beta}$ where

$$\epsilon_{\alpha\beta} = \epsilon^{\alpha\beta} = \begin{pmatrix} 0 & 1 & 0 & 0 \\ 1 & 0 & 0 & 0 \\ 0 & 0 & 0 & -1 \\ 0 & 0 & -1 & 0 \end{pmatrix}.$$

In NP notation we have

$$\begin{aligned} &{e^0}_a = l_a, \quad {e^1}_a = n_a, \quad {e^2}_a = m_a, \quad {e^3}_a = \overline{m}_a, \\ &{e_0}^a = n^a, \quad {e_1}^a = l^a, \quad {e_2}^a = -\overline{m}^a, \quad {e_3}^a = -m^a. \end{aligned} \tag{3.29}$$

(3.30)

We shall require that, to leading order, $l_a = u_{,a}$.

Setting $s = 2^{-1/2}$ we write the tetrads as[3]

[3]In our calculations we actually included one extra term in each of the asymptotic expansions below. E.g., the first component of ${e^0}_a$ was written as

$${e^0}_0 = 1 + c_{00}/r + d_{00}/r^2 + j_{00}/r^3 + O_4.$$

These "junk" terms show up in our expressions for the connection and curvature components. In any expression where a junk term occurs we regard all terms of that (and any higher order) as being junk, and not computable from the data described in section 3.1.

$$
\begin{aligned}
e^0{}_a &= (1 + c_{00}r^{-1} + d_{00}r^{-2} + O_3, \quad c_{01}r^{-1} + d_{01}r^{-2} + O_3, \\
&\qquad c_{02} + d_{02}r^{-1} + O_2, \quad c_{03} + d_{03}r^{-1} + O_2), \\
e^1{}_a &= (\tfrac{1}{2} + c_{10}r^{-1} + d_{10}r^{-2} + O_3, \quad 1 + c_{11}r^{-1} + d_{11}r^{-2} + O_3, \\
&\qquad c_{12} + d_{12}r^{-1} + O_2, \quad c_{13} + d_{13}r^{-1} + O_2), \\
e^2{}_a &= (c_{20}r^{-1} + d_{20}r^{-2} + O_3, \quad c_{21}r^{-1} + d_{21}r^{-2} + O_3, \\
&\qquad -sr + c_{22} + d_{02}r^{-1} + O_2, \quad isr\sin\theta + c_{23} + d_{23}r^{-1} + O_2), \\
e^3{}_a &= (c_{30}r^{-1} + d_{30}r^{-2} + O_3, \quad 1 + c_{31}r^{-1} + d_{31}/r^{-2} + O_3, \\
&\qquad -sr + c_{32} + d_{32}r^{-1} + O_2, \quad -isr\sin\theta + c_{33} + d_{33}r^{-1} + O_2),
\end{aligned}
\tag{3.31}
$$

and

$$
\begin{aligned}
e_0{}^a &= (1 + c^{00}r^{-1} + d^{00}r^{-2} + O_3, \quad -\tfrac{1}{2} + c^{01}r^{-1} + d^{01}r^{-2} + O_3, \\
&\qquad c^{02}r^{-2} + d^{02}r^{-3} + O_4, \quad c^{03}r^{-2} + d^{03}r^{-3} + O_4), \\
e_1{}^a &= (c^{10}r^{-1} + d^{10}r^{-2} + O_3, \quad 1 + c^{11}r^{-1} + d^{11}r^{-2} + O_3, \\
&\qquad c^{12}r^{-2} + d^{12}r^{-3} + O_4, \quad c^{13}r^{-2} + d^{13}r^{-3} + O_4), \\
e_2{}^a &= (c^{20}r^{-1} + d^{20}r^{-2} + O_3, \quad c^{21}r^{-1} + d^{21}r^{-2} + O_3, \\
&\qquad -sr^{-1} + c^{22}r^{-2} + d^{02}r^{-3} + O_4, \quad -is\csc\theta r^{-1} + c^{23}r^{-2} + d^{23}r^{-3} + O_4), \\
e_3{}^a &= (c^{30}r^{-1} + d^{30}r^{-2} + O_3, \quad 1 + c^{31}r^{-1} + d^{31}r^{-2} + O_3, \\
&\qquad -sr^{-1} + c^{32}r^{-2} + d^{32}r^{-3} + O_4, \quad is\csc\theta r^{-1} + c^{33}r^{-2} + d^{33}r^{-3} + O_4).
\end{aligned}
\tag{3.32}
$$

Each tetrad contains, at each order, 32 real coefficients. This is because, although c_{2n} and c_{3n} are complex, we also have $\overline{c_{2n}} = c_{3n}$ etc. The relation $e^\mu{}_a e_\nu{}^a = \delta^\mu{}_\nu$ allows one to determine the c^{mn} in terms of the c_{mn} and the d^{mn} in terms of the c_{mn} and the d_{mn}, reducing the number of unknowns, at each order, from 32 to 16. The first set of these is given as equation (A.4) in appendix A.1. The second set is rather lengthy and best generated using a computer algebra package.

We also have the relation $\epsilon_{\mu\nu}e^\mu{}_a e^\nu{}_b = g_{ab}$, and this enables us to determine $\{a_{mn}\}$ in terms of $\{c_{mn}\}$. Note that there are 10 real a_{mn} and 16 real c_{mn}. Given the tetrad, the metric is uniquely determined. But for a given metric there is a 6-parameter family of tetrads which give rise to it. They are of course Lorentz transformations of each other and the Lorentz group has 6

arbitrary parameters. We introduce 6 arbitrary first order Lorentz parameters $\alpha_m(u, \theta, \phi)$ and can determine the c_{mn} in terms of the a_{mn} and the α_m. There are many different ways of doing this, and one is written down explicitly as (A.5) in appendix A.1. We can of course write down the d_{mn} in terms of the a_{mn}, b_{mn}, α_m and extra second order Lorentz parameters β_m, but the expressions are rather lengthy and, once again, are best generated by computer algebra.

3.4 The Curvature Tensors

We now use the tetrads developed in §3.3 to evaluate the Ricci and Weyl curvature tensors using the algorithm outlined in appendix A.2. At each stage we convert all instances of $\{c^{mn}\}$ and $\{d^{mn}\}$ to instances of $\{c_{mn}\}$ and $\{d_{mn}\}$ using (A.4) and its second order analogue. Then we convert all instances of $\{c_{mn}\}$ and $\{d_{mn}\}$ to instances of the metric coefficients $\{a_{mn}\}$ and $\{b_{mn}\}$ using (A.5) and its second order analogue. These conversions are implicit and will not be mentioned explicitly again.

We start by looking at the Ricci tensor component $R_{11} = R_{ab}e_1{}^a e_1{}^b = R_{ab}l^a l^b$. We find

$$0 = R_{11} = a_{11,u}r^{-2} + O_3. \tag{3.33}$$

We chose our chart to ensure that u was approximately a null coordinate or equivalently $g^{00} = O_3$, or $g_{11} = O_1$. This means that we have to enforce $a_{11} = 0$, and so the leading order term in R_{11} vanishes. We look next at

$$0 = R_{01} = R_{ab}e_0{}^a e_1{}^b = R_{ab}n^a l^b = -\frac{1}{2}a_{11,uu}r^{-1} + O_2. \tag{3.34}$$

Again the leading order term vanishes automatically. Next consider

$$0 = R_{12}+R_{13} = -2sa_{12,u}r^{-2}+O_3, \qquad 0 = R_{12}-R_{13} = -2isa_{13,u}\csc\theta\, r^{-2}+O_3, \tag{3.35}$$

where $s = 2^{-1/2}$. We deduce that

$$a_{12,u} = a_{13,u} = 0. \tag{3.36}$$

Furthermore, we can compute

$$0 = R_{02}+R_{03} = sa_{12,uu}r^{-1}+O_2, \qquad 0 = R_{02}-R_{03} = isa_{13,uu}\csc\theta\, r^{-1}+O_2, \tag{3.37}$$

If we inspect R_{23} and use (3.36) we find

$$0 = R_{23} = \frac{1}{2}(a_{22,u} + a_{33,u}\csc^2\theta)r^{-2} + O_3, \tag{3.38}$$

and we deduce that

$$a_{22,u} + a_{33,u}\csc^2\theta = 0. \tag{3.39}$$

Next we compute

$$R_{00} = -\frac{1}{2}(a_{22,uu} + a_{33,uu}\csc^2\theta)r^{-1} + O_2, \tag{3.40}$$

and we see immediately from (3.39) that the leading term vanishes, and so this furnishes no new information. Finally, inspection of the leading O_2 terms in $R_{22} \pm R_{33}$ reveals that they vanish automatically because of $a_{11} = 0$, (3.36) and (3.39). Thus we have

$$R_{22} + R_{33} = O_3, \qquad R_{22} - R_{33} = O_3. \tag{3.41}$$

We have found, so far, that the conditions $a_{11} = 0$, (3.36) and (3.39) imply that R_{00}, R_{01}, R_{02} and R_{03} are O_2 while the other components are O_3.

At this point we need to examine (3.36) more closely. Using (A.3) we have

$$(h_{02} + h_{12} + y_2)_{,u} = 0 \qquad (h_{03} + h_{13} + z_2\sin^2\theta)_{,u} = 0. \tag{3.42}$$

Now we know that the functions y_2 and z_2 are arbitrary, apart form the constraints (3.27), and so (3.42) implies

$$(h_{02} + h_{12})_{,u} = 0 \qquad (h_{03} + h_{13})_{,u} = 0. \tag{3.43}$$

We may therefore choose, consistent with the constraints (3.27),

$$y_2 = -(h_{02} + h_{12}), \qquad z_2 = -(h_{03} + h_{13})\csc^2\theta, \tag{3.44}$$

which, using (A.3), sets

$$a_{12} = a_{13} = 0. \tag{3.45}$$

The choice (3.44) has an added advantage that if we now express b_{11} in terms of the h_{ab}, k_{ab}, m_1 and m_2, y_2 and z_2 we find that $b_{11} = 0$, so that $g_{11} = O_3$. At the same time we can examine b_{12} and b_{13} which are linear in y_3 and z_3 respectively. By choosing y_3 and z_3 appropriately we may arrange $b_{12} = b_{13} = 0$.

This is a convenient point at which to examine the choice of a specific Lorentz transformation. In our tetrad, this is determined at leading order by the parameters α_n (see (A.5)). Newman & Penrose [97] chose u to be a null

coordinate, $g^{ab}u_{,a}u_b = 0$, and also chose $l_a = u_{,a}$. For a symmetric connection, it follows easily that $l^a{}_{;b}l^b = 0$. Even if we set $l_a = f(x^c)u_{,a}$ we find that $l^a{}_{;b}l^b$ is proportional to l^a so that we still have a null geodesic, albeit not necessarily an affinely parameterized one. The rest of this paragraph relies on some details of the Newman-Penrose formalism which can be checked swiftly using, for example, appendix B of [135]. Within the NP formalism

$$l^a{}_{;b}l^b = (\epsilon + \overline{\epsilon})l^a - \bar{\kappa}m^a - \kappa\overline{m}^a, \tag{3.46}$$

where κ and ϵ are NP spin coefficients defined below. Now our coordinate u is only approximately null, and our covector l_a is only approximately its gradient. Here $\kappa = m^a l^b l_{a;b} = \gamma_{131}$ (using the notation of appendix A.2) turns out to be O_3. However if we choose $\alpha_4 = \alpha_5 = \beta_4 = \beta_5 = 0$, and anticipate $a_{01} = 0$ (see next paragraph), we obtain $\kappa = O_4$. Also $\epsilon + \overline{\epsilon} = n^a l^b l_{a;b} = \gamma_{011}$ is O_2, but if we choose $\alpha_1 = 0$, then we find $\epsilon + \overline{\epsilon}$ is O_3. We also find $\tau = \gamma_{130} = (\alpha_2 + i\alpha_3)r^{-2} + O_3$. If we impose $\alpha_2 = \alpha_3 = 0$ then $\tau = O_3$. At this stage we also choose $\alpha_6 = \beta_6 = 0$ for reasons given below.

Now we need to examine each of the remainder (next order) terms in (3.33), (3.34), (3.35), (3.37), (3.38), (3.40) and (3.41). For example, we now find that the O_3 terms in R_{11} vanish if and only if we set $a_{01} = 0$, and then $R_{11} = O_4$. This also implies that the O_2 terms in R_{01} vanish, so that $R_{01} = O_3$. We already established that $R_{12} \pm R_{13} = O_3$. Setting the leading order terms to zero furnishes expressions for a_{02} and a_{03} which we use for subsequent simplifications. Now $R_{12} \pm R_{13} = O_4$. We find then that our previous estimate (3.37) refines to $R_{02} \pm R_{03} = O_3$. We also need to refine our estimate (3.38) to $R_{23} = O_4$. We find $R_{22} \pm R_{33} = O_3$, where both O_3 terms deliver the same relation relating the u-derivatives of a_{22}, a_{23}, a_{33} and b_{22}, b_{23}, b_{33} which we save for later use. In deriving this result we had to choose $\alpha_6 = \beta_6 = 0$ and to impose the Bondi outgoing radiation condition (3.28). Then $R_{22} \pm R_{33} = O_4$. Next we re-examine (3.40). The leading O_2 term gives us an expression for $a_{00,u}$ which we store for later use. Now $R_{00} = O_3$. We have found, so far, that R_{00}, R_{01}, R_{02} and R_{03} are O_2 while the other components are O_3.

We now try to repeat the procedure of the previous paragraph. However we find that the O_4 contribution in R_{11} contains "junk" terms, i.e., terms which involve the third order metric components which we have not been including; see the footnote in §3.3. Thus we can obtain no further information from the

vacuum field equation $R_{11} = 0$. Similarly we find that the O_3 terms in R_{01} contain junk, as do the O_4 terms in $R_{12} \pm R_{13}$. The same applies to the O_3 terms in $R_{02} \pm R_{03}$, the O_4 terms in R_{23} and $R_{22} \pm R_{33}$, and finally the O_3 terms in R_{00}. We have therefore exhausted the information available from the vacuum field equations.

Assuming that we have a vacuum, we can now switch our attention to the Weyl tensor, and we compute first

$$\Psi_4 = R_{0202} = \left[\frac{1}{4}(a_{22,uu} - a_{33,uu}\csc^2\theta) + \frac{1}{2}ia_{23,uu}\csc\theta\right] r^{-1} + O_2. \tag{3.47}$$

Using (3.39), we may rewrite this as

$$\Psi_4 = \mathcal{N}_{,u} r^{-1} + O_2, \tag{3.48}$$

where

$$\mathcal{N} = \frac{1}{2}(a_{22} + ia_{23}\csc\theta)_{,u} \tag{3.49}$$

is the *Bondi news function* (see [18] and chapter 2).

This is a highly satisfactory result which, in spite of our rather ad hoc chart and tetrad, mimics the treatment of [18] and [100]. Furthermore we see that it is linear in the a_{mn} and so should appear in linearized theory. Also it does not involve the Lorentz parameters α_n and β_n and so is tetrad-invariant (for tetrads which are asymptotically Minkowskian). The remainder term in (3.48) contains some O_2 terms and junk O_3 terms.

Next consider

$$\Psi_3 = R_{0120} = \Psi_3^{(2)} r^{-2} + O_3, \tag{3.50}$$

where

$$\Psi_3^{(2)} = 2^{-1/2}(\mathcal{N}_{,\theta} - i\mathcal{N}_{,\phi}\csc\theta + \mathcal{N}\cot\theta) + (\alpha_4 + i\alpha_5)\mathcal{N}_{,u}. \tag{3.51}$$

Note first that the r-dependence is precisely what one would have expected from the peeling property. The first term in the coefficient $\Psi_3^{(2)}$ is linear and would have been predicted within linearized theory. However the second term is nonlinear for it depends on the α_n which determine the infinitesimal Lorentz transformation of the NP tetrads (3.31) and (3.32). This is to be expected. The NP tetrad used by Newman & Unti [100] was chosen very specifically,

while here we are considering a class of tetrads infinitesimally close to the Minkowski one. If we were to restrict attention to the subclass of tetrads where $\alpha_4 = \alpha_5 = 0$ then our result would be consistent with linearized theory. On the other hand another choice of $\alpha_4 + i\alpha_5$ would give $\Psi_3^{(2)} = 0$. The remainder term in (3.50) is junk.

Next we find that

$$\Psi_2 = R_{1320} = \Psi_2^{(3)} r^{-3} + O_4, \tag{3.52}$$

where the remainder term is junk. We will return to the leading term shortly.

We find next that

$$\Psi_1 = R_{0113} = \Psi_1^{(4)} r^{-4} + O_5, \tag{3.53}$$

The coefficient $\Psi_1^{(4)}$ contains nonlinear terms, but we are unable to determine it precisely because it also contains junk terms. The peeling property is still holding though.

The peeling property would demand that $\Psi_0 = R_{1313}$ should be O_5. However, in a similar manner to chapter 2 (2.21), we find

$$\Psi_0 = \Psi_0^{(4)} r^{-4} + O_5, \tag{3.54}$$

where

$$\begin{aligned}\Psi_0^{(4)} =& \frac{1}{8}\left[(a_{22} + a_{33}\csc^2\theta)(a_{22} - 2ia_{23}\csc\theta - a_{33}\csc^2\theta)\right. \\ &\left. + 4(b_{22} - b_{33}\csc^2\theta - 2ib_{23}\csc\theta)\right].\end{aligned} \tag{3.55}$$

This result is expected. Thus far we have not made the restrictions that were imposed in [18], [100] or chapter 2 to ensure peeling. The restriction of [100] was to *demand* $\Psi_0^{(4)} = 0$. The restriction of [18] was that the "outgoing radiation condition" held. In the chart and tetrad of chapter 2 the two conditions were equivalent. In our notation, the outgoing radiation condition is (3.28)

$$a_{22} = -a_{33}\csc^2\theta, \qquad b_{22} = b_{33}\csc^2\theta, \qquad b_{23} = 0. \tag{3.56}$$

Examining (3.55) we see that imposing the outgoing radiation condition (3.56)

ensures $\Psi_0^{(4)} = 0$, a result first obtained by Valiente Kroon [81]. With one or other condition we have

$$\Psi_0 = \Psi_0^{(5)} r^{-5} + O_6, \tag{3.57}$$

but the coefficient $\Psi_0^{(5)}$ contains junk terms and so we cannot evaluate it. It also contains nonlinear terms not predicted by linearized theory. This is consistent with the results in §2.2.

To summarize: if we impose the outgoing radiation condition (3.56) then we obtain the peeling property, and we can obtain explicitly the leading terms in Ψ_4, Ψ_3 and Ψ_2, but not those for Ψ_1 and Ψ_0 because they contain junk terms. Note that the outgoing radiation condition is not something that can be imposed during a numerical evolution. However, a numerical relativist can verify whether it holds by investigating the behaviour of Ψ_0 or by checking (3.56). This in turn provides a test on the validity of the asymptotic expansions used.

We now return to the discussion of Ψ_2 given by (3.52). The leading term coefficient is

$$\begin{aligned}\Psi_2^{(3)} =& \frac{1}{2}a_{00} - \frac{1}{4}ia_{23}\csc^3\theta + \frac{1}{2}b_{22,u} + \frac{1}{4}(a_{22} + ia_{23}\csc\theta)(a_{22,u} - ia_{23,u}\csc\theta) \\ &+ \frac{1}{4}i(a_{23,\theta} - 2a_{22,\phi})\cot\theta\csc\theta - \frac{1}{2}ia_{22,\theta\phi}\csc\theta \\ &+ \frac{1}{4}i(a_{23,\theta\theta} - \csc^2\theta a_{23,\phi\phi})\csc\theta.\end{aligned} \tag{3.58}$$

Here we have fixed the Lorentz parameters, as described earlier, and are imposing the outgoing radiation condition (3.28).

Now, motivated by the definition (2.19), the *Bondi mass* $M_B(u)$ can be defined by

$$4\pi M_B(u) = -\lim_{r\to\infty}\int\int r^3(\Psi_2 + \sigma\lambda)\,\mathrm{d}S, \tag{3.59}$$

where $\mathrm{d}S = \sin\theta\,\mathrm{d}\theta\,\mathrm{d}\phi$ is the area element of the unit sphere. Here σ and λ are NP spin coefficients given by

$$\sigma = m^a\delta l_a = \gamma_{313} = \sigma^{(2)}r^{-2} + O_3, \qquad \lambda = n^a\bar{\delta}\overline{m}_a = \gamma_{022} = \lambda^{(1)}r^{-1} + O_2, \tag{3.60}$$

where

$$\sigma^{(2)} = -\frac{1}{2}(a_{22} - ia_{23}\csc\theta), \qquad \lambda^{(1)} = -\frac{1}{2}(a_{22,u} + ia_{23,u}\csc\theta). \tag{3.61}$$

Taking the limit in (3.59) we have

$$4\pi M_B(u) = -\int\int(\Psi_2^{(3)} + \sigma^{(2)}\lambda^{(1)})\,\mathrm{d}S. \tag{3.62}$$

Of course the formula (3.59) is only valid in a specially chosen *Bondi frame*. The generalization to an arbitrary NP frame obtained via spins, boosts and a null rotation about l was first discussed in chapter 2. Here we make a further generalization by including null rotations about n. In the large r limit, our frame differs from the Bondi one by a Lorentz transformation which is close to the identity. A 2-parameter subgroup of the Lorentz group consists of "boosts" and "spins"

$$l \to a^2 l, \quad n \to a^{-2}n, \quad m \to e^{i\psi}m, \tag{3.63}$$

where a and ψ are real. As seen in §2.3, by using the formulae in appendix B of [135] it is easy to verify that the integrand of (3.62) is invariant under boosts and spins and that the news function (3.49) only undergoes a phase change. Next consider a 2-parameter subgroup of "null rotations about l" given by

$$l \to l, \quad m \to m + \bar{c}l, \quad n \to n + cm + \overline{cm} + c\bar{c}l, \tag{3.64}$$

where c is complex. Under such a transformation,

$$\begin{aligned} &\Psi_2 \to \Psi_2 + 2c\Psi_1 + c^2\Psi_0, \qquad \sigma \to \sigma + \bar{c}\kappa, \\ &\lambda \to \lambda + c\pi + 2c\alpha + c^2(\rho + 2\epsilon) + c^3\kappa + cl^a c_{;a} + \overline{m}^a c_{;a}. \end{aligned} \tag{3.65}$$

The NP scalars α, π, ρ and ϵ are all O_1, and we expect $c = O_1$. Thus the integrand of (3.62) is not changed. Finally, we consider null rotations about n given by

$$n \to n, \quad m \to m + \bar{c}n, \quad l \to l + cm + \overline{cm} + c\bar{c}n, \tag{3.66}$$

so that

$$\begin{aligned} &\Psi_2 \to \Psi_2 + 2c\Psi_3 + c^2\Psi_4, \qquad \lambda \to \lambda + \bar{c}\nu, \\ &\sigma \to \sigma + c\tau + 2c\beta + c^2(\mu + 2\gamma) + c^3\nu + cn^a c_{,a} + m^a c_{,a}. \end{aligned} \tag{3.67}$$

Now we have taken great care to ensure that l is almost geodesic ($\kappa = O_4$) and almost affinely parametrised ($\epsilon + \bar{\epsilon} = O_3$) and so we should only consider the transformation (3.66) where $c = O_3$, otherwise these properties are not conserved. Under this restriction the integrand of (3.62) is not changed. Thus the formula (3.62) evaluated in the new frame does indeed give the Bondi mass to leading order. Next note that

$$\begin{aligned}\mathrm{Im}(\Psi_2^{(3)} + \sigma^{(2)}\lambda^{(1)}) = &-\frac{1}{4}a_{23}\csc^3\theta + \frac{1}{4}a_{23,\theta}\csc\theta\cot\theta + \frac{1}{4}a_{23,\theta\theta}\csc\theta \\ &-\frac{1}{2}a_{22,\phi}\csc\theta\cot\theta - \frac{1}{2}a_{22,\theta\phi}\csc\theta - \frac{1}{4}a_{23,\phi\phi}\csc^3\theta.\end{aligned} \tag{3.68}$$

When we integrate this over the unit sphere, the terms in the second line give zero since their contribution to the integrand is 2π-periodic in ϕ. Those in the first line contribute

$$\frac{1}{2}\pi\left[\csc\theta(\sin\theta\, a_{23})_{,\theta}\right]_0^\pi .$$

Now a_{23} must scale like $\sin^2\theta$ at the end points or else the integrand is singular. It follows that the Bondi mass must be real, and

$$4\pi M_B(u) = -\frac{1}{2}\int_0^{2\pi}\int_0^\pi (a_{00} + b_{22,u} + a_{22}a_{22,u} + a_{23}a_{23,u}\csc^2\theta)\sin\theta\,\mathrm{d}\theta\,\mathrm{d}\phi. \tag{3.69}$$

Finally there is a standard result, [18], [100], [134], (2.14), for the rate of decrease of the Bondi mass

$$\begin{aligned}4\pi\frac{\mathrm{d}M_B}{\mathrm{d}u}(u) &= -\int\int|\mathcal{N}|^2\,\mathrm{d}S \\ &= -\frac{1}{4}\int\int\left((a_{22,u})^2 + (a_{23,u})^2\csc^2\theta\right)\mathrm{d}S,\end{aligned} \tag{3.70}$$

demonstrating the well-known result $\mathrm{d}M_B/\mathrm{d}u \leq 0$; the Bondi mass decreases as energy is radiated away, a result not deducible in linearized theory. Although (3.70) was originally derived in a special Bondi frame, it too holds in our approximate Bondi one, at least to leading order. We should emphasize that although the outgoing radiation condition was used in the derivation of (3.69), the mass loss formula (3.70) holds without the need for this restriction. In fact a definition of the Bondi mass, which is a monotonically decreasing function of retarded time, can be written down for polyhomogeneous spacetimes [30].

3.5 Implications for Numerical Relativity

At first glance the formalism we set up to carry out this study may seem to be cumbersome, but it has the advantage that the results can be translated back into the $X^a = (T, R, \Theta, \Phi)$ chart, after which the theoretical chart $x^a = (u, r, \theta, \phi)$ can be discarded.

We chose the x^a chart so that the metric coefficients a_{11} and b_{11} vanished, as well as a_{12} and a_{13}. Now

$$\begin{aligned}\left(\frac{\partial}{\partial u}\right)_r &= \left(\frac{\partial T}{\partial u}\right)_r \left(\frac{\partial}{\partial T}\right)_R + \left(\frac{\partial R}{\partial u}\right)_r \left(\frac{\partial}{\partial R}\right)_T \\ &= (1 - q_1 r^{-1}) \left(\frac{\partial}{\partial T}\right)_R + O_2,\end{aligned} \tag{3.71}$$

using (3.23). In principle the function q_1 is arbitrary. But the vacuum field equations implied $a_{01} = 0$, and then equations (A.3) imply

$$q_1 = \frac{1}{2}(h_{00} - h_{11}). \tag{3.72}$$

The vacuum field equations imply (3.39)

$$a_{22,u} + a_{33,u} \csc^2 \theta.$$

Using (A.3) and (3.44) we have, to leading order

$$[h_{22} + 2h_{02,\Theta} + 2h_{12,\Theta}]_{,T} + [h_{33} + (2h_{03,\Phi} + 2h_{13,\Phi}) \csc^2 \Theta]_{,T} \csc^2 \Theta = 0. \tag{3.73}$$

Other vacuum conditions can be handled in a similar way.

In order to discuss the Bondi news function and Bondi mass, it is convenient to introduce some auxiliary functions in the numerical chart,

$$\begin{aligned}
\mathcal{W} =& h_{03} + h_{13}, \\
\mathcal{A} =& h_{22} + 2(h_{02,\Theta} + h_{12,\Theta}), \\
\mathcal{B} =& h_{23} + h_{02,\Phi} + h_{12,\Phi} + \mathcal{W}_{,\Theta} - 2\mathcal{W}\cot\Theta, \\
\mathcal{C} =& k_{22} + 2\mathcal{W}h_{23}\cot\Theta\csc^2\Theta - 4\mathcal{W}^2\cot\Theta\csc^2\Theta + (k_{02}+k_{12})_{,\Theta} \\
& - (\tfrac{1}{2}h_{11} + h_{22})h_{02,\Theta} - ((\tfrac{1}{2}h_{00} + h_{01})h_{02})_{,\Theta} + (4\mathcal{W}\cot\Theta - h_{23})\mathcal{W}_{,\Theta}\csc^2\Theta \\
& - \tfrac{1}{2}h_{02}h_{11,\Theta} - h_{22}h_{12,\Theta} + (h_{02}+h_{12})h_{22,\Theta} + \mathcal{W}h_{23,\Theta}\csc^2\Theta - (\mathcal{W}_{,\Theta})^2\csc^2\Theta,
\end{aligned} \tag{3.74}$$

which should be readily available according to the assumptions in §3.1.

Then the leading term in the Bondi news function, given by (3.49), becomes

$$\mathcal{N} = \mathcal{A}_{,T} + i\mathcal{B}_{,T}\csc\Theta, \tag{3.75}$$

whose calculation might require some sophistication, although there is no reference to the intermediary $x^a = (u, r, \theta, \phi)$ chart. Because the news function is linear in the h_{ab} and their derivatives, it could have been calculated within linearized theory.

The formula (3.69) for the Bondi mass $M_B(u)$ translates into

$$M_B(T-R) = -\frac{1}{8\pi}\int_{\Phi=0}^{2\pi}\int_{\Theta=0}^{\pi}\Big(h_{11} + \mathcal{A}\mathcal{A}_{,T} + \mathcal{B}\mathcal{B}_{,T}\csc^2\Theta + \mathcal{C}_{,T}\Big)\,\sin\Theta\,\mathrm{d}\Theta\mathrm{d}\Phi. \tag{3.76}$$

In a similar way the formula (3.70) for the rate of change of M_B at fixed large R is

$$\dot{M}_B(T-R) = -\frac{1}{16\pi}\int_{\Phi=0}^{2\pi}\int_{\Theta=0}^{\pi}\Big((\mathcal{A}_{,T})^2 + (\mathcal{B}_{,T})^2\csc^2\Theta\Big)\,\sin\Theta\,\mathrm{d}\Theta\mathrm{d}\Phi. \tag{3.77}$$

In linearized theory, gravitational radiation has only two degrees of freedom. Numerical relativists often describe these degrees of freedom using the "gravitational waveform" quantities h_+ and $h_\times$ [121]. These represent the two possible polarizations of the gravitational waves, so that in *traceless-transverse*

gauge, the perturbed metric tensor h_{ab} takes the form

$$h_{ab} = \begin{pmatrix} 0 & 0 & 0 & 0 \\ 0 & h_+ & h_\times & 0 \\ 0 & h_\times & -h_+ & 0 \\ 0 & 0 & 0 & 0 \end{pmatrix}. \tag{3.78}$$

In traceless-transverse gauge, h_+ and $h_\times$ are related to Ψ_4 by the expression

$$\Psi_4 = -h_{+,TT} + ih_{\times,TT}, \tag{3.79}$$

and can therefore be obtained by evaluating $\mathcal{A}$ and $\mathcal{B}$. Equations (3.74) therefore enable a numerical relativist to evaluate h_+ and $h_\times$.

Again we emphasize that the intermediate x^a chart does not intrude—the formulae (3.75), (3.76) and (3.77) apply in the numerical $X^a = (T, R, \Theta, \Phi)$ chart. However, only (3.75) can be deduced from linearized theory.

Why are these formulae so complicated, when compared with the original papers, [18] and [100], or even the formulae in chapter 2 or §3.4? Well the coordinates and tetrads of the original papers were very carefully chosen to simplify the problem, and much of this chapter has been spent building the relationship between the numerical relativist's $X^a = (T, R, \Theta, \Phi)$ chart and the $x^a = (u, r, \theta, \phi)$ chart and adapted tetrad, in which the formulae look almost as simple as in the original approaches. One way to avoid the complexity is to design a numerical approach based on Penrose's geometrical approach [103], but that brings in different problems and complexities (see §1.2).

3.5.1 Polyhomogeneous Spacetimes

One of the fundamental assumptions made in the preceding two chapters is that asymptotic $1/r$ expansions of the metric variables exist. Bondi et al. [18] found that the outgoing radiation condition was necessary to prevent logarithmic terms appearing in the expansions. Similarly, the condition $\Psi_0 = O(r^{-5})$, imposed by Newman & Unti [100], was required to prevent the appearance of $\log r$ terms. This suggests that, in generic situations, logarithmic terms might naturally arise in the asymptotic expansions. This has led to the study of *polyhomogeneous spacetimes*. A polyhomogeneous spacetime has a metric

which admits an expansion in terms of $r^{-m}\,(\log r)^n$ for $m,\, n \in \mathbb{N}$.

One of the first notable studies of polyhomogeneous spacetimes was by Chruściel et al. [30]. They showed that the assumption of polyhomogeneity was very natural and does not lead to any significant analytical difficulties. Although the Weyl tensor no longer peels in the usual way, polyhomogeneity was shown to be formally consistent with the Einstein field equations and various results that hold for non-polyhomogeneous spacetimes were proved. Notably, an appropriate definition of the Bondi mass was obtained, which is a monotonically decreasing function of a retarded time coordinate. Chruściel et al. concluded that removing logarithmic terms from the asymptotic expansions is not sufficient justification for imposing the outgoing radiation condition. Furthermore, Valiente Kroon [80, 82–85] has found generalizations of the Newman-Penrose constants [99] for polyhomogeneous spacetimes.

The physical interpretation of the $\log r$ terms in polyhomogeneous spacetimes (and the resulting non-smooth null infinity) is still an open question. It is believed that the logarithmic terms are somehow connected to incoming radiation. The presence of a non-smooth null infinity may also have physical effects on the propagation of gravitational radiation (see, for example, [86]).

The fundamental assumption made in this chapter is that the numerically calculated spacetime can be expanded (asymptotically) in terms of negative powers of r. However, such behaviour is not generic and it is not possible to guarantee that a spacetime will possess a particular type of asymptotic decay or that the peeling property will hold. Indeed, if it is found that the outgoing radiation condition is not satisfied in the numerically calculated spacetime, then logarithmic terms will automatically be present and the Weyl scalars will not peel off in the "usual" way. The natural extension of the work in this chapter would therefore be to consider polyhomogeneous spacetimes, without imposing the outgoing radiation condition. The resulting calculations might well be valid in a more general setting than the one considered here. However, there may be a price to pay, as evaluating coefficients in a polyhomogeneous expansion of the metric variables is likely to be more difficult numerically than evaluating the coefficients in a $1/r$ expansion.

Chapter 4

Hertz Potentials

In chapters 2 and 3 we focused on the asymptotic behaviour of gravitational fields near future null infinity $\mathscr{I}^+$. By using $1/r$ expansions in the full non-linear theory of general relativity we were able to close the gap between the very specific choices of coordinate chart and tetrad used in theoretical calculations and the gauge choices that are accessible to a numerical relativist. This gives us free reign to choose whichever theoretical chart is the most convenient for us in which to formulate absorbing boundary conditions. The results of the preceding chapter will enable us to express the boundary conditions in a numerical chart later. In addition, provided we recall the limitations of linearized theory discussed in chapter 3, we can use a perturbative approach (see e.g. [139]) to simplify our calculations.

The notions of *incoming* and *outgoing* gravitational radiation are key when formulating absorbing boundary conditions. In [107] it was shown that Hertz potentials provide a very transparent way of describing incoming and outgoing radiation, linearized about a Minkowski background. Furthermore, Hertz potentials can describe perturbations about Schwarzschild and Kerr spacetimes. The method used by Buchman & Sarbach [22, 23] is applicable only on flat or Schwarzschild background spacetimes, and can not easily be extended to Kerr backgrounds. It is for this reason that Hertz potentials are of interest to us. In this chapter we will introduce Hertz potentials in more detail. Chapters 5, 6 and 7 will then build on this work to investigate the propagation of gravitational waves on Minkowski, Schwarzschild and Kerr backgrounds respectively. This will enable us to create boundary conditions for numerical relativity which are absorbing for linearized gravitational radiation on these backgrounds.

What is a Hertz potential? On a flat spacetime, a source-free electromagnetic field has precisely two degrees of freedom. The Einstein field equations describing linearized gravitational perturbations about a flat vacuum spacetime also have two degrees of freedom. In each case, the fields can be expressed in terms of the derivatives of a complex scalar field known as a Hertz potential. A gravitational field has spin 2, whereas an electromagnetic field has spin 1. It is similarly possible to use a Hertz potential to describe any zero rest-mass field of arbitrary spin propagating on a Minkowski background [104].

These ideas can be extended to certain curved spacetimes. Electromagnetic fields propagating on any algebraically special background can be represented by a Hertz potential [31, 33]. In addition, Hertz potential representations for gravitational perturbations about algebraically special spacetimes have been obtained [34, 76]. The field equations in such theories invariably involve the widespread use of antisymmetric tensors. Therefore a slightly less cumbersome approach is to use spinor notation. The resulting field equations for the Hertz potential are much simpler [133].

In this chapter we will introduce Hertz potentials using 2-component spinors (see e.g. [135] for an introduction to 2-component spinors). It is instructive to begin with the conceptually simpler case of Hertz potentials for electromagnetic fields (§4.1) before considering gravitational fields (§4.2).

4.1 Hertz Potentials for Electromagnetic Fields in a Vacuum Spacetime

Let χ_{AB} be a symmetric 2-component spinor with derivatives

$$\lambda_{AB'} = \nabla^{B}{}_{B'}\chi_{AB}, \tag{4.1}$$

$$\bar{\phi}_{A'B'} = \nabla^{A}{}_{A'}\lambda_{AB'} = \nabla^{A}{}_{A'}\nabla^{B}{}_{B'}\chi_{AB}. \tag{4.2}$$

Since $\bar{\phi}_{A'B'}$ is symmetric and traceless, it will represent a source-free Maxwell field if and only if Maxwell's equations are satisfied. This implies

$$0 = \nabla_{B}{}^{B'}\bar{\phi}_{A'B'} \tag{4.3}$$

$$= \nabla^{A}{}_{A'}\left(-\frac{1}{2}\Box\chi_{AB} + \Psi_{AB}{}^{CD}\chi_{CD}\right), \tag{4.4}$$

where $\Box = \nabla_{AA'}\nabla^{AA'}$, and $\Psi_{ABCD} = \Psi_{(ABCD)}$ is the Weyl spinor of the background spacetime. Clearly, if we impose

$$\Box\chi_{AB} - 2\Psi_{AB}{}^{CD}\chi_{CD} = 0, \tag{4.5}$$

then $\bar{\phi}_{A'B'}$ is a Maxwell field.

We can generalize (4.2) by introducing a "gauge change" via an arbitrary spinor $\alpha_{AB'}$

$$\bar{\tilde{\phi}}_{A'B'} = \nabla^{C}{}_{A'}\lambda_{CB'} - \nabla_{C(A'}\alpha^{C}{}_{B')}. \tag{4.6}$$

With a suitable choice of $\alpha_{AB'}$ it is often possible to cancel some of the terms from the field equation for χ_{AB} (4.5). We will specify our particular choice of $\alpha_{AB'}$ later. It can now be shown that $\bar{\tilde{\phi}}_{A'B'}$ is a Maxwell field if, for any $\alpha_{AB'}$, the spinor χ_{AB} satisfies

$$\Box\chi_{AB} - 2\Psi_{AB}{}^{CD}\chi_{CD} + 2\nabla^{C'}{}_{(A}\alpha_{B)C'} = 0. \tag{4.7}$$

Note that the choice of $\alpha_{AB'}$ is not a true gauge freedom because the new Maxwell field $\bar{\tilde{\phi}}_{A'B'}$ is different from the old one $\bar{\phi}_{A'B'}$, and the difference depends on the choice of $\alpha_{AB'}$.

We now restrict our attention to vacuum type D spacetimes, with a basis of repeated principal null spinors (o_A, ι_A) (this restriction will be justified in

§4.2, but note that the analysis below still works in the more general type II or *algebraically special* spacetimes). The spinor basis defines a Newman-Penrose null tetrad

$$l^a = o^A\bar{o}^{A'}, \quad n^a = \iota^A\bar{\iota}^{A'}, \quad m^a = o^A\bar{\iota}^{A'}, \quad \bar{m}^a = \iota^A\bar{o}^{A'}. \tag{4.8}$$

The covariant derivative ∇_a is contracted with each tetrad vector in turn to define the four standard differential operators used in the Newman-Penrose formalism

$$\begin{aligned} D \equiv l^a\nabla_a, \qquad \triangle \equiv D' \equiv n^a\nabla_a, \\ \delta \equiv m^a\nabla_a, \quad \delta' \equiv \bar{\delta} \equiv \bar{m}^a\nabla_a. \end{aligned} \tag{4.9}$$

Using the Geroch-Held-Penrose formalism [53], we introduce the four spin- and boost-weighted derivations Þ, Þ′, ð and ð′. Acting on a quantity η of GHP type $\{p, q\}$ these derivations are

$$\begin{aligned} \text{Þ}\eta \equiv (D - p\epsilon - q\bar{\epsilon})\eta, \quad \text{Þ}'\eta \equiv (D' + p\epsilon' + q\bar{\epsilon}')\eta, \\ \text{ð}\eta \equiv (\delta - p\beta + q\bar{\beta}')\eta, \quad \text{ð}'\eta \equiv (\delta' + p\beta' - q\bar{\beta})\eta. \end{aligned} \tag{4.10}$$

The use of the prime ($'$) in (4.9) and (4.10) denotes the operation

$$o^A \to i\iota^A, \quad \iota^A \to io^A, \quad \bar{o}^{A'} \to -i\bar{\iota}^{A'}, \quad \bar{\iota}^{A'} \to -i\bar{o}^{A'}. \tag{4.11}$$

If we choose

$$\chi_{AB} = \chi'\iota_A\iota_B, \tag{4.12}$$

and make the gauge choice

$$\alpha_{AB'} = -2\iota_A(\tau'\bar{\iota}_{B'} - \rho' o_{\bar{B}'})\chi', \tag{4.13}$$

then we find that (4.7) reduces to a single field equation for the complex scalar χ'

$$(\text{Þ}\text{Þ}' - \text{ð}\text{ð}' + \rho'\text{Þ} - \bar{\rho}\text{Þ}' - \tau'\text{ð} + \bar{\tau}'\text{ð}' - \Psi_2)\,\chi' = 0. \tag{4.14}$$

The scalar χ' has GHP type $\{2, 0\}$. The 4−vector potential A^a and the Maxwell

scalars ϕ_0, ϕ_1 and ϕ_2 can all now be expressed in terms of χ':

$$A^a = [\eth\chi' + \eth'\chi' + (\tau' + \bar{\tau}')\chi']\, n^a - [\text{Þ}\bar{\chi}' + \bar{\rho}\bar{\chi}']\, m^a - [\text{Þ}'\chi' + \rho'\chi']\, \bar{m}^a, \quad (4.15)$$

and

$$\phi_0 = \text{Þ}'^2\bar{\chi}', \quad \phi_1 = (\text{Þ}'\eth' + \tau\text{Þ}')\bar{\chi}', \quad \phi_2 = (\eth^2 + \sigma\text{Þ}' + \sigma\bar{\rho}')\bar{\chi}'. \quad (4.16)$$

Note that we could have chosen $\chi_{AB} = \chi o_A o_B$, as was done in the earlier paper [133]. The results in [133] are then related to ours by the GHP prime operation $'$. The reasons for our choice of χ_{AB} (4.12) will be justified in the next section.

In summary, the two degrees of freedom of the source-free electromagnetic field are encoded in the complex scalar χ', which satisfies a field equation. Quantities such as the vector potential and the Maxwell scalars can be expressed in terms of χ'.

4.2 Hertz Potentials for Linearized Gravitational Fields

The Weyl spinor Ψ_{ABCD} for a vacuum spacetime satisfies

$$\nabla^{DD'}\Psi_{ABCD} = 0. \tag{4.17}$$

Infinitesimal vacuum perturbations of the gravitational field have two degrees of freedom. Comparison of (4.17) with (4.3) then suggests that by using a similar approach to §4.1 we might be able to find a Hertz potential representation for linear perturbations of the Weyl spinor, such that the Einstein equations (1.2) would then reduce to a single field equation for a complex scalar potential.

In a background algebraically special vacuum spacetime, we introduce a symmetric spinor χ_{ABCD} with derivatives

$$\lambda_{ABCD'} = \nabla_{D'}{}^{D}\chi_{ABCD}, \tag{4.18}$$

$$\gamma_{ABC'D'} = \nabla_{C'}{}^{C}\lambda_{ABCD'}, \tag{4.19}$$

$$\mu_{AB'C'D'} = \nabla_{B'}{}^{B}\gamma_{ABC'D'}, \tag{4.20}$$

$$\nu_{A'B'C'D'} = \nabla_{A'}{}^{A}\mu_{AB'C'D'}. \tag{4.21}$$

If we impose

$$\Psi_{ABCD}\chi^{BCDE} = 0, \quad \Psi_{ABCD}\lambda^{BCD}{}_{E'} = 0, \tag{4.22}$$

then we obtain the symmetry properties

$$\gamma_{ABC'D'} = \gamma_{(AB)(C'D')}, \quad \mu_{AB'C'D'} = \mu_{A(B'C'D')}, \quad \nu_{A'B'C'D'} = \nu_{(A'B'C'D')}. \tag{4.23}$$

The real tensor γ_{ab} defined by

$$\gamma_{ab} = \Theta_{ABA'B'} = \gamma_{ABA'B'} + \bar{\gamma}_{ABA'B'}, \tag{4.24}$$

then satisfies

$$\gamma_{ab} = \gamma_{(ab)}, \quad \gamma_c{}^{c} = 0. \tag{4.25}$$

Since γ_{ab} is symmetric and traceless, we can interpret it as a linearized perturbation of the background metric induced by the potential χ_{ABCD}. In addition, we have

$$\nabla^b \gamma_{ab} = 0, \tag{4.26}$$

so the perturbation is in de Donder gauge. In a vacuum, the perturbed Riemann and Ricci tensors, $\hat{R}_{abcd}$ and $\hat{R}_{ab}$, are given by the standard identities [92]

$$\hat{R}_{abcd} = 2\nabla_{[c}\nabla_{[a}\gamma_{b]d]} - \gamma^{e}{}_{[a}R_{b]ecd}, \tag{4.27}$$

$$\hat{R}_{ab} = \Box\gamma_{ab} - 2\nabla^c\nabla_{(a}\gamma_{b)c}. \tag{4.28}$$

In analogy with (4.6) we make the "gauge change"

$$\gamma_{ABA'B'} \to \gamma_{ABA'B'} + \nabla^{C}{}_{(A'}\alpha_{B')ABC}, \tag{4.29}$$

where $\alpha_{A'ABC}$ is symmetric on its last three indices. Note once more that the introduction of $\alpha_{A'ABC}$ alters the perturbed metric so this is not a true gauge change. In addition the de Donder gauge condition (4.26) is no longer automatically satisfied. It can now be shown, via a long but straightforward calculation [133], that the perturbed Ricci tensor (4.28) will vanish if

$$\nabla_{(A}{}^{C'}\nabla^{E}{}_{|C'|}\chi_{BCD)E} + 3\Psi^{EF}{}_{(AB}\chi_{CD)EF} = \nabla_{C'(A}\alpha^{C'}{}_{BCD)}. \tag{4.30}$$

In order to make further progress, we restrict our attention to type D algebraically special spacetimes, with repeated principal null directions o_A and ι_A. This slight loss of generality poses no problem because the backgrounds of interest to us (such as Minkowski, Schwarzschild or Kerr spacetimes) are all of type D. Note once more that o_A and ι_A define a null tetrad of vectors

$$l^a = o^A\bar{o}^{A'}, \quad n^a = \iota^A\bar{\iota}^{A'}, \quad m^a = o^A\bar{\iota}^{A'}, \quad \bar{m}^a = \iota^A\bar{o}^{A'}, \tag{4.31}$$

and we define the same derivations as in §4.1,

$$\begin{aligned} D \equiv l^a\nabla_a, \quad & \triangle \equiv D' \equiv n^a\nabla_a, \\ \delta \equiv m^a\nabla_a, \quad & \delta' \equiv \bar{\delta} \equiv \bar{m}^a\nabla_a, \end{aligned} \tag{4.32}$$

and

$$\begin{aligned} \text{Þ}\eta &\equiv (D - p\epsilon - q\bar{\epsilon})\eta, \quad \text{Þ}'\eta \equiv (D' + p\epsilon' + q\bar{\epsilon}')\eta, \\ \text{ð}\eta &\equiv (\delta - p\beta + q\bar{\beta}')\eta, \quad \text{ð}'\eta \equiv (\delta' + p\beta' - q\bar{\beta})\eta, \end{aligned} \tag{4.33}$$

where η is a quantity with GHP type $\{p, q\}$.

The spinor χ_{ABCD} is now completely degenerate. Since we are interested in studying future null infinity, we take its repeated principal spinor to be ι_A rather than o_A, so that

$$\chi_{ABCD} = \chi' \iota_A \iota_B \iota_C \iota_D. \tag{4.34}$$

(For further justification of this choice of χ_{ABCD} see, for example, section 3.7 of [135].) The subsequent results will be related to those that were obtained by Stewart [133], in which $\chi_{ABCD} = \chi o_A o_B o_C o_D$, by the GHP prime operation (4.11). We now also make a "gauge choice" in order to simplify the field equation (4.30)

$$\alpha_{A'BCD} = 4\iota_B \iota_C \iota_D (\tau' \bar{\iota}_{A'} - \rho' \bar{o}_{A'}) \chi'. \tag{4.35}$$

With these choices of χ_{ABCD} and $\alpha_{A'BCD}$, (4.30) reduces to

$$\left(\text{Þ}\text{Þ}' - \text{ð}\text{ð}' + 3\rho'\text{Þ} - \bar{\rho}\text{Þ}' - 3\tau'\text{ð} + \bar{\tau}'\text{ð}' - 6\Psi_2\right)\chi' = 0. \tag{4.36}$$

The scalar χ' has GHP type $\{4, 0\}$. Thus, as postulated at the beginning of this section, the linearized vacuum Einstein equations have been reduced to a single field equation for the complex scalar χ'. The field equation (4.36) is the starting point for the calculations in chapters 5, 6 and 7.

In a similar manner to §4.1, in which the vector potential and the Maxwell scalars were expressed in terms of the Hertz potential, the perturbations to the Newman-Penrose scalars, the metric, the Weyl scalars and the NP tetrad can all be expressed in terms of χ'. Using (4.29) and (4.24), the perturbed metric can immediately be written in terms of the Hertz potential. This enables us to evaluate the perturbed tetrad. There are two ways of obtaining the perturbed NP scalars. By perturbing the GHP field equations, we can obtain a set of linear simultaneous equations which can be solved in terms of the perturbed NP scalars. A much easier way, however, is to note that the NP spin coefficients can be expressed in terms of antisymmetrized partial derivatives of the tetrad

vectors. For example

$$\kappa = 2l_{[a,b]}m^a l^b. \tag{4.37}$$

A complete set of such formulae was obtained by Cocke [32]. Since these expressions contain no covariant derivatives, they can be perturbed in a straightforward manner. Finally the perturbed Weyl scalars can be obtained from (4.27).

By repeatedly making use of the GHP commutator equations for the operators Þ, Þ′, ð and ð′ [53], the expressions for the perturbed quantities can be significantly simplified. Further simplifications occur if we restrict our attention to Minkowski or Schwarzschild background spacetimes. On a Minkowski background, the only non-zero NP scalars are ρ, ρ', β and β', which are all real. On a Schwarzschild background, ρ, ρ', β, β', ϵ' and also Ψ_2 are real and non-zero. On a Kerr background the NP scalars are, in general, complex and, in addition, τ and τ' are non-zero. The perturbations of the tetrad, metric, NP and Weyl scalars about Minkowski, Schwarzschild and Kerr backgrounds are given in appendix B.

As a useful guard against algebraic errors, we can use the GHP commutator equations [53] and the scalar equation (4.36) to check that the expressions for the perturbed quantities satisfy the GHP Bianchi identities and the GHP vacuum field equations.

In this section, we chose a potential of the form $\chi_{ABCD} = \chi' \iota_A \iota_B \iota_C \iota_D$ (4.34). The expressions for the perturbed quantities corresponding to the potential $\chi_{ABCD} = \chi o_A o_B o_C o_D$ are given in [133]. They are related to the results found here by the GHP prime operation (4.11) but are considerably lengthier than the expressions in appendix B because the GHP commutator equations were not used to simplify them.

The calculations mentioned in the preceding paragraphs are most easily carried out using a computer algebra system (the author used *Reduce 3.8*, and the script is available on request).

Chapter 5

The Homogeneous Euler-Poisson-Darboux Equation

The aim of chapters 5, 6 and 7 is to study the scalar field equation for Hertz potentials (4.36) on Minkowski, Schwarzschild and Kerr backgrounds respectively. By investigating the behaviour of the solutions in the far-field region we can begin to understand how linearized gravitational waves propagate, firstly on a flat space background, and then on curved spacetimes with mass M and angular momentum Ma. This will enable us to formulate absorbing boundary conditions for numerical relativity.

In §5.3 we find that, on a Minkowski background, by choosing standard double null coordinates with a suitable tetrad, (4.36) reduces to a special case of the homogeneous *Euler-Poisson-Darboux equation* [39, 45] whose solutions are known. In chapters 6 and 7, when suitable choices of coordinate chart and tetrad are made, inhomogeneous Euler-Poisson-Darboux equations are obtained, with additional terms depending on the mass and angular momentum parameters, M and a.

To illustrate these ideas, it is instructive to consider first the conceptually and algebraically simpler case of the wave equation for a spin-0 massless scalar field Φ

$$\Box\Phi = 0, \tag{5.1}$$

where $\Box \equiv \nabla^a\nabla_a$. Here, when double null coordinates are chosen, an Euler-

Poisson-Darboux equation is again obtained, which is homogeneous only on a Minkowski background.

Clearly, the Euler-Poisson-Darboux (EPD) equation is central to this investigation. In fact it has many applications in theoretical physics. For example, in the study of gravitational perturbations on a Schwarzschild background [111, 149] the field equations governing "odd parity" and "even parity" perturbations can be shown to be EPD equations. See, for example, [137] for an overview of other applications of the EPD equation in general relativity.

Much is known about the Euler-Poisson-Darboux equation and we begin this chapter by reviewing some useful results (§5.1). In particular the Riemann-Green function is known [50]. This means that integral representations of solutions to the Cauchy or characteristic initial value problems for both homogeneous and inhomogeneous EPD equations can be written down using Riemann's method [36, 37]. In the inhomogeneous cases (corresponding to perturbations about Schwarzschild or Kerr backgrounds), these solutions can then be estimated using a Picard iteration scheme [106]. This is the approach taken in chapters 6 and 7.

In §5.2 and §5.3, we restrict our attention to the homogeneous EPD equation. We obtain solutions first to the scalar wave equation (5.1), and then to the Hertz potential field equation (4.36), both on a Minkowski background. The inhomogeneous cases, corresponding to Schwarzschild and Kerr backgrounds, are dealt with in chapters 6 and 7 respectively.

5.1 General Properties of the Euler-Poisson-Darboux Equation

The homogeneous *Euler-Poisson-Darboux* equation is given by

$$z_{,uv} + \frac{\alpha z_{,u}}{v-u} - \frac{\beta z_{,v}}{v-u} + \frac{\gamma z}{v-u} = 0, \tag{5.2}$$

where α, β and γ are arbitrary constants and z is a function of u and v. It is a generalization of the standard wave equation and is the simplest second order hyperbolic differential equation whose coefficients contain singularities. We are interested in studying the behaviour of solutions as $v \to \infty$, and so the

singularities will not be dealt with here (see [137] for a discussion of solutions containing singularities). By making a change of dependent variable

$$z(u,v) = (v-u)^{\lambda}\omega(u,v), \tag{5.3}$$

for a suitable choice of λ, it is always possible to eliminate the term involving γ from (5.2). From now on we therefore consider the following simplified equation

$$z_{,uv} + \frac{\alpha z_{,u}}{v-u} - \frac{\beta z_{,v}}{v-u} = 0. \tag{5.4}$$

In general, α and β need not be integers, and indeed in many physical situations of interest EPD equations are obtained with non-integer parameters. (For example the "polarized Gowdy equation" [71, 75] is an Euler-Poisson-Darboux equation with $\alpha = \beta = \frac{1}{2}$. Similarly, in the study of plane symmetric spacetimes containing irrotational fluid flows [61, 138], an EPD equation with $\alpha = \beta = \frac{1}{2}$ is found, whose solutions contain spacelike singularities at $t = 0$.) The EPD equations resulting from the study of the spin-0 massless scalar field or a Hertz potential for linearized gravitational perturbations always have integer parameters of the same sign. By interchanging the independent variables u and v, or by setting $\lambda = 1-\alpha-\beta$ in the transformation (5.3), we can always arrange that both parameters are positive. Suppose then that $\alpha = m \in \mathbb{N}$ and $\beta = n \in \mathbb{N}$. In this case the general solution to (5.4) can be written in the form

$$z(u,v) = \left(\frac{\partial}{\partial u}\right)^{n-1} \frac{U(u)}{(v-u)^m} + \left(\frac{\partial}{\partial v}\right)^{m-1} \frac{V(v)}{(v-u)^n}, \tag{5.5}$$

where $U(u)$ and $V(v)$ are arbitrary functions of u and v respectively. We posit that the terms involving $U(u)$ represent outgoing radiation, whilst the terms involving $V(v)$ represent incoming radiation. This assertion will be justified in §5.2 when the characteristic initial value problem is discussed.

For general (non-integer) α and β, by seeking homogeneous solutions of the form $z(u,v) = v^{\lambda}y(x)$, where $x = \frac{u}{v}$, the EPD equation (5.4) is transformed into the hypergeometric differential equation, and we obtain

$$z(u,v) = v^{\lambda}{}_2F_1\left(-\lambda, \beta; 1-\alpha-\lambda; \frac{u}{v}\right), \tag{5.6}$$

for an arbitrary choice of λ. Here ${}_2F_1$ is a hypergeometric function [1, 102].

In order to write down integral representations of solutions to the EPD equation, the Riemann-Green function is required. This is defined as being the solution $R(u', v'; u, v)$ of the adjoint equation to (5.4) with independent variables u' and v', which depends on the parameters u and v and satisfies the characteristic boundary conditions

$$R(u', v; u, v) = \left(\frac{v - u'}{v - u}\right)^{\beta}, \tag{5.7}$$

and

$$R(u, v'; u, v) = \left(\frac{v' - u}{v - u}\right)^{\alpha}. \tag{5.8}$$

Using (5.6), it can be shown that

$$R(u', v'; u, v) = (v' - u')^{\alpha+\beta}(v' - u)^{-\beta}(v - u')^{-\alpha}{}_2F_1(\beta, \alpha, 1; t), \tag{5.9}$$

where

$$t = \frac{(v' - v)(u' - u)}{(v' - u)(u' - v)}. \tag{5.10}$$

Note that t is the ratio of two polynomials homogeneous in u' and v'.

5.2 The Massless Scalar Field on a Minkowski Background

Before dealing with the more complex examples of the EPD equation encountered in the study of Hertz potentials, it is instructive to consider the massless zero-spin scalar wave equation on Minkowski spacetime.

Consider a scalar field Φ on a Minkowski background, satisfying (5.1)

$$g^{ij}\Phi_{;ij} = 0. \tag{5.11}$$

We work in the standard double null coordinate chart for Minkowski spacetime (u, v, θ, ϕ), where

$$u = t - r, \quad v = t + r, \tag{5.12}$$

and (θ, ϕ) are spherical polar coordinates. We seek separable solutions by expanding the scalar field in terms of spherical harmonics

$$\Phi(u, v, \theta, \phi) = \sum_{l,m} \phi^{lm}(u, v) Y_{lm}(\theta, \phi). \tag{5.13}$$

Appendix C.1 contains details of the spherical harmonic conventions used here. Then (5.11) becomes

$$\sum_{l,m} Y_{lm}(\theta, \phi) \left\{ \frac{\partial^2 \phi^{lm}}{\partial u \partial v} + \frac{1}{v-u}\frac{\partial \phi^{lm}}{\partial u} - \frac{1}{v-u}\frac{\partial \phi^{lm}}{\partial v} - \frac{l(l+1)}{(v-u)^2}\phi^{lm} \right\} = 0, \tag{5.14}$$

where $-l \leq m \leq l$. By considering a single harmonic mode and changing the dependent variable from ϕ^{lm} to z^{lm}, where

$$\phi^{lm} = (v-u)^l z^{lm}(u, v), \tag{5.15}$$

we obtain the Euler-Poisson-Darboux equation

$$z^{lm}{}_{,uv} + \frac{l+1}{v-u} z^{lm}{}_{,u} - \frac{l+1}{v-u} z^{lm}{}_{,v} = 0. \tag{5.16}$$

The general solution to (5.16) is

$$z^{lm}(u,v) = \left(\frac{\partial}{\partial u}\right)^l \frac{U^{lm}(u)}{(v-u)^{l+1}} + \left(\frac{\partial}{\partial v}\right)^l \frac{V^{lm}(v)}{(v-u)^{l+1}}, \tag{5.17}$$

where $U^{lm}(u)$ and $V^{lm}(v)$ are arbitrary functions of u and v respectively.

We now seek solutions (5.17) corresponding to a given choice of initial data. The coordinates u and v are characteristic variables for the EPD equation (5.16) and are therefore the natural choice of coordinates with which to study incoming and outgoing radiation. We therefore choose to specify initial data on the surfaces $u = \text{const.}$ and $v = \text{const.}$ and solve the characteristic initial value problem rather than the Cauchy problem. Suppose we wish to find a solution to (5.16) at a point P with coordinates (u, v). The solution will uniquely be determined by the initial data specified on the characteristic surfaces $u = u_0$ and $v = v_0$.

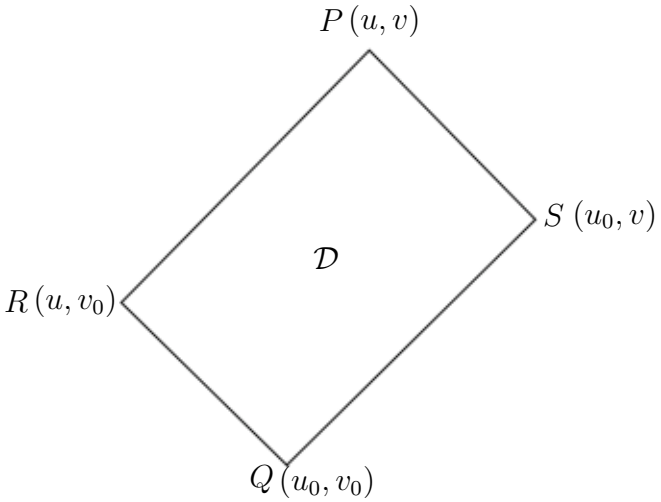

Figure 5.1: Specifying data on the edges QR and QS of the domain of dependence $\mathcal{D}$ defines the solution at the point P with coordinates (u, v).

Suppose that we specify a function $C^{lm}(u)$ as our initial data on the characteristic QR, $v = v_0$. The function $C^{lm}(u)$ can be written as

$$C^{lm}(u) = \left(\frac{\partial}{\partial u}\right)^l \frac{U^{lm}(u)}{(v_0-u)^{l+1}}, \tag{5.18}$$

for a suitable choice of $U^{lm}(u)$. If there are no initial data on QS, $u = u_0$ (that

is $V^{lm}(v') = 0$ for $v' \in [v_o, v]$) then the resulting solution to (5.16) at P is

$$z^{lm}(u,v) = \left(\frac{\partial}{\partial u}\right)^l \frac{U^{lm}(u)}{(v-u)^{l+1}}, \tag{5.19}$$

Similarly, general initial data $D^{lm}(v)$ on the characteristic QS, $u = u_0$ can be written as

$$D^{lm}(v) = \left(\frac{\partial}{\partial v}\right)^l \frac{V^{lm}(v)}{(v-u_0)^{l+1}}, \tag{5.20}$$

for some choice of $V^{lm}(v)$. If there are no initial data on the surface QR, $v = v_0$ (so that $U^{lm}(u') = 0$ for $u' \in [u_0, u]$) then the solution to (5.16) at P is

$$z^{lm}(u,v) = \left(\frac{\partial}{\partial v}\right)^l \frac{V^{lm}(v)}{(v-u)^{l+1}}. \tag{5.21}$$

In the general solution (5.17), the terms involving $U^{lm}(u)$ can then be interpreted as outgoing radiation and the terms involving $V^{lm}(v)$ can be interpreted as incoming radiation.

We now investigate equation (5.18) in more detail. Consider first the case $l = 0$ (and hence $m = 0$). Suppose that we specify some initial outgoing data $C^{00}(u)$ on $v = v_0$. Then (5.19) implies

$$C^{00}(u) = \frac{U^{00}(u)}{(v_0 - u)}. \tag{5.22}$$

If $C^{00}(u)$ has compact support then so does $U^{00}(u)$. The general solution $z^{00}(u,v)$ will therefore also have compact support in u. This is known as *sharp propagation*. Once the initial wave has passed a given point there is no longer any excitation of the field remaining. The sharp propagation occurs due to the spherical symmetry of the $l = 0$ mode. The spherical harmonic Y_{00} is constant, and so the solution propagates purely radially with no interference due to propagation in an angular direction.

Now consider the case $l = 1$ (so that $m = 0$ or ± 1). The general outgoing solution (5.19) is

$$z^{1\,m}(u,v) = \frac{\partial}{\partial u}\frac{U^{1\,m}(u)}{(v-u)^2}, \tag{5.23}$$

and so, for initial data $C^{1\,m}(u)$, we have

$$U^{1\,m}(u) = (v_0 - u)^2 \int_{u_0}^{u} C^{1\,m}(u')\mathrm{d}u'. \tag{5.24}$$

Now, if $C^{1\,m}(u)$ has compact support then in general we cannot infer that $U^{1\,m}(u)$ has compact support. Hence the general solution $z^{1\,m}(u, v)$ will not, in general, have compact support in u. (As a concrete example take $C^{1\,m}(u) = \delta(u - u_a)$. Then

$$U^{1\,m}(u) = (v_0 - u)^2 H(u - u_a), \tag{5.25}$$

which does not have compact support.) A similar analysis works for all $l \geq 1$. Once the initial outgoing wavefront has passed through the point (u, v), there is some residual radiation which persists. This is known as *spreading* of the initial data. The residual radiation is known as a *geometrical tail*.

An alternative way of viewing this phenomenon is by transforming the EPD equation (5.16) into (t, r) coordinates, to obtain

$$(rz^{lm})_{,tt} - (rz^{lm})_{,rr} = 2lz^{lm}{}_{,r}. \tag{5.26}$$

The case $l = 0$ corresponds to the spherically symmetric wave equation, whose solutions propagate sharply. If $l \geq 1$, then the extra "potential" term on the right-hand side of (5.26) gives rise to the geometrical tail.

An equation is said to satisfy *Huygens' principle* (as defined by Hadamard's "minor premise", [65] p. 54) if an initially sharp wave does not develop a tail. Huygens' principle can also be stated in terms of the Cauchy problem. It is satisfied if the value of z^{lm} at a point P depends only on the intersection of the characteristic cone $C(P)$ with the Cauchy surface S on which initial data are specified. Here, Huygens' principle is satisfied only in the case $l = 0$. The geometrical tail for $l \geq 1$ arises due to the angular dependence of the corresponding spherical harmonics (Y_{lm} is $\theta-$ and $\phi-$dependent if $l \geq 1$), which prevents such modes from propagating purely radially. The resulting interference causes an initially sharp wave to spread. In §7.2, we will consider the scalar wave equation on a Kerr background. Then, even if $l = 0$, the background curvature causes the initial data to spread. The solution contains a "gravitational tail" and so Huygens' principle cannot be satisfied. This is consistent with the results of Kundt & Newman [88].

Huygens' principle for scalar wave equations has recieved a good deal of attention in the literature (see e.g. [49]). McLenaghan [91] has shown that Huygens' principle for the scalar wave equation (5.11) is satisfied only on plane-wave or Minkowski background spacetimes. The results presented here are slightly different. McLenaghan investigated Huygens' principle for scalar waves Φ in physical, four-dimensional spacetimes. Here, we have factorized out the angular dependence of the field Φ and are considering Huygens' principle for the ϕ^{lm} (5.13), which propagate on a $1+1$-dimensional, "unphysical" spacetime. In one spatial dimension, Huygens' principle is not, in general, valid [37].

5.3 Linearized Gravitational Fields on a Minkowski Background

We now apply similar methods to those in §5.2 to the Hertz potential field equation (4.36) for linearized gravitational fields perturbed about a Minkowski background. Again, we obtain a homogeneous Euler-Poisson-Darboux equation with integer parameters. This enables us to write down solutions corresponding to incoming and outgoing gravitational radiation, and ultimately to formulate absorbing boundary conditions for gravitational radiation on a flat background.

5.3.1 Hertz Potentials on a Minkowski Background

Consider a Minkowski background with coordinate chart (u, v, θ, ϕ). Here, as in §5.2, θ and ϕ are spherical polar coordinates and u and v are the standard advanced and retarded time coordinates

$$u = t - r, \quad v = t + r. \tag{5.27}$$

With respect to the NP tetrad

$$\begin{aligned} &l^a = (0, 2, 0, 0), \quad n^a = (1, 0, 0, 0), \quad m^a = 2^{-1/2}(0, 0, r^{-1}, -ir^{-1}\csc\theta), \\ &l_a = (1, 0, 0, 0), \quad n_a = (0, \tfrac{1}{2}, 0, 0), \quad m_a = 2^{-1/2}(0, 0, -r, ir\sin\theta), \end{aligned} \tag{5.28}$$

the only non-vanishing NP scalars are

$$\rho = -r^{-1}, \quad \rho' = \tfrac{1}{2}r^{-1}, \quad \beta = \beta' = 2^{-3/2}r^{-1}\cot\theta. \tag{5.29}$$

The Hertz potential χ' (4.34) has GHP type $\{4, 0\}$ and therefore it has spin $s = 2$. Following the method detailed in [107] we decompose it in terms of spin-weighted spherical harmonics

$$\chi' = \sum_{l,m} \chi^{lm}(u, v)\,{}_2Y_{lm}(\theta, \phi). \tag{5.30}$$

There are many different conventions that can be used for spin-weighted spherical harmonics (see for example [21,57,99,135]). Appendix C.2 contains details

of the conventions used here. These conventions have been chosen to render the calculations in this thesis as simple as possible. Note that ${}_sY_{lm} \equiv 0$ for $l < |s|$, so the $l = 0$ (monopole) and $l = 1$ (dipole) cases would have to be treated separately. However, since gravitational monopoles and dipoles are non-radiative, these are not of interest in this study.

On a Minkowski background, the field equation for χ' (4.36) becomes

$$(\text{Þ}\text{Þ}' - \eth\eth' + 3\rho'\text{Þ} - \rho\text{Þ}')\,\chi' = 0. \tag{5.31}$$

Using the tetrad (5.28) and the NP scalars (5.29), the derivations Þ, Þ′, ð and ð′, which were defined in (4.33), can be expressed in terms of the coordinates u, v, θ and ϕ. For a quantity η of GHP type $\{p, q\}$

$$\begin{aligned}
\text{Þ}\eta &= 2\frac{\partial}{\partial v}\eta, \\
\text{Þ}'\eta &= \frac{\partial}{\partial u}\eta, \\
\eth\eta &= 2^{-1/2}r^{-1}\left(\frac{\partial}{\partial\theta} + i\csc\theta\,\frac{\partial}{\partial\phi} - \tfrac{1}{2}[p-q]\cot\theta\right)\eta, \\
\eth'\eta &= 2^{-1/2}r^{-1}\left(\frac{\partial}{\partial\theta} + i\csc\theta\,\frac{\partial}{\partial\phi} + \tfrac{1}{2}[p-q]\cot\theta\right)\eta.
\end{aligned} \tag{5.32}$$

Note that Þ and Þ′ contain u and v derivatives but no angular derivatives, and so have no effect on the spin-weighted spherical harmonics. The derivations ð and ð′ are precisely the same as those used in appendix C.2 to define the spin-weighted spherical harmonics (C.8), since $s = \frac{1}{2}(p-q)$. We can therefore make use of the eigenvalue equation (C.11). Substitution of (5.29), (5.30), (5.32) and (C.11) into (5.31) yields

$$\sum_{l,m}\left\{\chi^{lm}{}_{,uv} + \frac{1}{v-u}\chi^{lm}{}_{,u} + \frac{3}{v-u}\chi^{lm}{}_{,v} + \frac{(l+2)(l-1)}{(v-u)^2}\chi^{lm}\right\}{}_2Y_{lm}(\theta,\phi) = 0. \tag{5.33}$$

By considering a single mode, we conclude that

$$\chi^{lm}{}_{,uv} + \frac{1}{v-u}\chi^{lm}{}_{,u} + \frac{3}{v-u}\chi^{lm}{}_{,v} + \frac{(l+2)(l-1)}{(v-u)^2}\chi^{lm} = 0. \tag{5.34}$$

This is an Euler-Poisson-Darboux (EPD) equation. (It is interesting to note at this point that the "master equation" found in [22] governing the behaviour

of linearized gravitational waves on a Minkowski background is also an EPD equation. This can be seen by using characteristic variables u and v). The equation (5.34) can be cast into the form (5.4) by making a change of dependent variable

$$\chi^{lm}(u,v) = (v-u)^{l+2}\omega^{lm}(u,v), \tag{5.35}$$

to obtain

$$\omega^{lm}{}_{,uv} + \frac{l+3}{v-u}\omega^{lm}{}_{,u} - \frac{l-1}{v-u}\omega^{lm}{}_{,v} = 0, \tag{5.36}$$

which has the general solution

$$\omega^{lm}(u,v) = \left(\frac{\partial}{\partial v}\right)^{l+2} \frac{A^{lm}(v)}{(v-u)^{l-1}} + \left(\frac{\partial}{\partial u}\right)^{l-2} \frac{B^{lm}(u)}{(v-u)^{l+3}}, \tag{5.37}$$

for some $A^{lm}(v)$ and $B^{lm}(u)$. The general solution of (5.34) is then

$$\chi^{lm} = (v-u)^{l+2}\left[\left(\frac{\partial}{\partial v}\right)^{l+2} \frac{A^{lm}(v)}{(v-u)^{l-1}} + \left(\frac{\partial}{\partial u}\right)^{l-2} \frac{B^{lm}(u)}{(v-u)^{l+3}}\right]. \tag{5.38}$$

By considering the characteristic initial value problem in precisely the same way as in §5.2, we might interpret $B^{lm}(u)$ as representing "outgoing" radiation and $A^{lm}(v)$ as representing "incoming" radiation. In fact, we can be more specific than this. In §5.3.3 we construct the perturbed Weyl scalars induced by the Hertz potential χ'. It has been posited [104] that outgoing gravitational 2^l-poles on $\mathscr{I}^+$ peel; that is $\Psi_n \sim r^{n-5}$. An analogous result holds for incoming radiation on $\mathscr{I}^-$: $\Psi_n \sim r^{-n-1}$ (see chapters 2 and 3 for details on the peeling theorem in the full nonlinear theory of relativity). This peeling behaviour is matched precisely by the Weyl scalars constructed from "outgoing" solutions $B^{lm}(u)$ on $\mathscr{I}^+$, and by "incoming" solutions $A^{lm}(v)$ on $\mathscr{I}^-$ (see table 5.1). We conclude that the term

$$(v-u)^{l+2}\left(\frac{\partial}{\partial v}\right)^{l+2} \frac{A^{lm}(v)}{(v-u)^{l-1}}, \tag{5.39}$$

represents "incoming" linearized 2^l-pole gravitational radiation, whereas the term

$$(v-u)^{l+2}\left(\frac{\partial}{\partial u}\right)^{l-2} \frac{B^{lm}(u)}{(v-u)^{l+3}}, \tag{5.40}$$

represents "outgoing" 2^l-pole radiation (this result was first obtained in [107]).

It is this separation of incoming and outgoing radiation that will enable us to formulate absorbing boundary conditions for numerical relativity.

We consider now the characteristic initial value problem for the Euler-Poisson-Darboux equation (5.34). Suppose that an astrophysical event occurs which emits an outgoing gravitational wave on a Minkowski background. We take this wave to be our initial data. In the characteristic initial value problem, this corresponds to specifying data on the characteristic $v = v_0$, shown below in figure 5.2.

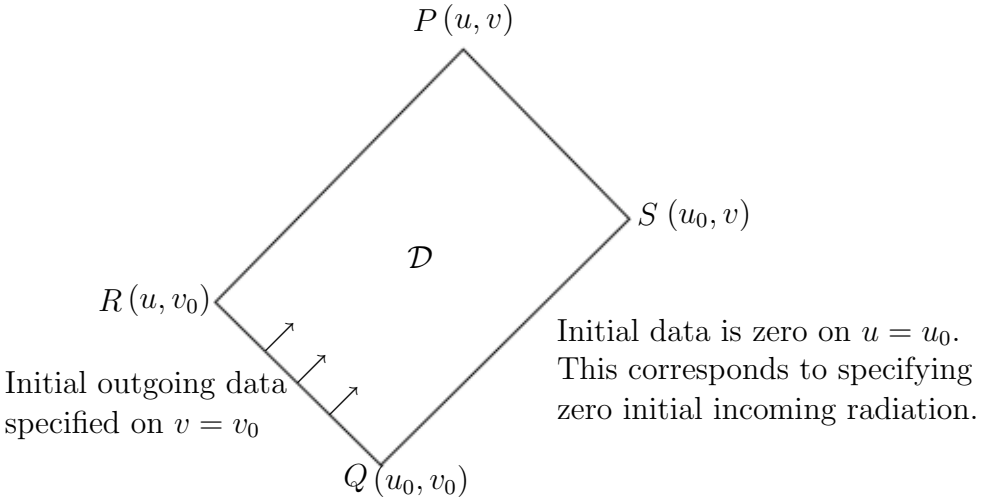

Figure 5.2: Specifying data only on $v = v_0$ results in a purely outgoing radiative solution.

Consider first the case $l = 2$ (so that $m = 0, \pm 1, \pm 2$). From (5.38), the general outgoing solution to (5.34) is

$$\chi^{2\,m}_{\text{out}} = \frac{B^{2\,m}(u)}{v - u}. \tag{5.41}$$

For initial data on $v = v_0$ given by $C^{2\,m}(u)$, it is then immediate that

$$B^{2\,m}(u) = (v_0 - u)C^{2\,m}(u). \tag{5.42}$$

Therefore compact support of the initial data leads to a general solution with compact support. This is sharp propagation and the gravitational wave obeys Huygens' principle (§5.2).

For $l = 3$ the general outgoing solution is

$$\chi^{3\,m}_{\rm out} = (v-u)^5 \frac{\partial}{\partial u} \frac{B^{3\,m}(u)}{(v-u)^6}. \tag{5.43}$$

Then for initial data $C^{3\,m}(u)$ on $v = v_0$, we have

$$B^{3\,m}(u) = (v_0-u)^6 \int_{u_0}^{u} \frac{C^{3\,m}(u')}{(v_0-u')^5} \mathrm{d}u'. \tag{5.44}$$

If $C^{3\,m}(u)$ has compact support, then the general solution (5.43) does not necessarily have compact support. (For example if $C^{3\,m}(u) = \delta(u-u_a)$ then $B^{3\,m} = \frac{(v_0-u)^6}{(v_0-u_a)^5}$.) It is easy to check that this is true for all $l \geq 3$. Thus for $l \geq 3$, gravitational radiation does not obey Huygens' principle. Once the initial wave has passed a given point, there is a leftover excitation in the field, known as the *geometrical tail*.

In a similar manner to the spin-zero massless scalar field (§5.2), the geometrical tail for $l \geq 3$ arises due to the complex angular dependence of the spin-weighted spherical harmonics. This angular dependence prevents solutions from propagating purely radially, and causes interference. However, for $l = 2$ the propagation of gravitational waves is not purely radial either. In fact ${}_2Y_{20} \propto \sin^2\theta$. Why then is there no geometrical tail in the case $l = 2$? In [19], by adding a perturbation approximation to the asymptotic expansion of Bondi et al. [18], it was shown that a quadrupole tail arises due to the interaction of quadrupole radiation with the gravitational monopole. Since we are perturbing about Minkowski spacetime here, there is no monopole present in the background, and therefore there is no quadrupole tail. In chapters 6 and 7, in which a gravitational monopole is present, we will find that the quadrupole radiation does in fact admit a tail. Huygens' principle is therefore never satisfied for gravitational radiation propagating on a curved spacetime.

Waylen [146] has shown, in a similar manner to McLenaghan [91], that linearized gravitational radiation satisfies Huygens' principle only on flat or plane-wave backgrounds. Just as in the scalar field case of the previous section, the results here are slightly different. Waylen considered the linearized Einstein field equations in the full four-dimensional spacetime. We have used spin-weighted spherical harmonics to factor out the angular dependence of the gravitational field and are considering wave equations for the χ^{lm} rather

than χ' (5.30). We are thus investigating Huygens' principle for the χ^{lm} in an unphysical two-dimensional spacetime.

We can extend the results above to fields of arbitrary spin on a Minkowski background. Let the complex scalar field Ψ have spin s. If we decompose Ψ in terms of spin-weighted spherical harmonics

$$\Psi(u,v) = \sum_{l,m} (v-u)^{l+s} \Psi^{lm}(u,v)\, {}_sY_{lm}(\theta,\phi), \tag{5.45}$$

then the spin-s wave equation becomes

$$\Psi^{lm}{}_{,uv} + \frac{l+s+1}{v-u}\Psi^{lm}{}_{,u} - \frac{l-s+1}{v-u}\Psi^{lm}{}_{,v} = 0, \tag{5.46}$$

which has the general solution

$$\Psi^{lm}(u,v) = \left(\frac{\partial}{\partial u}\right)^{l-s} \frac{\tilde{B}^{lm}(u)}{(v-u)^{l+s+1}} + \left(\frac{\partial}{\partial v}\right)^{l+s} \frac{\tilde{A}^{lm}(v)}{(v-u)^{l-s+1}}. \tag{5.47}$$

The terms involving $B^{lm}(u)$ represent outgoing radiation. Consistent with our earlier results, it is clear that sharp propagation is only possible if $l = s$. If $l > s$ then, for generic initial data $C^{lm}(u)$, spreading occurs and a geometrical tail is present. Note that for certain specific choices of $C^{lm}(u)$ with compact support, we can arrange that the first $l - s$ integrals of $C^{lm}(u)$ have compact support, and hence $\tilde{B}^{lm}(u)$ also has compact support, so that no spreading occurs. However this is not true of generic initial data.

5.3.2 Absorbing Boundary Conditions on a Minkowski Background

On a Minkowski background, the incoming and outgoing solutions propagate independently. If the initial data is posited to be purely outgoing then the solution should remain purely outgoing. However, if an artificial boundary $\partial\Omega$ of the computational domain is introduced then reflection off the boundary may produce incoming radiation. Boundary conditions imposed on $\partial\Omega$ should therefore remove all incoming radiation.

The Weyl scalars Ψ_i are chart-independent and contain all the information about the radiative behaviour of the gravitational field in a vacuum. They are

therefore the natural candidates for quantities on which to impose boundary conditions.

The general solution to the homogeneous Euler-Poisson-Darboux equation (5.38) can be expanded and written in the form

$$\begin{aligned}\chi^{lm} =& \frac{A_0^{lm}(v)}{(v-u)^{l-1}} + \frac{A_1^{lm}(v)}{(v-u)^{l-2}} + \cdots + A_{l+2}^{lm}(v)(v-u)^3 \\ &+ \frac{B_0^{lm}(u)}{(v-u)^{l-1}} + \frac{B_1^{lm}(u)}{(v-u)^{l-2}} + \cdots + \frac{B_{l-2}^{lm}(u)}{(v-u)},\end{aligned} \tag{5.48}$$

where the functions $A_i^{lm}(v)$ and $B_i^{lm}(u)$ can easily be expressed as linear combinations of the derivatives of the $A^{lm}(v)$ and $B^{lm}(u)$ respectively. Substituting (5.48) into the expressions for the $\hat{\Psi}_i$ (B.6) we find that the Weyl scalars can be written as the sum of incoming and outgoing contributions from each gravitational 2^l-pole

$$\Psi_i = \Psi_i^{\text{out}} + \Psi_i^{\text{in}}, \tag{5.49}$$

where

$$\Psi_i^{\text{out}} = \sum_{l,m} \left\{ \frac{\tilde{B}_0^{lm}(u)}{(v-u)^{l+3}} + \frac{\tilde{B}_1^{lm}(u)}{(v-u)^{l+2}} + \cdots + \frac{\tilde{B}_{l-2+i}^{lm}(u)}{(v-u)^{5-i}} \right\} {}_{i-2}Y_{lm}(\theta,\phi), \tag{5.50}$$

and

$$\Psi_i^{\text{in}} = \sum_{l,m} \left\{ \frac{\tilde{A}_0^{lm}(v)}{(v-u)^{l+3}} + \frac{\tilde{A}_1^{lm}(v)}{(v-u)^{l+2}} + \cdots + \frac{\tilde{A}_{l+2-i}^{lm}(v)}{(v-u)^{i+1}} \right\} {}_{i-2}Y_{lm}(\theta,\phi). \tag{5.51}$$

Again, the functions $\tilde{A}_k^{lm}(v)$ and $\tilde{B}_k^{lm}(u)$ could be expressed as linear combinations of the derivatives of the $A_k^{lm}(v)$ and $B_k^{lm}(u)$ respectively, but this is not necessary here. An absorbing boundary condition should set the $\tilde{A}_k^{lm}(v)$ in (5.51) to be zero on the boundary $\partial\Omega$, whilst ignoring the $\tilde{B}_k^{lm}(u)$.

We can read off, from (5.51), the leading order behaviour of the incoming and outgoing terms in each of the Weyl scalars. These are shown in table 5.1, which shows that Ψ_0 is dominated by incoming radiation. This is why many numerical relativity groups choose to impose their boundary conditions

	Incoming	Outgoing
Ψ_0	$O(r^{-1})$	$O(r^{-5})$
Ψ_1	$O(r^{-2})$	$O(r^{-4})$
Ψ_2	$O(r^{-3})$	$O(r^{-3})$
Ψ_3	$O(r^{-4})$	$O(r^{-2})$
Ψ_4	$O(r^{-5})$	$O(r^{-1})$

Table 5.1: The behaviour of the incoming and outgoing radiative parts of the Weyl scalars near $\mathscr{I}^+$

on it. Below we demonstrate how absorbing boundary conditions could be formulated in terms of Ψ_0.

From (5.51) we obtain

$$\Psi_0^{\text{out}} = \sum_{l,m} \left\{ \frac{\tilde{B}_0^{lm}(u)}{(v-u)^{l+3}} + \frac{\tilde{B}_1^{lm}(u)}{(v-u)^{l+2}} + \cdots + \frac{\tilde{B}_{l-2}^{lm}(u)}{(v-u)^5} \right\} {}_2Y_{lm}(\theta,\phi), \quad (5.52)$$

and

$$\Psi_0^{\text{in}} = \sum_{l,m} \left\{ \frac{\tilde{A}_0^{lm}(v)}{(v-u)^{l+3}} + \frac{\tilde{A}_1^{lm}(v)}{(v-u)^{l+2}} + \cdots + \frac{\tilde{A}_{l+2}^{lm}(v)}{(v-u)} \right\} {}_2Y_{lm}(\theta,\phi). \quad (5.53)$$

At $O(r^{-1})$, $O(r^{-2})$, $O(r^{-3})$ and $O(r^{-4})$ there are no contributions from the outgoing radiation. The outgoing radiative terms do not contribute until $O(r^{-5})$. Therefore an *approximately* absorbing boundary condition (accurate to fourth order) would be to demand that $\Psi_0 = O(r^{-5})$ on $\partial\Omega$. This is similar to the "freezing Ψ_0" condition commonly used in numerical relativity [78,90,114,124].

We can establish the condition $\Psi_0 = O(r^{-5})$ order by order to create a hierarchy of increasingly accurate boundary conditions, similar to those in [22]. From now on we use the symbol $\doteq$ to denote equality only on the boundary $\partial\Omega$. As a first approximation, we impose $\tilde{A}_{l+2}^{lm}(v) \doteq 0$ in (5.53). This removes the leading order incoming radiation term. In a numerical simulation, the $\tilde{A}_k^{lm}(v)$ are not known, but the condition $\tilde{A}_{l+2}^{lm}(v) \doteq 0$ can be expressed as

$$\hat{M}_1\Psi_0 \equiv (v-u)\Psi_0 \doteq O(r^{-1}). \quad (5.54)$$

At second order we must remove the term

$$\frac{\tilde{A}^{lm}_{l+1}(v)}{(v-u)^2}, \tag{5.55}$$

from (5.53). If we have already imposed $\hat{M}_1\Psi_0 \doteq O(r^{-1})$ then (5.55) can be removed by imposing

$$\hat{M}_2\Psi_0 \equiv (v-u)^2\Psi_0 \doteq O(r^{-1}). \tag{5.56}$$

Similarly, having imposed the second order boundary condition, we can impose the third and then the fourth order boundary conditions

$$\hat{M}_3\Psi_0 \equiv (v-u)^3\Psi_0 \doteq O(r^{-1}), \tag{5.57}$$

and

$$\hat{M}_4\Psi_0 \equiv (v-u)^4\Psi_0 \doteq O(r^{-1}). \tag{5.58}$$

At fifth order and above, we must adopt a slightly different approach, since outgoing terms are now also present in Ψ_0. For $k \geq 5$, we define the operators

$$\hat{M}_k \equiv \frac{\partial}{\partial v}(v-u)^k. \tag{5.59}$$

If we have already imposed the lower order boundary conditions ($\hat{M}_j\Psi_0 \doteq O(r^{-1})$ with $j \leq k$) then the leading order term in $\hat{M}_k\Psi_0$ is $\tilde{A}^{lm}_{l+3-k}$, and so we impose the condition

$$\hat{M}_k\Psi_0 \doteq O(r^{-1}). \tag{5.60}$$

Thus we now have a hierarchy of increasingly accurate absorbing boundary conditions. Inspection of (5.53) suggests that imposing this hierarchy up to $\hat{M}_{L+3}$ will remove all the $\tilde{A}^{lm}_j$ from all the gravitational multipoles with angular momentum number $l \leq L$, and so for $l \leq L$ these boundary conditions are perfectly absorbing.

How can a numerical relativist impose a condition such as $\hat{M}_k\Psi_0 \doteq O(r^{-1})$? One approach is to multiply by r and then take the limit $r \to \infty$. However, this is impractical numerically. Bayliss & Turkel [7] encountered a similar situation. They argued that it is valid to simply impose $\hat{M}_k\Psi_0 \doteq 0$.

It was argued in chapter 3 that Ψ_0 cannot in fact be estimated using linearized theory, since at leading order it contained third order terms from the asymptotic expansions of the metric variables. Therefore the boundary conditions defined above are of questionable use in numerical relativity. The calculations of chapter 3 suggest that Ψ_4 is the easiest Weyl scalar to evaluate numerically. Can we formulate appropriate boundary conditions for Ψ_4? Unfortunately, this appears to be a dead end. From (5.51) we obtain

$$\begin{aligned}\Psi_4^{\text{in}} &= \sum_{l,m}\left\{\frac{\tilde{A}_0^{lm}(v)}{(v-u)^{l+3}}+\frac{\tilde{A}_1^{lm}(v)}{(v-u)^{l+2}}+\cdots+\frac{\tilde{A}_{l-2}^{lm}(v)}{(v-u)^5}\right\}{}_2Y_{lm}(\theta,\phi),\\ \Psi_4^{\text{out}} &= \sum_{l,m}\left\{\frac{\tilde{B}_0^{lm}(u)}{(v-u)^{l+3}}+\frac{\tilde{B}_1^{lm}(u)}{(v-u)^{l+2}}+\cdots+\frac{\tilde{B}_{l+2}^{lm}(u)}{(v-u)}\right\}{}_2Y_{lm}(\theta,\phi),\end{aligned}\tag{5.61}$$

where the $\tilde{A}_i^{lm}(v)$ and $\tilde{B}_i^{lm}(u)$ can be expressed as a linear combination of the derivatives of the $A_i^{lm}(v)$ and $B_i^{lm}(u)$ respectively. In order to obtain absorbing boundary conditions we must remove all terms involving the $\tilde{A}_i^{lm}(v)$ on $\partial\Omega$. Such terms do not appear until fifth order. Hence, in order to obtain a boundary condition even for the *leading order* contribution from the incoming radiation, we would need to evaluate Ψ_4 to *fifth order*. This is unlikely to be possible numerically.

Having established that Ψ_0 and Ψ_4 are unsuitable for use in boundary conditions, a compromise is required. The obvious choice is Ψ_2. In chapter 3, we showed that Ψ_2 could be estimated to leading order using linearized theory. Furthermore, perusal of table 5.1 shows that the incoming and outgoing radiative parts in Ψ_2 are on an equal footing.[1] From (5.51) we find

$$\begin{aligned}\Psi_2^{\text{out}} &= \sum_{l,m}\left\{\frac{\tilde{B}_0^{lm}(u)}{(v-u)^{l+3}}+\frac{\tilde{B}_1^{lm}(u)}{(v-u)^{l+2}}+\cdots+\frac{\tilde{B}_l^{lm}(u)}{(v-u)^3}\right\}{}_0Y_{lm}(\theta,\phi),\\ \Psi_2^{\text{in}} &= \sum_{l,m}\left\{\frac{\tilde{A}_0^{lm}(v)}{(v-u)^{l+3}}+\frac{\tilde{A}_1^{lm}(v)}{(v-u)^{l+2}}+\cdots+\frac{\tilde{A}_l^{lm}(v)}{(v-u)^3}\right\}{}_0Y_{lm}(\theta,\phi).\end{aligned}\tag{5.62}$$

As before, we can proceed order by order, by removing the incoming terms (terms involving the $\tilde{A}_k^{lm}$). At leading order we obtain a Sommerfeld-type

[1] Could we also have chosen Ψ_1 or Ψ_3? It appears not. We argued in chapter 3 that Ψ_1 cannot be estimated in linearized theory. Furthermore Ψ_3 is dominated by outgoing radiation and so we would encounter a similar problem to the one described above for Ψ_4.

condition:

$$\hat{N}_1\Psi_2 \equiv \frac{\partial}{\partial v}(v-u)^3\Psi_2 \doteq O(r^{-1}), \tag{5.63}$$

which is equivalent to the condition $\tilde{A}_l^{lm}(u) \doteq 0$. Consider now the operator

$$\hat{N}_k\Psi_2 \equiv \frac{\partial}{\partial v}(v-u)^{2+k}\Psi_2. \tag{5.64}$$

Successively imposing $\hat{N}_k\Psi_2 \doteq O(r^{-1})$ for $k = 1, 2, \ldots$ removes the incoming radiation terms from Ψ_2, order by order. Again, we can argue that it is sufficient to impose $\hat{N}_k\Psi_2 \doteq 0$. By inspection of (5.62) we can deduce that using $\hat{N}_{L+3}$ in the hierarchy will result in perfectly absorbing boundary conditions for gravitational poles with $l \leq L$.

The operators $\hat{N}_k$ would be difficult to implement numerically owing to the high powers of r involved. An equivalent set of operators can be obtained by dividing through by $(v-u)^{2+k}$. We then define

$$\hat{O}_k \equiv \frac{\partial}{\partial v} + \frac{2+k}{v-u}, \tag{5.65}$$

and impose

$$\hat{O}_k\Psi_2 \doteq O(r^{-3-k}). \tag{5.66}$$

The sequence of boundary conditions defined by $\hat{O}_k$ has the same absorbing properties as the $\hat{N}_k$, but is easier to implement numerically. However, a numerical relativist cannot impose all the boundary conditions above at various different orders simultaneously. We therefore need to combine the $\hat{O}_k$ into a single boundary condition. Following the method of Bayliss & Turkel [7], we could impose the product

$$\prod_{k=1}^{L+3}\left(\frac{\partial}{\partial v} + \frac{2+k}{v-u}\right)\Psi_2 \doteq 0. \tag{5.67}$$

This sequence could then be used to any desired value of L, and would result in perfectly absorbing boundary conditions for gravitational radiation with $l \leq L$. It is the boundary condition (5.67) that a numerical relativist would ultimately use. It is no coincidence that the sequence of boundary conditions (5.67) is very similar in form to the B_m operators devised by Bayliss & Turkel [7]. Their approach was also to seek operators which kill off outgoing terms in solutions

to wave-like equations.

Buchman & Sarbach [22] also obtained a hierarchy of perfectly absorbing boundary conditions for linearized gravitational radiation on a Minkowski background with $l \leq L$. Their "master equation" governing the propagation of linearized gravitational radiation was expressed in terms of Ψ_2 and they were able to express their boundary conditions both in terms of Ψ_2 and Ψ_0. Within linearized theory both sets of boundary conditions could in principle be used to any desired order of accuracy. However, in the full nonlinear investigation of chapter 3 we found that nonlinear terms arose in the leading and second order terms of Ψ_0 and Ψ_2 respectively. Therefore we cannot justify the use of boundary conditions for the Weyl scalars, derived using linearized theory, beyond leading order.

5.3.3 An Aside on the Peeling of Linearized Gravitational Radiation

The study of Hertz potentials on a Minkowski background also enables us to investigate the peeling property of the Weyl scalars and the outgoing radiation condition, both in linearized theory. Both were discussed in the full nonlinear theory of relativity in chapters 2 and 3.

Gravitational fields are said to be *asymptotically regular* if they *peel* in the usual way as we approach null infinity; that is $\Psi_i = O(r^{-i-1})$ on $\mathscr{I}^-$ and $\Psi_i = O(r^{i-5})$ on $\mathscr{I}^+$. We will restrict our attention to future null infinity, $\mathscr{I}^+$, although the analysis works analogously on $\mathscr{I}^-$ by reversing the direction of time. Future null infinity is obtained by taking the limit $v \to \infty$ whilst u, θ and ϕ remain constant. For a solution consisting entirely of outgoing linearized gravitational radiation only and no incoming radiation, it is immediate from (5.51) and table 5.1 that $\Psi_i^{\text{out}} = O(r^{i-5})$ near $\mathscr{I}^+$ (and similarly $\Psi_i^{\text{in}} = O(r^{-i-1})$ near $\mathscr{I}^-$). Thus outgoing radiation peels in the usual way. For a solution containing only incoming radiation, recall from (5.51) that

$$\Psi_i^{\text{in}} = \sum_{l,m} \left\{ \frac{\tilde{A}_0^{lm}(v)}{(v-u)^{l+3}} + \frac{\tilde{A}_1^{lm}(v)}{(v-u)^{l+2}} + \cdots + \frac{\tilde{A}_{l+2-i}^{lm}(v)}{(v-u)^{i+1}} \right\} {}_{i-2}Y_{lm}(\theta,\phi). \quad (5.68)$$

Without specifying the behaviour of the $\tilde{A}_j^{lm}(v)$ as $v \to \infty$, we cannot de-

termine whether the fields peel as we approach $\mathscr{I}^+$. In order to guarantee $\Psi_i^{\text{in}} = O(r^{i-5})$ on $\mathscr{I}^+$, we must impose conditions on the asymptotic behaviour of the $A^{lm}(v)$ (which were defined in (5.38)):

$$A^{lm}(v) = O(v^{l-2}), \quad \left(\frac{\partial}{\partial v}\right) A^{lm}(v) = O(v^{l-3}), \ldots, \left(\frac{\partial}{\partial v}\right)^{l-1} A^{lm}(v) = O(v^{-1}), \tag{5.69}$$

as $v \to \infty$. These conditions can be satisfied by demanding that $A^{lm}(v)$ grows no faster than a polynomial of order $l-2$ as $v \to \infty$. We interpret this condition as the *outgoing radiation condition* for linearized gravitational waves, or the *linearized outgoing radiation condition*. This is analogous to the outgoing radiation condition found in the study of nonlinear gravitational radiation (see [18,40,81] and chapters 2 and 3), which regulates the amount of incoming radiation from $\mathscr{I}^+$ to ensure that the peeling assumption holds. The relationship between the two conditions cannot be made precise because we are now working in linearized theory. Analogous "incoming radiation conditions" hold on $\mathscr{I}^+$, which result in conditions similar to (5.69) being imposed on the $B^{lm}(u)$.

To measure the amount of energy carried by gravitational radiation one might compute the Bondi mass $M_B(u)$ and the news function $\mathcal{N}$ (see chapters 2 and 3 and [18, 40, 134]). With a suitable choice of radial coordinate r, the Bondi mass is given by

$$4\pi M_B(u) = -\lim_{r\to\infty} \int\int r^3 \left(\Psi_2 - \sigma\sigma'\right) \mathrm{d}S, \tag{5.70}$$

where $\mathrm{d}S$ is the area element of the unit sphere. Also

$$\mathcal{N} = -\lim_{r\to\infty} r\sigma'. \tag{5.71}$$

The perturbations induced by the Hertz potential are then given by

$$4\pi \hat{M}_B(u) = -\lim_{r\to\infty} \int\int r^3 \hat{\Psi}_2 \mathrm{d}S, \tag{5.72}$$

and

$$\hat{\mathcal{N}} = -\lim_{r\to\infty} r\hat{\sigma}' \tag{5.73}$$

However since the standard mass-loss equation involves the square of the news function we are unable to compute it consistently within linearized theory.

Chapter 6

Hertz Potentials on a Schwarzschild Background

In deriving the boundary conditions of chapter 5, we assumed that the spacetime in the far-field region could be described by a perturbation about flat space. We obtained a hierarchy of boundary conditions in a similar manner to Buchman & Sarbach [22]. In a numerical relativity simulation, a mass M might be present in the near-field region, and so it is more accurate to describe the far-field region by a perturbation about a Schwarzschild background. Buchman & Sarbach generalized their calculation to incorporate first order effects due to M [23]. By considering the Hertz potential field equation (4.36) on a Schwarzschild background we can also take M into account. We expect the solutions to (4.36) to be altered due to the presence of the background Weyl curvature. Our approach, based on integral representations of solutions to inhomogeneous Euler-Poisson-Darboux equations, is similar to that of Schmidt & Stewart [128], who studied the scalar wave equation on a Schwarzschild background.

Boundary conditions which take into account the Weyl curvature of the Schwarzschild background will naturally depend intrinsically on the mass parameter M. A numerical relativist would therefore need to accurately evaluate this quantity during the evolution of the spacetime. One possible approach would be to use the results of chapter 3 to evaluate the Bondi mass. Nevertheless, estimating M is a non-tivial problem in numerical relativity.

6.1 The Hertz Potential Field Equation on a Schwarzschild Background

We use the coordinate chart (u, v, θ, ϕ) with advanced and retarded time coordinates, v and u, given by

$$v = t + r^*, \quad u = t - r^*, \tag{6.1}$$

where

$$r^* = r + 2M \log\left(\frac{r}{2M} - 1\right). \tag{6.2}$$

We choose the Newman-Penrose tetrad

$$\begin{aligned} &l^a = (0, 2F^{-1}, 0, 0), \quad n^a = (1, 0, 0, 0), \quad m^a = 2^{-1/2}(0, 0, r^{-1}, -ir^{-1}\csc\theta), \\ &l_a = (1, 0, 0, 0), \quad n_a = (0, \tfrac{1}{2}F, 0, 0), \quad m_a = 2^{-1/2}(0, 0, -r, \mathrm{i}r\sin\theta), \end{aligned} \tag{6.3}$$

where

$$F = 1 - \frac{2M}{r}. \tag{6.4}$$

With respect to this tetrad, the only non-vanishing NP and Weyl scalars are

$$\begin{aligned} &\rho = -r^{-1}, \quad \rho' = \frac{1}{2}r^{-1}F, \quad \epsilon' = -\frac{1}{2}Mr^{-2}, \\ &\beta = \beta' = 2^{-3/2}r^{-1}\cot\theta, \quad \Psi_2 = -Mr^{-3}. \end{aligned} \tag{6.5}$$

As was done in §5.3, we decompose χ' in terms of spin-weighted spherical harmonics

$$\chi' = \sum_{l,m} \chi^{lm}(u, v)\,{}_2Y_{lm}(\theta, \phi). \tag{6.6}$$

On a Schwarzschild background the field equation (4.36) becomes

$$(\text{Þ}\text{Þ}' - \eth\eth' + 3\rho'\text{Þ} - \rho\text{Þ}' - 6\Psi_2)\,\chi' = 0. \tag{6.7}$$

Using the tetrad (6.3) and the NP scalars (6.5), the derivations Þ, Þ′, ð and ð′ can be expressed in terms of the coordinates u, v, θ and ϕ. For a quantity

η of GHP type $\{p, q\}$,

$$\begin{aligned}
\text{Þ}\eta &= 2\frac{\partial}{\partial v}\eta \\
\text{Þ}'\eta &= \left(\frac{\partial}{\partial u} - \tfrac{1}{2}[p+q]Mr^{-2}\right)\eta \\
\eth\eta &= 2^{-1/2}r^{-1}\left(\frac{\partial}{\partial\theta} + i\csc\theta\,\frac{\partial}{\partial\phi} - \tfrac{1}{2}[p-q]\cot\theta\right)\eta \\
\eth'\eta &= 2^{-1/2}r^{-1}\left(\frac{\partial}{\partial\theta} + i\csc\theta\,\frac{\partial}{\partial\phi} + \tfrac{1}{2}[p-q]\cot\theta\right)\eta.
\end{aligned} \tag{6.8}$$

Note again that Þ and Þ′ do not involve angular derivatives and so have no effect on the spin-weighted spherical harmonics. Due to our choice of m^a, the $\eth$ and $\eth'$ above match precisely the $\eth$ and $\eth'$ of (C.8) and so, as in §5.3.1, we are able to use the eigenvalue equation (C.11) once more. For $l \geq 2$, the field equation (6.7) becomes

$$\begin{aligned}
\sum_{l,m}\Big\{&\chi^{lm}{}_{,uv} + \frac{1}{2r}\chi^{lm}{}_{,u} + \frac{3}{2r}\chi^{lm}{}_{,v} + \frac{l_c}{4r^2}\chi^{lm} \\
&-\frac{M}{r^2}\chi^{lm}{}_{,u} - \frac{5M}{r^2}\chi^{lm}{}_{,v} - \frac{M}{r^3}\left(l_c - 4F\right)\chi^{lm}\Big\}\,{}_2Y_{lm}(\theta,\phi),
\end{aligned} \tag{6.9}$$

where

$$l_c = \frac{1}{2}(l+2)(l-1). \tag{6.10}$$

Since the angular dependence of the field has decoupled, we can consider a single harmonic mode and deduce that

$$\begin{aligned}
&\chi^{lm}{}_{,uv} + \frac{1}{2r}\chi^{lm}{}_{,u} + \frac{3}{2r}\chi^{lm}{}_{,v} + \frac{l_c}{4r^2}\chi^{lm} \\
&\qquad = \frac{M}{r^2}\chi^{lm}{}_{,u} + \frac{5M}{r^2}\chi^{lm}{}_{,v} + \frac{M}{r^3}\left(l_c - 4F\right)\chi^{lm},
\end{aligned} \tag{6.11}$$

Substituting the expression

$$r^{-1} = r^{*-1}\left(1 + \frac{2M}{r}\log\left(\frac{r}{2M} - 1\right)\right), \tag{6.12}$$

into (6.11), we obtain

$$\begin{aligned}\chi^{lm}{}_{,uv}&+\frac{1}{v-u}\chi^{lm}{}_{,u}+\frac{3}{v-u}\chi^{lm}{}_{,v}+\frac{l_c}{(v-u)^2}\chi^{lm}\\ &=-\frac{2M}{r(v-u)}\log\left(\frac{r}{2M}-1\right)\chi^{lm}{}_{,u}-\frac{6M}{r(v-u)}\log\left(\frac{r}{2M}-1\right)\chi^{lm}{}_{,v}\\ &\quad-\frac{l_c}{(v-u)^2}\left(\frac{4M}{r}\log\left(\frac{r}{2M}-1\right)+\frac{4M^2}{r^2}\left[\log\left(\frac{r}{2M}-1\right)\right]^2\right)\\ &\quad+\frac{M}{r^2}\chi^{lm}{}_{,u}+\frac{5M}{r^2}\chi^{lm}{}_{,v}+\frac{M}{r^3}\left(l_c-4F\right)\chi^{lm},\end{aligned}\tag{6.13}$$

The relationship with the Minkowski background calculation now becomes apparent. Equation (6.13) is the same Euler-Poisson-Darboux equation as (5.34) but now with additional "source" terms which are present only if $M\neq 0$.

Since we are interested in the behaviour of solutions as $v\to\infty$, we next use the expression

$$r^{-1}=\frac{2}{v-u}+\frac{8M\log\left(\frac{v-u}{2M}\right)}{(v-u)^2}+O\left(\frac{\left[M\log\left(\frac{v-u}{2M}\right)\right]^2}{(v-u)^3}\right),\tag{6.14}$$

which is obtained from (6.12), to make a polyhomogeneous expansion of the source term in terms of $v-u$,

$$\begin{aligned}\chi^{lm}{}_{,uv}&+\frac{1}{v-u}\chi^{lm}{}_{,u}+\frac{3}{v-u}\chi^{lm}{}_{,v}+\frac{(l+2)(l-1)}{(v-u)^2}\chi^{lm}\\ &=-\left[\frac{4M\log\left(\frac{v-u}{2M}\right)}{(v-u)^2}-\frac{4M}{(v-u)^2}+O\left(\frac{\left[M\log\left(\frac{v-u}{2M}\right)\right]^2}{(v-u)^3}\right)\right]\chi^{lm}{}_{,u}\\ &\quad+\left[-\frac{12M\log\left(\frac{v-u}{2M}\right)}{(v-u)^2}+\frac{20M}{(v-u)^2}+O\left(\frac{\left[M\log\left(\frac{v-u}{2M}\right)\right]^2}{(v-u)^3}\right)\right]\chi^{lm}{}_{,v}\\ &\quad+\left[-\frac{8Ml_c\log\left(\frac{v-u}{2M}\right)}{(v-u)^3}+\frac{M(8l_c-32)}{(v-u)^3}+O\left(\frac{\left[M\log\left(\frac{v-u}{2M}\right)\right]^2}{(v-u)^4}\right)\right]\chi^{lm}.\end{aligned}\tag{6.15}$$

Finally it will be convenient to make a change of dependent variable via

$$\chi'_{lm}(u,v)=(v-u)^{1-l}\omega^{lm}(u,v).\tag{6.16}$$

With this change of variable, (6.15) becomes

$$\omega^{lm}{}_{,uv} - \frac{l-2}{v-u}\omega^{lm}{}_{,u} + \frac{l+2}{v-u}\omega^{lm}{}_{,v} = S^{lm}(u,v;\omega^{lm}(u,v)), \tag{6.17}$$

where

$$\begin{aligned} S^{lm}(u,v;\omega^{lm}) = &\left(\omega^{lm}{}_{,u} - \frac{(1-l)}{v-u}\omega^{lm}\right) S_1(u,v) \\ &+ \left(\omega^{lm}{}_{,v} + \frac{(1-l)}{v-u}\omega^{lm}\right) S_2(u,v) + \omega^{lm} S_3(u,v), \end{aligned} \tag{6.18}$$

and

$$\begin{aligned} S_1(u,v) &= -\frac{4M\log\left(\frac{v-u}{2M}\right)}{(v-u)^2} + \frac{4M}{(v-u)^2} + O\left(\frac{\left[M\log\left(\frac{v-u}{2M}\right)\right]^2}{(v-u)^3}\right) \\ S_2(u,v) &= -\frac{12M\log\left(\frac{v-u}{2M}\right)}{(v-u)^2} + \frac{20M}{(v-u)^2} + O\left(\frac{\left[M\log\left(\frac{v-u}{2M}\right)\right]^2}{(v-u)^3}\right) \\ S_3(u,v) &= -\frac{8Ml_c\log\left(\frac{v-u}{2M}\right)}{(v-u)^3} + \frac{M(8l_c-32)}{(v-u)^3} + O\left(\frac{\left[M\log\left(\frac{v-u}{2M}\right)\right]^2}{(v-u)^4}\right). \end{aligned} \tag{6.19}$$

In §6.2 we will estimate the effect of the source terms (6.18) on the solutions of (6.17). Firstly however, we discuss how the use of spin-weighted spherical harmonics enables us to recover the Hertz potential from the curvature perturbations given in appendix B.2.

6.1.1 An Aside on Recovering the Hertz Potential from the Curvature Perturbation

The spherical harmonic decomposition (6.6) allowed us to factor out the angular dependence of the Hertz potential. By seeking a linear combination of the perturbed Newman-Penrose scalars which only depend on the angular derivatives of χ' (that is $\eth\chi'$ and $\eth'\chi'$) it is possible to recover the potential from the curvature perturbation.

Perusing appendix B.2 we note that, using the commutator equations for the GHP operators Þ, $\text{Þ}'$, $\eth$ and $\eth'$ [53] and the field equation for χ' (4.36), $\hat{\kappa}$

can be written as

$$\hat{\kappa} = -\eth^3\bar{\chi}' + \eth\eth'^2\chi' - 2\rho'\eth'\text{Þ}\chi' + 2\rho\eth'\text{Þ}'\chi' + 4\Psi_2\eth\chi'. \tag{6.20}$$

It follows that

$$\Psi_2\hat{\kappa} - \tfrac{4}{3}\eth'\hat{\Psi}_0 = -\eth^3\bar{\chi}' + \eth\eth'^2\chi' - \tfrac{2}{3}\eth'\eth^4\bar{\chi}'. \tag{6.21}$$

Substituting the spin-weighted spherical harmonic decomposition (6.6) into (6.21) yields

$$\Psi_2\hat{\kappa} - \tfrac{4}{3}\eth'\hat{\Psi}_0 = \left\{Ar^{-3}\chi^{lm} + (Br^{-3} + Cr^{-5})\bar{\chi}^{lm}\right\}{}_1Y_{lm}(\theta,\phi), \tag{6.22}$$

where

$$\begin{aligned} A &= 2^{-3/2}\left(\frac{(l-2)(l-1)l}{(l+3)(l+2)(l+1)}\right)^{1/2}, \\ B &= -2^{-3/2}\left(\frac{(l+2)}{(l-1)}\right)^{1/2}, \\ C &= -\frac{1}{3}2^{-3/2}\left(\frac{(l+2)}{(l-1)}\right)^{1/2}. \end{aligned} \tag{6.23}$$

Therefore by evaluating the real and imaginary parts of

$$\lim_{r\to\infty} r^3 \int\int \left(\Psi_2\hat{\kappa} - \tfrac{4}{3}\eth'\hat{\Psi}_0\right){}_1\bar{Y}_{lm}(\theta,\phi)\mathrm{d}S, \tag{6.24}$$

where $\mathrm{d}S$ is the area element of the unit sphere, we can evaluate χ^{lm} and thus recover the Hertz potential χ'.

6.2 The Inhomogeneous Euler-Poisson-Darboux Equation

6.2.1 The Riemann Representation of Solutions to the Characteristic Initial Value Problem

The field equation (6.17) is an inhomogeneous Euler-Poisson-Darboux equation whose solutions can be written down in integral form using Riemann's method. Most of the literature on Riemann's method deals only with the Cauchy problem (see for example [36,37]) rather than the characteristic initial value problem, which is of interest to us here. The derivation of the integral representation of solutions to the characteristic initial value problem is very similar to that of the Cauchy problem [137]. We state the general result below.

Consider the inhomogeneous partial differential equation for the variable $z(u, v)$,

$$L[z] = z_{,uv} + a(u, v)z_{,u} + b(u, v)z_{,v} + cz = S(u, v), \tag{6.25}$$

where a and b are functions and $S(u, v)$ is a "source term". Characteristic initial data are specified on the surfaces QR ($v = v_0$) and QS ($u = u_0$), shown in figure 6.1. The initial data on QR and QS are $z(u, v_0) = f(u)$ and $z(u_0, v) = g(v)$ respectively (note that we also require $f(u_0) = g(v_0)$). The characteristic initial value problem then requires us to find the unique solution to (6.25) at the point P, which satisfies these initial data.

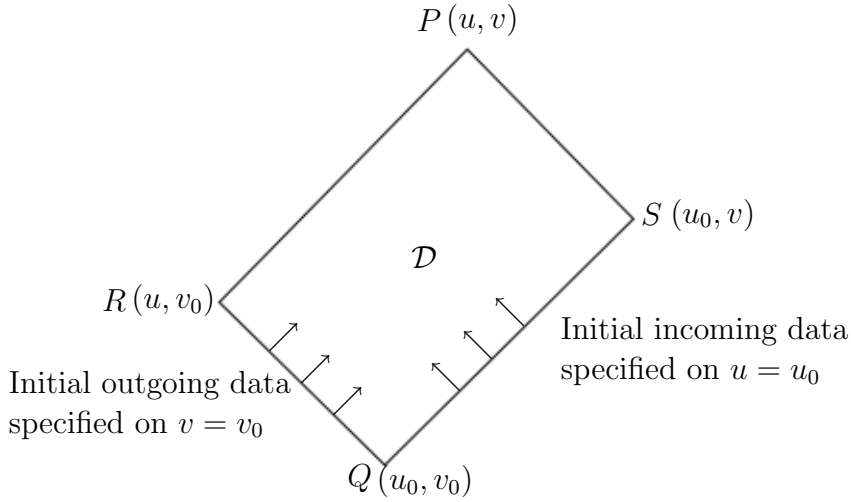

Figure 6.1: Characteristic initial value problem for the inhomogeneous partial differential equation (6.25).

The Riemann-Green function $R(u',v';u,v)$ for (6.25) is defined to be the solution to the adjoint equation

$$L^*[R]=0, \tag{6.26}$$

satisfying

$$\begin{aligned} &R(u,v;u,v)=1,\\ &R_{,u'}=bR \text{ on } v'=v,\\ &R_{,v'}=aR \text{ on } u'=u. \end{aligned} \tag{6.27}$$

The unique solution to (6.25) at point P, satisfying the given initial conditions, is then composed of the sum of line integrals along QS and QR and an area integral over the entire domain of dependence $\mathcal{D}$ of the point P. The solution is most transparently expressed by using the notation $z(X)$ to denote the

function z evaluated at the point X. For example, $z(S) \equiv z(u_0, v)$. Then

$$\begin{aligned} z(P) =& \frac{1}{2}\left[z(R)R(R;P) + z(S)R(S;P)\right] \\ &+ \frac{1}{2}\int_{QR}\left[R(u',v_0;P)z(u',v_0)_{,u'} - z(u',v_0)R(u',v_0;P)_{,u'}\right. \\ &\qquad \left. +2b(u',v_0)z(u',v_o)R(u',v_0;P)\right]\mathrm{d}u' \\ &+ \frac{1}{2}\int_{QS}\left[R(u_0,v';P)z(u_0,v')_{,v'} - z(u_0,v')R(u_0,v';P)_{,v'}\right. \\ &\qquad \left. +2a(u_0,v')z(u_0,v')R(u_0,v';P)\right]\mathrm{d}v' \\ &+ \int_{v_0}^{v}\int_{u_0}^{u} R(u',v';P)S(u',v')\mathrm{d}u'\mathrm{d}v'. \end{aligned} \tag{6.28}$$

Suppose that within the domain of dependence $\mathcal{D}$ of P, we have $S(u', v') = 0$, so that (6.25) is homogeneous. Then the double integral in (6.28) vanishes, whilst the remaining terms are unaffected. We conclude that the first three terms on the right-hand side of (6.28) constitute the homogeneous solution to (6.25). Suppose in addition that the initial "incoming" data vanish (i.e. we prescribe $z = 0$ on QS). Then the second line integral in (6.28) will also vanish. Similarly if there are no initial "outgoing" data (so that $z = 0$ on QR) then the first line integral will vanish. Therefore the two line integrals in (6.28) correspond to the propagation of "outgoing" and "incoming" homogeneous solutions, originating from the characteristic surfaces QR and QS respectively. Let z^{hom} denote the unique solution of $L[z] = 0$ which satisfies some given initial data on QR and QS. Then in general the solution (6.28) of $L[z] = S(u, v)$ can be written as

$$z(u,v) = z^{\mathrm{hom}}(u,v) + \int_{v_0}^{v}\int_{u_0}^{u} R(u',v';u,v)S(u',v')\mathrm{d}u'\mathrm{d}v'. \tag{6.29}$$

6.2.2 The Solution to the Hertz Potential Field Equation on a Schwarzschild Background

We now apply the techniques of §6.2.1 to the field equation (6.17). We are interested in the behaviour of solutions in the limit $v \to \infty$.

Consider the characteristic initial value problem with initial data on $u = u_0$

and $v = v_0$. Using (6.29), the general solution of (6.17) at (u, v) is

$$\omega^{lm}(u,v) = \omega_0^{lm}(u,v) + \int_{v_0}^{v}\int_{u_0}^{u} R^{lm}(u',v';u,v)S^{lm}(u',v';\omega^{lm}(u',v'))\mathrm{d}u'\mathrm{d}v', \tag{6.30}$$

where $\omega_0^{lm}(u,v)$ is the homogeneous solution of the Euler-Poisson-Darboux equation and $S^{lm}(u,v;\omega^{lm})$ is the source term (6.18). Suppose that an astrophysical event (such as a binary black hole merger) emits an outgoing gravitational wave. We take this to be our initial data. In the characteristic initial value problem, this corresponds to specifying data on $v = v_0$ and imposing $\omega^{lm}(u_0, v) = 0$. Note that, for continuity, we require $\omega^{lm}(u_0, v_0) = 0$.

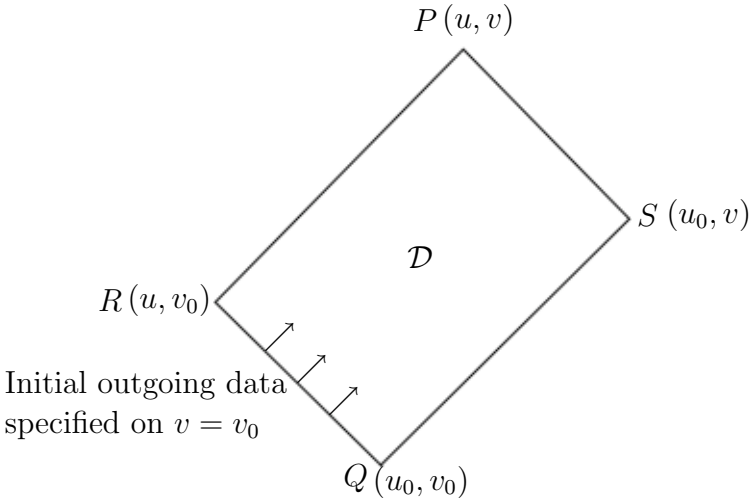

Figure 6.2: Characteristic initial value problem for a Hertz potential on a Schwarzschild background with outgoing initial data.

Since the integral in (6.30) vanishes on QR and QS (see figure 6.2), the initial outgoing data satisfy $\omega^{lm}(u, v_0) = \omega_0^{lm}(u, v_0)$. This means that the initial data can be can be written as an outgoing solution of the *homogeneous* EPD equation (the *flat space* equation) even though the subsequent solution propagates on a Schwarzschild background.

The Riemann-Green function $R^{lm}(u', v'; u, v)$ is given by

$$R^{lm}(u',v';u,v) = (v'-u')^{-2l}(v'-u)^{l+2}(v-u')^{l-2}{}_2F_1(-2-l,2-l;1;t), \tag{6.31}$$

where

$$t = \frac{(v'-v)(u'-u)}{(v'-u)(u'-v)}. \tag{6.32}$$

Picard's method [106] can be used to obtain an approximate solution to any desired order of accuracy via successive iterations of the form

$$\omega_i^{lm}(u,v) = \omega_0^{lm}(u,v) + \Delta\omega_{i-1}^{lm}(u,v), \tag{6.33}$$

where

$$\Delta\omega_{i-1}^{lm}(u,v) = \int_{v_0}^{v}\int_{u_0}^{u} R^{lm}(u',v';u,v)S^{lm}(u',v';\omega_{i-1}^{lm}(u',v'))\mathrm{d}u'\mathrm{d}v'. \tag{6.34}$$

In the limit $i \to \infty$, it can be shown that $\omega_i^{lm} \to \omega^{lm}$, the inhomogeneous solution of (6.17). We will argue later that a single iteration of Picard's method is sufficient to estimate the leading order contribution from the Weyl curvature.

The initial outgoing data on QR can be written in the form

$$\omega_0^{lm}(u,v_0) = (v_0-u)^{2l+1}\frac{\partial^{l-2}}{\partial u^{l-2}}\left(\frac{B^{lm}(u)}{(v_0-u)^{l+3}}\right), \tag{6.35}$$

for some function $B^{lm}(u)$. The *homogeneous* (flat space) solution to the characteristic initial value problem is then

$$\omega_0^{lm}(u,v) = (v-u)^{2l+1}\frac{\partial^{l-2}}{\partial u^{l-2}}\left(\frac{B^{lm}(u)}{(v-u)^{l+3}}\right), \tag{6.36}$$

which has the asymptotic expansion

$$\begin{aligned} &= B^{lm^{(l-2)}}(v-u)^{l-2} - (l-2)(l+3)B^{lm^{(l-1)}}(v-u)^{l-3} \\ &\quad + O\left((v-u)^{l-4}\right). \end{aligned} \tag{6.37}$$

The condition $\omega_0^{lm}(u_0,v) = 0$ as $v \to \infty$ now becomes a condition on the derivatives of $B^{lm}(u)$

$$B^{lm}(u_0) = B^{lm^{(1)}}(u_0) = \cdots = B^{lm^{(l-2)}}(u_0) = 0. \tag{6.38}$$

Using (6.37) and (6.18), we find

$$\begin{aligned} S^{lm}(u,v;\omega_0^{lm}(u,v)) = &-4MB^{lm^{(l-1)}}(u)(v-u)^{l-4}\log\left(\frac{v-u}{2M}\right) \\ &+4MB^{lm^{(l-1)}}(u)(v-u)^{l-4} \\ &+O\left((v-u)^{l-5}\left[M\log\left(\frac{v-u}{2M}\right)\right]^2\right). \end{aligned} \tag{6.39}$$

By inspection, noting that ${}_2F_1(-2-l,2-l;1;t)$ is a polynomial in t of order $l-2$, we expect to find that $\Delta\omega_0^{lm} = O(v^{l-2})$ as $v\to\infty$. At first glance, this appears to be a contradiction since, if $\Delta\omega_0^{lm}$ is of the same order of magnitude as the homogeneous solution, the iteration scheme (6.33) will not converge. The resolution of this apparent paradox lies in the coefficient of v^{l-2} in $\Delta\omega_0^{lm}$. By inspection, it must be proportional to $\left(\frac{M}{v_0}\right)^a$ for some $a\geq 1$. Therefore *provided that we are in the far-field region* (so that $M\ll v_0$), then $\Delta\omega_0^{lm}\ll\omega_0^{lm}$. Subsequent iterations of Picard's method will introduce higher powers of $\frac{M}{v_0}$ and so $\Delta\omega_{i+1}^{lm}\ll\Delta\omega_i^{lm}$. The boundary conditions subsequently derived in this chapter are therefore only valid if the boundary of the computational domain lies in the far-field region, so that the condition $M\ll v_0$ holds. This provides a consistency requirement on the location of the numerical boundary.

We illustrate the arguments above by considering the simplest case, $l=2$. We have

$$\Delta\omega_0^{2\,m} = \int_{v_0}^{v}\int_{u_0}^{u} 4MB^{2\,m^{(1)}}(u')\frac{(v'-u)^4}{(v'-u')^6}\left(1-\log\left(\frac{v'-u'}{2M}\right)\right)\mathrm{d}u'\mathrm{d}v'. \tag{6.40}$$

The leading order term in $\Delta\omega_0$ is obtained by taking the v_0 limit in the integral above. It is therefore $O(1)$ with respect to v, as expected.

As a concrete example, suppose we take $B^{2\,m^{(1)}}(u)=\delta(u-u_A)$ for some $u_A\in(u_0,u)$. Expanding in powers of $1/v'$ we find

$$\Delta\omega_0^{2\,m} = \int_{v_0}^{v} 4M\left(1-\log\left(\frac{v'-u_A}{2M}\right)\right)\left(\frac{1}{v'^2}+\frac{2(3u_A-2u)}{v'^3}+O\left(\frac{1}{v'^4}\right)\right)\mathrm{d}v'. \tag{6.41}$$

To leading order in $1/v_0$ we have

$$\Delta\omega_0^{2\,m} = -\frac{4M}{v_0}\left(\log\left(\frac{v_0-u_A}{2M}\right)-1\right)+O\left(\frac{M^2}{v_0^2}\right). \tag{6.42}$$

If v_0 is in the far-field region (so that $M \ll v_0$), then $\Delta\omega_0^{2\,m} \ll \omega_0^{2\,m}$. Note that the $v-$dependence of $\Delta\omega_0^{2\,m}$ to leading order is

$$\frac{4M}{v}\left(\log\left(\frac{v-u_A}{2M}\right)-1\right). \tag{6.43}$$

In equation (6.40), suppose instead that we choose a general function $B^{2\,m}(u)$ such that $B^{2\,m^{(1)}}(u) = O(1)$ and $B^{2\,m^{(1)}}(u_0) = 0$. Taylor expanding the integrand, we find

$$\begin{aligned}\Delta\omega_0^{2\,m} &= 4M\int_{v_0}^{v}\int_{u_0}^{u} B^{2\,m^{(1)}}(u')\left(1-\log\left(\frac{v'-u'}{2M}\right)\right)\left(\frac{1}{v'^2}+\frac{2(3u'-2u)}{v'^3}+O\left(\frac{1}{v'^4}\right)\right)\mathrm{d}u'\mathrm{d}v' \\ &= 4M\int_{v_0}^{v} B^{2\,m}(u)\left(1-\log\left(\frac{v'-u}{2M}\right)\right)\left(\frac{1}{v'^2}+O\left(\frac{1}{v'^3}\right)\right)\mathrm{d}v', \end{aligned} \tag{6.44}$$

where the $u'-$integral has been done by parts, neglecting the higher order terms. Thus we find that

$$\begin{aligned}\Delta\omega_0^{2\,m} = &-\frac{4MB^{2\,m}(u)}{v_0}\left(\log\left(\frac{v_0-u}{2M}\right)-1\right)+O\left(\frac{M^2}{v_0^2}\right) \\ &+\frac{4MB^{2\,m}(u)}{v}\left(\log\left(\frac{v-u}{2M}\right)-1\right)+O\left(\frac{M^2}{v^2}\right).\end{aligned} \tag{6.45}$$

As a useful check of the validity of our approximations, we can substitute (6.45) back into (6.17). The first line in (6.45) is a function of u only and can therefore be written as a homogeneous solution to (6.17). However, when we substitute the $v-$dependent term

$$\frac{4MB^{2\,m}(u)}{v}\left(\log\left(\frac{v-u}{2M}\right)-1\right), \tag{6.46}$$

into the left-hand side of (6.17) we recover the source term (6.18), as required.

We now translate these results back in terms of the original Hertz potential χ^{lm}, using (6.16). For $l = 2$, as $v \to \infty$, and for the general outgoing initial data given by

$$\chi^{2\,m}_{\mathrm{out}}(u, v_0) = \frac{B^{2\,m}(u)}{v_0-u}, \tag{6.47}$$

the solution to the inhomogeneous Euler-Poisson-Darboux equation (6.11) is

$$\chi^{2\,m}_{\text{out}} = \frac{B^{2\,m}(u)}{v} - \frac{4B^{2\,m}(u)}{v}\left(\frac{M}{v_0}\left(\log\left(\frac{v_0-u}{2M}\right)-1\right)+O\left(\frac{M^2}{v_0^2}\right)\right) + \frac{4MB^{2\,m}(u)}{v^2}\left(\log\left(\frac{v-u}{2M}\right)-1\right)+O\left(\frac{M^2}{v^3}\right). \tag{6.48}$$

If we take the limit $M \to 0$ then we recover the leading order term in the asymptotic expansion of the flat space solution, as expected. Note that the second term in (6.48) is also a homogeneous solution to the Euler-Poisson-Darboux equation (6.11). Therefore the first line in (6.48) is a homogeneous solution but with $B^{2\,m}(u)$ replaced by $F(u)$ where

$$F(u) = B^{2\,m}(u)\left(1 - 4\frac{M}{v_0}\left(\log\left(\frac{v_0-u}{2M}\right)-1\right)+O\left(\frac{M^2}{v_0^2}\right)\right). \tag{6.49}$$

The final term in (6.48)

$$\frac{4MB^{2\,m}(u)}{v^2}\left(\log\left(\frac{v-u}{2M}\right)-1\right), \tag{6.50}$$

is not a homogeneous solution. It is the contribution to the solution from the Weyl curvature. We therefore interpret it as the *gravitational tail*. Similar calculations can be performed for higher values of l. For $l \geq 2$, even if the initial data have compact support, the gravitational tail will not in general have compact support. A wave propagating on a Schwarzschild background then consists of a combination of the geometrical tail and the gravitational tail due to the Weyl curvature.

In order to formulate absorbing boundary conditions, we must also investigate the behaviour of an incoming wave propagating on a Schwarzschild background, since such waves can be created by the reflection of outgoing waves off $\partial\Omega$. Suppose that we specify some initial incoming 2^l-pole data on QS. Then we can write the data in the form

$$\omega^{lm}(u_0, v) = (v-u_0)^{2l+1}\left(\frac{\partial}{\partial v}\right)^{l+2}\frac{A^{lm}(v)}{(v-u_0)^{l-1}}, \tag{6.51}$$

for a suitable function $A^{lm}(v)$. The homogeneous solution satisfying these data

is

$$\omega_0^{lm}(u,v) = (v-u)^{2l+1}\left(\frac{\partial}{\partial v}\right)^{l+2}\frac{A^{lm}(v)}{(v-u)^{l-1}}. \tag{6.52}$$

We restrict our attention to fields which are asymptotically regular so that the peeling theorem holds. Recall from §5.3.3 that we must then impose the linearized outgoing radiation condition, which places a constraint upon the behaviour of $A^{lm}(v)$ as $v \to \infty$. Restricting our attention further to the case $l = 2$, we discover that the homogeneous solution has the asymptotic expansion

$$\omega_0^{2\,m}(u,v) = A_1(v) + \frac{A_2(v)}{v-u} + O\left(\frac{1}{(v-u)^2}\right), \tag{6.53}$$

for some functions $A_1(v)$ and $A_2(v)$, both of order $O(1)$ as $v \to \infty$, and both of which vanish at $v = v_0$.

To estimate the effect of the background Weyl curvature on the incoming solution, we follow the same method used in the study of the outgoing solution. One iteration of Picard's method is performed. Substituting (6.53) into the source term in (6.18) we obtain

$$S^{2\,m}(u,v;\omega_0^{2\,m}) = \frac{M\tilde{A}_1(v)\log\left(\frac{v-u}{2M}\right)}{(v-u)^2} + \frac{M\tilde{A}_2(v)}{(v-u)^2} + O\left(\frac{\log\left(\frac{v-u}{2M}\right)}{(v-u)^3}\right). \tag{6.54}$$

The functions $\tilde{A}_1(v)$ and $\tilde{A}_2(v)$ could be expressed in terms of $A_1(v)$ and $A_2(v)$, but this is not necessary here, since we are only interested in the general behaviour of the incoming solution. It is sufficient for our purposes to note that $\tilde{A}_1(v)$ and $\tilde{A}_2(v)$ are both $O(1)$ as $v \to \infty$. Then $\Delta\omega_0^{2\,m}$ (6.33) is given by

$$\begin{aligned}\Delta\omega_0^{2\,m} = \int_{v_0}^{v}\int_{u_0}^{u} & M\tilde{A}_1(v)(v'-u)^4\frac{\log\left(\frac{v'-u'}{2M}\right)}{(v'-u')^6} + M\tilde{A}_2(v)\frac{(v'-u)^4}{(v'-u')^6} \\ & + O\left((v'-u)^4\frac{\log\left(\frac{v'-u'}{2M}\right)}{(v'-u')^7}\right)\mathrm{d}u'\mathrm{d}v'.\end{aligned} \tag{6.55}$$

The $u'-$integral in $\Delta\omega_0^{2\,m}$ can easily be evaluated. The $v'-$integral is done by parts, neglecting higher order terms, to give

$$\Delta\omega_0^{2\,m} = \frac{M\hat{A}_1(v)\log\left(\frac{v-u}{2M}\right)}{v} + \frac{M\hat{A}_2(v)}{v} + O\left(\frac{M^2}{v^2}\right). \tag{6.56}$$

Again $\hat{A}_1(v)$ and $\hat{A}_2(v)$ are both of order $O(1)$ as $v \to \infty$ and could be expressed in terms of $\tilde{A}_1(v)$ and $\tilde{A}_2(v)$. Translating this result back in terms of the Hertz potential χ^{lm}, using (6.16), we find that the general $l = 2$ incoming mode can be written in the form

$$\chi^{2\,m}_{\text{in}} = \frac{\bar{A}_1(v)}{v} + M\bar{A}_2(v)\frac{\log\left(\frac{v-u}{2M}\right) - 1}{v^2} + O\left(\frac{M^2}{v^3}\right), \tag{6.57}$$

where, once more, the functions $\bar{A}_1(v)$ and $\bar{A}_2(v)$ are both of order $O(1)$ as $v \to \infty$. As was found in the analysis of outgoing radiation, the leading order term is a solution to the homogeneous EPD equation, but at second order there is a contribution due to the Weyl curvature which is not a homogeneous solution to the EPD equation.

6.2.3 Absorbing Boundary Conditions on a Schwarzschild Background

To obtain boundary conditions for linearized gravitational radiation on a Schwarzschild background, we adopt a similar approach to that used to obtain the operators (5.67) for Ψ_2. However, we will restrict our attention to the $l = 2$ pole. The quadrupole contribution to $\hat{\Psi}_2$ can be calculated by substituting (6.48) and (6.57) into the expressions for the perturbed Weyl scalars (B.11). We obtain

$$\hat{\Psi}^{l=2}_{2\text{ out}} = \frac{\frac{1}{2}F^{(2)}(u)}{v^3} + 2MB^{(2)}(u)\frac{\left(\log\left(\frac{v-u}{2M}\right) - 1\right)}{v^4} + O\left(\frac{M^2}{v^5}\right), \tag{6.58}$$

and

$$\hat{\Psi}^{l=2}_{2\text{ in}} = \frac{\bar{A}_1(v)}{v^3} + M\bar{A}_1(v)\frac{\log\left(\frac{v-u}{2M}\right) - 1}{v^4} + O\left(\frac{M^2}{v^5}\right). \tag{6.59}$$

Here we are not interested in the specific behaviour of the functions $F(u)$, $B(u)$, $\bar{A}_1(v)$ or $\bar{A}_2(v)$.

The boundary conditions here will be slightly different in form from the boundary conditions on a Minkowski background (5.65) because we have expanded the solution in powers of v rather than $v - u$. Consider the operator

$$\hat{P}_1 \equiv \frac{\partial}{\partial v} + \frac{3}{v}. \tag{6.60}$$

The operator $\hat{P}_1$ removes the leading order outgoing term from $\hat{\Psi}_2$. Imposing

$$\hat{P}_1 \hat{\Psi}_2 \doteq O(v^{-4}), \tag{6.61}$$

will then remove the leading order incoming radiative term from $\hat{\Psi}_2$ on $\partial\Omega$. The first order boundary condition $\hat{P}_1$ is similar to the first order Bayliss & Turkel condition [7] and similar to $\hat{O}_1$ (5.65). This is expected because at leading order the background Weyl curvature has no effect.

Suppose now that we have removed the first order contribution from the incoming radiation (using $\hat{P}_1$) and now wish to remove the second order terms. At second order, the presence of logarithms complicates matters. Consider the operator

$$\hat{P}_2 \equiv \frac{\partial}{\partial v}(v-u)\frac{\partial}{\partial v}v^4. \tag{6.62}$$

At second order, the quantity $\hat{P}_2\hat{\Psi}_2$ contains only incoming radiation. Imposing

$$\hat{P}_2 \hat{\Psi}_2 \doteq O(v^{-1}), \tag{6.63}$$

will then remove these terms. We have now obtained the first two boundary conditions in an increasingly accurate hierarchy similar to (5.67).

Buchman & Sarbach [23] also obtained a boundary condition, $\mathcal{D}_2$, which is perfectly absorbing for quadrupolar radiation on a Schwarzschild background. Their boundary condition is non-local, as it involves an integral over the past boundary of the computational domain.

In practice (6.62) is unlikely to be of use in a numerical simulation. It differs in form considerably from the simple and elegant Bayliss & Turkel-type conditions of chapter 5 (5.67), which were devised to be as easy as possible to implement numerically. Due to the presence of the logarithmic terms, the operator (6.62) now involves multiplying by five powers of the radial coordinate and taking two radial derivatives just to obtain second order accuracy in the boundary condition. It would be desirable to obtain a much simpler sequence of operators than the $\hat{P}_i$ defined above. This will be done in chapter 7, in which a careful choice of coordinates, which removes the logarithmic terms, will enable us to consider both Schwarzschild and Kerr background spacetimes.

Chapter 7

Hertz Potentials on a Kerr Background

In chapter 5, the far-field region of spacetime was modelled as a linear perturbation about flat space. This model was improved in chapter 6, in which it was assumed that the far-field region could more accurately be described by a perturbation about a Schwarzschild background with mass parameter M. In a similar manner to Buchman & Sarbach [22, 23], the first order effects due to M/R were incorporated, although the resulting boundary conditions were rather cumbersome.

One might expect that more accurate boundary conditions could be obtained by working to second order in M/R. However, at second order there is also a contribution due to the angular momentum Ma of the background spacetime. The method used by Buchman & Sarbach cannot incorporate these effects and so their calculation was not extended to second order. By considering Hertz potentials that generate gravitational perturbations about a Kerr background spacetime [77], however, we can determine the second order effect of the background angular momentum on the propagation of linearized gravitational waves, thereby taking the results of Buchman & Sarbach one stage further.

Any boundary conditions which take into account the background Kerr spacetime will depend on the mass and angular momentum parameters M and a. Both parameters must accurately be estimated during the numerical evolution if the boundary conditions are to be used. As mentioned in chapter 6,

one possible approach to estimating M is to evaluate the Bondi mass using the results of chapter 3. However, there appears to be no easy way of estimating the value of a. This remains an outstanding problem in numerical relativity.

The scalar field equation (4.36) for a Hertz potential χ' is valid in any type D spacetime so in principle the methods used in chapters 5 and 6 should work on a Kerr background. However, the analysis now becomes even more complex than in chapter 6. Unless we simplify the calculations considerably, any boundary conditions obtained will be too unwieldy to implement numerically.

In chapters 5 and 6, double null coordinate charts and "standard" tetrads were chosen. The Hertz potential was decomposed in terms of spin-weighted spherical harmonics and it was found that the angular dependence decoupled completely from the $u-$ and $v-$dependence. Furthermore, the null coordinates u and v were also characteristic coordinates for the resulting Euler-Poisson-Darboux equations. On a Kerr background, the calculation is somewhat different. Firstly, there is no obvious choice of double null coordinate chart. We will therefore choose a single outgoing null coordinate u and transform the resulting Euler-Poisson-Darboux equation into characteristic coordinates later. Secondly, due to the presence of the angular momentum parameter a, the angular dependence of the potential, when decomposed into spin-weighted spherical harmonics, will not decouple. Some mixing of the harmonic modes will occur. One might expect that decomposing the Hertz potential in terms of spin-weighted *spheroidal* harmonics (originally defined by Teukolsky [142,143]) would result in the decoupling of the angular dependence. However, this proves not to be the case. In addition, there are very few analytical results known about spin-weighted spheroidal harmonics (see, for example, [14, 21]). In this calculation, their use appears to be a dead end.

In chapter 6, logarithmic terms were present in the inhomogeneous Euler-Poisson-Darboux equation (6.13). If we use the standard Boyer-Lindquist coordinates [20] for the corresponding calculation on a Kerr background, then such terms will still be present. Together with the trigonometric terms that arise at second order, due to the lack of decoupling, this is enough to render the calculation virtually intractable. We require a coordinate chart and tetrad better adapted to the study of the Kerr spacetime near future null infinity, to minimise the number of logarithmic and trigonometric terms present in the Hertz potential field equation. Luckily, Bai et al. [6, 59] have obtained such a

chart and tetrad.

Section 7.1 contains details of the coordinate chart and tetrad of Bai et al. In §7.2 we illustrate our methods by considering the massless spin-0 scalar field equation on a Kerr background. An inhomogeneous Euler-Poisson-Darboux equation is obtained. We are able to investigate the effect of the mass M and angular momentum Ma on the solution by solving the characteristic initial value problem to second order using a Picard iteration scheme. In addition, we are able to demonstrate how the background angular momentum results in mode-mixing between the $l-$poles. In §7.3 we apply these methods to the more complex Hertz potential field equation for linearized gravitational waves on a Kerr background. Again, an inhomogeneous Euler-Poisson-Darboux equation is obtained, whose solutions we can estimate using Picard's method. At second order, some mode-mixing between the gravitational 2^l-poles is present. Finally, we use the solutions to formulate absorbing boundary conditions for numerical relativity.

7.1 A Coordinate Chart and Tetrad Adapted to the Study of the Kerr Metric near $\mathscr{I}^+$

Bai et al. [6,59] have obtained a coordinate chart $(u, \lambda, \tilde{\theta}, \tilde{\phi})$ and tetrad $(l, n, m, \bar{m})$, both of which are adapted to the study of the Kerr metric near future null infinity $\mathscr{I}^+$. To define the chart, null hypersurfaces that intersect $\mathscr{I}^+$ in shear-free cuts are first constructed. Each hypersurface corresponds to a particular value of a null coordinate u, which satisfies the relativistic eikonal equation (7.4). The Boyer-Lindquist radial coordinate r is then replaced with an affine parameter λ of the null generators of these hypersurfaces. Angular coordinates are defined on the unit sphere generated by the intersection of the $u = \text{const.}$ hypersurfaces with $\mathscr{I}^+$.

The tetrad is defined by demanding that l is hypersurface-forming and that the tetrad is parallelly transported along the null generator of constant u hypersurfaces. The definitions above are made possible by expanding the tetrad components in powers of $1/\lambda$ and working to the desired order of accuracy. Further details are given below.

In Boyer-Lindquist coordinates (t, r, θ, ϕ) [20], the Kerr metric [77] for a vacuum spacetime containing a mass M, with angular momentum Ma, centered on the origin, is

$$\begin{aligned} \mathrm{d}s^2 = &\left(1 - \frac{2Mr}{\rho^2}\right)\mathrm{d}t^2 - \frac{\rho^2}{\Delta}\mathrm{d}r^2 + \frac{4Mar\sin^2\theta}{\rho^2}\mathrm{d}t\mathrm{d}\phi \\ &- \rho^2\mathrm{d}\theta^2 - \left(r^2 + a^2 + \frac{2Ma^2r}{\rho^2}\sin^2\theta\right)\sin^2\theta\,\mathrm{d}\phi^2, \end{aligned} \tag{7.1}$$

where

$$\begin{aligned} \Delta &= r^2 - 2Mr + a^2, \\ \rho^2 &= r^2 + a^2\cos^2\theta. \end{aligned} \tag{7.2}$$

The Boyer-Lindquist chart (t, r, θ, ϕ) is related to the standard spherical polar

chart for Minkowski spacetime (T, R, Θ, Φ) via

$$\begin{aligned} T &= t, \\ R &= \sqrt{r^2 + a^2 \sin^2\theta}, \\ \sin\Theta &= \sqrt{\frac{r^2 + a^2}{r^2 + a^2 \sin^2\theta}} \sin\theta, \\ \Phi &= \phi. \end{aligned} \tag{7.3}$$

By solving the asymptotic expansion of the relativistic eikonal equation

$$g^{ij} u_{,i} u_{,j} = 0, \tag{7.4}$$

order by order, a Bondi-Sachs type null coordinate u can be constructed, such that the $u =$ const. null hypersurfaces intersect future null infinity in shear-free cuts. In terms of the Boyer-Lindquist coordinates, u is given by

$$u = t - \left(r + 2M \log\frac{r}{2M} - \frac{4M^2 - \frac{1}{2}a^2 \sin^2\theta}{r} - \frac{4M^3 - Ma^2}{r^2} + O\left(\frac{1}{r^3}\right)\right). \tag{7.5}$$

A Newman-Penrose tetrad adapted to the $u =$ const. hypersurfaces (so that l_a is hypersurface forming) can then be written down

$$\begin{aligned} l_a &= (\mathrm{d}u)_a = (1, -h_1, -h_2, 0), \\ n_a &= \frac{1}{g^{00} - g^{11}h_1^2 - g^{22}h_2^2}(1, h_1, h_2, 0), \\ m_a &= \left(g_{03}\frac{i}{\sin\theta}\sqrt{\frac{\rho^2}{2\Sigma^2}}, \quad -g_{11}\sqrt{\frac{-h_2^2}{2g_{11}h_2^2 + 2g_{22}h_1^2}}, \right. \\ &\qquad \left. g_{22}\sqrt{\frac{-h_1^2}{2g_{11}h_2^2 + 2g_{22}h_1^2}}, \quad g_{33}\frac{i}{\sin\theta}\sqrt{\frac{\rho^2}{2\Sigma^2}}\right), \end{aligned} \tag{7.6}$$

where

$$\begin{aligned}
\Sigma &= (r^2+a^2)^2 - \Delta a^2 \sin^2\theta, \\
h_1 &= 1 + \frac{2M}{r} + \frac{4M^2 - \frac{1}{2}a^2\sin^2\theta}{r^2} + \frac{8M^3 - 2Ma^2}{r^3} + O\left(\frac{1}{r^4}\right), \\
h_2 &= \frac{a^2 \sin\theta\cos\theta}{r} - \frac{\frac{1}{2}a^4\sin^3\theta\cos\theta}{r^3} + O\left(\frac{1}{r^4}\right).
\end{aligned} \tag{7.7}$$

Next, we define an affine parameter λ of the null generators of the constant u hypersurfaces, so that $l^a = \left(\frac{\partial}{\partial\lambda}\right)^a$. We replace the Boyer-Lindquist radial coordinate r with λ. The Boyer-Lindquist angular coordinates (θ, ϕ) are not constant along the null generators of the $u =$ const. hypersurfaces. We therefore define two new angular coordinates $(\tilde{\theta}, \tilde{\phi})$. On the unit sphere generated by the intersection of a constant$-u$ hypersurface with $\mathscr{I}^+$, $(\tilde{\theta}, \tilde{\phi})$ become standard polar coordinates. The Boyer-Lindquist coordinates can be expressed asymptotically in terms of λ, $\tilde{\theta}$ and $\tilde{\phi}$:

$$\begin{aligned}
r &= \lambda - \frac{a^2\sin^2\tilde{\theta}}{2\lambda} - \frac{Ma^2\sin^2\tilde{\theta}}{2\lambda^2} + O\left(\frac{1}{\lambda^3}\right), \\
\theta &= \tilde{\theta} - \frac{a^2\sin\tilde{\theta}\cos\tilde{\theta}}{2\lambda^2} + O\left(\frac{1}{\lambda^4}\right), \\
\phi &= \tilde{\phi} - \frac{Ma}{\lambda^2} - \frac{4M^2a}{3\lambda^2} + O\left(\frac{1}{\lambda^4}\right).
\end{aligned} \tag{7.8}$$

In terms of the new coordinate chart $(u, \lambda, \tilde{\theta}, \tilde{\phi})$, the Kerr metric (7.1) becomes

$$\begin{aligned} \mathrm{d}s^2 = &\left(1 - \frac{2M}{\lambda} + \frac{(3\cos^2\tilde{\theta} - 1)Ma^2}{\lambda^3} + O\left(\frac{1}{\lambda^4}\right)\right)\mathrm{d}u^2 + 2\mathrm{d}u\mathrm{d}\lambda \\ &+ 2\left(-\frac{3Ma^2\cos\tilde{\theta}\sin\tilde{\theta}}{\lambda^2} + \frac{a^4\cos\tilde{\theta}\sin^3\tilde{\theta}}{2\lambda^3} + O\left(\frac{1}{\lambda^4}\right)\right)\mathrm{d}u\mathrm{d}\tilde{\theta} \\ &+ 2\left(\frac{2Ma\sin^2\tilde{\theta}}{\lambda} + \frac{Ma^3\sin^2\tilde{\theta}(1 - 5\cos^2\tilde{\theta})}{\lambda^3} + O\left(\frac{1}{\lambda^4}\right)\right)\mathrm{d}u\mathrm{d}\tilde{\phi} \\ &+ O\left(\frac{1}{\lambda^3}\right)\mathrm{d}\lambda\mathrm{d}\tilde{\theta} + O\left(\frac{1}{\lambda^3}\right)\mathrm{d}\lambda\mathrm{d}\tilde{\phi} - \left(\lambda^2 - \frac{Ma^2\sin^2\tilde{\theta}}{\lambda} + O\left(\frac{1}{\lambda^2}\right)\right)\mathrm{d}\tilde{\theta}^2 \\ &- \left(\frac{12M^2a^3\cos\tilde{\theta}\sin^3\tilde{\theta}}{\lambda^3} + O\left(\frac{1}{\lambda^4}\right)\right)\mathrm{d}\tilde{\theta}\mathrm{d}\tilde{\phi} \\ &- \left(\sin^2\tilde{\theta}\,\lambda^2 + \frac{Ma^2\sin^4\tilde{\theta}}{\lambda^3} + O\left(\frac{1}{\lambda^4}\right)\right)\mathrm{d}\tilde{\phi}^2. \end{aligned} \tag{7.9}$$

Finally, we transform the tetrad (7.6) such that the new tetrad is parallelly transported along a null generator of the constant u hypersurfaces. Performing a phase shift on m^a only has an effect at $O(1/\lambda^5)$. For n^a to be parallelly transported, we perform a null rotation about l^a,

$$\begin{aligned} l &\to l, \\ m &\to m + bl, \\ n &\to n + \bar{b}m + b\bar{m} + b\bar{b}l, \end{aligned} \tag{7.10}$$

where

$$b = -\frac{3iMa\sin\tilde{\theta}}{2\sqrt{2}\lambda^2} - \frac{Ma^2\sin\tilde{\theta}\cos\tilde{\theta}}{\sqrt{2}\lambda^3} + O\left(\frac{1}{\lambda^4}\right). \tag{7.11}$$

The new tetrad, expressed in the $(u, \lambda, \tilde{\theta}, \tilde{\phi})$ chart is

$$
\begin{aligned}
l_a &= \left(1, \quad O\left(\frac{1}{\lambda^4}\right), \quad \frac{a^4 \sin^3\tilde{\theta}\cos\tilde{\theta}}{2\lambda^3} + O\left(\frac{1}{\lambda^4}\right), \quad 0\right), \\
n_a &= \left(\frac{1}{2} - \frac{M}{\lambda} + \frac{Ma^2(\cos^2\tilde{\theta} - \frac{1}{2}\sin^2\tilde{\theta})}{\lambda^3} + O\left(\frac{1}{\lambda^4}\right),\right. \\
&\qquad 1 - \frac{2Ma^2\cos^2\tilde{\theta}}{\lambda^3} + O\left(\frac{1}{\lambda^4}\right), \\
&\qquad \left. -\frac{2Ma^2\sin\tilde{\theta}\cos\tilde{\theta}}{\lambda^2} + O\left(\frac{1}{\lambda^3}\right), \quad \frac{3Ma\sin^2\tilde{\theta}}{2\lambda} + O\left(\frac{1}{\lambda^3}\right)\right), \\
m_a &= \left(\frac{iMa\sin\tilde{\theta}}{2\sqrt{2}\lambda^2} - \frac{Ma^2\sin\tilde{\theta}\cos\tilde{\theta}}{\sqrt{2}\lambda^3} + O\left(\frac{1}{\lambda^4}\right), \quad O\left(\frac{1}{\lambda^4}\right),\right. \\
&\qquad -\frac{\lambda}{\sqrt{2}} + \frac{Ma^2(2 - \frac{3}{2}\sin^2\tilde{\theta} - 2\cos^2\tilde{\theta})}{\sqrt{2}\lambda^2} + O\left(\frac{1}{\lambda^3}\right), \\
&\qquad \left. -\frac{i\lambda\sin\tilde{\theta}}{\sqrt{2}} - \frac{iMa^2\sin^3\tilde{\theta}}{2\sqrt{2}\lambda^2} + O\left(\frac{1}{\lambda^3}\right)\right).
\end{aligned} \tag{7.12}
$$

With respect to the tetrad (7.12), the Newman-Penrose scalars are

$$
\begin{aligned}
\kappa, \tau', \epsilon &= O\left(\frac{1}{\lambda^5}\right), \quad \rho = -\frac{1}{\lambda} + O\left(\frac{1}{\lambda^5}\right), \quad \sigma = -\frac{3Ma^2\sin^2\tilde{\theta}}{2\lambda^4} + O\left(\frac{1}{\lambda^5}\right), \\
\kappa' &= -\frac{3iMa\sin\tilde{\theta}}{4\sqrt{2}\lambda^3} + \frac{Ma^2\sin\tilde{\theta}\cos\tilde{\theta}}{\sqrt{2}\lambda^4} + O\left(\frac{1}{\lambda^5}\right), \quad \sigma' = \frac{Ma^2\sin^2\tilde{\theta}}{4\lambda^4} + O\left(\frac{1}{\lambda^5}\right), \\
\tau &= -\frac{3iMa}{2\sqrt{2}\lambda^3} + \frac{2\sqrt{2}Ma^2\sin\tilde{\theta}\cos\tilde{\theta}}{\lambda^4} + O\left(\frac{1}{\lambda^5}\right), \quad \beta' = \frac{\cot\tilde{\theta}}{2\sqrt{2}\lambda} + O\left(\frac{1}{\lambda^4}\right), \\
\beta &= \frac{\cot\tilde{\theta}}{2\sqrt{2}\lambda} - \frac{3iMa\sin\tilde{\theta}}{2\sqrt{2}\lambda^3} + O\left(\frac{1}{\lambda^4}\right), \quad \epsilon' = -\frac{M}{2\lambda^2} - \frac{3iMa\cos\tilde{\theta}}{4\lambda^3} + O\left(\frac{1}{\lambda^4}\right), \\
\rho' &= \frac{1}{2\lambda} - \frac{M}{\lambda^2} - \frac{3iMa\cos\tilde{\theta}}{2\lambda^3} + O\left(\frac{1}{\lambda^4}\right).
\end{aligned} \tag{7.13}
$$

The Weyl scalars are given by

$$\Psi_0 = \frac{3Ma^2 \sin^2\tilde{\theta}}{\lambda^5} + O\left(\frac{1}{\lambda^6}\right), \quad \Psi_1 = \frac{3iMa\sin\tilde{\theta}}{\sqrt{2}\lambda^4} + O\left(\frac{1}{\lambda^5}\right),$$
$$\Psi_2 = -\frac{M}{\lambda^3} - \frac{3iMa\cos\tilde{\theta}}{\lambda^4} + O\left(\frac{1}{\lambda^5}\right), \quad \Psi_3 = -\frac{3iMa\sin\tilde{\theta}}{2\sqrt{2}\lambda^4} + O\left(\frac{1}{\lambda^5}\right),$$
$$\Psi_4 = \frac{3Ma^2 \sin^2\tilde{\theta}}{4\lambda^5} + O\left(\frac{1}{\lambda^6}\right). \tag{7.14}$$

The relationship between the Minkowski (T, R, Θ, Φ), Boyer-Lindquist (t, r, θ, ϕ) and Bai et al. $(u, \lambda, \tilde{\theta}, \tilde{\phi})$ coordinate charts is best understood by considering the limits $M \to 0$ and $a \to 0$.

Consider first the limit $M \to 0$, $a \to 0$, in which the Kerr background tends to Minkowski spacetime. In this case the Boyer-Lindquist and Minkowski charts coincide, and the Bai et al. coordinates reduce to the standard flat space retarded time chart. Consistent with the Minkowski background results of chapter 5, the Weyl scalars (7.14) vanish and the only non-zero Newman-Penrose scalars are ρ, ρ', β and β'.

Consider now the case $M \neq 0$, $a \to 0$, in which case we recover the Schwarzschild spacetime. Again, in this limit the Boyer-Lindquist and Minkowski charts coincide. This is because the Boyer-Lindquist chart is based on a foliation of the spacetime by concentric spheroids, centered on the origin. In the limit $a \to 0$, these spheroids become the spheres on which the Minkowski spherical polar coordinates are based. If $a \to 0$ then the null coordinate u becomes the standard retarded time null coordinate for a Schwarzschild spacetime (6.1). Similarly, λ, $\tilde{\theta}$ and $\tilde{\phi}$ tend to r, θ and ϕ respectively, and so we recover the standard retarded time chart (u, r, θ, ϕ) for Schwarzschild spacetime. The metric (7.9), tetrad (7.12), Newman-Penrose scalars (7.13) and Weyl scalars (7.14) reduce to the standard results for a Schwarzschild spacetime found in chapter 6.

Finally, consider the case $M \to 0$, $a \neq 0$. The spacetime is now flat (since $M = 0$). However, the three coordinate charts all differ, due to the presence of the angular momentum parameter a. The Boyer-Lindquist coordinates differ from the Minkowski coordinates because, since $a \neq 0$, the spheroids on which the (θ, ϕ) chart is based no longer reduce to spheres, as was the case in the previous paragraph. Similarly, since $a \neq 0$, the null coordinate u (7.5) does

not reduce to the standard flat space retarded time coordinate. Although $\tilde{\phi} \to \phi$ as $M \to 0$, the same is not true of θ and $\tilde{\theta}$ or r and λ, and this is the fundamental difference between the Boyer-Lindquist chart and the Bai et al. chart. In the limit $M \to 0$, $a \neq 0$ the tetrad vectors n, m and $\bar{m}$ (7.12) reduce to the standard Minkowski tetrad vectors of chapter 5. However the same is not true of l. The only non-zero Newman-Penrose scalars are ρ, ρ', β and β', and the Weyl scalars (7.14) all vanish. This is expected since we are dealing with a flat spacetime, albeit in a rotating coordinate chart and frame.

For the remainder of this chapter we will use the $(u, \lambda, \tilde{\theta}, \tilde{\phi})$ chart only. For convenience, we will drop the $\sim$ from $\tilde{\theta}$ and $\tilde{\phi}$.

7.2 The Massless Scalar Field on a Kerr Background

Before investigating gravitational radiation linearized about a Kerr background it is instructive to consider the simpler case of a massless spin-0 scalar field Φ on a Kerr background, which obeys the field equation

$$g^{ij}\Phi_{;ij} = 0, \tag{7.15}$$

where the contravariant form of the Kerr metric g^{ij} in the $(u, \lambda, \theta, \phi)$ chart of §7.1 can be obtained from (7.9).

The scalar field Φ is expanded in terms of spherical harmonics (see appendix C.1 for details of the spherical harmonic conventions we use),

$$\Phi = \sum_{l,m} \phi^{lm}(u, \lambda) Y_{lm}(\theta, \phi). \tag{7.16}$$

Substituting (7.16) into (7.15) and using the eigenvalue equation (C.2) to remove angular derivatives of spherical harmonics we obtain

$$\begin{aligned}\sum_{l,m} Y_{lm}(\theta,\phi) \Bigg\{ & \frac{\partial^2\phi^{lm}}{\partial\lambda^2} - 2\frac{\partial^2\phi^{lm}}{\partial\lambda\partial u} + \frac{2}{\lambda}\left(\frac{\partial\phi^{lm}}{\partial\lambda} - \frac{\partial\phi^{lm}}{\partial u} - M\frac{\partial^2\phi^{lm}}{\partial\lambda^2}\right) \\ & - \frac{1}{\lambda^2}\left(l(l+1)\phi^{lm} + 2M\frac{\partial\phi^{lm}}{\partial\lambda}\right) \\ & + \frac{1}{\lambda^3}\left(-4iMam\frac{\partial\phi^{lm}}{\partial\lambda} - Ma^2\frac{\partial^2\phi^{lm}}{\partial\lambda^2} + 3Ma^2\cos^2\theta\frac{\partial^2\phi^{lm}}{\partial\lambda^2}\right) \\ & + \frac{2}{\lambda^4}iMam\phi^{lm} + O\left(\frac{Ma^2\phi^{lm}}{\lambda^4}\right)\Bigg\} = 0. \end{aligned} \tag{7.17}$$

The presence of a term involving $\cos\theta$ in (7.17) means that we cannot completely decouple the angular dependence of the field, as was done in chapters 5 and 6. However, in appendix C.1 a recurrence relation (C.5) is derived relating

$\cos\theta\, Y_{lm}$ to $Y_{l+1\,m}$ and $Y_{l-1\,m}$. This enables us to rewrite (7.17) as

$$\sum_{l,m} Y_{lm}(\theta,\phi)\left\{\frac{\partial^2\phi^{lm}}{\partial\lambda^2} - 2\frac{\partial^2\phi^{lm}}{\partial\lambda\partial u} + \frac{2}{\lambda}\left(\frac{\partial\phi^{lm}}{\partial\lambda} - \frac{\partial\phi^{lm}}{\partial u} - M\frac{\partial^2\phi^{lm}}{\partial\lambda^2}\right)\right.$$
$$- \frac{1}{\lambda^2}\left(l(l+1)\phi^{lm} + 2M\frac{\partial\phi^{lm}}{\partial\lambda}\right)$$
$$+ \frac{1}{\lambda^3}\left(-4iMam\frac{\partial\phi^{lm}}{\partial\lambda} - Ma^2\frac{\partial^2\phi^{lm}}{\partial\lambda^2}\right.$$
$$\left.+3Ma^2\left[A_{l-2\,m}\frac{\partial^2\phi^{l-2\,m}}{\partial\lambda^2} + B_{lm}\frac{\partial^2\phi^{lm}}{\partial\lambda^2} + C_{l+2\,m}\frac{\partial^2\phi^{l+2\,m}}{\partial\lambda^2}\right]\right)$$
$$\left.+\frac{2}{\lambda^4}iMam\phi^{lm} + O\left(\frac{Ma^2\phi^{lm}}{\lambda^4}\right)\right\} = 0, \tag{7.18}$$

It is the presence of the $\phi^{l\pm2\,m}$ in (7.18) which gives rise to the "mode-mixing" between different $l-$poles (note that there is no mode-mixing between the $m-$poles). By inspection, noting that the coefficient of the mode-mixing terms in (7.18) is proportional to Ma^2, we expect the mode-mixing not to occur at leading order. Now consider a single harmonic mode in (7.18). In order to cast the equation into a more familiar form, we make a change of variables $(u,\lambda)\to(u,v)$ where

$$v = u + 2\lambda. \tag{7.19}$$

Note that unlike u, v is not a null coordinate for the Kerr spacetime background (unless $M = a = 0$) but it has been chosen because it is a characteristic coordinate of the homogeneous EPD equation. It will also be convenient to change the dependent variable via

$$\phi^{lm} = (v-u)^l z^{lm}(u,v). \tag{7.20}$$

With these changes (7.18) becomes

$$z^{lm}{}_{,uv} + \frac{l+1}{v-u}z^{lm}{}_{,u} - \frac{l+1}{v-u}z^{lm}{}_{,v} = S^{lm}(u,v;z^{lm}), \tag{7.21}$$

where

$$
\begin{aligned}
S^{lm}(u,v;z^{lm}) = &-\frac{4M}{v-u}\left(l(l-1)(v-u)^{-2}z^{lm}+2l(v-u)^{-1}z^{lm}{}_{,v}+z^{lm}{}_{,vv}\right)\\
&-\frac{4M}{(v-u)^2}\left(l(v-u)^{-1}z^{lm}+z^{lm}{}_{,v}\right)\\
&-\frac{16iMam}{(v-u)^3}\left(l(v-u)^{-1}z^{lm}+z^{lm}{}_{,v}\right)\\
&-\frac{8Ma^2}{(v-u)^3}\left(l(l-1)(v-u)^{-2}z^{lm}+2l(v-u)^{-1}z^{lm}{}_{,v}+z^{lm}{}_{,vv}\right)\\
&+\frac{24Ma^2}{(v-u)^3}\Big(A_{l-2\,m}[(l-2)(l-3)(v-u)^{-4}z^{l-2\,m}\\
&\qquad\qquad +2(l-2)(v-u)^{-3}z^{l-2\,m}{}_{,v}+(v-u)^{-2}z^{l-2\,m}{}_{,vv}]\\
&\qquad +B_{lm}[l(l-1)(v-u)^{-2}z^{lm}+2l(v-u)^{-1}z^{lm}{}_{,v}+z^{lm}{}_{,vv}]\\
&\qquad +C_{l+2\,m}[(l+2)(l+1)z^{l+2\,m}+2l(v-u)z^{l+2\,m}{}_{,v}\\
&\qquad\qquad +(v-u)^2z^{l+2\,m}{}_{,vv}]\Big)\\
&+\frac{8iMam}{(v-u)^4}z^{lm}+O\left(\frac{Ma^2z^{lm}}{(v-u)^4}\right).
\end{aligned}
\tag{7.22}
$$

As one might expect, (7.21) is an inhomogeneous Euler-Poisson-Darboux equation with a source term (7.22) which vanishes if $M=0$, in which case we recover (5.16). The general homogeneous solution is

$$
z_0^{lm}(u,v)=\left(\frac{\partial}{\partial u}\right)^l\frac{U^{lm}(u)}{(v-u)^{l+1}}+\left(\frac{\partial}{\partial v}\right)^l\frac{V^{lm}(v)}{(v-u)^{l+1}},
\tag{7.23}
$$

for some arbitrary functions U^{lm} and V^{lm}. As argued in §5.2, the terms involving U^{lm} correspond to outgoing radiation and those involving V^{lm} correspond to incoming radiation. For $l\geq 1$ the solutions contain a *geometrical tail*, in which characteristic initial data with compact support leads to a solution which does not have compact support.

To obtain solutions to the inhomogeneous Euler-Poisson-Darboux equation (7.21) we use the same approach as chapter 6. The solution to the characteristic initial value problem can be expressed in integral form using Riemann's method (6.28). An iterative succession of approximations can be obtained using Picard's method [106].

Consider the characteristic initial value problem described by figure below. We specify some characteristic initial outgoing data z_0^{lm} on QR. The initial

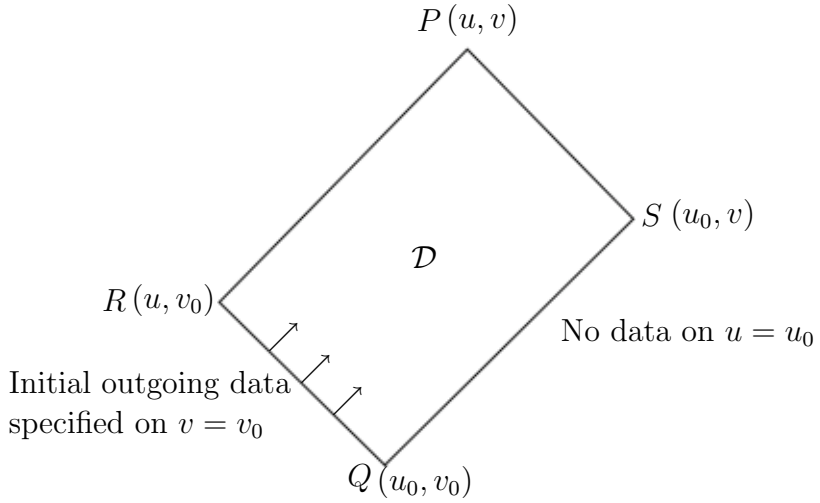

Figure 7.1: Characteristic initial value problem for a scalar field on a Kerr background with outgoing initial data.

data are written in the form

$$z_0^{lm}(u,v_0)=\left(\frac{\partial}{\partial u}\right)^l\frac{U^{lm}(u)}{(v_0-u)^{l+1}}, \tag{7.24}$$

so that the corresponding homogeneous solution is

$$z_0^{lm}(u,v)=\left(\frac{\partial}{\partial u}\right)^l\frac{U^{lm}(u)}{(v-u)^{l+1}}. \tag{7.25}$$

Following the argument of §6.2.2, the solution to (7.21) at (u,v) is given by

$$z^{lm}(u,v)=z_0^{lm}(u,v)+\int_{v_0}^{v}\int_{u_0}^{u}R^{lm}(u',v';u,v)S^{lm}\left(u',v';z^{lm}(u',v')\right)\mathrm{d}u'\mathrm{d}v', \tag{7.26}$$

where the Riemann-Green function $R^{lm}(u',v';u,v)$ is given by

$$R^{lm}(u',v';u,v)=(v'-u')^{2l+2}(v'-u)^{-(l+1)}(v-u')^{-(l+1)}{}_2F_1(l+1,l+1,1,t), \tag{7.27}$$

and

$$t=\frac{(v'-v)(u'-u)}{(v'-u)(u'-v)}. \tag{7.28}$$

Note again that we require that U^{lm} and its derivatives vanish at u_0, so that the solution is well-defined at (u_0, v_0).

Picard's method [106] enables us to approximate the inhomogeneous solution at (u, v) via a series of iterations of the form

$$z_i^{lm}(u,v) = z_0^{lm}(u,v) + \Delta z_{i-1}^{lm}(u,v), \tag{7.29}$$

where

$$\Delta z_{i-1}^{lm}(u,v) = \int_{v_0}^{v}\int_{u_0}^{u} R^{lm}(u',v';u,v) S^{lm}\left(u',v';z_{i-1}^{lm}(u',v')\right) \mathrm{d}u'\mathrm{d}v', \tag{7.30}$$

for $i \geq 1$. Thus the solution to (7.21) consists of the homogeneous solution $z_0^{lm}(u,v)$ together with the *gravitational tail*.

We can estimate the behaviour of the gravitational tail for general values of l as $v \to \infty$. Suppose that initial data are given in the far-field region (so that $M/v_0 \ll 1$ and $a/v_0 \ll 1$). By inspection we note that $R^{lm}(u',v';u,v)$ can be written in the form

$$R^{lm}(u',v';u,v) = \frac{(v'-u')}{(v-u)^{2l+1}} P(u,v,u',v'), \tag{7.31}$$

where $P(u,v,u',v')$ is a polynomial in u, v, u' and v' of order l and is homogeneous in u, v and u', v'. Consider the first iteration of Picard's method. A general term in $S^{lm}(u',v';z_{i-1}^{lm})$ (7.22) can be written in the form

$$\frac{1}{(v'-u')^x} \tag{7.32}$$

for some integer x. The leading order contribution in Δz_{i-1}^{lm} is obtained by taking the lower limit of the $v'-$integral. We deduce that $\Delta z_{i-1}^{lm} = O(1/v^{l+1})$ as $v \to \infty$.

This conclusion appears to be a contradiction since it implies that Picard's method will not converge. However we must also consider the *coefficient* of $1/v^{l+1}$. By inspection, this coefficient will, in general, involve factors of the form $M^x a^y / v_0^z$ where $z > x + y$. Provided that v_0 is in the far field region (so that $M/v_0 \ll 1$ and $a/v_0 \ll 1$), then the coefficient of $1/v^{l+1}$ in Δz_{i-1}^{lm} will be small and $\Delta z_i^{lm} \ll \Delta z_{i-1}^{lm}$. Picard's method will therefore converge. By inspection once more, we note that the first order contribution to the coefficient

of $1/v^{l+1}$ in the gravitational tail will involve the mass parameter M but not the angular momentum parameter a. At second order both a and M will be involved. At third order, mode-mixing terms proportional to Ma^2 will be present (although we have not listed all the third order terms in (7.22)). A general term in the coefficient of $1/v^{l+1}$ in the gravitational tail Δz^{lm}_{i-1} will take the form

$$\frac{M^x a^y F(u)}{v_0^z}, \tag{7.33}$$

where $z > x + y$, and $F(u)$ is a function which depends on the choice of initial data.

As was mentioned in chapter 6, the condition $M \ll v_0$, required for the convergence of Picard's method, provides a consistency condition on the location of the outer boundary and the validity of any boundary conditions derived for the scalar field.

We illustrate these arguments explicitly by considering the modes $l = 0$, 1 and 2. Although we did not list all the $O(Ma^2/v^4)$ terms in (7.22) (there are too many to write down here), we are nevertheless able to illustrate the mode-mixing that occurs at this order.

7.2.1 The Monopole Case, $l = 0$

In the case $l = 0$, the initial data are written in the form

$$z^0(u, v_0) = \frac{U^0(u)}{(v_0 - u)}, \tag{7.34}$$

where $U^0(u_0) = 0$. Note that $l = 0$ implies that $m = 0$ so we have dropped the m suffix for convenience. The Riemann-Green function (7.27) is given by

$$R^0(u', v'; u, v) = \frac{v' - u'}{v - u}. \tag{7.35}$$

Performing one iteration of Picard's method, we obtain

$$\begin{aligned}\Delta z^0_0 &= \frac{1}{v-u}\int_{v_0}^{v}\int_{u_0}^{u}\left[-\frac{4MU^0(u')}{(v'-u')^3} + O\left(\frac{Ma^2}{v'^5}\right)\right]\mathrm{d}u'\mathrm{d}v' \\ &= \frac{1}{v-u}\int_{v_0}^{v}\left[-\frac{4MU^{0(-1)}(u)}{(v'-u)^3} + \frac{12MU^{0(-2)}(u)}{(v'-u)^4} + O\left(\frac{Ma^2}{v'^5}\right)\right]\mathrm{d}v', \end{aligned} \tag{7.36}$$

were the $u'-$integral has been done by parts, neglecting higher order terms. For convenience we have defined

$$U^{0(-1)}(u) = \int_{u_0}^{u} U^0(u')\mathrm{d}u', \quad U^{0(-2)}(u) = \int_{u_0}^{u} U^{0(-1)}(u')\mathrm{d}u'. \tag{7.37}$$

The $v'-$integral can be evaluated explicitly. We obtain

$$z_1^0(u,v) = \frac{1}{v-u}\left(U^0(u) - \frac{2MU^{0(-1)}(u)}{(v_0-u)^2} + \frac{4MU^{0(-2)}(u)}{(v_0-u)^3} + O\left(\frac{Ma^2}{v_0^4}\right)\right) + O\left(\frac{1}{(v-u)^2}\right). \tag{7.38}$$

A second iteration of Picard's method can be performed by repeating the calculation above, but with $U^0(u)$ replaced by

$$U^0(u) - \frac{2MU^{0(-1)}(u)}{(v_0-u)^2} + \frac{4MU^{0(-2)}(u)}{(v_0-u)^3} + O\left(\frac{Ma^2}{v_0^4}\right). \tag{7.39}$$

It is easy to check that the terms displayed in (7.38) are unaltered by the second iteration (and hence by all subsequent iterations).

Perusal of (7.22) suggests that at $O(Ma^2/v_0^4)$ there will be some mode-mixing behaviour. The $O(Ma^2/v_0^4)$ contribution cannot be determined precisely because there are further terms present that were not displayed in (7.22), but it is nevertheless instructive to evaluate the mode mixing terms. If $l = 0$, then $A_{l-2\,m}$ in (7.22) vanishes and $C_{l+2\,m} = 2/3\sqrt{5}$. Hence there is a contribution from the $l = 2$ mode. Suppose that the initial characteristic outgoing data for the $l = 2$ mode are given by

$$z^2(u,v_0) = \left(\frac{\partial}{\partial u}\right)^2 \frac{U^2(u)}{(v_0-u)^3}, \tag{7.40}$$

for some function $U^2(u)$. If we perform a single iteration of Picard's method using these data, we find that the leading order mode-mixing contribution to the $l = 0$ mode due to the $l = 2$ mode is

$$\frac{1}{v-u}\left(\frac{56Ma^2U^2(u)}{5\sqrt{5}(v_0-u)^4}\right). \tag{7.41}$$

7.2.2 The Dipole Case, $l = 1$

The initial outgoing data for $l = 1$ can be written in the form

$$z^1(u, v_0) = \frac{\partial}{\partial u}\frac{U^1(u)}{(v_0 - u)^2}, \tag{7.42}$$

for some function $U^1(u)$. Again for convenience we drop the m suffix here. The Riemann-Green function (7.27) is given by

$$R^1(u', v'; u, v) = \frac{v' - u'}{(v - u)^3}\left[(v' - u)(u' - v) + (v' - v)(u' - u)\right]. \tag{7.43}$$

We find that

$$S^1(u', v'; z_0^1) = -\frac{4MU^{1^{(1)}}(u')}{(v' - u')^5} - \frac{56MU^1(u')}{(v' - u')^6} + \frac{24iMamU^{1^{(1)}}(u')}{(v' - u')^6} + O\left(\frac{Ma^2}{(v' - u')^7}\right). \tag{7.44}$$

Since the Riemann-Green function is more complicated than the one dealt with in §7.2.1, we now adopt a slightly different approach. The $v'-$integral in Δz_0^1 can be evaluated precisely (this is best done using a computer algebra package). Next we make a Taylor expansion of the result in powers of $1/v$ to obtain

$$\Delta z_0^1 = \frac{1}{v^2}\int_{u_0}^{u}\left\{\frac{2MU^{1^{(1)}}(u')(4u - u' - 3v_0)}{3(v_0 - u')^3} + \frac{28MU^1(u')(3u - u' - 2v_0)}{3(v_0 - u')^4} - \frac{4iMamU^{1^{(1)}}(u')(3u - u' - 2v_0)}{(v_0 - u')^4} + O\left(\frac{Ma^2}{v_0^4}\right)\right\}\mathrm{d}u' + O\left(\frac{1}{v^3}\right). \tag{7.45}$$

The integrand is then expanded in powers of $1/v_0$ to give

$$\Delta z_0^1 = \frac{1}{v^2}\int_{u_0}^{u}\Bigg\{-\frac{2MU^{1(1)}(u')}{v_0^2}+\frac{4MU^{1(1)}(u')(2u-5u')}{3v_0^3} + \frac{2MU^{1(1)}(u')u'(4u-7u')}{v_0^4}-\frac{56MU^{1}(u')}{3v_0^3} + \frac{28MU^{1}(u')(u-3u')}{v_0^4}+\frac{8iMamU^{1(1)}(u')}{3v_0^3} -\frac{4iMamU^{1(1)}(u')(u-3u')}{v_0^4}+O\left(\frac{Ma^2}{v_0^4}\right)\Bigg\}\,\mathrm{d}u'+O\left(\frac{1}{v^3}\right). \tag{7.46}$$

The $u'-$integral can now be performed. We find

$$z_1^1(u,v) = \frac{\partial}{\partial u}\frac{U^1(u)}{(v-u)^2}+\frac{1}{v^2}\left(-\frac{2MU^1(u)}{v_0^2} + \frac{-36MU^{1\,(-1)}(u)-12MuU^1(u)+8iMamU^1(u)}{3v_0^3} +O\left(\frac{Ma^2}{v_0^4}\right)\right)+O\left(\frac{1}{v^3}\right). \tag{7.47}$$

As was found in the monopole case, a second iteration of Picard's method has no effect on the terms displayed in (7.47).

By inspection of the source term (7.22), we note that for $l=1$, $A_{l-2\,m}=0$ but $C_{l+2\,m}\neq 0$. We therefore expect that at $O(Ma^2/v_0^4)$ there will be a mode-mixing contribution from the $l=3$ (octopole) solution. Suppose that the initial octopole data are given by

$$z^3(u,v_0) = \left(\frac{\partial}{\partial u}\right)^3\frac{U^3(u)}{(v_0-u)^4}, \tag{7.48}$$

for some function $U^3(u)$. Then the contribution to Δz_0^1 can be evaluated. We find that the leading order octopole contribution to the dipole mode is

$$\frac{1}{v^2}432Ma^2C_{3\,m}\frac{U^{3(2)}(u)}{v_0^4}. \tag{7.49}$$

Note once more that there are other terms of $O(Ma^2/v_0^4)$ which we have not evaluated here.

7.2.3 The Quadrupole Case, $l = 2$

To calculate the quadrupole contribution to the gravitational tail, we adopt a similar approach to the dipole calculation in §7.2.2. The initial data on $v = v_0$ are written in the form

$$z^2(u, v_0) = \left(\frac{\partial}{\partial u}\right)^2 \frac{U^2(u)}{(v_0 - u)^3}. \tag{7.50}$$

The source term $S^2(u', v'; z_0^2)$ for the first Picard-iteration is given by

$$S^2(u', v'; z_0^2) = \frac{-4MU^{2^{(2)}}(u')}{(v' - u')^6} - \frac{96MU^{2^{(1)}}(u')}{(v' - u')^7} - \frac{24iMamU^{2^{(2)}}(u')}{(v' - u')^7} + O\left(\frac{Ma^2}{(v' - u')^8}\right). \tag{7.51}$$

The $v'-$integral in Δz_0^2 can be evaluated explicitly (this is best done using a computer algebra package). We expand the result in powers of $1/v$ to obtain

$$\begin{aligned}\Delta z_0^2 = \frac{1}{v^3}\int_{u_0}^{u} \Bigg\{ & \frac{-2MU^{2^{(2)}}(u')(3u^2 - 2uu' - 4uv_0 + 2u'v_0 + v_0^2)}{(v_0 - u')^4} \\ & + \frac{16MU^{2^{(1)}}(u')(-36u^2 + 27uu' + 45uv_0 - u'^2 - 25u'v_0 - 10v_0^2)}{5(v_0 - u')^5} \\ & + \frac{4iMamU^{2^{(2)}}(u')(-36u^2 + 27uu' + 45uv_0 - u'^2 - 25u'v_0 - 10v_0^2)}{5(v_0 - u')^5} \\ & + O\left(\frac{Ma^2}{v_0^4}\right)\Bigg\}\,\mathrm{d}u' + O\left(\frac{1}{v^4}\right). \end{aligned} \tag{7.52}$$

The integrand is now expanded in powers of $1/v_0$,

$$\begin{aligned}\Delta z_0^2 = \frac{1}{v^3}\int_{u_0}^{u} \Bigg\{ & -\frac{2MU^{2^{(2)}}(u')}{v_0^2} - \frac{4MU^{2^{(2)}}(u')(3u' - 2u)}{v_0^3} \\ & - \frac{32MU^{2^{(1)}}(u')}{v_0^3} - \frac{8iMamU^{2^{(2)}}(u')}{v_0^3} \\ & + O\left(\frac{Ma^2}{v_0^4}\right)\Bigg\}\,\mathrm{d}u' + O\left(\frac{1}{v^4}\right). \end{aligned} \tag{7.53}$$

Finally, performing the $u'-$integral we obtain

$$z_1^2(u,v) = \left(\frac{\partial}{\partial u}\right)^2 \frac{U^2(u)}{(v-u)^3} + \frac{1}{v^3}\left(-\frac{2MU^{2^{(1)}}(u)}{v_0^2} - \frac{20MU^2(u) + 4MU^{2^{(1)}}(u) + 8iMamU^{2^{(1)}}(u)}{v_0^3} + O\left(\frac{Ma^2}{v_0^4}\right)\right) + O\left(\frac{1}{v^4}\right). \tag{7.54}$$

Again, it is easy to check that subsequent iterations of Picard's method have no effect upon the terms displayed in (7.54).

Inspection of (7.22) suggests that at $O(Ma^2/v_0^4)$ there will be a contribution from $l = 4$ mode and, in addition, if $m = 0$ there will be a contribution from the $l = 0$ mode. Although there are other contributions at this order which we will not evaluate, it is nevertheless interesting to calculate this mode-mixing effect. Suppose the initial data for the $l = 0$ and $l = 4$ modes are given by

$$z^0(u, v_0) = \frac{U^0(u)}{(v_0 - u)}, \tag{7.55}$$

and

$$z^4(u, v_0) = \left(\frac{\partial}{\partial u}\right)^4 \frac{U^4(u)}{(v_0 - u)^5}, \tag{7.56}$$

respectively. Then the corresponding contribution to $S^2(u', v'; z_0^2)$ is

$$\frac{24Ma^2}{(v'-u')^8}\left[2A_{0\,m}U^0(u') + 22C_{4\,m}U^{2^{(4)}}(u')\right]. \tag{7.57}$$

(Note that $A_{0\,m} = 0$ if $m \neq 0$.) Evaluating the integrals to leading order, we find that the mode mixing contribution at $O(Ma^2/v_0^4)$ is

$$\frac{1}{v^3}\frac{24Ma^2}{v_0^4}\left[2A_{0\,m}U^{0^{(-1)}}(u) + 22C_{4\,m}U^{4^{(3)}}(u)\right]. \tag{7.58}$$

To summarize: the scalar field consists of the homogeneous solution (corresponding to propagation on flat space, §5.2), together with a "gravitational tail" which is present even if $l = 0$. This gravitational effect is transmitted slower than light. An initially sharp wave will then develop a tail due to the

curvature of the background spacetime. Huygens' principle is not satisfied.

The gravitational tail decays in the same way as the homogeneous solution as $v \to \infty$. However, the ratio X of the size of the gravitational tail to the size of the homogeneous solution is small, provided that the characteristic initial value problem is solved in the far-field region. The leading order contribution to X is of the form M/v_0^2. The second order contribution to X is of the form Ma/v_0^3. The third order contribution is of the form Ma^2/v_0^4. In addition, at third order, some mode-mixing occurs. For a given harmonic mode (i.e. a given value of l and m) there is a contribution from the $l+2, m-$mode. In addition, provided that $l \geq 2$ and $m \leq l-2$, there is also a contribution from the $l-2, m-$mode.

7.3 Linearized Gravitational Radiation on a Kerr Background

We now apply the techniques developed in the previous section to linearized gravitational waves on a Kerr background. Our starting point is the scalar field equation for the Hertz potential (4.36), which on a Kerr background is

$$(\text{Þ}\text{Þ}' - \eth\eth' + 3\rho'\text{Þ} - \bar{\rho}\text{Þ}' - 3\tau'\eth + \bar{\tau}'\eth' - 6\Psi_2)\,\chi' = 0. \tag{7.59}$$

As in §7.2, we choose the chart and tetrad that were introduced in §7.1. The Newman-Penrose scalars and the Weyl scalars are given by (7.13) and (7.14) respectively. We expand the Hertz potential in terms of spin-weighted spherical harmonics,

$$\chi' = \sum_{l,m} \chi^{lm}(u,\lambda)\,{}_2Y_{lm}(\theta,\phi). \tag{7.60}$$

The spin-weighted spherical harmonic conventions used here are defined in appendix C.2. Note that the operators $\eth$ and $\eth'$ in (7.59) are contractions of the covariant derivative ∇ with the tetrad (7.12). Unlike in the calculations of chapters 5 and 6, these now differ from the $\eth$ and $\eth'$ used in appendix C.2, which are defined by (C.8). Therefore, rather than using the eigenvalue equation (C.11), we use (C.12), which reads

$$\begin{aligned}\left(\frac{\partial^2}{\partial\theta^2} + \csc^2\theta\frac{\partial^2}{\partial\phi^2} - (1+2s)i\frac{\cos\theta}{\sin^2\theta}\frac{\partial}{\partial\phi} - \frac{s+s^2\cos^2\theta}{\sin^2\theta}\right){}_sY_{lm}(\theta,\phi)\\ = -(l+s)(l-s+1)\,{}_sY_{lm}(\theta,\phi).\end{aligned} \tag{7.61}$$

Substituting the spin-weighted spherical harmonic expansion (7.60) into (7.59), and making use of (7.61) yields

$$\sum_{l,m} {}_2Y_{lm}(\theta,\phi)\left\{\frac{\partial^2\chi^{lm}}{\partial\lambda^2}-2\frac{\partial^2\chi^{lm}}{\partial\lambda\partial u}-\frac{2}{\lambda}\left(\frac{\partial\chi^{lm}}{\partial u}+\frac{\partial\chi^{lm}}{\partial\lambda}+M\frac{\partial^2\chi^{lm}}{\partial\lambda^2}\right)\right.$$
$$+\frac{1}{\lambda^2}\left(-(l+2)(l-1)\chi^{lm}+10M\frac{\partial\chi^{lm}}{\partial\lambda}\right)$$
$$+\frac{1}{\lambda^3}\left(-16M\chi^{lm}+4iMa(3\cos\theta-1)\frac{\partial\chi^{lm}}{\partial\lambda}\right.$$
$$\left.+Ma^2(3\cos^2\theta-1)\frac{\partial^2\chi^{lm}}{\partial\lambda^2}\right)$$
$$\left.+\frac{8iMam\chi^{lm}}{\lambda^4}+O\left(\frac{Ma^2\chi^{lm}}{\lambda^4}\right)\right\}=0. \tag{7.62}$$

The trigonometric terms render (7.62) difficult to solve. However, in appendix C.2, we derive some new recurrence relations, (C.20) and (C.24), connecting $\cos\theta\,{}_sY_{lm}$ with ${}_sY_{l+1\,m}$ and ${}_sY_{l-1\,m}$. This enables us to rewrite (7.62) as

$$\sum_{l,m} {}_2Y_{lm}(\theta,\phi)\left\{\frac{\partial^2\chi^{lm}}{\partial\lambda^2}-2\frac{\partial^2\chi^{lm}}{\partial\lambda\partial u}-\frac{2}{\lambda}\left(\frac{\partial\chi^{lm}}{\partial u}+\frac{\partial\chi^{lm}}{\partial\lambda}+M\frac{\partial^2\chi^{lm}}{\partial\lambda^2}\right)\right.$$
$$+\frac{1}{\lambda^2}\left(-(l+2)(l-1)\chi^{lm}+10M\frac{\partial\chi^{lm}}{\partial\lambda}\right)-\frac{1}{\lambda^3}16M\chi^{lm}$$
$$+\frac{1}{\lambda^3}12iMa\left({}_2A_{l-1\,m}\frac{\partial\chi^{l-1\,m}}{\partial\lambda}+[{}_2B_{lm}-\tfrac{1}{3}]\frac{\partial\chi^{lm}}{\partial\lambda}+{}_2C_{l+1\,m}\frac{\partial\chi^{l+1\,m}}{\partial\lambda}\right)$$
$$+\frac{1}{\lambda^3}3Ma^2\left({}_2E_{l-2\,m}\frac{\partial^2\chi^{l-2\,m}}{\partial\lambda^2}+{}_2F_{l-1\,m}\frac{\partial^2\chi^{l-1\,m}}{\partial\lambda^2}+[{}_2G_{lm}-\tfrac{1}{3}]\frac{\partial^2\chi^{lm}}{\partial\lambda^2}\right.$$
$$\left.+{}_2H_{l+1\,m}\frac{\partial^2\chi^{l+1\,m}}{\partial\lambda^2}+{}_2I_{l+2\,m}\frac{\partial^2\chi^{l+2\,m}}{\partial\lambda^2}\right)$$
$$\left.+\frac{8iMam\chi^{lm}}{\lambda^4}+O\left(\frac{Ma^2\chi^{lm}}{\lambda^4}\right)\right\}=0. \tag{7.63}$$

Consider a single harmonic mode in (7.63). The presence of $\chi^{l\pm1\,m}$ and $\chi^{l\pm2\,m}$ gives rise to the mode-mixing. Inspecting the terms of order Ma/λ^3, we deduce that for a given l and m there will always be a contribution from the $l+1,m-$mode. If $m\leq l-1$ then there will also be a contribution from $l-1,m-$mode (otherwise ${}_2A_{l-1\,m}$ is zero). The exception to this rule is the case

$l = 2$ for which ${}_2A_{1\,m}$ is always zero. Consider now the terms of order Ma^2/λ^3. At this order, contributions from the $l+1, m-$ and $l+2, m-$modes will always be present. If $m \leq l-1$ then ${}_2F_{l-1\,m}$ is non-zero and so there will be a contribution from $l-1, m-$mode. Similarly, if $m \leq l-2$ then ${}_2E_{l-2\,m}$ is non-zero and so there will be a contribution from the $l-2, m-$mode. The exceptions to this rule are $l = 2$ (for which ${}_2E_{0\,m}$ and ${}_2F_{1\,m}$ are always zero) and $l = 3$ (for which ${}_2E_{1\,m}$ vanishes). These exceptions are expected since $l = 0$ (monopole) and $l = 1$ (dipole) gravitational poles are non-radiative and should not contribute to the mode-mixing.

In order to make further analytical progress we make a change of independent variables $(u, \lambda) \to (u, v)$, where

$$v = u + 2\lambda. \tag{7.64}$$

It is also convenient to change the dependent variable via

$$\chi^{lm} = (v-u)^{1-l}\omega^{lm}(u, v). \tag{7.65}$$

With these changes, considering a single harmonic mode in (7.63) implies

$$\omega^{lm}{}_{,uv} - \frac{l-2}{v-u}\omega^{lm}{}_{,u} + \frac{l+2}{v-u}\omega^{lm}{}_{,v} = S^{lm}(u, v; \omega^{lm}), \tag{7.66}$$

where

$$
\begin{aligned}
S^{lm}(u,v;\omega^{lm}) = &-\frac{4M}{v-u}\left(\omega^{lm}{}_{,vv}-\frac{2l+3}{v-u}\omega^{lm}{}_{,v}+\frac{(l+1)(l+3)}{(v-u)^2}\omega^{lm}\right)\\
&+\frac{16iMa}{(v-u)^2}\left(3_2A_{l-1\,m}\left[\omega^{l-1m}{}_{,v}-\frac{l-2}{v-u}\omega^{l-1\,m}\right]\right.\\
&\qquad+(3_2B_{lm}+2m-1)\left[\frac{1}{v-u}\omega^{lm}{}_{,v}-\frac{l-1}{(v-u)^2}\omega^{lm}\right]\\
&\qquad\left.+3_2C_{l+1\,m}\left[\frac{1}{(v-u)^2}\omega^{l+1\,m}{}_{,v}-\frac{l}{(v-u)^3}\omega^{l+1\,m}\right]\right)\\
&+\frac{24Ma^2}{(v-u)^3}\left(_2E_{l-2\,m}[(v-u)^2\omega^{l-2\,m}{}_{,vv}-2(l-3)(v-u)^2\omega^{l-2\,m}{}_{,v}\right.\\
&\qquad+(l-2)(l-3)\omega^{l-2\,m}]\\
&\qquad+{}_2F_{l-1\,m}\left[(v-u)\omega^{l-1\,m}{}_{,vv}-2(l-2)\omega^{l-1\,m}{}_{,v}\right.\\
&\qquad\left.+\frac{(l-2)(l-1)}{v-u}\omega^{l-1\,m}\right]\\
&\qquad+({}_2G_{lm}-\tfrac{1}{3})\left[\omega^{lm}{}_{,vv}-\frac{2(l-1)}{v-u}\omega^{lm}{}_{,v}+\frac{l(l-1)}{(v-u)^2}\omega^{lm}\right]\\
&\qquad+{}_2H_{l+1\,m}\left[\frac{1}{v-u}\omega^{l+1\,m}{}_{,vv}-\frac{2l}{(v-u)^2}\omega^{l+1\,m}{}_{,v}\right.\\
&\qquad\left.+\frac{l(l+1)}{(v-u)^3}\omega^{l+1\,m}\right]\\
&\qquad+{}_2I_{l+2\,m}\left[\frac{1}{(v-u)^2}\omega^{l+2\,m}{}_{,vv}-\frac{2(l+1)}{(v-u)^3}\omega^{l+2\,m}{}_{,v}\right.\\
&\qquad\left.\left.+\frac{(l+1)(l+2)}{(v-u)^4}\omega^{l+2\,m}\right]\right)\\
&+O\left(\frac{Ma^2w^{lm}}{(v-u)^4}\right),
\end{aligned}
\tag{7.67}
$$

Once again we have obtained an inhomogeneous Euler-Poisson-Darboux equation (7.66) with a source term (7.67) which is non-zero if $a \neq 0$ and $M \neq 0$. We seek solutions by considering the, now familiar, characteristic initial value problem and using a Picard iteration scheme.

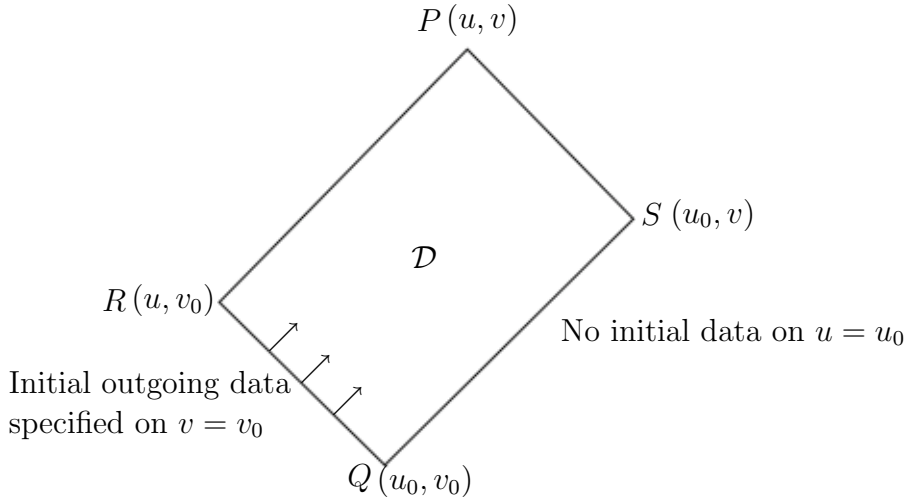

Figure 7.2: Characteristic initial value problem for Hertz potential on a Kerr background with outgoing initial data.

The solution to (7.66) can be written down in integral form as

$$\omega^{lm}(u,v)=\omega_0^{lm}(u,v)+\int_{v_0}^{v}\int_{u_0}^{u}R^{lm}(u',v';u,v)S^{lm}\left(u',v';\omega^{lm}(u',v')\right)\mathrm{d}u'\mathrm{d}v', \tag{7.68}$$

where the Riemann-Green function is given by

$$R^{lm}(u',v';u,v)=(v'-u')^{-2l}(v'-u)^{l+2}(v-u')^{l-2}{}_2F_1(-2-l,2-l;1;t), \tag{7.69}$$

and

$$t=\frac{(v'-v)(u'-u)}{(v'-u)(u'-v)}. \tag{7.70}$$

The general homogeneous solution is

$$\omega_0^{lm}(u,v)=(v-u)^{2l+1}\left[\left(\frac{\partial}{\partial v}\right)^{l+2}\frac{V^{lm}(v)}{(v-u)^{l-1}}+\left(\frac{\partial}{\partial u}\right)^{l-2}\frac{U^{lm}(u)}{(v-u)^{l+3}}\right], \tag{7.71}$$

In §5.3, we argued that setting $V^{lm}(v)=0$ corresponds to an outgoing radiative solution. We also showed that on the edges QR and QS of the domain of dependence $\mathcal{D}$ of the point (u,v), the homogeneous and inhomogeneous solutions are identical, since the integral in (7.68) vanishes. In order to investigate the propagation of outgoing gravitational radiation, we therefore choose

$$\omega^{lm}(u,v_0)=(v_0-u)^{2l+1}\frac{\partial^{l-2}}{\partial u^{l-2}}\frac{U^{lm}(u)}{(v_0-u)^{l+3}}=\omega_0^{lm}(u,v_0), \tag{7.72}$$

as the outgoing characteristic initial data on v_0, and specify $\omega^{lm}(u_0, v) = 0$ (note that $U^{lm}(u)$ and its derivatives must vanish on u_0). The solution (7.68) is approximated using Picard's method:

$$\omega_i^{lm} = \omega_0^{lm} + \Delta\omega_{i-1}^{lm}, \tag{7.73}$$

where

$$\Delta\omega_{i-1}^{lm} = \int_{v_0}^{v}\int_{u_0}^{u} R^{lm}(u', v'; u, v) S^{lm}\left(u', v'; \omega_{i-1}^{lm}(u', v')\right) \mathrm{d}u'\mathrm{d}v'. \tag{7.74}$$

In general ${}_2F_1$ is a polynomial of order $l-2$ in t. As $v \to \infty$ we expect $\Delta\omega_i^{lm} = O(v^{l-2})$. This is of the same order of magnitude as the homogeneous solution. However, if the initial data are in the far-field region (so that $a/v_0 \ll 1$ and $M/v_0 \ll 1$) then the coefficient of v^{l-2} in $\Delta\omega^{lm}$ will be small compared to the homogeneous solution, and $\Delta\omega_i^{lm} \ll \Delta\omega_{i-1}^{lm}$. The boundary conditions subsequently derived in this section are therefore only valid if the boundary of the computational domain lies in the far-field region, so that the conditions $M \ll v_0$ and $a \ll v_0$ hold. This provides a consistency requirement on the location of the numerical boundary.

7.3.1 The Quadrupole Case, $l = 2$

We illustrate the arguments above by considering the case $l = 2$. The initial data are written in the form

$$\omega^{2\,m}(u, v_0) = U^{2\,m}(u), \tag{7.75}$$

so that the corresponding homogeneous solution is

$$\omega_0^{2\,m}(u, v) = U^{2\,m}(u). \tag{7.76}$$

We also need initial data from the $l = 3$ mode, since this will also contribute to the propagation of the $l = 2$ mode. We posit

$$\omega^{3\,m}(u, v_0) = (v_0 - u)^7 \frac{\partial}{\partial u}\frac{U^{3\,m}(u)}{(v_0 - u)^6}, \tag{7.77}$$

which corresponds to the homogeneous solution

$$\omega_0^{3\,m}(u,v) = (v-u)^7 \frac{\partial}{\partial u}\frac{U^{3\,m}(u)}{(v-u)^6}. \tag{7.78}$$

The Riemann-Green function is

$$R^{2\,m}(u',v';u,v) = \left(\frac{v'-u}{v'-u'}\right)^4. \tag{7.79}$$

The source function for the first iteration of Picard's method $S^{2\,m}(u,v;\omega_0^{lm})$ is given by

$$\begin{aligned} S^{2\,m}(u,v;\omega_0^{lm}) = &-\frac{60MU^{2\,m}(u)}{(v-u)^3} - \frac{16iMa(3\,{}_2B_{2\,m}+2m-1)U^{2\,m}(u)}{(v-u)^4} \\ &- \frac{48iMa\,{}_2C_{3\,m}U^{3\,m^{(1)}}(u)}{(v-u)^4} + O\left(\frac{Ma^2}{(v-u)^5}\right). \end{aligned} \tag{7.80}$$

We then find that

$$\begin{aligned} \Delta\omega_0^{2\,m} = \int_{v_0}^{v}\int_{u_0}^{u} &-60M\frac{U^{2\,m}(u')(v'-u)^4}{(v'-u')^7} - 16iMa(3\,{}_2B_{2\,m}+2m-1)\frac{U^{2\,m}(u')(v'-u)^4}{(v'-u')^8} \\ &- 48iMa\,{}_2C_{3\,m}\frac{U^{3\,m^{(1)}}(u')(v'-u)^4}{(v'-u')^8} + O\left(\frac{Ma^2}{(v'-u')^5}\right)\mathrm{d}u'\mathrm{d}v' \end{aligned} \tag{7.81}$$

The $u'-$integral is evaluated by parts, neglecting higher order terms in v'. Evaluating the $v'-$integral, we find.

$$\begin{aligned}\Delta\omega_0^{2\,m} = \int_{v_0}^{v} \Bigg[& -60M\frac{U^{2\,m^{(-1)}}(u)}{(v'-u)^3} + 420M\frac{U^{2\,m^{(-2)}}(u)}{(v'-u)^4} - 16iMa({}_2B_{2\,m}+2m-1)\frac{U^{2\,m^{(-1)}}(u)}{(v'-u)^4} \\ & -48iMa\,{}_2C_{3\,m}\frac{U^{3\,m}(u)}{(v'-u)^4} + O\left(\frac{Ma^2}{(v'-u)^5}\right)\Bigg]\,\mathrm{d}v', \\ = & \left\{-30M\frac{U^{2\,m^{(-1)}}(u)}{(v_0-u)^2} + 140M\frac{U^{2\,m^{(-2)}}(u)}{(v_0-u)^3} - \frac{16}{3}({}_2B_{2\,m}+2m-1)\frac{U^{2\,m^{(-1)}}(u)}{(v_0-u)^3}\right. \\ & \left. -16iMa\,{}_2C_{3\,m}\frac{U^{3\,m}(u)}{(v_0-u)^3} + O\left(\frac{Ma^2}{(v_0-u)^4}\right)\right\} \\ & + \left\{30M\frac{U^{2\,m^{(-1)}}(u)}{(v-u)^2} - 140M\frac{U^{2\,m^{(-2)}}(u)}{(v-u)^3} + \frac{16}{3}({}_2B_{2\,m}+2m-1)\frac{U^{2\,m^{(-1)}}(u)}{(v-u)^3}\right. \\ & \left. +16iMa\,{}_2C_{3\,m}\frac{U^{3\,m}(u)}{(v-u)^3} + O\left(\frac{Ma^2}{(v-u)^4}\right)\right\}. \end{aligned} \tag{7.82}$$

It is easy to check that subsequent iterations have no effect on the terms displayed above. As a further check of our calculations, the $v-$dependent terms in (7.82) can be substituted into the Euler-Poisson-Darboux equation (7.66) to recover the source terms. There is a contribution to the gravitational tail (7.82) from the $l = 3$ mode. At higher order there are also contributions from the harmonic modes with $l \geq 4$.

We summarise these results by translating them back in terms of the Hertz potential $\chi^{2\,m}$ using (7.65). Initial outgoing data on the surface $v = v_0$ are written as

$$\chi_0^{2\,m}(u,v) = \frac{U^{2m}(u)}{v_0-u}. \tag{7.83}$$

The homogeneous solution to the Euler-Poisson-Darboux equation satisfying these initial data is given by

$$\chi_0^{2\,m} = \frac{U^{2\,m}(u)}{v-u}. \tag{7.84}$$

The solution to the inhomogeneous EPD equation is

$$\begin{aligned}\chi^{2\,m}(u,v) =& \frac{F(u)}{v-u} + 30M\frac{U^{2\,m^{(-1)}}(u)}{(v-u)^3} - 140M\frac{U^{2\,m^{(-2)}}(u)}{(v-u)^4} \\ &+ \frac{16}{3}(3\,{}_2B_{2\,m} + 2m - 1)\frac{U^{2\,m^{(-1)}}(u)}{(v-u)^4} \\ &+ 16iMa\,{}_2C_{3\,m}\frac{U^{3\,m}(u)}{(v-u)^4} + O\left(\frac{1}{(v-u)^5}\right), \end{aligned} \tag{7.85}$$

where

$$\begin{aligned}F(u) =& U^{2\,m}(u) - 30M\frac{U^{2\,m^{(-1)}}(u)}{(v_0-u)^2} + 140M\frac{U^{2\,m^{(-2)}}(u)}{(v_0-u)^3} \\ &- \frac{16}{3}(3\,{}_2B_{2\,m} + 2m - 1)\frac{U^{2\,m^{(-1)}}(u)}{(v_0-u)^3} - 16iMa\,{}_2C_{3\,m}\frac{U^{3\,m}(u)}{(v_0-u)^3} \\ &+ O\left(\frac{Ma^2}{(v_0-u)^4}\right). \end{aligned} \tag{7.86}$$

The solution then consists the homogeneous solution (7.84), but with $U^{2\,m}(u)$ replaced by $F(u)$. In addition, there is an extra gravitational tail term,

$$\begin{aligned}&30M\frac{U^{2\,m^{(-1)}}(u)}{(v-u)^3} - 140M\frac{U^{2\,m^{(-2)}}(u)}{(v-u)^4} + \frac{16}{3}(3\,{}_2B_{2\,m} + 2m - 1)\frac{U^{2\,m^{(-1)}}(u)}{(v-u)^4} \\ &\qquad + 16iMa\,{}_2C_{3\,m}\frac{U^{3\,m}(u)}{(v-u)^4} + O\left(\frac{1}{(v-u)^5}\right), \end{aligned} \tag{7.87}$$

which cannot be expressed as a solution to the homogeneous EPD equation. In general, the Hertz potential that generates outgoing quadrupole gravitational radiation, linearized about a Kerr background, can be written in the simple form

$$\chi^{2\,m}_{\text{out}} = \frac{F(u)}{v-u} + \frac{G(u)}{(v-u)^3} + \frac{H(u)}{(v-u)^4} + O\left(\frac{1}{(v-u)^5}\right), \tag{7.88}$$

for some functions $F(u)$, $G(u)$ and $H(u)$.

In order to formulate absorbing boundary conditions we must also investigate the propagation of incoming gravitational radiation, since this can be produced by reflection of outgoing radiation off the boundary of the computational domain $\partial\Omega$. We work in terms of the variable $\omega^{lm}(u,v)$ once more (7.65). In

§6.2.2 we argued that, if the linearized outgoing radiation condition is imposed, then an incoming quadrupole gravitational wave on flat space behaves asymptotically as

$$\omega_0^{2\,m}(u,v) = A_1(v) + \frac{A_2(v)}{v-u} + O\left(\frac{1}{(v-u)^2}\right), \tag{7.89}$$

for some functions $A_1(v)$ and $A_2(v)$, both of order $O(1)$ as $v \to \infty$ and both vanishing at $v = v_0$. We perform one iteration of Picard's method. Firstly, (7.89) is substituted into the source term (7.67). The gravitational tail term $\Delta\omega_0^{2\,m}$ (defined in (7.74)) is then given by

$$\Delta\omega_0^{2\,m} = \int_{v_0}^{v}\int_{u_0}^{u} \frac{\hat{A}_1(v')(v'-u)^4}{(v'-u')^7} + \frac{\hat{A}_2(v')(v'-u)^4}{(v'-u')^8} + O\left(\frac{Ma^2}{(v'-u')^5}\right) \mathrm{d}u\mathrm{d}v, \tag{7.90}$$

where the functions $\hat{A}_1(v)$ and $\hat{A}_2(v)$ could be expressed in terms of $A_1(v)$ and $A_2(v)$ but this is not necessary. For our purposes it is sufficient to note that they are both of $O(1)$ as $v \to \infty$. The $u'-$integral in (7.90) is evaluated first. The $v'-$integral is then done by parts, neglecting higher order terms, to obtain

$$\Delta\omega_0^{2\,m} = \frac{\tilde{A}_1(v)}{(v-u)^2} + \frac{\tilde{A}_2(v)}{(v-u)^3} + O\left(\frac{1}{(v-u)^4}\right), \tag{7.91}$$

where, again, $\tilde{A}_1(v)$ and $\tilde{A}_2(v)$ could be expressed in terms of $\hat{A}_1(v)$ and $\hat{A}_2(v)$. Note that the terms obtained from the lower limit of the $u'-$integral, which are of the form

$$\frac{F(v)}{(v-u_0)^x}, \tag{7.92}$$

for some $F(v)$ and x, have been incorporated into the definitions of $\tilde{A}_1(v)$ and $\tilde{A}_2(v)$. Using (7.65), we conclude that the Hertz potential that generates incoming quadrupole radiation on a Kerr background can be written as

$$\chi_{\mathrm{in}}^{2\,m} = \frac{\bar{A}_1(v)}{v-u} + \frac{\bar{A}_2(v)}{(v-u)^2} + O\left(\frac{1}{(v-u)^3}\right), \tag{7.93}$$

for some functions $\bar{A}_1(v)$ and $\bar{A}_2(v)$. This expression will be used later in order to formulate absorbing boundary conditions.

7.3.2 The Limits $M \to 0$ and $a \to 0$

Are the results of §7.3.1 consistent with those of chapters 5 and 6? In the limits $M \to 0$ and $a \to 0$, does the Hertz potential on a Kerr background (7.85) reduce to the Hertz potentials that were calculated on Minkowski and Schwarzschild backgrounds?

Consider first the limit $M \to 0$. Under this limit, we recover the homogeneous (flat space) solution immediately. This is because all the terms in the source term (7.67) vanish as $M \to 0$. This result is expected since the case $M = 0$, $a \neq 0$ corresponds to flat space, but in rotating coordinates. Clearly then, taking the limits $M \to 0$ and $a \to 0$ together will also recover the homogeneous (flat space) solution.

Consider now the limit $a \to 0$, with $M \neq 0$. Now, in (7.85) we are left with the first order contributions due to M only. These first order corrections to the homogeneous solution are different from those that were calculated in chapter 6 (6.48). This is because, although the u, θ and ϕ coordinates in both calculations are now identical, the v coordinates still differ. The v of chapter 6, which we will now denote by v^{s} to avoid confusion, was an advanced time null coordinate for Schwarzschild spacetime. The v coordinate used in this chapter, now denoted by v^k, is a characteristic coordinate for the homogeneous Euler-Poisson-Darboux equation. If we were to consider the Hertz potential field equation (4.36) on a Schwarzschild background using the standard (u, r, θ, ϕ) coordinate chart and then make the coordinate change $v^k = u + 2r$, then, if $a = 0$, we would recover (7.85). We conclude that the results of this chapter are consistent with those of chapters 5 and 6.

It is not possible to make the relationship between the Kerr and Schwarzschild calculations more precise here because the two characteristic initial value problems are subtly different. In both cases, initial data were specified on $v = \text{const.}$ hypersurfaces. But since $v^s \neq v^k$, these surfaces were different in each case, so the $B(u)$ which defined the initial data in chapter 6 (6.48) will not match the $U^{2\,m}(u)$ of (7.85). We can, however, illustrate the relationship in more detail by considering quadrupole radiation once more. The leading order outgoing radiation term on a Kerr background is given by

$$\chi_0^{2\,m}(u, v^k) = \frac{U^{2\,m}(u)}{(v^k - u)}. \tag{7.94}$$

We can transform v^k into v^s using

$$v^k = v^s - 2M \log\left(\frac{r}{2M} - 1\right). \tag{7.95}$$

Substituting (7.95) into (7.94) and using the asymptotic expansion of r (6.14), we obtain

$$\chi_0^{2\,m}(u, v^s) = \frac{U^{2\,m}(u)}{v^s - u} + 2MU^{2\,m}(u)\frac{\log(v^s - u)}{(v^s - u)^2}. \tag{7.96}$$

As expected, this is similar in form to the original Schwarzschild solution (6.48). The slight differences in the two expressions are due to the two different characteristic initial value problems.

7.3.3 Absorbing Boundary Conditions on a Kerr Background

In order to obtain absorbing boundary conditions on a Kerr background, we adopt a similar approach to chapter 5, in which boundary conditions on a Minkowski background were obtained. Here, however, we only consider quadrupole radiation.

Recall that the outgoing quadrupole mode of the Hertz potential can be written in the form (7.88)

$$\chi_{\text{out}}^{2\,m} = \frac{F(u)}{v - u} + \frac{G(u)}{(v - u)^3} + \frac{H(u)}{(v - u)^4} + O\left(\frac{1}{(v - u)^5}\right), \tag{7.97}$$

for appropriate functions $F(u)$, $G(u)$ and $H(u)$. The term involving $F(u)$ is a solution to the homogeneous EPD equation; the terms involving $G(u)$ and $H(u)$ are not. The incoming quadrupole mode can be written as (7.93)

$$\chi_{\text{in}}^{2\,m} = \frac{\bar{A}_1(v)}{v - u} + \frac{\bar{A}_2(v)}{(v - u)^2} + O\left(\frac{1}{(v - u)^3}\right), \tag{7.98}$$

Using (B.16), the quadrupole contribution to the perturbation of Ψ_2 can be calculated:

$$\hat{\Psi}_{2\text{ out}}^{l=2} = \frac{\tilde{F}(u)}{(v - u)^3} + \frac{\tilde{G}(u)}{(v - u)^4} + \frac{\tilde{H}(u)}{(v - u)^5} + O\left(\frac{1}{(v - u)^6}\right), \tag{7.99}$$

and

$$\hat{\Psi}^{l=2}_{2\text{ in}} = \frac{\tilde{A}(v)}{(v-u)^3} + \frac{\tilde{B}(v)}{(v-u)^4} + \frac{\tilde{C}(v)}{(v-u)^5} + O\left(\frac{1}{(v-u)^6}\right), \tag{7.100}$$

where the functions $\tilde{F}(u)$, $\tilde{G}(u)$ and $\tilde{H}(u)$ depend on $F(u)$ and $G(u)$ and $\tilde{A}(v)$, $\tilde{B}(v)$ and $\tilde{C}(v)$ depend on $\bar{A}_1(v)$ and $\bar{A}_2(v)$.

The expressions for $\hat{\Psi}_2$ above are similar to the corresponding expressions for $\hat{\Psi}_2$ on a Minkowski background (5.62) (although the coordinate charts used in each case differ). We can therefore use the same approach as in §5.3.2. We define the Bayliss & Turkel-type operators [7]

$$\hat{Q}_k \equiv \frac{\partial}{\partial v} + \frac{2+k}{v-u}. \tag{7.101}$$

At leading order $O(r^{-3})$, $\hat{Q}_1\hat{\Psi}_2$ contains only incoming radiative terms. Imposing $\hat{Q}_1\hat{\Psi}_2 \doteq O(r^{-4})$ will remove these terms. Next, imposing $\hat{Q}_2\hat{\Psi}_2 \doteq O(r^{-5})$ will remove the incoming terms at $O(r^{-4})$. This process can be repeated as many times as necessary: $\hat{Q}_k\hat{\Psi}_2$ contains incoming terms at order $O(r^{-2-k})$ which can be removed by imposing the condition

$$\hat{Q}_k\hat{\Psi}_2 \doteq O(r^{-3-k}). \tag{7.102}$$

The sequence

$$\prod_{k=1}^{L}\left(\frac{\partial}{\partial v} + \frac{2+k}{v-u}\right)\hat{\Psi}_2 \doteq 0. \tag{7.103}$$

will then result in an increasingly accurate hierarchy of absorbing boundary conditions for linearized gravitational radiation on a Kerr background.

The boundary conditions (7.103) appear to be identical to the flat space boundary conditions (5.67). However, it is the specific choice of u and v in (7.103) that incorporates the effects of the background Weyl curvature.

On a Minkowski background, we argued that using the sequence (5.67) results in perfectly absorbing boundary conditions for all gravitational modes with $l \leq L$. On a Kerr background, using (7.103), we can no longer make this assertion. Firstly, throughout this section we only considered quadrupole radiation. Secondly, we only evaluated the effect of the Weyl curvature at second order, and so we cannot justify choosing $L > 2$ in (7.103). However,

by inspecting the asymptotic expansions made throughout this chapter, it is reasonable to suppose that gravitational 2^l-poles with $l > 2$ might give similar expressions to (7.100) for the perturbed Weyl scalar $\hat{\Psi}_2$. We might therefore postulate that, within linearized theory, the hierarchy of boundary conditions (7.103) should be absorbing for general multipole gravitational radiation on a Kerr background, however, without performing further calculations, we cannot justify the boundary conditions for $L > 2$.

Chapter 8

Boundary Conditions in a Numerical Chart

The boundary conditions of chapters 5, 6 and 7 were derived using very specific choices of coordinate chart and tetrad, adapted to the theoretical study of gravitational radiation. These charts and tetrads are unlikely to match those used in numerical relativity. In chapter 3, techniques were developed which allow us to transform between theoretical and numerical charts. Furthermore, quantities such as the Bondi mass and the Weyl scalars were expressed purely in terms of the metric variables in a numerical chart. In this chapter we will use these techniques to transform the boundary conditions derived in chapters 5, 6 and 7 into a numerical chart.

In chapter 3 it was assumed that the theoretical chart contained a single null coordinate, the retarded time u (together with a radial coordinate and two angular coordinates). This was indeed the case for the calculation on a Kerr background, which used the $(u, \lambda, \theta, \phi)$ chart introduced in §7.1. In chapters 5 and 6 however, double null coordinate charts were used. Therefore, in order to express these boundary conditions in a numerical chart, we must first extend the techniques of chapter 3 so that we can deal with a theoretical chart containing two null coordinates. This is done in §8.1.

In §8.2 we use these results to transform the boundary conditions of chapter 5 (in which linearized gravitational radiation on a Minkowski background was considered) into a numerical chart. We previously argued that the boundary conditions of chapter 6 (for gravitational perturbations on a Schwarzschild

background) would be too difficult to implement numerically and so we do not attempt to transform them into a numerical chart here. Instead, in §8.3 we transform the boundary conditions of chapter 7 (for gravitational perturbations on a Kerr background) into the numerical chart. Boundary conditions for gravitational radiation on a Schwarzschild background can then be obtained by taking the limit $a \to 0$.

8.1 Asymptotically Flat Spacetimes in Double Null Coordinates

Suppose that the chart used by a numerical relativist is a quasi-spherical one $X^a = (T, R, \Theta, \Phi)$ and that the theoretical chart $x^a = (u, v, \theta, \phi)$ contains two null coordinates, retarded time u and advanced time v. A radial coordinate $r(u, v)$ can also be defined and, as in chapter 3, we assume $r = R$.

Following the method of §3.1 we assume that the spacetime is asymptotically Minkowskian. We find that in the numerical chart the metric takes the form

$$\begin{aligned}
&g_{00} = 1 + h_{00}R^{-1} + O(R^{-2}), && g_{01} = h_{01}R^{-1} + O(R^{-2}),\\
&g_{02} = h_{02} + O(R^{-1}), && g_{03} = h_{03} + O(R^{-1}),\\
&g_{11} = -1 + h_{11}R^{-1} + O(R^{-2}), && g_{12} = h_{12} + O(R^{-1}),\\
&g_{13} = h_{13} + O(R^{-1}), && g_{22} = -R^2 + h_{22}R + O(1)\\
&g_{23} = h_{23}R + O(1), && g_{33} = -R^2\sin^2\Theta + h_{33}R + O(1),
\end{aligned} \tag{8.1}$$

where the h_{ij} are functions of T, Θ and Φ.

We investigate $u(T, R, \Theta, \Phi)$ and $v(T, R, \Theta, \Phi)$ by considering the relativistic eikonal equation

$$g^{ij}u_{,i}u_{,j} = 0, \tag{8.2}$$

Following the method outlined in §3.2, we seek solutions which satisfy

$$g^{ij}u_{,i}u_{,j} = O(R^{-3}), \tag{8.3}$$

where in equation (8.3) only the indices range over 0 and 1. This results in a quadratic equation for the quantity $u_{,R}/u_{,T}$. There are two solutions,

corresponding to the advanced and retarded time coordinates:

$$\begin{aligned} u_{,R} &= -(1+2m_u R^{-2})u_{,T} + O(R^{-2}), \\ v_{,R} &= (1+2m_v R^{-2})v_{,T} + O(R^{-2}), \end{aligned} \tag{8.4}$$

where

$$\begin{aligned} m_u &= -\tfrac{1}{4}(h_{00} + 2h_{01} + h_{11}), \\ m_v &= -\tfrac{1}{4}(h_{00} - 2h_{01} + h_{11}). \end{aligned} \tag{8.5}$$

Note that $m_u = m_v$ if and only if $h_{01} = 0$. We leave some freedom in u and v by setting

$$\begin{aligned} u_{,T} &= 1 + q_u R^{-1} + O(R^{-2}), \\ v_{,T} &= 1 + q_v R^{-1} + O(R^{-2}), \end{aligned} \tag{8.6}$$

where q_u and q_v are arbitrary functions, independent of R. We now have

$$\begin{aligned} \mathrm{d}R &= \tfrac{1}{2}(1 - [q_v + m_u + m_v]R^{-1})\mathrm{d}v - \tfrac{1}{2}(1 - [q_u + m_u + m_v]R^{-1})\mathrm{d}u + O(R^{-2}), \\ \mathrm{d}T &= \tfrac{1}{2}(1 + [m_u - m_v - q_v]R^{-1})\mathrm{d}v + \tfrac{1}{2}(1 + [m_v - m_u - q_u]R^{-1})\mathrm{d}u + O(R^{-2}). \end{aligned} \tag{8.7}$$

Rather than writing down expressions for $\theta(R, \Theta, \Phi)$ and $\phi(R, \Theta, \Phi)$ it is more convenient to use the inverse transformations:

$$\Theta = \theta + y_\theta r^{-1} + O(r^{-2}), \quad \Phi = \phi + y_\phi r^{-1} + O(r^{-2}), \tag{8.8}$$

where y_θ and y_ϕ are functions independent of r.

The expansions (8.7) and (8.8) enable us to write down the Jacobian $\partial X^a/\partial x^b$ for the coordinate change between the theoretical chart (u, v, θ, ϕ) and the numerical chart (T, R, Θ, Φ):

$$\frac{\partial X^a}{\partial x^b} = \begin{pmatrix} \frac{1}{2} + \frac{1}{2}[m_v - m_u - q_u]R^{-1} + O(R^{-2}) & \frac{1}{2} + \frac{1}{2}[m_u - m_v - q_v]R^{-1} + O(R^{-2}) \\ -\frac{1}{2} + \frac{1}{2}[q_u + m_u + m_v]R^{-1} + O(R^{-2}) & \frac{1}{2} - \frac{1}{2}[q_v + m_u + m_v]R^{-1} + O(R^{-2}) \\ y_{\theta,u}R^{-1} + O(R^{-2}) & y_{\theta,v}R^{-1} + O(R^{-2}) \\ y_{\phi,u}R^{-1} + O(R^{-2}) & y_{\phi,v}R^{-1} + O(R^{-2}) \end{pmatrix}$$

$$\begin{pmatrix} O(R^{-2}) & O(R^{-2}) \\ O(R^{-2}) & O(R^{-2}) \\ 1 + y_{\theta,\theta}R^{-1} + O(R^{-2}) & y_{\theta,\phi}R^{-1} + O(R^{-2}) \\ y_{\phi,\theta}R^{-1} + O(R^{-2}) & 1 + y_{\phi,\phi}R^{-1} + O(R^{-2}) \end{pmatrix} \tag{8.9}$$

At this point, we do not need to take the calculation any further. The Jacobian (8.9) and the expression for Ψ_2 in terms of the metric variables in the numerical chart (3.58) are sufficient to allow us to transform the boundary conditions (5.67) into the numerical chart (see §8.2). However, we can still obtain some useful information by continuing in a similar manner to §3.2. Using (8.9), the metric in the numerical chart (8.1) can be transformed into the theoretical chart to give

$$\begin{aligned}
g_{00} &= -y_{\theta,u}^2 - y_{\phi,u}^2 \sin^2\theta + a_{00}r^{-1} + O(r^{-2}), \\
g_{01} &= \tfrac{1}{2} - y_{\theta,u}y_{\theta,v} - y_{\phi,u}y_{\phi,v} \sin^2\theta + a_{01}r^{-1} + O(r^{-2}), \\
g_{02} &= -y_{\theta,u}r + a_{02} + O(r^{-1}), \\
g_{03} &= -y_{\phi,u} \sin^2\theta r + a_{03} + O(r^{-1}), \\
g_{11} &= -y_{\theta,v}^2 - y_{\phi,v}^2 \sin^2\theta + a_{11}r^{-1} + O(r^{-2}), \\
g_{12} &= -y_{\theta,v} + a_{12} + O(r^{-1}), \\
g_{13} &= -y_{\phi,v} \sin^2\theta + a_{13} + O(r^{-1}), \\
g_{22} &= -r^2 + ra_{22} + O(1), \\
g_{23} &= a_{23}r + O(1), \\
g_{33} &= -r^2 \sin^2\theta + a_{33}r + O(1).
\end{aligned} \tag{8.10}$$

The a_{ij} are expressed in terms of the h_{ij} in (A.19). In order for the metric to be

asymptotically Minkowskian we must impose that y_ϕ and y_θ are independent of u and v.

We choose a Newman-Penrose tetrad which asymptotically resembles the tetrad (5.28),

$$\begin{aligned}
l_a &= \big(1 + c_{00}r^{-1} + O(r^{-2}), \quad c_{01}r^{-1} + O(r^{-2}), \quad c_{02} + O(r^{-1}), \quad c_{03} + O(r^{-1})\big) \\
n_a &= \big(c_{10}r^{-1} + O(r^{-2}), \quad \tfrac{1}{2} + c_{11}r^{-1} + O(r^{-2}), \quad c_{12} + O(r^{-1}), \quad c_{13} + O(r^{-1})\big) \\
m_a &= \big([c_{20} + ic_{30}]r^{-1} + O(r^{-2}), \quad [c_{21} + ic_{31}]r^{-1} + O(r^{-2}) \\
&\qquad -sr + c_{22} + ic_{32} + O(r^{-1}), \quad irs\sin\theta + c_{23} + ic_{33} + O(r^{-1})\big) .
\end{aligned} \tag{8.11}$$

Here the c_{ij} are real functions of u, v, θ and ϕ, and $s = 2^{-1/2}$. The contravariant tetrad vectors can then be written down:

$$\begin{aligned}
l^a &= \big(c^{00}r^{-1} + O(r^{-2}), \quad 2 + c^{01}r^{-1} + O(r^{-2}), \\
&\qquad c^{02}r^{-2} + O(r^{-3}), \quad c^{03}r^{-2} + O(r^{-3})\big) \\
n^a &= \big(1 + c^{10}r^{-1} + O(r^{-2}), \quad c^{11}r^{-1} + O(r^{-2}), \\
&\qquad c^{12}r^{-2} + O(r^{-3}), \quad c^{13}r^{-2} + O(r^{-3})\big) \\
m^a &= \big([c^{20} + ic^{30}]r^{-1} + O(r^{-2}), \quad [c^{21} + ic^{31}]r^{-1} + O(r^{-2}), \\
&\qquad sr^{-1} + [c^{22} + ic^{32}]r^{-2} + O(r^{-3}), \quad -ir^1 s\csc\theta + [c^{23} + ic^{33}]r^{-2} + O(r^{-3})\big) .
\end{aligned} \tag{8.12}$$

Again the c^{ij} are real functions of u, v, θ and ϕ. The c^{ij} are related to the c_{ij} by the expressions in (A.20). We can also relate the c_{ij} to the a_{ij} using

$$g_{ab} = 2l_{(a}n_{b)} - 2m_{(a}\bar{m}_{b)}. \tag{8.13}$$

Since there are 16 c_{ij} and only 10 a_{ij}, this relation introduces 6 arbitrary constants A_i corresponding to the Lorentz transformations of the tetrad, at first order, which preserve the metric. One possible representation of these relations is given in (A.21).

Imposing the vanishing of the Ricci curvature in a similar manner to §3.4 provides us with a set of constraints on the a_{ij}, given by (A.22). From these we can deduce a corresponding set of constraints on the h_{ij} (A.23).

8.2 Boundary Conditions on a Minkowski Background

In chapter 5 we defined the operators

$$\hat{O}_k \equiv \frac{\partial}{\partial v} + \frac{2+k}{v-u}, \tag{8.14}$$

and imposed

$$\hat{O}_k \Psi_2 \doteq O(r^{-3-k}), \tag{8.15}$$

where the symbol $\doteq$ denotes equality only on the boundary of the computational domain $\partial\Omega$. This resulted in the hierarchy of boundary conditions

$$\prod_{k=1}^{L+3} \left(\frac{\partial}{\partial v} + \frac{2+k}{v-u} \right) \Psi_2 \doteq 0. \tag{8.16}$$

These boundary conditions can be imposed to any desired value of L and are perfectly absorbing for linearized gravitational 2^l-poles on a Minkowski background with $l \leq L$.

There are two steps involved in transforming (8.16) into a numerical chart. Firstly, Ψ_2 must be expressed in the numerical chart. Secondly, we must deal with the null coordinates u and v.

In terms of the metric variables in the theoretical (u, r, θ, ϕ) chart of chapter 3, the leading order term in Ψ_2 was given by (3.58). Using (A.3) and its second order analogue we can express this in terms of the metric variables in the numerical chart. We find

$$\Psi_2 = \Psi_2^{(3)} R^{-3} + O(R^{-4}), \tag{8.17}$$

where

$$\begin{aligned} \Psi_2^{(3)} =& \frac{1}{2} h_{11} - \frac{1}{4} i\mathcal{B} \csc^3\Theta + \frac{1}{2}\mathcal{C}_{,T} + \frac{1}{4}(\mathcal{A} + i\mathcal{B}\csc\Theta)(\mathcal{A}_{,T} - i\mathcal{B}_{,T}\csc\Theta) \\ &+ \frac{1}{4}(\mathcal{B}_{,\Theta} - 2\mathcal{A}_{,\Phi})\cot\Theta\csc\Phi - \frac{1}{2} i\mathcal{A}_{,\Theta\Phi} + \frac{1}{4} i(\mathcal{B}_{,\Theta\Theta} - \mathcal{B}_{,\Phi\Phi})\csc\Theta. \end{aligned} \tag{8.18}$$

Here, $\mathcal{A}$ and $\mathcal{B}$ are the auxiliary functions first defined in (3.74),

$$\begin{aligned}\mathcal{A} =& h_{22} + 2(h_{02,\Theta} + h_{12,\Theta}),\\ \mathcal{B} =& h_{23} + h_{02,\Phi} + h_{12,\Phi} + \mathcal{W}_{,\Theta} - 2\mathcal{W}\cot\Theta,\\ \mathcal{W} =& h_{03} + h_{13}.\end{aligned} \tag{8.19}$$

In flat space, $v-u = 2r$. If we assume that the radial coordinates, r and R, in the theoretical and numerical charts are identical, then we can replace $v-u$ in (8.16) with $2R$. Furthermore, recalling the condition that y_θ and y_ϕ (8.8) are independent of u and v, the partial derivative $\partial/\partial v$ can be transformed into the numerical chart

$$\begin{aligned}\frac{\partial}{\partial v} =& \left(\frac{\partial T}{\partial v}\right)\frac{\partial}{\partial T} + \left(\frac{\partial R}{\partial v}\right)\frac{\partial}{\partial R} + \left(\frac{\partial \Theta}{\partial v}\right)\frac{\partial}{\partial \Theta} + \left(\frac{\partial \Phi}{\partial v}\right)\frac{\partial}{\partial \Phi}\\ =& \frac{1}{2}\left(1 + [m_u - m_v - q_v]R^{-1} + O(R^{-2})\right)\frac{\partial}{\partial T}\\ &+ \frac{1}{2}\left(1 - [q_v + m_u + m_v]R^{-1} + O(R^{-2})\right)\frac{\partial}{\partial R}\\ &+ O(R^{-2})\frac{\partial}{\partial \Theta} + O(R^{-2})\frac{\partial}{\partial \Phi}.\end{aligned} \tag{8.20}$$

The operator

$$\hat{O}_k \equiv \frac{\partial}{\partial v} + \frac{2+k}{v-u} \tag{8.21}$$

then becomes

$$\begin{aligned}\hat{O}_k \equiv& \left(1 + [m_u - m_v - q_v]R^{-1} + O(R^{-2})\right)\frac{\partial}{\partial R}\\ &+ \left(1 - [q_v + m_u + m_v]R^{-1} + O(R^{-2})\right)\frac{\partial}{\partial T}\\ &+ \frac{2+k}{R}.\end{aligned} \tag{8.22}$$

Note that we have dropped the factor of $\frac{1}{2}$ that appears when transforming (8.21) into (8.22). The quantities m_u and m_v in (8.22) are easily evaluated via (8.5). However q_v depends on the relationship between the theoretical retarded time coordinate u and the numerical chart and is thus more difficult to evaluate. The simplest case, corresponding to a numerical evolution in standard flat space coordinates is

$$\hat{O}_k \equiv \frac{\partial}{\partial R} + \frac{\partial}{\partial T} + \frac{2+k}{R}. \tag{8.23}$$

The hierarchy of boundary conditions (8.16) then becomes

$$\prod_{k=1}^{L+3} \left\{ \frac{\partial}{\partial R} + \frac{\partial}{\partial T} + \frac{2+k}{R} \right\} \Psi_2 \doteq 0, \tag{8.24}$$

where Ψ_2 is given by (8.17) and (8.18). These boundary conditions are identical to those of Buchman & Sarbach [22]. Note also the similarity between the boundary conditions above and those of Bayliss & Turkel [7], who were also seeking absorbing boundary conditions for wave-like equations.

In principle the sequence of boundary conditions (8.24) could be applied for any desired value of L. Within linearized theory, we have shown (§5.3.2) that they are perfectly absorbing for gravitational radiation on a Minkowski background with angular momentum number $l \leq L$. However, we showed in chapter 3 that, within linearized theory, we can only obtain Ψ_2 to leading order. Hence in the full nonlinear theory of relativity, we can only justify using (8.24) to first order.

8.3 Boundary Conditions on Schwarzschild and Kerr Backgrounds

We argued in §6.2.3 that the boundary conditions on a Schwarzschild background (6.62) were too cumbersome to be used in numerical relativity. However, by setting $a = 0$ in the boundary conditions for linearized gravitational radiation on a Kerr background (7.103), we can obtain boundary conditions on a Schwarzschild background. We therefore restrict our attention to the hierarchy of boundary conditions (7.103):

$$\prod_{k=1}^{L} \left(\frac{\partial}{\partial v} + \frac{2+k}{v-u} \right) \hat{\Psi}_2 \doteq 0, \tag{8.25}$$

where the coordinates u and v were defined in (7.5) and (7.64) respectively.

The Weyl scalar Ψ_2 was given in terms of the metric variables in the numerical chart by (8.17) in the preceding section. Here, however, we are interested in the *perturbed* quantity $\hat{\Psi}_2$. In the chart and tetrad of §7.1, the unperturbed Weyl scalars on a Kerr background were given by (7.14). To leading order in the numerical chart, $\Psi_2 = -MR^{-3}$. We can therefore obtain the perturbation induced by the Hertz potential:

$$\hat{\Psi}_2 = \hat{\Psi}_2^{(3)} R^{-3} + O(R^{-4}), \tag{8.26}$$

where

$$\begin{aligned} \hat{\Psi}_2^{(3)} =& \frac{1}{2} h_{11} - \frac{1}{4} i\mathcal{B} \csc^3\Theta + \frac{1}{2}\mathcal{C}_{,T} + \frac{1}{4}(\mathcal{A} + i\mathcal{B}\csc\Theta)(\mathcal{A}_{,T} - i\mathcal{B}_{,T}\csc\Theta) \\ &+ \frac{1}{4}(\mathcal{B}_{,\Theta} - 2\mathcal{A}_{,\Phi})\cot\Theta\csc\Phi - \frac{1}{2} i\mathcal{A}_{,\Theta\Phi} + \frac{1}{4} i(\mathcal{B}_{,\Theta\Theta} - \mathcal{B}_{,\Phi\Phi})\csc\Theta + M. \end{aligned} \tag{8.27}$$

Now consider the operator

$$\hat{Q}_k \equiv \frac{\partial}{\partial v} + \frac{2+k}{v-u}. \tag{8.28}$$

We make the transformation $v = u + 2\lambda$, and drop the resulting factor of $\frac{1}{2}$

that appears, to obtain

$$\hat{Q}_k \equiv \frac{\partial}{\partial\lambda} + \frac{2+k}{\lambda}, \tag{8.29}$$

where λ is the radial coordinate defined in (7.8). Suppose now that the numerical chart (T, R, Θ, Φ) is the "standard" flat space chart (if this was not the case then we could easily add further $1/R$ terms in the coordinate transformations, as was done in §3.1). We now have three charts to consider:

(i) the $(u, \lambda, \tilde{\theta}, \tilde{\phi})$ chart of Bai et al. [6, 59],
(ii) the Boyer-Lindquist chart (t, r, θ, ϕ) [20],
(iii) the numerical chart (T, R, Θ, Φ).

Our goal is to transform the operator $\hat{Q}_k$ (8.29) from the $(u, \lambda, \tilde{\theta}, \tilde{\phi})$ chart into the numerical chart, via the Boyer-Lindquist chart.

We consider first the radial coordinates λ, r, and R. Recall the relationships between the three charts which were introduced in §7.1. From (7.8), we have

$$\lambda = r + \frac{a^2 \sin^2\theta}{2r} + \frac{Ma^2 \sin^2\theta}{2r^2} + O\left(r^{-3}\right) \tag{8.30}$$

Furthermore, the numerical chart (T, R, Θ, Φ) is related to the Boyer-Lindquist chart (t, r, θ, ϕ) by (7.3),

$$R = \sqrt{r^2 + a^2 \sin^2\theta}, \tag{8.31}$$

and

$$\sin\Theta = \sqrt{\frac{r^2 + a^2}{r^2 + a^2 \sin^2\theta}} \sin\theta. \tag{8.32}$$

This enables us to relate λ and R:

$$\lambda = R + \frac{Ma^2 \sin^2\Theta}{2R^2} + O\left(R^{-3}\right). \tag{8.33}$$

Next we deal with the partial derivative $\partial/\partial\lambda$. This can be transformed into (T, R, Θ, Φ) coordinates by using the chain rule twice. First we transform

into Boyer-Lindquist coordinates, using (7.5) and (7.8):

$$\begin{aligned}\frac{\partial}{\partial\lambda} &= \frac{\partial t}{\partial\lambda}\frac{\partial}{\partial t} + \frac{\partial r}{\partial\lambda}\frac{\partial}{\partial r} + \frac{\partial\theta}{\partial\lambda}\frac{\partial}{\partial\theta} + \frac{\partial\phi}{\partial\lambda}\frac{\partial}{\partial\phi}. \\ &= \left(1 + \frac{2M}{r} + \frac{4M^2 - \frac{1}{2}a^2\sin^2\theta}{r^2} + O\left(r^{-3}\right)\right)\frac{\partial}{\partial t} \\ &\quad + \left(1 + \frac{a^2\sin^2\theta}{2r^2} + O\left(r^{-3}\right)\right)\frac{\partial}{\partial r} \\ &\quad + O\left(r^{-3}\right)\frac{\partial}{\partial\theta} + O\left(r^{-3}\right)\frac{\partial}{\partial\phi}. \end{aligned} \tag{8.34}$$

Next, using (8.31) and (8.32), we apply the chain rule once more to transform into the numerical chart,

$$\begin{aligned}\frac{\partial}{\partial\lambda} &= \left(1 + \frac{2M}{R} + \frac{4M^2 - \frac{1}{2}a^2\sin^2\Theta}{R^2} + O\left(R^{-3}\right)\right)\frac{\partial}{\partial T} \\ &\quad + \left(1 + O\left(R^{-3}\right)\right)\frac{\partial}{\partial R} + O\left(R^{-3}\right)\frac{\partial}{\partial\Theta} + O\left(R^{-3}\right)\frac{\partial}{\partial\Phi}. \end{aligned} \tag{8.35}$$

The operator $\hat{Q}_k$ (8.29) is then given in the numerical chart by

$$\begin{aligned}\hat{Q}_k &= \left(1 + \frac{2M}{R} + \frac{4M^2 - \frac{1}{2}a^2\sin^2\Theta}{R^2}\right)\frac{\partial}{\partial T} + \frac{\partial}{\partial R} \\ &\quad + \frac{2+k}{R} + O\left(R^{-3}\right), \end{aligned} \tag{8.36}$$

The hierarchy of boundary conditions (8.25) now becomes

$$\begin{aligned}\prod_{k=1}^{L}\Bigg\{&\left(1 + \frac{2M}{R} + \frac{4M^2 - \frac{1}{2}a^2\sin^2\Theta}{R^2}\right)\frac{\partial}{\partial T} \\ &+ \frac{\partial}{\partial R} + \frac{2+k}{R} + O\left(R^{-3}\right)\Bigg\}\hat{\Psi}_2 \doteq 0. \end{aligned} \tag{8.37}$$

We can clearly see that in the limits $M \to 0$, $a \to 0$ we recover the flat space boundary conditions of the previous section. In the limit $a \to 0$, $M \neq 0$ we obtain boundary conditions for linearized gravitational radiation on a Schwarzschild background, with a first order contribution from the mass parameter M.

In the limit $M \to 0$, $a \neq 0$ one might expect to obtain boundary conditions for linearized gravitational radiation on a Minkowski background similar to

(8.24). However, due to the presence of the term

$$\frac{\frac{1}{2}a^2 \sin^2 \Theta}{R^2} \tag{8.38}$$

in (8.37) this appears not to be the case. The reason for this is as follows. If $a \neq 0$, then the tetrad (7.12) in which $\hat{\Psi}_2$ is evaluated is rotating at second order. Therefore the case $M = 0$, $a \neq 0$ corresponds to a boundary condition for linearized gravitational radiation on a flat space background, but applied to $\hat{\Psi}_2$ evaluated in a *rotating frame*. The Weyl scalar $\hat{\Psi}_2$ is given to leading order by (8.27). The effect of the rotating tetrad only becomes apparent at second order.

In principle, the sequence (8.37) could be applied for any choice of L. However, within linearized theory we only established that the boundary conditions were perfectly absorbing for $L = 2$ (although it was postulated, without proof, that within linearized theory, the higher the value of L, the more accurate the boundary conditions might be). Furthermore, in chapter 3 we showed that Ψ_2 can only be evaluated to first order in linearized theory. At higher order, nonlinear terms contribute. Therefore in the full nonlinear theory of general relativity we are only able to justify using the boundary conditions (8.37) at first order (this corresponds to the case $L = 1$ with $M = 0$ and $a = 0$).

Finally we note that the boundary conditions (8.37) involve radial derivatives $\partial/\partial R$, which are difficult to implement accurately on $\partial\Omega$ in a numerical simulation. This problem can be overcome by defining a sequence of *auxiliary variables* on $\partial\Omega$. The boundary conditions can then be expressed in terms of these variables, enabling the radial derivatives to be removed [54, 55, 68].

Chapter 9

Conclusions and Outlook

9.1 Conclusions

The main results of this thesis are as follows.

In the first half of the thesis we attempted to close the gap between analytical and numerical studies of gravitational radiation. Theoretical results concerning gravitational radiation (such as the discovery of the news function and the mass-loss formula by Bondi et al. [18]) rely upon very specific choices of chart and tetrad, which are not necessarily the same as those used in numerical relativity.

In chapter 2 we generalized a calculation by Stewart [134], in which the results of Bondi et al. [18] were expressed in the Newman-Penrose formalism. We were able to remove the assumption of axisymmetry from Stewart's calculation. In addition we obtained a new interpretation of the outgoing radiation condition, which is required to prevent coordinate singularities from occurring in the Bondi coordinates.

The results of chapter 2 required a careful choice of coordinate chart and Newman-Penrose tetrad and are therefore of limited use in numerical relativity. In chapter 3 we extended the results by demonstrating how they can be related to the general chart and tetrad that might be used in a numerical relativity simulation.

Under the assumption that the spacetime is asymptotically Minkowskian, we made $1/r$ expansions of the metric variables (in both the analytical and

numerical charts) and the Newman-Penrose tetrad. Imposing the vanishing of the Ricci curvature in the far-field region provided us with a set of constraints on the metric variables. Expressing the numerical chart asymptotically in terms of the analytical one enabled us to transform from one chart to the other with $O(r^{-2})$ accuracy. Thus we were able to express quantities such as the Weyl scalars, the news function and the Bondi mass purely in terms of the metric variables in the numerical chart. We also demonstrated Valiente Kroon's result [81] on how the outgoing radiation condition results in the peeling behaviour of the Weyl scalars: $\Psi_i = O(r^{i-5})$ as $r \to \infty$.

Finally, in chapter 3, we discussed the limitations of linearized theory in general relativity that our calculations had highlighted. We found that Ψ_4, Ψ_3 and Ψ_2 can accurately be evaluated using linearized theory, but that Ψ_1 and Ψ_0 (which is often used by numerical relativists to formulate boundary conditions) cannot, since there are nonlinear contributions at leading order.

In summary, in the first half of the thesis we demonstrated how to link theoretical and numerical studies in relativity, and investigated the validity of linearized theory.

In the second half of the thesis, we turned our attention to absorbing outer boundary conditions in numerical relativity. Keeping in mind the restrictions suggested by the previous chapters, we used Hertz potentials to generate linear perturbations about Minkowski, Schwarzschild and Kerr backgrounds and to investigate the propagation of the resulting gravitational waves. In chapter 4, we were able to simplify considerably the original formulae for the perturbed Newman-Penrose and Weyl scalars induced by a Hertz potential [133].

On a Minkowski background (chapter 5), with a suitable choice of chart and tetrad, the field equation for the Hertz potential reduces to a homogeneous Euler-Poisson-Darboux equation, whose solutions are known. The solutions enable us to transparently represent incoming and outgoing gravitational radiation. We were thus able to obtain a hierarchy of outer boundary conditions, similar in form to those of Bayliss & Turkel [7], which are perfectly absorbing for gravitational 2^l-poles with $l \leq L$. The Weyl scalar Ψ_0 cannot be estimated in linearized theory, and we found that Ψ_4 is dominated by outgoing radiation and so neither are suitable for use in boundary conditions. We therefore formulated this sequence of boundary conditions in terms of Ψ_2.

In addition, in chapter 5 we were able to introduce a version of the out-

going radiation condition for linearized theory, which ensures that the peeling theorem for the Weyl scalars holds. We also investigated Huygens' principle for both scalar waves and gravitational waves on a Minkowski background.

In chapter 6, we used Hertz potentials to generate gravitational perturbations on a Schwarzschild background. An inhomogeneous Euler-Poisson-Darboux equation was obtained, whose solutions we could write down in integral form. The solutions consist of the sum of the homogeneous solution and a *gravitational tail* caused by the background Weyl curvature. Using a Picard iteration scheme, we were able to estimate the leading order (M/v) contribution to the gravitational tail as $v \to \infty$ and hence obtain absorbing boundary conditions which take into account the first order contribution due to M/R. Unfortunately, due to the presence of logarithmic terms in our calculations, the boundary conditions we obtained are rather cumbersome and unlikely to be of use in numerical relativity.

Finally in chapter 6 we demonstrated how the Hertz potential may be recovered from the curvature perturbation.

Previously, Buchman & Sarbach [22,23] had also obtained absorbing boundary conditions for linearized gravitational radiation on a Schwarzschild background. Their boundary conditions incorporated the first order contribution due to M/R. We were able to extend this work in chapter 7 by using Hertz potentials to generate gravitational perturbations on a Kerr background. This meant that that we could incorporate the second order contribution from the Weyl curvature, in which the angular momentum of the background has an effect. A careful choice of coordinate chart and tetrad enabled us to avoid the problems encountered in chapter 6, in which the presence of logarithmic terms in the solutions to the Hertz potential field equation meant that the resulting boundary conditions were too unwieldy to use numerically.

The method used in chapter 7 was similar to that of chapter 6. The Hertz potential was expanded in terms of spin-weighted spherical harmonics. An inhomogeneous Euler-Poisson-Darboux equation was obtained, whose solutions were written in integral form and then estimated using Picard's method. However, unlike the Minkowski and Schwarzschild calculations, the angular dependence of the field equations no longer decoupled. We derived a recurrence relation (see appendix C.2) for the spin-weighted spherical harmonics which enabled us to express this lack of decoupling as *mode-mixing* between

the various gravitational 2^l-poles. By calculating the first and second order contributions to the gravitational tail for $l = 2$, we were able to obtain a hierarchy of increasingly accurate absorbing boundary conditions for gravitational quadrupole radiation on a Kerr background. Again, these boundary conditions were formulated in terms of Ψ_2. Although we only considered the $l = 2$ modes, the calculation suggested that these boundary conditions might also be absorbing for general gravitational 2^l-poles with $l > 2$.

In chapter 8 we linked the two investigations carried out in this thesis. The machinery of chapter 3 was used to express Ψ_2 in terms of the metric variables in a typical numerical chart. We then transformed the boundary conditions for linearized gravitational radiation on Minkowski and Kerr backgrounds into the numerical chart. At leading order (in which the Weyl curvature has no effect), we obtained the very simple Bayliss & Turkel type boundary conditions [7]. At first order there was a contribution due to the mass M of the background spacetime. At second order there was also a contribution from the angular momentum Ma of the background.

Within linearized theory, it was shown that our sequences of boundary conditions are absorbing for quadrupolar gravitational radiation ($L \leq 2$), and account for the mass and angular momentum of the background spacetime. Our calculations did not deal explicitly with the case $L > 2$ but inspection of the asymptotic expansions used suggested that the hierarchy of boundary conditions might well be valid for larger values of L, although this is only a postulate. By considering the full nonlinear theory of relativity, we were able to highlight the limitations of these boundary conditions. At leading order, linearized theory correctly predicts Ψ_2. At higher orders however, nonlinear effects become significant and linearized theory is no longer valid. Therefore we can only justify imposing boundary conditions devised within linearized theory (such as those in chapter 8 or those of Buchman & Sarbach) to leading order.

9.2 Outlook

There were three main threads in this thesis: asymptotic flatness in numerical relativity, the propagation of linearized gravitational waves on a curved

background spacetime and the problem of outer boundary conditions. Further study is warranted in each of these areas.

Our calculation regarding asymptotically flat spacetimes (chapter 3) was based on a $1/r$ expansion of the metric variables and the tetrad components. A more accurate representation of reality might be to use a polyhomogeneous expansion, in which logarithmic terms are also present (see e.g. Chruściel et al. [30] and Valiente Kroon [80, 82–86]). This was discussed in more detail in §3.5.1.

The matching process between numerical and analytical charts that we devised relied on using the first few terms in the $1/r$ expansions and is therefore only valid in the far-field i.e. for large r. For the purposes of obtaining outer boundary conditions this was not restrictive. However, our calculations do not allow quantities such as the Bondi mass or the Weyl scalars to be evaluated in the near-field region.

We next considered the propagation of gravitational waves linearized about curved spacetime backgrounds. We were able to estimate the behaviour of the resulting gravitational tails. It is interesting to compare this calculation with that of Price [109], who considered gravitational perturbations on a Schwarzschild background. Whereas we investigated the behaviour of the gravitational tails as $v \to \infty$, Price was interested in the late time behaviour of the tails with r constant but $t \to \infty$. The tails decay as either $t^{-(2l+2)}$ or $t^{-(2l+3)}$, where l is the angular momentum number of the gravitational waves. This is known as *Price's Law*. Our two investigations are distinct. A similar investigation has more recently been performed for late-time gravitational tails on a Kerr background [56]. Dafermos [38] has investigated the effect that boundary conditions in numerical relativity might have on tails that obey Price's law. Typical radiation-controlling boundary conditions cause the tails to decay faster than any polynomial power.

Price extended his investigation to the late-time tails of massless scalar fields of arbitrary spin [110]. An interesting extension of our Hertz potential calculations would be to consider the propagation of such fields on a curved background. In this thesis, Hertz potentials were used to describe gravitational perturbations ($s = \pm 2$), electromagnetic fields ($s = \pm 1$) and massless scalar fields with $s = 0$. However, complex scalar fields of arbitrary spin can also be described using Hertz potentials. In §5.3.1 we demonstrated how,

on a Minkowski background, the radiative modes of a complex scalar field of arbitrary spin contain geometrical tails if $l > s$. On a curved spacetime, inhomogeneous Euler-Poisson-Darboux equations would be obtained and the solutions would contain gravitational tails for all values of $l \geq s$. The techniques used in chapters 6 and 7 could be used to estimate the behaviour of the gravitational tails as $v \to \infty$.

Finally we discuss the outer boundary conditions that we obtained in chapter 8. Within linearized theory, the boundary conditions are absorbing for gravitational waves propagating on a Kerr background. However, further investigations are required to establish whether the higher order effects of our boundary conditions (and indeed all boundary conditions derived using linearized theory) are in agreement with the full nonlinear theory of relativity.

In §1.3 we stated three properties desirable for boundary conditions in numerical relativity: they should form a well-posed initial boundary value problem, they should be constraint-preserving and they should be absorbing. We have obtained absorbing boundary conditions and we have demonstrated how to implement them in a numerical chart. However, we have not considered the first two items in the list. Furthermore, the boundary conditions obtained in this thesis depend on the mass and angular momentum parameters, M and a, of the background spacetime. Accurately estimating these quantities is a non-trivial, open problem.

Can a well-posed initial boundary value problem be found using our boundary conditions? Furthermore, can additional boundary conditions be specified so that no constraint violations are introduced via the computational boundary? The first well-posed initial boundary value problem for the vacuum Einstein field equations was found by Friedrich & Nagy [52] in 1999. Since then, many groups have attempted to generalize this work by specifying constraint-preserving boundary conditions for other Einstein evolution systems (for example [124, 141]). Many of these studies involve boundary conditions based on combinations of Ψ_0 and Ψ_4, so we are hopeful that our boundary conditions can successfully be implemented numerically. One approach to these issues is to use the framework of Ruiz et al. [122]. There, the well-posedness of a set of constraint-preserving boundary conditions for Einstein's equations in harmonic gauge was investigated in the high-frequency limit. In addition, the boundary conditions of Buchman & Sarbach [22, 23] were incorporated into

their class of constraint-preserving boundary conditions. It should be possible to apply those techniques to the boundary conditions found in this thesis. Once well-posedness and constraint-preserving properties are established, a scheme similar to that of Rinne et al. [117] could be used to test the boundary conditions. In [117], two outer boundaries $\partial\Omega_1$ and $\partial\Omega_2$ were used, such that $\Omega_1 \in \Omega_2$. The boundary conditions being tested were imposed on the inner boundary $\partial\Omega_1$ and the resulting numerical solution was compared to the solution obtained when no conditions were imposed on this boundary.

In summary, in this thesis we investigated the propagation of linearized gravitational radiation on curved spacetime background. This enabled us to obtain absorbing outer boundary conditions for numerical relativity which are valid in linearized theory. We also showed how our boundary conditions could be implemented, by demonstrating how quantities such as the Weyl scalars or the Bondi mass can be evaluated in numerically. Finally, we have highlighted some of the limitations of perturbative studies in numerical relativity.

In the coming years, computing power will continue to increase and numerical relativity studies will become more ambitious. Events such as binary black hole coalescence will continue to be modelled by numerical relativists to provide waveform templates for the second generation of gravitational wave instruments. The detection of such gravitational waves would provide further experimental evidence of the existence of black holes and the validity of Einstein's theory of general relativity in the strong-field regime.

Appendix A

Computational Details for Chapters 3 and 8

A.1 Computational Details for Chapter 3

The h^{ab} and k^{ab} occurring in (3.11) are related to the h_{ab} and the k_{ab} by

$$\begin{aligned}
h^{00} &= -h_{00}, & h^{01} &= h_{01}, \\
h^{02} &= h_{02}, & h^{03} &= h_{03}\csc^2\theta, \\
h^{11} &= -h_{11}, & h^{12} &= -h_{12}, \\
h^{13} &= -h_{13}\csc^2\theta, & h^{22} &= -h_{22}, \\
h^{23} &= -h_{23}\csc^2\theta, & h^{33} &= -h_{33}\csc^4\theta,
\end{aligned} \tag{A.1}$$

and

$$\begin{aligned}
k^{00} &= -k_{00} + h_{00}^2 - h_{01}^2 - h_{02}^2 - h_{03}^2 \csc^2\theta, \\
k^{01} &= k_{01} - h_{00}h_{01} + h_{01}h_{11} + h_{02}h_{12} + h_{03}h_{23} \csc^2\theta, \\
k^{02} &= k_{02} - h_{00}h_{02} + h_{01}h_{12} + h_{02}h_{22} + h_{03}h_{23} \csc^2\theta, \\
k^{03} &= (k_{03} - h_{00}h_{03} + h_{01}h_{13} + h_{02}h_{23} + h_{03}h_{33} \csc^2\theta) \csc^2\theta, \\
k^{11} &= -k_{11} + h_{01}^2 - h_{11}^2 - h_{12}^2 - h_{13}^2 \csc^2\theta, \\
k^{12} &= -k_{12} + h_{01}h_{02} - h_{11}h_{12} - h_{12}h_{22} - h_{13}h_{23} \csc^2\theta, \\
k^{13} &= (-k_{13} + h_{01}h_{03} - h_{11}h_{13} - h_{12}h_{23} - h_{13}h_{33} \csc^2\theta) \csc^2\theta, \\
k^{22} &= -k_{22} + h_{02}^2 - h_{12}^2 - h_{22}^2 - h_{23}^2 \csc^2\theta, \\
k^{23} &= (-k_{23} + h_{02}h_{03} - h_{12}h_{13} - h_{22}h_{23} - h_{23}h_{33} \csc^2\theta) \csc^2\theta, \\
k^{33} &= (-k_{33} + h_{03}^2 - h_{13}^2 - h_{23}^2 - h_{33}^2 \csc^2\theta) \csc^4\theta.
\end{aligned} \tag{A.2}$$

The a_{ab} occurring in (3.26) (after imposing the conditions (3.27)) are given by

$$\begin{aligned}
a_{00} &= h_{00} - 2q_1, \\
a_{01} &= h_{00} + h_{01} + 2m_1 - q_1, \\
a_{02} &= h_{02} - y_{3,u}, \\
a_{03} &= h_{03} - z_{3,u} \sin^2\theta, \\
a_{11} &= h_{00} + 2h_{01} + h_{11} + 4m_1, \\
a_{12} &= h_{02} + h_{12} + y_2, \\
a_{13} &= h_{03} + h_{13} + z_2 \sin^2\theta, \\
a_{22} &= h_{22} - 2y_{2,\theta}, \\
a_{23} &= h_{23} - y_{2,\phi} - z_{2,\theta} \sin^2\theta, \\
a_{33} &= h_{33} - 2z_{2,\phi}.
\end{aligned} \tag{A.3}$$

The relation between the tetrad components c^{mn} and the c_{mn} is

$$\begin{aligned}
c^{00} &= \tfrac{1}{2}c_{01} - c_{00},\\
c^{01} &= \tfrac{1}{2}c_{00} - \tfrac{1}{4}c_{01} - c_{10} + \tfrac{1}{2}c_{11},\\
c^{02} &= s(c_{20} + c_{30}) - \tfrac{1}{2}s(c_{21} + c_{31}),\\
c^{03} &= is[(c_{20} - c_{30}) - \tfrac{1}{2}s(c_{21} - c_{31})\csc\theta],\\
c^{10} &= -c_{01},\\
c^{11} &= \tfrac{1}{2}c_{01} - c_{11},\\
c^{12} &= s(c_{21} + c_{31}),\\
c^{13} &= is(c_{21} - c_{31})\csc\theta,\\
c^{20} &= s(c_{02} + ic_{03}\csc\theta),\\
c^{21} &= s(c_{12} - \tfrac{1}{2}c_{02}) - is(\tfrac{1}{2}c_{03} - c_{13})\csc\theta,\\
c^{22} &= -\tfrac{1}{2}(c_{22} + c_{32}) - \tfrac{1}{2}i(c_{23} + c_{33})\csc\theta,\\
c^{23} &= -\tfrac{1}{2}i(c_{22} - c_{32})\csc\theta + \tfrac{1}{2}(c_{23} - c_{33})\csc^2\theta,\\
c^{30} &= s(c_{02} - ic_{03}\csc\theta),\\
c^{31} &= s(c_{12} - \tfrac{1}{2}c_{02}) + is(\tfrac{1}{2}c_{03} - c_{13})\csc\theta,\\
c^{32} &= -\tfrac{1}{2}(c_{22} + c_{32}) + \tfrac{1}{2}i(c_{23} + c_{33})\csc\theta,\\
c^{33} &= -\tfrac{1}{2}i(c_{22} - c_{32})\csc\theta - \tfrac{1}{2}(c_{23} - c_{33})\csc^2\theta,
\end{aligned} \tag{A.4}$$

where $s = 2^{-1/2}$.

One possible relation between the tetrad coefficients c_{mn} and the metric coefficients a_{mn} is

$$\begin{aligned}
c_{00} &= \alpha_1, \\
c_{01} &= \tfrac{1}{2}a_{11}, \\
c_{02} &= a_{12} - 2s\alpha_4, \\
c_{03} &= a_{13} + 2s\alpha_5 \sin\theta, \\
c_{10} &= \tfrac{1}{2}a_{00} - \tfrac{1}{2}\alpha_1, \\
c_{11} &= a_{01} - \tfrac{1}{4}a_{11} - \alpha_1, \\
c_{12} &= a_{02} - \tfrac{1}{2}a_{12} - s(2\alpha_2 - \alpha_4), \\
c_{13} &= a_{03} - \tfrac{1}{2}a_{13} + s(2\alpha_3 - \alpha_5)\sin\theta, \\
c_{20} &= \alpha_2 + i\alpha_3, \\
c_{21} &= \alpha_4 + i\alpha_5, \\
c_{22} &= \tfrac{1}{2}sa_{22} - is(a_{23} - \alpha_6)\csc\theta, \\
c_{23} &= s\alpha_6 - \tfrac{1}{2}isa_{33}\csc\theta, \\
c_{30} &= \alpha_2 - i\alpha_3, \\
c_{31} &= \alpha_4 - i\alpha_5, \\
c_{32} &= \tfrac{1}{2}sa_{22} + is(a_{23} - \alpha_6)\csc\theta, \\
c_{33} &= s\alpha_6 + \tfrac{1}{2}isa_{33}\csc\theta,
\end{aligned} \tag{A.5}$$

where α_m are the Lorentz parameters and $s = 2^{-1/2}$. Other representations are possible.

A.2 The Tetrad Formalism used in Chapter 3

Here we define the notation used and summarize the results. The reader to whom this material is unfamiliar should consult introductory material e.g. [27] chapter 1, section 7.

In this appendix $a, b, c, \ldots$ are coordinate indices while $\alpha, \beta, \gamma, \ldots$ are tetrad indices.

At each spacetime point P we introduce a basis of vectors

$$e_\alpha{}^a, \qquad \alpha \in [0,3], \quad a \in [0,3]. \tag{A.6}$$

Then the matrix

$$e_\alpha{}^a = \begin{pmatrix} e_0{}^0 & e_0{}^1 & \ldots \\ e_1{}^0 & e_1{}^1 & \ldots \\ \vdots & \vdots & \ddots \end{pmatrix}$$

is non-singular and we denote its inverse by $e^\alpha{}_a$. Thus

$$e_\alpha{}^a e^\beta{}_a = \delta_\alpha{}^\beta, \qquad e_\alpha{}^a e^\alpha{}_b = \delta^a{}_b. \tag{A.7}$$

The $e^\alpha{}_a$ represent the dual basis of covectors. As usual, chart indices are lowered using g_{ab} and raised using g^{ab}.

An additional assumption made here is that

$$\epsilon_{\alpha\beta} = g_{ab}\, e_\alpha{}^a e_\beta{}^b \tag{A.8}$$

is a **constant** symmetric matrix with inverse $\epsilon^{\alpha\beta}$. Thus

$$\epsilon_{\alpha\beta}\, \epsilon^{\beta\gamma} = \delta_\alpha{}^\gamma. \tag{A.9}$$

The choice $\epsilon_{\alpha\beta} = \mathrm{diag}(1,-1,-1,-1)$ gives an *orthonormal tetrad*, but here we choose

$$\epsilon_{\alpha\beta} = \epsilon^{\alpha\beta} = \begin{pmatrix} 0 & 1 & 0 & 0 \\ 1 & 0 & 0 & 0 \\ 0 & 0 & 0 & -1 \\ 0 & 0 & -1 & 0 \end{pmatrix}, \tag{A.10}$$

which gives a Newman-Penrose tetrad [97].

Then it is easy to see that

$$\epsilon_{\alpha\beta}\, e^{\beta}{}_{a} = e_{\alpha a}, \qquad \epsilon^{\alpha\beta}\, e_{\beta}{}^{a} = e^{\alpha a}, \tag{A.11}$$

so that tetrad indices can be lowered using $\epsilon_{\alpha\beta}$ and raised using $\epsilon^{\alpha\beta}$.

The *Ricci rotation coefficients* $\gamma_{\lambda\mu\nu}$ are defined via

$$e_{\mu b;c} = \gamma_{\lambda\mu\nu} e^{\lambda}{}_{b} e^{\nu}{}_{c}, \tag{A.12}$$

where the metric covariant derivative has been used. Since $\epsilon_{\alpha\beta}$ is constant, we must have $\gamma_{\lambda\mu\nu} = \gamma_{[\lambda\mu]\nu}$.

The tetrad *structure constants* $C^{\gamma}{}_{\alpha\beta}$ are defined via

$$[e_{\alpha}, e_{\beta}] = C^{\gamma}{}_{\alpha\beta} e_{\gamma}. \tag{A.13}$$

Clearly $C^{\gamma}{}_{\alpha\beta} = C^{\gamma}{}_{[\alpha\beta]}$. If we let (A.13) act on a scalar function f, note that the metric connection is symmetric, and use (A.12), then it is easy to see that

$$C^{\gamma}{}_{\alpha\beta} = \gamma^{\gamma}{}_{\beta\alpha} - \gamma^{\gamma}{}_{\alpha\beta}, \tag{A.14}$$

which implies

$$\gamma_{\lambda\mu\nu} = \tfrac{1}{2}(C_{\nu\lambda\mu} - C_{\lambda\mu\nu} - C_{\mu\nu\lambda}). \tag{A.15}$$

It is important to realise that the $C^{\lambda}{}_{\mu\nu}$ do not involve the connection. Using (A.14), (A.12) and the fact that the connection is symmetric, we can deduce that

$$C^{\lambda}{}_{\mu\nu} = e^{\lambda}{}_{a,b}(e_{\mu}{}^{a} e_{\nu}{}^{b} - e_{\mu}{}^{b} e_{\nu}{}^{a}). \tag{A.16}$$

Next, the Ricci identity applied to $e^{\alpha}{}_{b}$ gives

$$R_{\alpha\beta\gamma\delta} = \gamma_{\alpha\beta\gamma,a} e_{\delta}{}^{a} - \gamma_{\alpha\beta\delta,a} e_{\gamma}{}^{a} + \gamma_{\alpha\beta\epsilon} C^{\epsilon}{}_{\gamma\delta} + \gamma^{\epsilon}{}_{\alpha\gamma}\gamma_{\epsilon\beta\delta} - \gamma^{\epsilon}{}_{\alpha\delta}\gamma_{\epsilon\beta\eta}, \tag{A.17}$$

and finally

$$R_{\alpha\gamma} = \epsilon^{\beta\delta} R_{\alpha\beta\gamma\delta}. \tag{A.18}$$

Note that throughout chapter 3 we use these forms for the curvature tensors. Thus R_{12} means $R_{\alpha\beta}$ with $\alpha = 1$ and $\beta = 2$, which is not the same as R_{ab} with $a = 1$ and $b = 2$.

The algorithm used to obtain the $R_{\alpha\beta}$ in §3.4 starts from the sets $\{e_\alpha{}^a\}$ and $\{e^\alpha{}_a\}$. We compute $C^\alpha{}_{\beta\gamma}$ from (A.16) and of course $C_{\gamma\alpha\beta} = \epsilon_{\gamma\delta}C^\delta{}_{\alpha\beta}$. Next we compute $\gamma_{\alpha\beta\gamma}$ from (A.15) and finally the curvature tensors from (A.17) and (A.18). Although this looks ponderous it can easily be automated using a computer algebra system.

A.3 Computational Details for Chapter 8

The a_{ij} are related to the h_{ij} by

$$\begin{aligned}
a_{00} &= m_v + \tfrac{1}{4}(h_{00} - 2h_{01} + h_{11}) = 0,\\
a_{01} &= \tfrac{1}{4}(h_{00} - h_{11}) - \tfrac{1}{2}(m_u + m_v) - \tfrac{1}{2}(q_u + q_v) = \tfrac{1}{2}h_{00} - \tfrac{1}{2}(q_u + q_v),\\
a_{02} &= \tfrac{1}{2}(h_{02} - h_{12}),\\
a_{03} &= \tfrac{1}{2}(h_{03} - h_{13}),\\
a_{11} &= m_u + \tfrac{1}{4}(h_{00} + 2h_{01} + h_{11}) = 0,\\
a_{12} &= \tfrac{1}{2}(h_{12} + h_{02}),\\
a_{13} &= \tfrac{1}{2}(h_{13} + h_{03}),\\
a_{22} &= h_{22} - 2y_{\theta,\theta},\\
a_{23} &= h_{23} - y_{\theta,\phi} - y_{\phi,\theta}\sin^2\theta,\\
a_{33} &= h_{33} - 2y_{\phi,\phi}\sin^2\theta.
\end{aligned} \tag{A.19}$$

The relation between the covariant and contravariant tetrad coefficients, c_{ij} and c^{ij}, is

$$\begin{aligned}
c^{00} &= -2c_{01}, & c^{01} &= -4c_{11},\\
c^{02} &= 4sc_{21}, & c^{03} &= -4sc_{31}\csc\theta,\\
c^{10} &= -c_{00}, & c^{11} &= -2c_{10},\\
c^{12} &= 2sc_{20}, & c^{13} &= -2sc_{30}\csc\theta,\\
c^{20} &= -sc_{02}, & c^{21} &= -2sc_{12},\\
c^{22} &= c_{22}, & c^{23} &= -c_{32}\csc\theta,\\
c^{30} &= sc_{03}\csc\theta, & c^{31} &= 2sc_{13}\csc\theta,\\
c^{32} &= -c_{23}\csc\theta, & c^{33} &= c_{23}\csc^2\theta,
\end{aligned} \tag{A.20}$$

where $s = 2^{-1/2}$.

The tetrad coefficients c_{ij} are related to the a_{ij} via

$$\begin{aligned}
c_{00} &= -2A_1 + 2a_{01}, & c_{01} &= a_{11}, \\
c_{02} &= -4sA_3 + 2a_{12}, & c_{03} &= 4sA_5 \sin\theta + 2a_{13}, \\
c_{10} &= \tfrac{1}{2}a_{00}, & c_{11} &= A_1, \\
c_{12} &= -2sA_2 + a_{02}, & c_{13} &= 2sA_4 \sin\theta + a_{03}, \\
c_{20} &= A_2, & c_{21} &= A_3, \\
c_{22} &= \tfrac{1}{2}sa_{22}, & c_{23} &= A_6 \sin\theta + sa_{23}, \\
c_{30} &= A_4, & c_{31} &= A_5, \\
c_{32} &= A_6, & c_{33} &= -\tfrac{1}{2}sa_{33} \csc\theta,
\end{aligned} \tag{A.21}$$

where the A_i are the Lorentz parameters, depending on u, v, θ, ϕ. Other representations are possible.

The vanishing of the Ricci curvature provides us with the following constraints on the a_{ij}:

$$\begin{aligned}
a_{01,uv} &= 0, & a_{02,uv} &= a_{12,uu}, \\
a_{02,vv} &= a_{12,uv}, & a_{03,uv} &= a_{13,uu}, \\
a_{03,vv} &= a_{13,uv}, & a_{22,uv} &= 0, \\
a_{23,uv} &= 0, & a_{33,uu} &= -a_{22,uu} \sin^2\theta, \\
a_{33,uv} &= 0, & a_{33,vv} &= -a_{22,vv} \sin^2\theta.
\end{aligned} \tag{A.22}$$

Using (A.19) and (A.22) we obtain the following constraints on the h_{ij}:

$$\begin{aligned}
\tfrac{1}{2}h_{00,uv} - \tfrac{1}{2}(q_{u,uv} + q_{v,uv}) &= 0,\\
\tfrac{1}{2}(h_{02,uv} - h_{12,uv}) &= \tfrac{1}{2}(h_{12,uu} + h_{02,uu}),\\
\tfrac{1}{2}(h_{02,vv} - h_{12,vv}) &= \tfrac{1}{2}(h_{12,uv} + h_{02,uv}),\\
\tfrac{1}{2}(h_{03,uv} - h_{13,uv}) &= \tfrac{1}{2}(h_{13,uu} + h_{03,uu}),\\
\tfrac{1}{2}(h_{03,vv} - h_{13,vv}) &= \tfrac{1}{2}(h_{13,uv} + h_{03,uv}),\\
h_{22,uv} - 2y_{\theta,\theta uv} &= 0,\\
h_{23,uv} - y_{\theta,\phi uv} - y_{\phi,\theta uv}\sin^2\theta &= 0,\\
h_{33,uu} - 2y_{\phi,\phi uu}\sin^2\theta &= -(h_{22,uu} - 2y_{\theta,\theta uu})\sin^2\theta,\\
h_{33,uv} - 2y_{\phi,\phi uv}\sin^2\theta &= 0,\\
h_{33,vv} - 2y_{\phi,\phi vv}\sin^2\theta &= -(h_{22,vv} - 2y_{\theta,\theta vv})\sin^2\theta.
\end{aligned} \tag{A.23}$$

Appendix B

Perturbed Quantities Induced by a Hertz Potential

On a type D background spacetime, the Hertz potential

$$\chi_{ABCD} = \chi' \iota_A \iota_B \iota_C \iota_D, \tag{B.1}$$

generates perturbations to the metric, the tetrad, the Newman-Penrose scalars and the Weyl scalars. In this appendix, we state the perturbations on Minkowski, Schwarzschild and Kerr backgrounds. A hat $\wedge$ above a symbol denotes its perturbation.

B.1 Perturbations about a Minkowski Background

On a Minkowski background, using the tetrad (5.28), ρ, ρ', β and β' are real and non-zero. The remaining Newman-Penrose scalars and the Weyl scalars vanish.

Expressed in terms of the unperturbed tetrad $(l, n, m, \bar{m})$, the perturbed

metric is given by

$$\begin{aligned}\gamma_{ab} = &\left[\eth\eth\bar{\chi}' + \eth'\eth'\chi'\right] n_a n_b \\ &+ \left[(\text{Þ}' + 2\rho')\text{Þ}'\bar{\chi}'\right] m_a m_b + \left[(\text{Þ}' + 2\rho')\text{Þ}'\chi'\right] \bar{m}_a \bar{m}_b \\ &- 2\left[(\text{Þ}' + \rho')\eth\bar{\chi}'\right] n_{(a} m_{b)} - 2\left[(\text{Þ}' + \rho')\eth'\chi'\right] n_{(a}\bar{m}_{b)}. \end{aligned} \tag{B.2}$$

The covariant tetrad perturbation is

$$\begin{aligned}\hat{l}_a &= \tfrac{1}{2}\left[\eth\eth\bar{\chi}' + \eth'\eth'\chi'\right] n_a - \left[(\text{Þ}' + \rho')\eth\bar{\chi}'\right] m_a - \left[(\text{Þ}' + \rho')\eth'\chi'\right] \bar{m}_a, \\ \hat{n}_a &= 0, \\ \hat{m}_a &= -\tfrac{1}{2}\left[(\text{Þ}' + 2\rho')\text{Þ}'\chi'\right] \bar{m}_a, \\ \hat{\bar{m}}_a &= -\tfrac{1}{2}\left[(\text{Þ}' + 2\rho')\text{Þ}'\bar{\chi}'\right] m_a, \end{aligned} \tag{B.3}$$

and the contravariant perturbation is

$$\begin{aligned}\hat{l}^a &= -\tfrac{1}{2}\left[\eth\eth\bar{\chi}' + \eth'\eth'\chi'\right] n^a, \\ \hat{n}^a &= 0, \\ \hat{m}^a &= -\left[(\text{Þ}' + \rho')\eth'\chi'\right] n^a + \tfrac{1}{2}\left[(\text{Þ}' + 2\rho')\text{Þ}'\chi'\right] \bar{m}^a, \\ \hat{\bar{m}}^a &= -\left[(\text{Þ}' + \rho')\eth\bar{\chi}'\right] n^a + \tfrac{1}{2}\left[(\text{Þ}' + 2\rho')\text{Þ}'\bar{\chi}'\right] m^a. \end{aligned} \tag{B.4}$$

The perturbed NP scalars are given by

$$
\begin{aligned}
\hat{\kappa} &= -\tfrac{1}{2}\eth\eth\eth\bar{\chi}' + \tfrac{1}{2}\text{Þ}\text{Þ}'\eth'\chi', \\
\hat{\kappa}' &= 0, \\
\hat{\sigma} &= \tfrac{1}{2}\text{Þ}\text{Þ}'\text{Þ}'\chi' + \rho'\text{Þ}\text{Þ}'\chi' + \rho\rho'\text{Þ}'\chi', \\
\hat{\sigma}' &= \tfrac{1}{2}\text{Þ}'\text{Þ}'\text{Þ}'\bar{\chi}' + \rho'\text{Þ}'\text{Þ}'\bar{\chi}' + \rho'^2\text{Þ}'\bar{\chi}', \\
\hat{\rho} &= \tfrac{1}{2}\left[\text{Þ}'(\eth'\eth'\chi' - \eth\eth\bar{\chi}') - \rho'(\eth'\eth'\chi' + \eth\eth\bar{\chi}')\right], \\
\hat{\rho}' &= 0, \\
\hat{\tau} &= \tfrac{1}{2}\text{Þ}'\text{Þ}'\eth'\chi', \\
\hat{\tau}' &= \tfrac{1}{2}\text{Þ}'\text{Þ}'\eth\bar{\chi}', \\
\hat{\beta} &= -\tfrac{1}{2}\beta\text{Þ}'\text{Þ}'\chi' + \tfrac{1}{2}\rho'\text{Þ}'\eth'\chi' - \rho'\beta\text{Þ}'\chi', \\
\hat{\beta}' &= \tfrac{1}{2}\text{Þ}'\text{Þ}'\eth\bar{\chi}' - \tfrac{1}{2}\beta\text{Þ}'\text{Þ}'\bar{\chi}' + \tfrac{1}{2}\rho'\text{Þ}'\eth\bar{\chi}' - \rho'\beta\text{Þ}'\bar{\chi}', \\
\hat{\epsilon} &= -\tfrac{1}{2}\text{Þ}'\eth\eth\bar{\chi}', \\
\hat{\epsilon}' &= 0.
\end{aligned}
\tag{B.5}
$$

The perturbed Weyl scalars are given by

$$
\begin{aligned}
\hat{\Psi}_4 &= \tfrac{1}{2}\text{Þ}'^4\bar{\chi}', \\
\hat{\Psi}_3 &= \tfrac{1}{2}\text{Þ}'^3\eth\bar{\chi}', \\
\hat{\Psi}_2 &= \tfrac{1}{2}\text{Þ}'^2\eth^2\bar{\chi}', \\
\hat{\Psi}_1 &= \tfrac{1}{2}\text{Þ}'\eth^3\bar{\chi}', \\
\hat{\Psi}_0 &= \tfrac{1}{2}\eth^4\bar{\chi}'.
\end{aligned}
\tag{B.6}
$$

B.2 Perturbations about a Schwarzschild Background

On a Schwarzschild background, in the tetrad (6.3), ρ, ρ', β, β', ϵ' and Ψ_2 are real and non-zero. The remaining Newman-Penrose and Weyl scalars vanish.

Expressed in terms of the unperturbed tetrad $(l, n, m, \bar{m})$, the metric perturbation is given by

$$\begin{aligned}\gamma_{ab} = &\left[\text{ð}\text{ð}\bar{\chi}' + \text{ð}'\text{ð}'\chi'\right] n_a n_b \\ &+ \left[(\text{Þ}' + 2\rho')\text{Þ}'\bar{\chi}'\right] m_a m_b + \left[(\text{Þ}' + 2\rho')\text{Þ}'\chi'\right] \bar{m}_a \bar{m}_b \\ &- 2\left[(\text{Þ}' + \rho')\text{ð}\bar{\chi}'\right] n_{(a} m_{b)} - 2\left[(\text{Þ}' + \rho')\text{ð}'\chi'\right] n_{(a} \bar{m}_{b)}. \end{aligned} \tag{B.7}$$

The covariant tetrad perturbation is

$$\begin{aligned}\hat{l}_a &= \tfrac{1}{2}\left[\text{ð}\text{ð}\bar{\chi}' + \text{ð}'\text{ð}'\chi'\right] n_a - \left[(\text{Þ}' + \rho')\text{ð}\bar{\chi}'\right] m_a - \left[(\text{Þ}' + \rho')\text{ð}'\chi'\right] \bar{m}_a, \\ \hat{n}_a &= 0, \\ \hat{m}_a &= -\tfrac{1}{2}\left[(\text{Þ}' + 2\rho')\text{Þ}'\chi'\right] \bar{m}_a, \\ \hat{\bar{m}}_a &= -\tfrac{1}{2}\left[(\text{Þ}' + 2\rho')\text{Þ}'\bar{\chi}'\right] m_a, \end{aligned} \tag{B.8}$$

and the contravariant tetrad perturbation is

$$\begin{aligned}\hat{l}^a &= -\tfrac{1}{2}\left[\text{ð}\text{ð}\bar{\chi}' + \text{ð}'\text{ð}'\chi'\right] n^a, \\ \hat{n}^a &= 0, \\ \hat{m}^a &= -\left[(\text{Þ}' + \rho')\text{ð}'\chi'\right] n^a + \tfrac{1}{2}\left[(\text{Þ}' + 2\rho')\text{Þ}'\chi'\right] \bar{m}^a, \\ \hat{\bar{m}}^a &= -\left[(\text{Þ}' + \rho')\text{ð}\bar{\chi}'\right] n^a + \tfrac{1}{2}\left[(\text{Þ}' + 2\rho')\text{Þ}'\bar{\chi}'\right] m^a. \end{aligned} \tag{B.9}$$

The perturbed NP scalars are given by

$$\begin{aligned}
\hat{\kappa} &= -\tfrac{1}{2}\eth\eth\eth\bar{\chi}' + \tfrac{1}{2}\text{Þ}\text{Þ}'\eth'\chi' + \tfrac{1}{2}\Psi_2\eth'\chi', \\
\hat{\kappa}' &= 0, \\
\hat{\sigma} &= \tfrac{1}{2}\text{Þ}\text{Þ}'\text{Þ}'\chi' + \rho'\text{Þ}\text{Þ}'\chi' + (\rho\rho' - \Psi_2)\text{Þ}'\chi', \\
\hat{\sigma}' &= \tfrac{1}{2}\text{Þ}'\text{Þ}'\text{Þ}'\bar{\chi}' + \rho'\text{Þ}'\text{Þ}'\bar{\chi}' + \rho'^2\text{Þ}'\bar{\chi}', \\
\hat{\rho} &= \tfrac{1}{2}\left[\text{Þ}'(\eth'\eth'\chi' - \eth\eth\bar{\chi}') - \rho'(\eth'\eth'\chi' + \eth\eth\bar{\chi}')\right], \\
\hat{\rho}' &= 0, \\
\hat{\tau} &= \tfrac{1}{2}\text{Þ}'\text{Þ}'\eth'\chi', \\
\hat{\tau}' &= \tfrac{1}{2}\text{Þ}'\text{Þ}'\eth\bar{\chi}', \\
\hat{\beta} &= -\tfrac{1}{2}\beta\text{Þ}'\text{Þ}'\chi' + (\tfrac{1}{2}\rho' + \epsilon')\text{Þ}'\eth'\chi' - \rho'(\beta\text{Þ}'\chi' - \epsilon'\eth'\chi'), \\
\hat{\beta}' &= \tfrac{1}{2}\text{Þ}'\text{Þ}'\eth\bar{\chi}' - \tfrac{1}{2}\beta\text{Þ}'\text{Þ}'\bar{\chi}' + (\tfrac{1}{2}\rho' - \epsilon')\text{Þ}'\eth\bar{\chi}' - \rho'(\beta\text{Þ}'\bar{\chi}' + \epsilon'\eth\bar{\chi}'), \\
\hat{\epsilon} &= -\tfrac{1}{2}\text{Þ}'\eth\eth\bar{\chi}' + \tfrac{1}{2}\epsilon'(\eth'\eth'\chi' + \eth\eth\bar{\chi}'), \\
\hat{\epsilon}' &= 0.
\end{aligned} \tag{B.10}$$

The perturbed Weyl scalars are given by

$$\begin{aligned}
\hat{\Psi}_4 &= \tfrac{1}{2}\text{Þ}'^4\bar{\chi}', \\
\hat{\Psi}_3 &= \tfrac{1}{2}\text{Þ}'^3\eth\bar{\chi}', \\
\hat{\Psi}_2 &= \tfrac{1}{2}\text{Þ}'^2\eth^2\bar{\chi}', \\
\hat{\Psi}_1 &= \tfrac{1}{2}\text{Þ}'\eth^3\bar{\chi}' - \tfrac{3}{2}\Psi_2(\text{Þ}'\eth'\chi' + \rho'\eth'\chi'), \\
\hat{\Psi}_0 &= \tfrac{1}{2}\eth^4\bar{\chi}' - \tfrac{3}{2}\Psi_2\rho'\text{Þ}\chi' + \tfrac{3}{2}\Psi_2\rho\text{Þ}'\chi' + 3\Psi_2^2\chi'.
\end{aligned} \tag{B.11}$$

Note that the perturbations about a Minkowski background can be obtained by substituting $\epsilon' = \Psi_2 = 0$ into the expressions above.

B.3 Perturbations about a Kerr Background

In a Kerr spacetime, using the tetrad (7.12), ρ, ρ', ϵ', β, β', τ, τ' and Ψ_2 are non-zero and, in general, complex. In the formulae below, red expressions are specific to the Kerr background and are not present on Schwarzschild or Minkowski backgrounds. They involve the angular momentum parameter a and the mass parameter M. Blue expressions are present in perturbations about Schwarzschild and Kerr backgrounds. They involve M but not a. Expressions in black are present in the perturbations about either Minkowski, Schwarzschild or Kerr backgrounds and are independent of M and a.

The metric perturbation is

$$\gamma_{ab} = (X + \bar{X}) n_a n_b + Y m_a m_b + \bar{Y} \bar{m}_a \bar{m}_b - 2Z n_{(a} m_{b)} - 2\bar{Z} n_{(a} \bar{m}_{b)}, \tag{B.12}$$

the covariant tetrad perturbation is

$$\begin{aligned} \hat{l}_a &= \tfrac{1}{2}(X + \bar{X}) n_a - Z m_a - \bar{Z} \bar{m}_a, \\ \hat{n}_a &= 0, \\ \hat{m}_a &= -\tfrac{1}{2} \bar{Y} \bar{m}_a, \\ \hat{\bar{m}}_a &= -\tfrac{1}{2} Y m_a, \end{aligned}$$

and the contravariant tetrad perturbation is

$$\begin{aligned} \hat{l}^a &= -\tfrac{1}{2}(X + \bar{X}) n^a, \\ \hat{n}^a &= 0, \\ \hat{m}^a &= -Z n^a + \tfrac{1}{2} \bar{Y} \bar{m}^a, \\ \hat{\bar{m}}^a &= -Z n^a + \tfrac{1}{2} Y m^a, \end{aligned} \tag{B.13}$$

where

$$\begin{aligned} X &= \text{ð}'\text{ð}'\chi' + 2\tau' \text{ð}' \chi', \\ Y &= \text{Þ}'\text{Þ}'\bar{\chi}' + 2\bar{\rho}' \text{Þ}' \bar{\chi}', \\ Z &= \text{Þ}'\text{ð}\bar{\chi}' + \bar{\rho}' \text{ð}\bar{\chi}' + (\tau + \bar{\tau}') \text{Þ}' \bar{\chi}'. \end{aligned} \tag{B.14}$$

The perturbed NP scalars are given by

$$
\begin{aligned}
\hat{\kappa} =& -\tfrac{1}{2}\text{ð}\text{ð}\text{ð}\bar{\chi}' + \tfrac{1}{2}\text{Þ}\text{Þ}'\text{ð}'\chi' + \tfrac{1}{2}\Psi_2\text{ð}'\chi' - \tfrac{1}{2}\tau(\text{ð}\text{ð}\bar{\chi}' + \text{ð}'\text{ð}'\chi') + \tfrac{1}{2}(\bar{\tau} + 2\tau')\text{Þ}\text{Þ}'\chi' \\
& -\tfrac{1}{2}\bar{\tau}'\text{ð}\text{ð}\bar{\chi}' - \tau(\tau'\text{ð}'\chi' + \bar{\tau}'\text{ð}\bar{\chi}') + [\text{Þ}\tau' + \tfrac{1}{2}\bar{\rho}(\bar{\tau} - \tau')]\text{Þ}'\chi', \\
\hat{\kappa}' =& 0, \\
\hat{\sigma} =& \tfrac{1}{2}\text{Þ}\text{Þ}'\text{Þ}'\chi' + \tfrac{1}{2}(\rho - \bar{\rho})\text{Þ}'\text{Þ}'\chi' + \rho'\text{Þ}\text{Þ}'\chi' + (\rho\rho' - \Psi_2)\text{Þ}'\chi' + (\bar{\tau}' - \tau)\text{Þ}'\text{ð}'\chi' \\
& + \rho'(\bar{\tau}' - \tau)\text{ð}'\chi' + ((\text{ð}\tau') + \bar{\tau}\bar{\tau}' - \tau\bar{\tau} - \tau\tau')\text{Þ}'\chi', \\
\hat{\sigma}' =& \tfrac{1}{2}\text{Þ}'\text{Þ}'\text{Þ}'\bar{\chi}' + \tfrac{1}{2}(\rho' + \bar{\rho}')\text{Þ}'\text{Þ}'\bar{\chi}' + \rho'\bar{\rho}'\text{Þ}'\bar{\chi}', \\
\hat{\rho} =& \tfrac{1}{2}\text{Þ}'(\text{ð}'\text{ð}'\chi' - \text{ð}\text{ð}\bar{\chi}') - \tfrac{1}{2}\bar{\rho}'(\text{ð}'\text{ð}'\chi' + \text{ð}\text{ð}\bar{\chi}') + (\bar{\tau} + \tau')\text{Þ}'\text{ð}'\chi' - 2\tau\text{Þ}'\text{ð}\bar{\chi}' \\
& -\bar{\rho}'(\tau\text{ð}\bar{\chi}' + \tau'\text{ð}'\chi') + (\bar{\tau}^2 + \bar{\tau}\tau' + \tau'^2)\text{Þ}'\chi' - \tau(\bar{\tau}' + 2\tau)\text{Þ}'\bar{\chi}', \\
\hat{\rho}' =& 0, \\
\hat{\tau} =& \tfrac{1}{2}\text{Þ}'\text{Þ}'\text{ð}'\chi' + (\tfrac{1}{2}\bar{\tau} + \tau')\text{Þ}'\text{Þ}'\chi' + (\tfrac{1}{2}(\text{Þ}'\bar{\tau}) + \rho'(\tau' - \bar{\tau}))\text{Þ}'\chi', \\
\hat{\tau}' =& \tfrac{1}{2}\text{Þ}'\text{Þ}'\text{ð}\bar{\chi}' + (\tau + \tfrac{1}{2}\bar{\tau}')\text{Þ}'\text{Þ}'\bar{\chi}' + \tfrac{1}{2}(\text{Þ}'\tau)\text{Þ}'\bar{\chi}', \\
\hat{\beta} =& -\tfrac{1}{2}\beta'\text{Þ}'\text{Þ}'\chi' + (\tfrac{1}{2}\rho' + \epsilon')\text{Þ}'\text{ð}'\chi' - \rho'(\beta'\text{Þ}'\chi' - \epsilon'\text{ð}'\chi') + (\epsilon'(\tau' + \bar{\tau}') + \rho'(\tfrac{1}{2}\bar{\tau} + \tau'))\text{Þ}'\chi', \\
\hat{\beta}' =& \tfrac{1}{2}\text{Þ}'\text{Þ}'\text{ð}\bar{\chi}' - \tfrac{1}{2}\beta\text{Þ}'\text{Þ}'\bar{\chi}' + (\tfrac{1}{2}\rho' - \epsilon')\text{Þ}'\text{ð}\bar{\chi}' - \bar{\rho}'(\beta\text{Þ}'\bar{\chi}' + \epsilon'\text{ð}\bar{\chi}') + \tau\text{Þ}'\text{Þ}'\bar{\chi}' \\
& + (\tfrac{1}{2}[(\text{Þ}'\tau) + \bar{\rho}'\tau] - \epsilon'(\tau + \bar{\tau}'))\text{Þ}'\bar{\chi}', \\
\hat{\epsilon} =& -\tfrac{1}{2}\text{Þ}'\text{ð}\text{ð}\bar{\chi}' + \tfrac{1}{2}\epsilon'(\text{ð}'\text{ð}'\chi' + \text{ð}\text{ð}\bar{\chi}') + \tfrac{1}{2}\tau'\text{Þ}'\text{ð}'\chi' - (\tau + \tfrac{1}{2}\bar{\tau}')\text{Þ}'\text{ð}\bar{\chi}' \\
& + \epsilon'(\tau'\text{ð}'\chi' + \bar{\tau}'\text{ð}\bar{\chi}') + \tau'(\tau + \tfrac{1}{2}\bar{\tau})\text{Þ}'\chi' - \tau(\tau + \tfrac{1}{2}\bar{\tau}')\text{Þ}'\bar{\chi}', \\
\hat{\epsilon}' =& 0.
\end{aligned}
\tag{B.15}
$$

The perturbed Weyl scalars are given by

$$
\begin{aligned}
\hat{\Psi}_4 =& \tfrac{1}{2}\text{Þ}'^4\bar{\chi}', \\
\hat{\Psi}_3 =& \tfrac{1}{2}\text{Þ}'^3\text{ð}\bar{\chi}' + \tfrac{3}{2}\tau\text{Þ}'^3\bar{\chi}' + \tfrac{3}{2}(\text{Þ}'\tau)\text{Þ}'^2\bar{\chi}' + \tfrac{1}{2}(\text{Þ}'^2\tau)\text{Þ}'\bar{\chi}', \\
\hat{\Psi}_2 =& \tfrac{1}{2}\text{Þ}'^2\text{ð}^2\bar{\chi}' + 2\tau\text{Þ}'^2\text{ð}\bar{\chi}' + 3\tau^2\text{Þ}'^2\bar{\chi}' + (\text{Þ}'\tau)\text{Þ}'\text{ð}\bar{\chi}' + 3\tau(\text{Þ}'\tau)\text{Þ}'\bar{\chi}', \\
\hat{\Psi}_1 =& \tfrac{1}{2}\text{Þ}'\text{ð}^3\bar{\chi}' - \tfrac{3}{2}\Psi_2(\text{Þ}'\text{ð}'\chi' + \rho'\text{ð}'\chi') + \tfrac{3}{2}\tau\text{Þ}'\text{ð}\text{ð}\bar{\chi}' + 3\tau^2\text{Þ}'\text{ð}\bar{\chi}' - \tfrac{3}{2}\Psi_2(\bar{\tau} + \tau')\text{Þ}'\chi' + 3\tau^3\text{Þ}'\bar{\chi}', \\
\hat{\Psi}_0 =& \tfrac{1}{2}\text{ð}^4\bar{\chi}' + \tfrac{3}{2}\Psi_2(\rho\text{Þ}'\chi' - \rho'\text{Þ}\chi') + 3{\Psi_2}^2\chi' + \tfrac{3}{2}\Psi_2(\tau'\text{ð}\chi' - \tau\text{ð}'\chi').
\end{aligned}
\tag{B.16}
$$

The perturbations about a Schwarzschild background can be obtained from the expressions above by setting $\tau = \tau' = 0$ and $\rho = \bar{\rho}$. If we also set $\epsilon' = 0$ and $\Psi_2 = 0$ then we obtain the perturbations on a Minkowski background.

Appendix C

Spherical Harmonic Conventions

C.1 Spherical Harmonics

For $l \geq 0$ and $-l \leq m \leq l$, the spherical harmonics $Y_{lm}(\theta, \phi)$ are given by

$$Y_{lm}(\theta, \phi) = \sqrt{\frac{(2l+1)(l-m)!}{4\pi(l+m)!}} P_{lm}(\cos\theta) \mathrm{e}^{im\phi}. \tag{C.1}$$

They form a complete set of orthonormal functions on the unit sphere. The spherical harmonics are eigenfunctions of the Laplacian operator on the unit sphere,

$$\left(\frac{\partial^2}{\partial\theta^2} + \csc^2\theta \frac{\partial^2}{\partial\phi^2} - i\frac{\cos\theta}{\sin^2\theta}\frac{\partial}{\partial\phi} \right) Y_{lm}(\theta, \phi) = -l(l+1) Y_{lm}(\theta, \phi). \tag{C.2}$$

In (C.1), the $P_{lm}(\cos\theta)$ are associated Legendre functions with the Condon-Shortley phase factor $(-1)^m$ included:

$$P_{lm}(x) = \frac{(-1)^m}{2^l l!} (1-x^2)^{m/2} \frac{\mathrm{d}^{l+m}}{\mathrm{d}x^{l+m}} (x^2-1)^l. \tag{C.3}$$

There is a well known recurrence formula for the associated Legendre functions

$$x P_{lm}(x) = \left(\frac{l-m+1}{2l+1} \right) P_{l+1\,m}(x) + \left(\frac{l+m}{2l+1} \right) P_{l-1\,m}(x), \tag{C.4}$$

which enables us to write

$$\cos\theta\, Y_{lm} = \sqrt{\frac{(l+m+1)(l-m+1)}{(2l+3)(2l+1)}}\, Y_{l+1\,m} + \sqrt{\frac{(l-m)(l+m)}{(2l+1)(2l-1)}}\, Y_{l-1\,m}. \quad \text{(C.5)}$$

Hence we obtain

$$\cos^2\theta\, Y_{lm} = A_{lm} Y_{l+2\,m} + B_{lm} Y_{lm} + C_{lm} Y_{l-2\,m}, \quad \text{(C.6)}$$

where

$$\begin{aligned} A_{lm} &= \sqrt{\frac{(l-m+1)(l-m+2)(l+m+1)(l+m+2)}{(2l+1)(2l+3)^2(2l+5)}}, \\ B_{lm} &= \frac{(l-m+1)(l+m+1)}{(2l+1)(2l+3)} + \frac{(l+m)(l-m)}{(2l+1)(2l-1)}, \\ C_{lm} &= \sqrt{\frac{(l-m-1)(l-m)(l+m-1)(l+m)}{(2l-3)(2l-1)^2(2l+1)}} = A_{l-2\,m}, \end{aligned} \quad \text{(C.7)}$$

This recurrence relation is used in §7.2. Note that the relation (C.5) is still valid for $l = 0$ or $m = l$, since the coefficient of $Y_{l-1\,m}$ vanishes in both cases. Similarly the relation (C.6) is valid if $l = 0,\ 1$, or $m = l,\ l-1$ (since C_{lm} vanishes in each case).

C.2 Spin-Weighted Spherical Harmonics

We use the spin-weighted spherical harmonic conventions found in [135]. For a quantity $\eth$ of spin s, we define the operators $\eth$ and $\eth'$ such that

$$\begin{aligned}\eth\eta &= \frac{1}{\sqrt{2}r}\left(\partial_\theta\eta - s\cot\theta\eta - i\csc\theta\partial_\phi\eta\right)\\ \eth'\eta &= \frac{1}{\sqrt{2}r}\left(\partial_\theta\eta + s\cot\theta\eta + i\csc\theta\partial_\phi\eta\right).\end{aligned} \tag{C.8}$$

For $l \geq |s|$ and $-l \leq m \leq l$, the spin-weighted spherical harmonics ${}_sY_{lm}(\theta,\phi)$ are defined by

$${}_sY_{lm} = \begin{cases} (-1)^s r^s \sqrt{\dfrac{2^s(l-s)!}{(l+s)!}}\eth^s{}_0Y_{lm} & \text{if } 0 \leq s \leq l,\\ \\ r^{-s}\sqrt{\dfrac{2^{-s}(l+s)!}{(l-s)!}}\eth'^{-s}{}_0Y_{lm} & \text{if } 0 \geq s \geq -l. \end{cases} \tag{C.9}$$

The ${}_0Y_{lm}$ are the standard spin-0 spherical harmonics Y_{lm} defined in appendix C.1. For any given s the ${}_sY_{lm}$ form a complete set of orthonormal functions on the unit sphere. The operators $\eth$ and $\eth'$ then act as spin-raising and -lowering operators respectively:

$$\begin{aligned}\eth\,{}_sY_{lm} &= 2^{-1/2}r^{-1}\left(\frac{l-s}{l+s+1}\right)^{1/2}{}_{s+1}Y_{lm},\\ \eth'\,{}_sY_{lm} &= -2^{-1/2}r^{-1}\left(\frac{l+s}{l-s+1}\right)^{1/2}{}_{s-1}Y_{lm}.\end{aligned} \tag{C.10}$$

This implies the eigenvalue equation

$$\eth\eth'\,{}_sY_{lm} = -\frac{1}{2r^2}(l+s)(l-s+1)\,{}_sY_{lm}, \tag{C.11}$$

which can also be written as

$$\begin{aligned}&\left(\frac{\partial^2}{\partial\theta^2} + \csc^2\theta\frac{\partial^2}{\partial\phi^2} - (1+2s)i\frac{\cos\theta}{\sin^2\theta}\frac{\partial}{\partial\phi} - \frac{s+s^2\cos^2\theta}{\sin^2\theta}\right){}_sY_{lm}(\theta,\phi)\\ &\quad = -(l+s)(l-s+1)\,{}_sY_{lm}(\theta,\phi).\end{aligned} \tag{C.12}$$

Note that some conventions (such as e.g. [21]) do not include the factors of r in the definitions (C.8) or (C.9). We include them here to simplify the calculations in chapters 5 and 6.

We can factor out the $\theta-$ and $\phi-$dependence of the spin-weighted spherical harmonics by writing

$$ {}_sY_{lm}(\theta,\phi) = {}_sN_{lm}\, P_l^{m+s,\,m-s}(\cos\theta)\mathrm{e}^{im\phi}, \tag{C.13} $$

where ${}_sN_{lm}$ is a normalization factor and $P_l^{m+s,\,m-s}$ is a function whose behaviour we now investigate. Substitution of (C.13) into the eigenvalue equation (C.11) yields the differential equation

$$ \left\{(1-x^2)\frac{\mathrm{d}^2}{\mathrm{d}x^2} - 2x\frac{\mathrm{d}}{\mathrm{d}x} - \frac{(m+s)^2}{2(1-x)} - \frac{(m-s)^2}{2(1+x)} + l(l+1)\right\} P_l^{m+s,\,m-s}(x) = 0. \tag{C.14} $$

This differential equation is known as the generalized associated Legendre equation. Its regular solutions are the generalized associated Legendre functions of the first kind $P_l^{p,\,q}$ with $p = m+s$ and $q = m-s$ (see, for example, [41,145]) . For general (non-integer) p, q and k, Kuipers [87] obtained the normalisation relation

$$ \int_{-1}^{1} P_k^{p,\,q}(x)^2\mathrm{d}x = \frac{1}{2^{p-q+1}}\frac{1}{2k+1}\frac{\Gamma(k+\frac{p-q}{2}+1)\Gamma(k+\frac{p+q}{2}+1)}{\Gamma(k-\frac{p-q}{2}+1)\Gamma(k-\frac{p+q}{2}+1)}. \tag{C.15} $$

By enforcing

$$ \int\int {}_sY_{lms}\,\bar{Y}_{lm}\mathrm{d}S = 1, \tag{C.16} $$

where $\mathrm{d}S$ is the area element of the unit sphere, and using (C.15) we then obtain

$$ {}_sN_{lm} = \sqrt{\frac{(2l+1)(l-s)!(l-m)!}{2^{2-2s}\pi(l+s)!(l+m)!}}. \tag{C.17} $$

In [87] the recurrence relation

$$ xP_l^{m+s,\,m-s}(x) = {}_s\alpha_{lm}P_{l+1}^{m+s,\,m-s}(x) + {}_s\beta_{lm}P_l^{m+s,\,m-s}(x) + {}_s\gamma_{lm}P_{l-1}^{m+s,\,m-s}(x), \tag{C.18} $$

was derived, where

$$\begin{aligned} {}_s\alpha_{lm} &= \frac{(l-s+1)(l-m+1)}{(l+1)(2l+1)}, \\ {}_s\beta_{lm} &= \frac{ms}{l(l+1)}, \\ {}_s\gamma_{lm} &= \frac{(l+s)(l+m)}{l(2l+1)}. \end{aligned} \tag{C.19}$$

We can deduce from (C.18) a new recurrence relation for the spin-weighted spherical harmonics:

$$\cos\theta\, {}_sY_{lm}(\theta,\phi) = {}_sA_{lm}\, {}_sY_{l+1\,m}(\theta,\phi) + {}_sB_{lm}\, {}_sY_{lm}(\theta,\phi) + {}_sC_{lm}\, {}_sY_{l-1\,m}(\theta,\phi), \tag{C.20}$$

where

$${}_sA_{lm} = \frac{{}_sN_{lm}}{{}_sN_{l+1\,m}}\, {}_s\alpha_{lm} = \sqrt{\frac{(l+s+1)(l-s+1)(l+m+1)(l-m+1)}{(2l+1)(2l+3)(l+1)^2}}, \tag{C.21}$$

$${}_sB_{lm} = {}_s\beta_{lm} = \frac{ms}{l(l+1)}, \tag{C.22}$$

$${}_sC_{lm} = \frac{{}_sN_{lm}}{{}_sN_{l-1\,m}}\, {}_s\gamma_{lm} = \sqrt{\frac{(l-s)(l+s)(l-m)(l+m)}{(2l+1)(2l-1)l^2}}. \tag{C.23}$$

It follows that

$$\begin{aligned} \cos^2\theta\, {}_sY_{lm}(\theta,\phi) = {}& {}_sE_{lm}\, {}_sY_{l+2\,m}(\theta,\phi) + {}_sF_{lm}\, {}_sY_{l+1\,m}(\theta,\phi) \\ & + {}_sG_{lm}\, {}_sY_{lm}(\theta,\phi) + {}_sH_{lm}\, {}_sY_{l-1\,m}(\theta,\phi) \\ & + {}_sI_{lm}\, {}_sY_{l-2\,m}(\theta,\phi), \end{aligned} \tag{C.24}$$

where

$$\begin{aligned} {}_sE_{lm} &= {}_sA_{lm}\, {}_sA_{l+1\,m}, \\ {}_sF_{lm} &= {}_sA_{lm}\left[{}_sB_{l+1\,m} + {}_sB_{lm}\right], \\ {}_sG_{lm} &= {}_sA_{lm}\, {}_sC_{l+1\,m} + {}_sB_{lm}^2 + {}_sC_{lm}\, {}_sA_{l-1\,m}, \\ {}_sH_{lm} &= {}_sC_{lm}\left[{}_sB_{lm} + {}_sB_{l-1\,m}\right], \\ {}_sI_{lm} &= {}_sC_{lm}\, {}_sC_{l-1\,m}. \end{aligned} \tag{C.25}$$

Note that although spin-weighted spherical harmonics are only defined for $l \geq |s|$ and $-1 \leq m \leq l$, the recurrence relation (C.20) is still valid if $l = s$ (since ${}_sC_{sm} = 0$) and $m = l$ (since ${}_sC_{ll} = 0$). Similarly (C.24) is still valid in the cases $l = s,\ s+1$ and $m = l,\ l-1$.

Bibliography

[1] M. Abramowitz and I. A. Stegun. *Handbook of mathematical functions: with formulas graphs and mathematical tables*. Dover Publications, 1965.

[2] M. Alcubierre, G. Allen, B. Brügmann, G. Lanfermann, E. Seidel, W-M. Suen, and M. Tobias. Gravitational collapse of gravitational waves in 3D numerical relativity. *Physical Review D*, 61:041501, January 2000.

[3] K. Alvi. First-Order Symmetrizable Hyperbolic Formulations of Einstein's Equations Including Lapse and Shift as Dynamical Fields. *Classical and Quantum Gravity*, 19(20):5153–5162, October 2002.

[4] D. N. Arnold and A. Mukherjee. Adaptive Finite Elements and Colliding Black Holes. *arXiv Preprint: 970903v1*, 1997.

[5] R. Arnowitt, S. Deser, and C. W. Misner. The Dynamics of General Relativity. re-published at arxiv:gr-qc/0405109, May 2004.

[6] S. Bai, Z. Cao, X. Gong, Y. Shang, X. Wu, and Y. K. Lau. Light cone structure near null infinity of the Kerr metric. *Physical Review D*, 75(4):044003, 2007.

[7] A. Bayliss and E. Turkel. Radiation Boundary Conditions for Wave-Like Equations. *Communications on Pure and Applied Mathematics*, 33(6):707–725, November 1980.

[8] C. Beetle, M. Bruni, L. M. Burko, and A. Nerozzi. Towards a Wave-Extraction Method for Numerical Relativity: I. Foundations and initial-value formulation. *Physical Review D*, 72:024013, 2005.

[9] C. Beetle and L. M. Burko. A Radiation Scalar for Numerical Relativity. *Physical Review Letters*, 89(27):271101, December 2002.

[10] B. K. Berger. Numerical Approaches to Spacetime Singularities. *Living Reviews in Relativity*, 5(1), 2002: `http://relativity.livingreviews.org/Articles/lrr-2002-1`.

[11] M. Berger and P. Colella. Local Adaptive Mesh Refinement for Shock Hydrodynamics. *Journal of Computational Physics*, 82:64–84, May 1989.

[12] M. Berger and J. Oliger. Adaptive Mesh Refinement for Hyperbolic Partial Differential Equations. *Journal of Computational Physics*, 53:484–512, August 1984.

[13] M. Berger and I. Rigoutsos. An Algorithm for Point Clustering and Grid Generation. *IEEE Transactions on Systems, Man and Cybernetics*, 21(5):1278–1286, September/October 1991.

[14] E. Berti, V. Cardoso, and M. Casals. Eigenvalues and Eigenfunctions of Spin-Weighted Spheroidal Harmonics in Four and Higher Dimensions. *arXiv Preprint*, 2008.

[15] G. D. Birkhoff. *Relativity and Modern Physics*. Harvard University Press, 1923.

[16] C. Bona, T. Ledvinka, C. Palenzuela, and M. Zacek. General-Covariant Evolution Formalism for Numerical Relativity. *Physical Review D*, 67(10):104005–1 – 104005–5, May 2003.

[17] C. Bona, L. Lehner, and C. Palenzuela-Luque. Geometrically Motivated Hyperbolic Coordinate Conditions for Numerical Relativity: Analysis, Issues and Implementations. *Physical Review D*, 72(10):104009–1 – 104009–15, November 2005.

[18] H. Bondi, M. G. J. van der Burg, and A. W. K. Metzner. Gravitational Waves in General Relativity. VII. Waves from Axisymmetric Isolated Systems. *Proceedings of the Royal Society of London. Series A, Mathematical and Physical Sciences*, 269(1336):21–52, August 1962.

[19] W. B. Bonnor and M. A. Rotenberg. Gravitational Waves from Isolated Sources. *Proceedings of the Royal Society of London. Series A, Mathematical and Physical Sciences*, 289:247–274, 1966.

[20] R. H. Boyer and R. W. Lindquist. Maximal Analytic Extension of the Kerr Metric. *Journal of Mathematical Physics*, 8(2):265–281, February 1967.

[21] R. A. Breuer, M. P. Ryan, and S. Waller. Some Properties of Spin-Weighted Spheroidal Harmonics. *Proceedings of the Royal Society of London. Series A, Mathematical and Physical Sciences*, 358(1692):71–86, December 1977.

[22] L. T. Buchman and O. C. A. Sarbach. Towards Absorbing Outer Boundaries in General Relativity. *Classical and Quantum Gravity*, 23(23):6709–6744, December 2006.

[23] L. T. Buchman and O. C. A. Sarbach. Improved Outer Boundary Conditions for Einstein's Field Equations. *Classical and Quantum Gravity*, 24:S307–S326, June 2007.

[24] A. Buonanno, G. B. Cook, and F. Pretorius. Inspiral, merger, and ring-down of equal-mass black-hole binaries. *Physical Review D*, 75(12):124018, June 2007.

[25] L. M. Burko, T. W. Baumgarte, and C. Beetle. Towards a Wave-Extraction Method for Numerical Relativity: III. Analytical examples for the Beetle-Burko radiation scalar. *Physical Review D*, 73:024002, 2006.

[26] S. J. Campbell and J. Wainwright. Algebraic Computing and the Newman-Penrose Formalism in General Relativity. *General Relativity and Gravitation*, 8(12):987–1001, December 1977.

[27] S. Chandrasekhar. *The Mathematical Theory of Black Holes*. Oxford University Press, 1983.

[28] M. Choptuik. Universality and Scaling in Gravitational Collapse of a Massless Scalar Field. *Physical Review Letters*, 70(1):9–12, January 1993.

[29] M. Choptuik, L. Lehner, I. Olabarrieta, R. Petryk, F. Pretorius, and H. Villegas. Towards the final fate of an unstable black string. *Physical Review D*, 68:044001, August 2003.

[30] P. T. Chruściel, M. A. H. MacCallum, and D. B. Singleton. Gravitational waves in general relativity: XIV. Bondi expansions and the "polyhomogeneity" of scri. *Proceedings of the Royal Society of London. Series A, Mathematical and Physical Sciences*, 436:299–316, 1992.

[31] P. L. Chrzanowski. Vector potential and metric perturbations of a rotating black hole. *Physical Review D*, 11(8), 1975.

[32] W. J. Cocke. Table for constructing spin coefficients in general relativity. *Physical Review D*, 40(2):650–651, July 1989.

[33] J. M. Cohen and L. S. Kegeles. Electromagnetic Fields in Curved Spaces: A Constructive Procedure. *Physical Review D*, 10(4):1070–1084, August 1974.

[34] J. M. Cohen and L. S. Kegeles. Space-Time Perturbations. *Physics Letters*, 54A(1):5–7, August 1975.

[35] G. B. Cook. Initial Data for Numerical Relativity. *Living Reviews in Relativity*, 3(5), 2000:
`http://www.livingreviews.org/lrr-2000-5`.

[36] E. T. Copson. On the Riemann-Green Function. *Archive for Rational Mechanics and Analysis*, 1(1):324–348, January 1957.

[37] R. Courant and D. Hilbert. *Methods of Mathematical Physics*. Wiley-Interscience, 1989.

[38] M. Dafermos. A note on boundary value problems for black hole evolutions. *arXiv Preprint: 0403034*, March 2004.

[39] G. Darboux. *Leçons sur la Théorie Générale des Surfaces II*. Gauthier, 1899.

[40] E. Deadman and J. M. Stewart. Numerical Relativity and Asymptotic Flatness. *Classical and Quantum Gravity*, 26(6):065008, March 2009.

[41] G. T. Torres del Castillo. *3-D Spinors, Spin-weighted Functions and Their Applications*. Springer, 2003.

[42] A. Einstein. Die Feldgleichungen der Gravitation. *Sitzungsberichte der Königlich Preußischen Akademie der Wissenschaften*, pages 844–847, 1915.

[43] A. Einstein. Die Grundlage der allgemeinen Relativitätstheorie. *Annalen der Physik*, 354(7):769–822, 1916.

[44] K. Eppley. Evolution of time-symmetric gravitational waves: Initial data and apparent horizons. *Physical Review D*, 16(6):1609–1614, September 1977.

[45] A. Erdélyi. On the Euler-Poisson-Darboux Equation. *Jounral d'Analyse Mathématique*, 23:89–102, 1974.

[46] J. A. Font. Numerical Hydrodynamics and Magnetohydrodynamics in General Relativity. *Living Reviews in Relativity*, 11(7), 2008: `http://relativity.livingreviews.org/Articles/lrr-2008-7`.

[47] J. Frauendiener. Conformal Infinity. *Living Reviews in Relativity*, 7(1), 2004: `http://relativity.livingreviews.org/Articles/lrr-2004-1`.

[48] J. Frauendiener. Numerical treatment of the hyperboloidal initial value problem for the vacuum Einstein equations. II. The evolution equations. *Physical Review D*, 58:064003, August 1998.

[49] F. G. Friedlander. *The wave equation on a curved space-time*. Cambridge University Press, 1975.

[50] F. G. Friedlander and A. E. Heins. On the Representation Theorems of Poisson, Riemann and Volterra for the Euler-Poisson-Darboux Equation. *Archive for Rational Mechanics and Analysis*, 33(3):219–230, January 1969.

[51] H. Friedrich. Cauchy Problems for the Conformal Vacuum Field Equations in General Relativity. *Communications in Mathematical Physics*, 91:445–472, 1983.

[52] H. Friedrich and G. Nagy. The Initial Boundary Value Problem for Einstein's Vacuum Field Equation. *Communications in Mathematical Physics*, 201:619–655, 1999.

[53] R. Geroch, A. Held, and R. Penrose. A Space-Time Calculus Based on Pairs of Null Directions. *Journal of Mathematical Physics*, 14(7):874–881, July 1973.

[54] D. Givoli. High-Order Non-Reflecting Boundary Conditions: A Review. *Wave Motion*, 39(4):319–326, April 2004.

[55] D. Givoli and B. Neta. High-Order Non-Reflecting Boundary Scheme for Time-Dependent Waves. *Journal of Computational Physics*, 186(1):24–46, March 2003.

[56] R. J. Gleiser, R. H. Price, and J. Pullin. Late-time tails in the Kerr spacetime. *Classical and Quantum Gravity*, 25:072001, March 2008.

[57] J. N. Goldberg, A. J. Macfarlane, E. Newman, F. Rohrlich, and E. C. G. Sudarshan. Spin-s Spherical Harmonics and ð. *Journal of Mathematical Physics*, 8:2155, 1967.

[58] R. Gómez, L. Lehner, R. L. Marsa, and J. Winicour. Moving black holes in 3D. *Physical Review D*, 57:4778–4788, 1998.

[59] X. Gong, Y. Shang, S. Bai, Z. Cao, Z. Luo, and Y. K. Lau. Newman-Penrose constants of the Kerr-Newman metric. *Physical Review D*, 76(10):107501, 2007.

[60] P. Grandclément and J. Novak. Spectral Methods for Numerical Relativity. *Living Reviews in Relativity*, 12(1), 2009: `http://www.livingreviews.org/lrr-2009-1`.

[61] J. B. Griffiths. *Colliding plane waves in general relativity*. Oxford University Press, 1991.

[62] C. Gundlach, G. Calabrese, I. Hinder, and J. M. Martin-Garcia. Constraint Damping in the Z4 Formulation and Harmonic Gauge. *Classical and Quantum Gravity*, 22(17):3767–3773, September 2005.

[63] C. Gundlach and J. M. Martin-Garcia. Critical phenomena in gravitational collapse. *Living Reviews in Relativity*, 10(5), 2007: `http://relativity.livingreviews.org/Articles/lrr-2007-5`.

[64] B. Gustafsson, H-O. Kreiss, and J. Oliger. *Time Dependent Problems and Difference Methods*. Wiley-Interscience, 1996.

[65] J. Hadamard. *Lectures on Cauchy's Problem*. Yale University Press, 1923.

[66] T. Hagstrom. New Results on Absorbing Layers and Radiation Boundary Conditions. *Topics in Computational Wave Propagation: Direct and Inverse Problems*, pages 1–39, 2003.

[67] T. Hagstrom and S. I. Hariharan. A Formulation of Asymptotic and Exact Boundary Conditions using Local Operators. *Applied Numerical Mathematics*, 27(4):403–416, August 1998.

[68] T. Hagstrom and T. Warburton. A New Auxiliary Variable Formulation of High-Order Local Radiation Boundary Conditions. *Wave Motion*, 39(4):327–338, April 2004.

[69] S. G. Hahn and R. W. Lindquist. The Two-Body Problem in Geometrodynamics. *Annals of Physics*, 29:304–331, September 1964.

[70] S. W. Hawking. Black Holes in General Relativity. *Communications in Mathematical Physics*, 25:152–166, 1972.

[71] S. N. Hern and J. M. Stewart. The Gowdy T3 cosmologies revisited. *Classical and Quantum Gravity*, 15:1581–1593, February 1998.

[72] F. Herrmann, I. Hinder, D. Shoemaker, and P. Laguna. Unequal mass binary black hole plunges and gravitational recoil. *Classical and Quantum Gravity*, 24:S33–S42, May 2007.

[73] R. L. Higdon. Absorbing Boundary Conditions for Difference Approximations to the Multi-Dimensional Wave Equation. *Mathematics of Computation*, 47(176):437–459, October 1986.

[74] M. Holst, L. Lindblom, R. Owen, H. P. Pfeiffer, M. A Scheel, and L. E. Kidder. Optimal Constraint Projection for Hyperbolic Evolution Systems. *Physical Review D*, 70(8):4017–4034, October 2004.

[75] T. Jurke. On future asymptotics of polarized Gowdy T3-models. *Classical and Quantum Gravity*, 20:173–191, 2003.

[76] L. S. Kegeles and J. M. Cohen. Constructive Procedure for Perturbations of Spacetimes. *Physical Review D*, 19(6):1641–1663, March 1979.

[77] R. P. Kerr. Gravitational Field of a Spinning Mass as an Example of Algebraically Special Metrics. *Physical Review Letters*, 11(5):237–238, September 1963.

[78] L. E. Kidder, L. Lindblom, M. A Scheel, L. T. Buchman, and H. P. Pfeiffer. Boundary conditions for the Einstein evolution system. *Physical Review D*, 71:064020, March 2005.

[79] W. Kinnersley. Type D Vacuum Metrics. *Journal of Mathematical Physics*, 10(7):1195–1203, July 1969.

[80] J. A. Valiente Kroon. Conserved quantities for polyhomogeneous spacetimes. *Classical and Quantum Gravity*, 15:2479–2491, 1998.

[81] J. A. Valiente Kroon. A Comment on the Outgoing Radiation Condition for the Gravitational Field and the Peeling Theorem. *General Relativity and Gravitation*, 31(8):1219–1224, 1999.

[82] J. A. Valiente Kroon. Logarithmic Newman-Penrose Constants for Arbitrary Polyhomogeneous Spacetimes. *Classical and Quantum Gravity*, 16(5):1653–1665, May 1999.

[83] J. A. Valiente Kroon. On Killing Vector Fields and Newman-Penrose Constants. *Journal of Mathematical Physics*, 41(2):898–923, February 2000.

[84] J. A. Valiente Kroon. On the existence and convergence of polyhomogeneous expansions of zero-rest-mass-fields. *Classical and Quantum Gravity*, 17:4365–4375, 2000.

[85] J. A. Valiente Kroon. Polyhomogeneity and zero-rest-mass fields with applications to Newman-Penrose constants. *Classical and Quantum Gravity*, 17:605–621, 2000.

[86] J. A. Valiente Kroon. Can one detect a non-smooth null infinity? *Classical and Quantum Gravity*, 18:4311–4316, 2001.

[87] L. Kuipers. Generalized Legendre's Associated Functions (Integral Theorems, Recurrence Formulas). *Monatshefte für Mathematik*, 63(1), March 1958.

[88] W. Kundt and E. Newman. Hyperbolic Differential Equations in Two Dimensions. *Journal of Mathematical Physics*, 9(12):2193–2210, December 1968.

[89] L. Lindblom, K. D. Matthews, O. Rinne, and M. A. Scheel. Gauge drivers for the generalized harmonic Einstein equations. *Physical Review D*, 77:084001, 2008.

[90] L. Lindblom, M. A Scheel, L. E. Kidder, R. Owen, and O. Rinne. A New Generalized Harmonic Evolution System. *Classical and Quantum Gravity*, 23(16):447–462, July 2006.

[91] R. G. McLenaghan. An explicit determination of the empty space-times on which the wave-equation satisfies Huygens' principle. *Proceedings of the Cambridge Philosophical Society*, 65(1):139–155, 1969.

[92] C. W. Misner, K. S. Thorne, and J. A. Wheeler. *Gravitation*. W. H. Freeman, 1973.

[93] V. Moncrief. Gravitational perturbations of spherically symmetric systems. I. The exterior problem. *Annals of Physics*, 88(2):323–342, December 1974.

[94] V. Moncrief and O. Rinne. Regularity of the Einstein equations at future null infinity. *Classical and Quantum Gravity*, 26:125010, 2009.

[95] A. Nagar and L. Rezzolla. Gauge-invariant non-spherical metric perturbations of Schwarzschild black-hole spacetimes. *Classical and Quantum Gravity*, 22:R167–R192, July 2005.

[96] A. Nerozzi, C. Beetle, M. Bruni, L. M. Burko, and D. Pollney. Towards a Wave-Extraction Method for Numerical Relativity: II. The quasi-Kinnersley Frame. *Physical Review D*, 72, July 2005.

[97] E. Newman and R. Penrose. An Approach to Gravitational Radiation by a Method of Spin Coefficients. *Journal of Mathematical Physics*, 3(3):566=578, May-June 1962.

[98] E. Newman and R. Penrose. Errata: An Approach to Gravitational Radiation by a Method of Spin Coefficients. *Journal of Mathematical Physics*, 4(7):998, July 1963.

[99] E. Newman and R. Penrose. New Conservation Laws for Zero Rest-Mass Fields in Asymptotically Flat Space-Time. *Proceedings of the Royal Society of London. Series A, Mathematical and Physical Sciences*, 305(1481):175–204, June 1968.

[100] E. Newman and T. W. J. Unti. Behaviour of Asymptotically Flat Empty Spaces. *Journal of Mathematical Physics*, 3(5):891–901, 1962.

[101] J. Novak and S. Bonazzola. Absorbing boundary conditions for simulations of gravitational waves with spectral methods in spherical coordinates. *Journal of Computational Physics*, 197:186–196, 2004.

[102] F. W. J. Olver. *Asymptotics and Special Functions.* AK Peters, 1997.

[103] R. Penrose. *Conformal Treatment of Infinity.* Gordon & Breach, 1963.

[104] R. Penrose. Zero rest-mass fields including gravitation: asymptotic behaviour. *Proceedings of the Royal Society of London. Series A, Mathematical and Physical Sciences*, 284:159–203, February 1965.

[105] R. Penrose and W. Rindler. *Spinors and Space-Time: 1. Two Spinor Calculus and Relativistic Fields. 2. Spinor and Twistor Methods in Space-Time Geometry.* Cambridge University Press, 1984, 1986.

[106] E. Picard. Memoire sur la théorie des équations aux dérivées partielles et la méthode des approximations successives. *Journal de Mathématiques Pures et Appliquées*, 4(6):145–209, 1890.

[107] J. Porrill and J. M. Stewart. Electromagnetic and Gravitational Fields in a Schwarzschild Space-Time. *Proceedings of the Royal Society of London. Series A, Mathematical and Physical Sciences*, 376(1766):451–463, May 1981.

[108] F. Pretorius. Evolution of Binary Black-Hole Spacetimes. *Physical Review Letters*, 95(12):1101, September 2005.

[109] R. H. Price. Nonspherical Perturbations of Relativistic Gravitational Collapse. I. Scalar and Gravitational Perturbations. *Physical Review D*, 5(10):2419–2438, May 1972.

[110] R. H. Price. Nonspherical Perturbations of Relativistic Gravitational Collapse. II. Integer-Spin, Zero-Rest-Mass Fields. *Physical Review D*, 5(10):2439–2454, May 1972.

[111] T. Regge and J. A. Wheeler. Stability of a Schwarzschild Singularity. *Physical Review*, 108(4):1063–1069, November 1957.

[112] A. D. Rendall. Theorems on the Existence and Global Dynamics for the Einstein Equations. *Living Reviews in Relativity*, 6(8), 2005: `http://relativity.livingreviews.org/Articles/lrr-2005-6`.

[113] O. Rinne. *Axisymmetric Numerical Relativity*. PhD thesis, University of Cambridge, 2005.

[114] O. Rinne. Stable radiation-controlling boundary conditions for the generalized harmonic Einstein equations. *Classical and Quantum Gravity*, 23:6275–6300, October 2006.

[115] O. Rinne. Constrained evolution in axisymmetry and the gravitational collapse of prolate Brill waves. *Classical and Quantum Gravity*, 25(135009), 2008.

[116] O. Rinne, L. T. Buchman, M. A. Scheel, and H. P. Pfeiffer. Implementation of absorbing boundary conditions for the Einstein equations. *Classical and Quantum Gravity*, 26:075009, 2009.

[117] O. Rinne, L. Lindblom, and M. A. Scheel. Testing outer boundary treatments for the Einstein equations. *Classical and Quantum Gravity*, 24:4053–4078, 2007.

[118] O. Rinne and J. M. Stewart. A strongly hyperbolic and regular reduction of Einstein's equations for axisymmetric spacetimes. *Classical and Quantum Gravity*, 22:1143–1166, 2005.

[119] D. C. Robinson. Classification of black holes with electromagnetic fields. *Physical Review D*, 10(2):458–460, July 1974.

[120] D. C. Robinson. Uniqueness of the Kerr Black Hole. *Physical Review Letters*, 34(14):905–906, April 1975.

[121] M. Ruiz, M. Alcubierre, D. Núñez, and R. Takahaski. Multipole expansions for energy and momenta carried by gravitational waves. *General Relativity and Gravitation*, 40(8):1705–1729, August 2008.

[122] M. Ruiz, O. Rinne, and O. C. A. Sarbach. Outer boundary conditions for Einstein's field equations in harmonic coordinates. *Classical and Quantum Gravity*, 24:6349–6377, 2007.

[123] R. K. Sachs. Gravitational Waves in General Relativity. VIII. Waves in Asymptotically Flat Space-Time. *Proceedings of the Royal Society of London. Series A, Mathematical and Physical Sciences*, 270(1340):103–126, October 1962.

[124] O. C. A. Sarbach and M. Tiglio. Boundary conditions for Einstein's field equations: Mathematical and numerical analysis. *Journal of Hyperbolic Differential Equations*, 2(4):839–883, 2005.

[125] B. S. Sathyaprakash and B. F. Schutz. Physics, Astrophysics and Cosmology with Gravitational Waves. *Living Reviews in Relativity*, 12(2), 2009:
`http://relativity.livingreviews.org/Articles/lrr-2009-2`.

[126] M. A Scheel, M. Boyle, T. Chu, L. E. Kidder, K. D. Matthews, and H. P. Pfeiffer. High-accuracy waveforms for binary black hole inspiral, merger, and ringdown. *Physical Review D*, 79(2), 2009.

[127] M. A Scheel, H. P. Pfeiffer, L. Lindblom, L. E. Kidder, O. Rinne, and S. A. Teukolsky. Solving Einstein's Equations with Dual Coordinate Frames. *arXiv Preprint*, July 2006.

[128] B. G. Schmidt and J. M. Stewart. The Scalar Wave Equation in a Schwarzschild Space-Time. *Proceedings of the Royal Society of London. Series A, Mathematical and Physical Sciences*, 367(1731):503–525, September 1979.

[129] J. A. Schouten. *Ricci Calculus*. Springer, 1954.

[130] L. Smarr. *The structure of general relativity with a numerical illustration: The collision of two black holes*. PhD thesis, Texas University, Austin, 1975.

[131] R. F. Stark and T. Piran. Gravitational-Wave Emission from Rotating Gravitational Collapse. *Physical Review Letters*, 55(8):891–894, August 1985.

[132] H. Stephani, D. Kramer, M. A. H. MacCallum, and C. Hoenselaers. *Exact Solutions of Einstein's Field Equations*. Cambridge University Press, 2002.

[133] J. M. Stewart. Hertz-Bromwich-Debye-Whittaker-Penrose Potentials in General Relativity. *Proceedings of the Royal Society of London. Series A, Mathematical and Physical Sciences*, 367(1731):527–538, September 1979.

[134] J. M. Stewart. Numerical Relativity III. The Bondi Mass Revisited. *Proceedings of the Royal Society of London. Series A, Mathematical and Physical Sciences*, 424(1866):211–222, July 1989.

[135] J. M. Stewart. *Advanced General Relativity*. Cambridge University Press, 2nd edition, 1991.

[136] J. M. Stewart. The Cauchy Problem and the Initial Boundary Value Problem in Numerical Relativity. *Classical and Quantum Gravity*, 15(9):2865–2889, September 1998.

[137] J. M. Stewart. The Euler-Poisson-Darboux equation for Relativists. *General Relativity and Gravitation*, DOI 10.1007/s10714-009-0829-3, 2009.

[138] J. M. Stewart and P. Le Floch. to be confirmed. *forthcoming*, 2009.

[139] J. M. Stewart and M. Walker. Perturbations of Space-Times in General Relativity. *Proceedings of the Royal Society of London. Series A, Mathematical and Physical Sciences*, 341(1624):49–74, October 1974.

[140] P. Szekeres. The Gravitational Compass. *Journal of Mathematical Physics*, 6(9):1387–1391, September 1965.

[141] B. Szilágyi and J. Winicour. Well-posed initial-boundary evolution in general relativity. *Physical Review D*, 68:041501, August 2003.

[142] S. A. Teukolsky. Perturbations of a Rotating Black Hole. I. Fundamental Equations for Gravitational, Electromagnetic, and Neutrino-Field Perturbations. *Astrophysical Journal*, 185:635–647, October 1973.

[143] S. A. Teukolsky. Perturbations of a Rotating Black Hole. II. Dynamical Stability of the Kerr Metric. *Astrophysical Journal*, 185:649–673, October 1973.

[144] J. Thornburg. Event and Apparent Horizon Finders for 3+1 Numerical Relativity. *Living Reviews in Relativity*, 10(3), 2007: `http://relativity.livingreviews.org/Articles/lrr-2007-3`.

[145] N. O. Virchenko and I. Fedotova. *Generalized associated Legendre functions and their applications*. World Scientific, 2001.

[146] P. C. Waylen. On the degree of sharpness is solutions of Einstein's field equations. *Proceedings of the Royal Society of London. Series A, Mathematical and Physical Sciences*, 321(1546):397–408, February 1971.

[147] J. Winicour. Characteristic Evolution and Matching. *Living Reviews in Relativity*, 12(3), 2009: `http://relativity.livingreviews.org/Articles/lrr-2009-3`.

[148] J. W. York. *Kinematics and Dynamics of General Relativity*. Cambridge University Press, 1979.

[149] F. J. Zerilli. Gravitational Field of a Particle Falling in a Schwarzschild Geometry Analyzed in Tensor Harmonics. *Physical Review D*, 2(10):2141–2160, November 1970.